UNITED STATES PATENT AND TRADEMARK OFFICE

UNITED STATES DEPARTMENT OF COMMERCE
United States Patent and Trademark Office
Address: COMMISSIONER OF PATENTS AND TRADEMARKS
Washington, D.C. 20231
www.uspto.gov

RECEIVED
DEC 12 2001

NOTICE OF ALLOWANCE AND FEE(S) DUE

7590   12/03/2001

Intellectual Property Office
The Pennsylvania State University
113 Technology Center
University Park, PA 16802

EXAMINER
ZITOMER, FRED

ART UNIT	CLASS-SUBCLASS
1713	526-255000

DATE MAILED: 12/03/2001

APPLICATION NO.	FILING DATE	FIRST NAMED INVENTOR	ATTORNEY DOCKET NO.	CONFIRMATION NO.
09/730,088	12/05/2000	Tze-Chiang Chung	2000-2282	7453

TITLE OF INVENTION: SEMICRYSTALLINE FERROELECTRIC FLUOROPOLYMERS AND PROCESS FOR PREPARING SAME

TOTAL CLAIMS	APPLN. TYPE	SMALL ENTITY	ISSUE FEE	PUBLICATION FEE	TOTAL FEE(S) DUE	DATE DUE
8	nonprovisional	YES	$640	$300	$940	03/04/2002

THE APPLICATION IDENTIFIED ABOVE HAS BEEN EXAMINED AND IS ALLOWED FOR ISSUANCE AS A PATENT.

PROSECUTION ON THE MERITS IS CLOSED. THIS NOTICE OF ALLOWANCE IS NOT A GRANT OF PATENT RIGHTS. THIS APPLICATION IS SUBJECT TO WITHDRAWAL FROM ISSUE AT THE INITIATIVE OF THE OFFICE OR UPON PETITION BY THE APPLICANT. SEE 37 CFR 1.313 AND MPEP 1308.

THE ISSUE FEE AND PUBLICATION FEE (IF REQUIRED) MUST BE PAID WITHIN THREE MONTHS FROM THE MAILING DATE OF THIS NOTICE OR THIS APPLICATION SHALL BE REGARDED AS ABANDONED. THIS STATUTORY PERIOD CANNOT BE EXTENDED. SEE 35 U.S.C. 151.

HOW TO REPLY TO THIS NOTICE:

I. Review the SMALL ENTITY status shown above. If the SMALL ENTITY is shown as YES, verify your current SMALL ENTITY status:
A. If the status is changed, pay the PUBLICATION FEE (if required) and twice the amount of the ISSUE FEE shown above and notify the United States Patent and Trademark Office of the change in status, or
B. If the status is the same, pay the TOTAL FEE(S) DUE shown above.

If the SMALL ENTITY is shown as NO:

A. Pay TOTAL FEE(S) DUE shown above, or

B. If applicant claimed SMALL ENTITY status before, or is now claiming SMALL ENTITY status, check the box below and enclose the PUBLICATION FEE and 1/2 the ISSUE FEE shown above.

☐ Applicant claims SMALL ENTITY status.
See 37 CFR 1.27.

II. PART B - FEE(S) TRANSMITTAL should be completed and returned to the United States Patent and Trademark Office (USPTO) with your ISSUE FEE and PUBLICATION FEE (if required). Even if the fee(s) have already been paid, Part B - Fee(s) Transmittal should be completed and returned. If you are charging the fee(s) to your deposit account, section "4b" of Part B - Fee(s) Transmittal should be completed and an extra copy of the form should be submitted.

III. All communications regarding this application must give the application number. Please direct all communications prior to issuance to Box ISSUE FEE unless advised to the contrary.

IMPORTANT REMINDER: Utility patents issuing on applications filed on or after Dec. 12, 1980 may require payment of maintenance fees. It is patentee's responsibility to ensure timely payment of maintenance fees when due.

Page 1 of 3

PTOL-85 (REV. 07-01) Approved for use through 01/31/2004.

SEMICRYSTALLINE FERROELECTRIC FLUOROPOLYMERS AND
PROCESS FOR PREPARING SAME

" U.S. patent application No. 09/750,088 "

RELATED APPLICATIONS

This application is based on a Provisional Application (PSU Reference No. 2000-2282), which was filed on June 2, 2000, and which is entitled "Ferroelectric Polymers With Giant Electrostriction: Based On Semicrystalline Terpolymers Containing Vinylidene Fluoride, Trifluoroethylene and Third Monomer."

FIELD OF THE INVENTION

The present invention relates to a new class of polymeric materials that generate exceptionally high dielectric constant and high electro-mechanical response at ambient temperature. More particularly, the invention relates to a class of semicrystalline ferroelectric terpolymers comprising vinylidene fluoride (VDF), trifluoroethylene (TrFE), and at least one bulky monomer, such as chlorotrifluoroethylene (CTFE) or hexafluoropropene (HFP) or the like, prepared by borane/oxygen initiation in bulk reaction conditions.

BACKGROUND OF THE INVENTION

Ferroelectric materials that generate mechanical actuation induced by external electric field have attracted a great deal of attention and have been recognized for applications in a variety of transducers, actuators and sensors. Most of the current commercial applications for ferroelectric materials are based on piezoceramics and magnetostrictive materials, despite the fact that they exhibit many deficiencies, such as low strain levels (< 0.2%), brittleness, heavy weight, high processing temperatures and processing difficulties when producing parts having complicated shapes. In sharp contrast, ferroelectric polymers exhibit many desirable properties, such as flexibility, light weight, high mechanical strength, an ability to be processed readily into large area films, and an ability to be molded readily into a variety of configurations. However, despite these advantages over ceramic materials, most ferroelectric polymers suffer the disadvantage of having a low electric field sensitivity, in terms of dielectric constant,

piezoelectric coefficient, electromechanical coupling coefficient and field induced strain, which limit their applications.

One of the phenomena in ferroelectric polymers that has a great potential in generating high strain with high force level and broad frequency bandwidth is the phase transformation between ferroelectric (polar) and paraelectric (nonpolar) crystalline domains. The crystalline phase change produces large lattice strain and large change in sample dimension. Electrostriction refers to a coupling effect between the strain and the square of polarization, and is a desirable mechanism for achieving a large electric-induced mechanical response. It is interesting to note that the electrostrictive response due to crystalline phase transition is very different from electrostatic force in dielectric elastomers [R. Pelrine, R. Kornbluh, Q. Pei, and J. Joseph, Science, 287, 836, 2000], which can produce a large strain but a very weak force.

In the past decade, most of the research activities involving ferroelectric polymers have focussed on ferroelectric fluorocarbon polymers, especially semicrystalline VDF/TrFE copolymers. Many research efforts have been devoted to a general goal of reducing the energy barrier for ferroelectric-paraelectric (Curie) phase transition, and for generating a large and fast electric-induced mechanical (piezoelectric) response at ambient temperature. Although VDF/TrFE copolymers (stretched film poled at 120 °C) exhibit a relatively high piezoelectric constant (on the order of from about 10 pC/N to about 25 pC/N; $pC = 10^{-12}$ coulomb and N = newton) [K. Koga, and H. Ohigashi, J. Appl. Phys., 59, 2142,1986], the response of the dipoles to an electric field is very slow at ambient temperature, and the polarization hysteresis loop (polarity vs. electric field) of the copolymer is very large. As shown in Figure 3, a VDF/TrFE copolymer comprising 55 mole % VDF and 45 mole % TrFE, which exhibits the narrowest polarization hysteresis loop and lowest Curie temperature of the copolymers in the VDF/TrEF family [Y. Higashihata, J. Sako, and T. Yagi, Ferroelectrics, 32, 85, 1981], still exhibits a significantly wider hysteresis loop than those exhibited by the VDF/TrEF/bulky monomer terpolymers of this invention.

The close connection between crystalline structure and electric properties led to many attempts to alter copolymer morphology by creating non-equilibrium states; and a number of such attempts resulted in ferroelectric polymers that exhibit somewhat improved electric responses. Such attempts have included, for example, subjecting ferroelectric polymers to mechanical deformation [K. Tashiro, S. Nishimura, and M. Kobayashi, Macromolecules, 21,

2463, 1988, and 23, 2802, 1990], electron-radiation [B. Daudin, and M. Dubus, J. Appl. Phys., 62, 994, 1987], uniaxial drawing [T. Furukawa, and N. Seo, Japanese Journal of Applied Physics, 29, 675, 1990], crystallization under high pressure [T. Yuki, S. Ito, T. Koda, and S. Ikeda, Jpn. J. Appl. Phys., 37, 5372, 1998], and crystallization under high electric field [S. Ikeda, H. Suzaki, and S. Nakami, Jpn. J. Appl. Phys., 31, 1112, 1992],

Zhang et al. [Science, 280, 2102, 1998 and WO99/26261] recently reported their work involving electron-radiation treatment of ferroelcetric polyvinylidene fluoride polymers. The polymers that were generically disclosed in their work include polyvinylidene fluoride, polyvinylidene fluoride-trifluoroethylene, polyvinylidene fluoride-tetrafluoroethylene, polyvinylidene fluoride-trifluoroethylene-hexafluoropropylene and polyvinylidene fluoride-hexafluoropropylene. However, the only polymers actually prepared and studied were 50/50 and 65/35 copolymers of vinylidene fluoride/trifluoroethylene (VDF-TrFE). The Zhang et al work, which included a systematic study of the radiation conditions, such as dosage, temperature, inert atmosphere, stretching sample, etc., revealed an exceptionally high electrostrictive response (~ 4%) of the irradiated copolymer that behaves like a relaxor ferroelectric with fast electric-induced mechanical response at ambient temperature. Their work also revealed that the polarization hysteresis loop of the irradiated copolymer became very narrow at room temperature, compared with the hysteresis loop of a sample of the copolymer before irradiation. However, the polarization of the irradiated copolymer also was significantly reduced and the irradiated copolymer became completely insoluble because of the severe crosslinking side reaction that had occurred during the high-energy radiation. The increase of hardness of the irradiated copolymer sample due to the crosslinking also was revealed in its electric response, i.e., a very high electric field (150 MV/m) was required before the irradiated copolymer exhibited a high strain response (~ 4%). Thus, it appears that irradiating a ferroelectric copolymer not only reduces the polar crystalline domain size, but also produces many undesirable side reactions that increase the amorphous phase and diminish the processibility of the irradiated copolymer. At page 11, lines 25-27 [in WO 99/26261], Zhang et al, in a quite off-handed manner, suggested that the effects achieved by irradiation can be accomplished chemically, by adding a bulky side group to the main polymer chain which operates as an internal plasticizer. Zhang et al provided no examples of bulky side chain additions and made no further reference to chemically modified polymers.

4

As will be apparent from the following description of the invention, the present approach for altering the crystalline domains, and creating relaxor ferroelectric behavior, of VDF/TrFE copolymers is to introduce into the copolymer structure a controlled amount of bulky monomer units, such as chlorotrifluroethylene (CTFE) and hexafluoropropene (HFP) units, with a homogeneous fashion. The resulting terpolymers are solution and melt processible and form a desirable film morphology with uniform nano-crystalline domains that have Curie (polar-nonpolar crystalline phase) transition at about ambient temperature. Therefore, these terpolymers exhibit exceptionally high dielectric constant at ambient temperature and fast and high electro-mechanical response induced by external electric field.

Prior to the present invention, there have been several reports that discussed VDF/TrFE/CTFE terpolymers with significantly different thermal and electric properties. The terpolymers were prepared by emulsion and suspension polymerization processes at elevated temperature. For example, U.S. Patent 4,554,335 discloses the stable dielectric constants over a wide range of temperatures in the terpolymers that are composed of 25-90 mol% of VDF units, 5-70 mol% TrFE units, and 1-13 mol% CTFE units. However, these polymers have a dielectric constant of at most about 20 at ambient temperature (20 °C) at 1 kHz. The stability of dielectric constants over a wide range of temperatures implies a terpolymer with a broad Curie (polar-nonpolar crystalline phase transition) temperature that is associated with a broad range of crystalline domains and a broad terpolymer composition distribution. U.S. Patent 5,087,679 discloses VDF/TrFE/CTFE terpolymers having a TrFE content in the range of 18-22 mole %. The terpolymers disclosed in that patent exhibit a dielectric constant higher than 25 (but below than 40) at 20 °C 1 kHz. The properties that are disclosed in these two patents are very different from those exhibited by the terpolymers of the present invention, in which the VDF/TrFE/CTFE terpolymers were prepared by bulk process at ambient temperature using borane/oxygen initiation. Figure 1 compares the dielectric constant of a terpolymer sample (Example 6 in this disclosure) with that of the best sample shown in the previous disclosures (U.S. Patent 5,087,679). The dielectric constant of the sample in this disclosure is significantly higher over a wide temperature range, and the dielectric constant reaches about 100 at 20 °C 1 kHz. In fact, this terpolymer (of Example 6) has a mole ratio of VDF/TrFE/CTFE = 58/33.1/8.9, which is well off the best composition suggested in the previous disclosure (U.S. Patent 5,087,679). In

5

addition, the dielectric constant remains very high over a wide frequency range (650 Hz to 300 kHz), as shown in Figure 2.

There also have been reports that discuss VDF/TrFE/HFP terpolymers containing bulky hexafluoropropene (HFP) monomer units. For example, Freimuth et al. [H. Freimuth, C. Sinn, and M. Dettenmaier, Polymer, 37, 831, 1996] disclose that the incorporation of HFP into VDF/TrFE copolymer did not affect the crystalline structure, but strongly reduced the degree of crystallinity of the resulting polymer. Sako et al. [J. Sako, T. Yagi, Y. Higashihata, M. Tatemoto, N. Tomihashi, Y. Shimizu, U.S.Patent 4,577,005] reported improved specific permittivity (dielectric constant) for VDF/TFE/HFP terpolymers, compared to VDF/TFE copolymers. However, the dielectric constant of the terpolyemrs remained low (< 20) at room temperature and 1 kHz, even after heat treatment. Tajitsu et al. [Y. Tajitsu, A. Hirooka, A. Yamagish, and M. Date, Jpn. J. Appl. Phys., 36, 6114, 1997] reported a switching phenomenon in the VDF/TrFE/HFP terpolymers having a low HFP content (< 2.5 mole %). The switching phenomenon is associated with the rotations of individual molecular chains around their axes in crystalline domains. Overall, the switching time was found to have a very low dependence on the HFP content of the terpolymer. With an increase in the HFP content, both polarization and dielectric constant were found to decrease at the Curie temperature, which usually is above 40° C.

To date, methods of preparing VDF/TrFE/CTFE and VDF/TrFE/HFP copolymrs have included free radical emulsion and suspension polymerization processes in aqueous solution using a batch reactor [F. J. Honn, et al., U.S. Patent 3,053,818; J. E. Dohany, et al., U.S. Patent 3,790,540; T. Sakagami, et al., U.S. Patent 4,554,335; and H. Inukai, et al., U.S. Patent 5,087,679]. The combination of heterogeneous reaction conditions, significant difference in comonomer reactivity ratios, and high monomer conversion in batch reactions inevitably results in terpolymers having a broad composition distribution and inhomogeneous crystalline domains. In addition, it is also very difficult to completely remove emulsifying and suspending agents (containing polar groups) after emulsion and suspension polymerization processes, respectively.

SUMMARY OF THE INVENTION

It is an object of the present invention to provide a new class of ferroelectric terpolymers, which exhibit an exceptionally high dielectric constant and large strain response under the influence of an electric field at ambient temperature.

It is another object to provide a new class of terpolymers, which are both melt and solution processible, and which possess a combination of uniform molecular and nano-crystalline structures, so that they have a crystal phase (polar-nonpolar) transition temperature (Curie temperature) at near ambient temperature and exhibit typical relaxor ferroelectric behavior.

Yet another object is to provide a process for preparing the subject ferroelectric terpolymers, which process utilizes homogeneous reaction conditions involving only the various monomers and a very small amount of borane and oxygen, which, in situ, form a borane/oxygen free radical initiator.

The above and other objects and advantages of the invention are achieved by providing easily processible (by solution or melt) semicrystalline terpolymers, which comprises 50-80 mole % of vinylidene fluoride (VDF), 15-40 mole % of trifluoroethylene (TrFE) and 2-20 mole % of at least one bulky monomer, such as chlorotrifluoroethylene (CTFE) or hexafluoropropene (HFP). The terpolymers have a number average molecular weight in excess of about 10,000, and preferably in excess of about 30,000. Typically, the molecular weight of the terpolymers would be on the order of from about 10,000 to about 500,000, and preferably from about 30,000 to about 100,000.

The terpolymers exhibit a high dielectric constant and a crystal phase (polar-nonpolar) transition temperature (Curie temperature) near ambient temperature. Typically, the dielectric constant of the present terpolymers would be at least about 40, and preferably at least about 50, e.g., on the order of from about 40 to about 100, and preferably from about 50 to about 100. The Curie temperature of the terpolymers typically would be from about $15^\circ C$ to about $40^\circ C$, and preferably from about $18^\circ C$ to about $35^\circ C$.

The terpolymers also exhibit an exceptionally large electrostrictive strain response under an external field at ambient temperature. As used in this specification and claims, the term "ambient temperature" is understood to be at 1 atmosphere and room temperature between $20\text{-}25^\circ C$. Also, the term "exceptionally large strain response" is understood to mean > 0.5 % strain at 50 MV/m and > 2.5 % at 100 MV/m.

As used in this specification and claims, the term "terpolymer" is meant to include not only polymers that contain units derived from three distinct monomers, but also polymers that contain units derived from greater than three monomers. For example, the term "terpolymer" includes polymers prepared from vinylidene fluoride, trifluoroethylene, and chlorotrifluoro-

7

ethylene (VDF/TrFE/CTFE), as well as polymers prepared from vinylidene fluoride, trifluoroethylene, chlorotrifluoroethylene and hexafluoropropylene (VDF/TrFE/CTFE/HFP). In other words, the ferroelectric terpolymers of this invention include terpolymers of vinylidene fluoride, trifluoroethylene, and at least one bulky co-monomer, such as, chlorotrifluoroethylene (CTFE), hexafluoropropene (HFP), vinylidene chloride (VDC), tetrafluoroethylene (TFE), vinyl fluoride, vinyl chloride, acrylonitrile, acrylamide, methyl methacrylate, ethyl methacrylate, butyl methacrylate, octyl methacylate, methacrylic acid, methyl acrylate, ethyl acrylate, butyl acrylate, octyl acylate, 2-hydroxyethyl acrylate, glycidyl acrylate, acrylic acid, maleic anhydride, vinyl acetate, styrene, alpha-methyl styrene, trimethoxyvinylsilane, triethoxyvinylsilane and the like.

As used in this specification and claims the term "substantially uniform molecular and nano-crystalline structures" is understood to mean that the terpolymer under consideration has a narrow terpolymer composition that results in the terpolymer having uniform nano-crystalline domains. Both melting and Curie transitions in Differential Scanning Calorimetry (DSC) thermograms are strongly dependent on the terpolymer composition, with sharp melting peaks and diminished Curie (polar-nonpolar) phase transitions.. The combination of significant reductions of both melting temperature and heat for polar-nonpolar crystal phase (Curie) transition indicates the terpolymers having very small crystalline domains. The crystalline phase was further examined by X-ray diffraction region for the (200) and (110) reflections. Only one narrow peak is observed in all terpolymers, and the peak systematically moves to the lower angle (2θ) as the CTFE content increases in a given terpolymer. The angle about $18.2°$ (corresponding to a lattice spacing of 4.9 angstrom) for the terpolymer VDF/TrFE/CTFE = 61.4/25.3/13.3 indicates the paraelectric phase in this terpolymer, which is different from the ferreoelectric phase of the corresponding (VDF/TrFE=60/40) copolymer. The systematic increase of the lattice spacing clearly is due to the uniform terpolymer structure, and the uniformly distributed CTFE units serve as the defects in the crystalline phase.

The terpolymers of the invention are characterized by a unique combination of substantially uniform molecular and nano-crystalline structures, such that they exhibit typical relaxor ferroelectric behavior (with extremely low heat for polar-nonpolar crystalline phase transition). The expanding and contracting of these crystalline domains under an external electric field, coupled with a large difference in the lattice strain between the polar and non-polar crystal phases, generates the exceptionally large electrostrictive strain response that is characteristic of

the terpolymers of this invention. The unique properties of the present terpolymers are believed to be due, at least in part, to the new chemistry that is used in their preparation, i.e., using oxidation adducts of an organoborane as a free radical initiator in a homogeneous bulk polymerization process to prepare semicrystalline terpolymers having a homogeneous molecular structure that results in uniform crystalline structure and desirable crystalline domains.

BRIEF DESCRIPTION OF THE DRAWINGS

Figure 1 is a graph comparing dielectric constants at 1 kHz of a VDF/TrFE/CTFE terpolymer in accordance with the present invention (Example 6) with a comparative VDF/TrFE/CTFE terpolymer shown in the disclosure of U. S. patent 5,087,679.

Figure 2 is a graph illustrating the dielectric constants (with frequency range from 650 to 300,000 Hz) of a VDF/TrFE/CTFE terpolymer comprising 58 mole % VDF, 33.1 mole % TrFE and 8.9 mole % CTFE (Example 6 of the present invention).

Figure 3 is a graph comparing the polarization hysteresis loops of two VDF/TrFE/CTFE terpolymers in accordance with the present invention (Examples 2 and 8) with that of a conventional VDF/TrFE copolymer comprising 55 mole % VCD and 45 mole % TrFE.

Figure 4 is a graph illustrating the longitudinal strain (in %) of three terpolymers in accordance with the present invention versus the magnitude of an external field (in MV/m) to which the terpolymers were subjected for a VDF/TrFE/CTFE terpolymer comprising 72.2 mole % VDF, 17.8 mole % TrFE and 10 mole % CTFE (Example 1), for a VDF/TrFE/CTFE terpolymer comprising 66 mole % VDF, 22.5 mole % TrFE and 11.5 mole % CTFE (Example 2), and for a VDF/TrFE/CTFE terpolymer comprising 58 mole % VDF, 33.1 mole % TrFE and 8.9 mole % CTFE (Example 6).

DETAILED DISCRIPTION OF THE INVENTION

This invention discloses a new class of ferroelectric polymers that exhibit exceptionally large electrostrictive response (~ 4%) under external electric field at ambient temperature. These polymers are based on the terpolymer, which comprises 50-80 mole% of vinylidene fluoride (VDF), 15-40 mole% of trifluoroethylene (TrFE) and 2-20 mole% of a bulky monomer, such as chlorotrifluoroethylene (CTFE) or hexafluoropropene (HFP). These terpolymers are high

molecular weight (> 10,000 g/mole) semicrystalline polymers with homogeneous molecular and nano-crystalline structures.

It is well established that VDF/TrFE copolymer segments form ferroelectric crystalline domains with high Curie temperature (> 50° C), which causes the low electric field-induced mechanical response at ambient temperature. The major objective of this invention is to incorporate a certain amount of bulky monomer units into the copolymer structure with a homogeneous fashion, so that the bulky groups located along the polymer chain can reduce crystalline domain size without destroying the overall crystallinity. Therefore, the resulting terpolymer exhibits a reduced Curie temperature (ideally at ambient temperature), and still maintains high dielectric constant. Consequently, a rapid switch between polar and nonpolar crystal phases can take place at ambient temperature under an external electric field. The large difference in the lattice dimensions between the polar and nonpolar crystals causes the expansion and contraction of the terpolymer solid, which generates an exceptionally large electric-field induced mechanical response at ambient temperature.

As disclosed in Tables 1 and 2, a broad composition range of semicrystalline VDF/TrFE/CTFE and VDF/TrFE/HFP terpolymers have been prepared with high molecular weight (>10,000 g/mole). The thermal properties of the terpolymers were measured by differential scanning calarometry (Perkin-Elmer DSC-7). The terpolymers exhibited a melting temperature between about 100 and about 140° C, a heat of fusion between about 30 and about 15 J/g, and Curie temperature between about 15 and 40° C, a heat of phase transition below 3 J/g. In some terpolymers, the Curie temperature was undetectable. The actual values of the thermal properties are governed by the terpolymer composition.

Polymer films (~30 μm thickness) may be prepared either by solution casting on a glass slide from a solution containing 1-10 wt % polymer in a solvent, such as N, N-dimethylformamide, or by melt-pressing polymer powder at above 160° C. The polymer films usually are used in the form in which they are prepared. However, they may be stretched by uniaxial stretching to 2 or more times their original length at room temperature. The films may be heat treated, e.g., annealed, for example, at a temperature of from about 80 to about 110°C under vacuum for 5 hrs. The films also may be subjected to a radiation treatment under an inert atmosphere with a dosage in the range of 5 to 30 Mrad irradiation. For electrical measurement, a gold electrode may be sputtered on a small area on both major surfaces of the polymer film. The
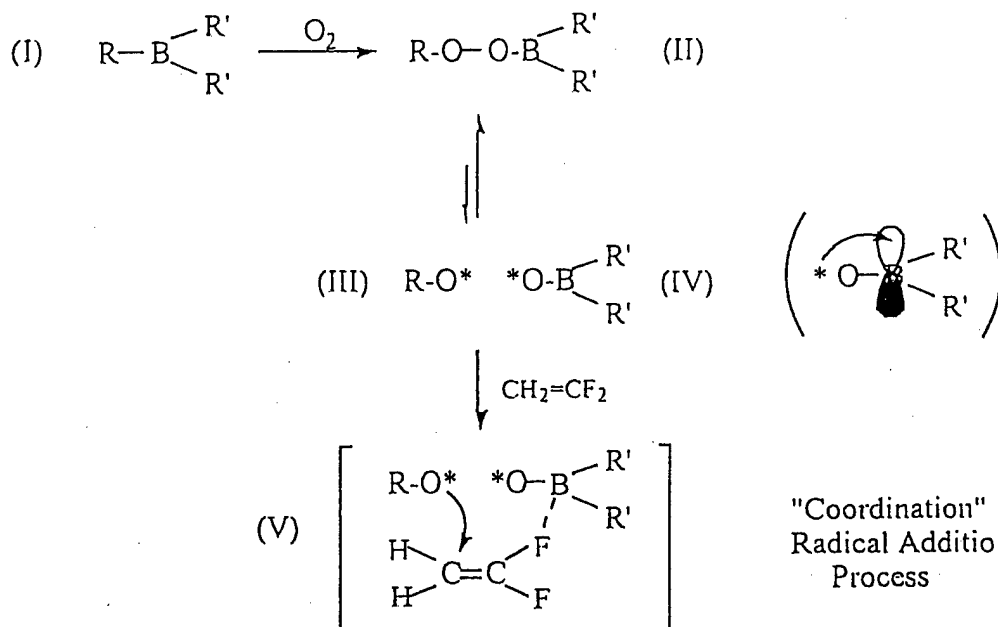
polarization hysteresis loop of each terpolymer was measured by a Sawyer-Tower circuit, with the frequency range from about 1 to 10 Hz. The dielectric constant (with the frequency range between 650 Hz to 300 kHz) was measured by a LCR meter (HP 4284A Impedance Analyzer) at a temperature range between – 20 to 120° C, and the electric field-induced strain may be measured by a bimorph-based strain sensor designed specifically for polymer film strain measurement.

The terpolymers exhibit a high dielectric constant at ambient temperature. As shown in Figures 1 and 2, and summarized in Table 3 (described more fully in Examples 21-32), the dielectric constant of the present terpolymers at 25° C and 1 kHz is at least about 40, and preferably at least about 50, e.g., on the order of from about 40 to about 100, and preferably from about 50 to about 100. The high dielectric constant at ambient temperature is strongly related to the Curie temperature of the terpolymers (which is controlled in the range from 15° C to 40° C, and preferably from about 18° C to about 35° C) and the very small heat of polar-nonpolar crystalline phase transition. Moreover, the dielectric peaks of terpolymer are broad (diffuse) and depend on the frequency, which are common features of a ferroelectric relaxor. The higher dielectric constant is advantageous when preparing capacitors having relatively small size and large capacity.

The terpolymers also exhibit large electric responses at ambient temperature under the external fields. Figure 3 illustrates the diminished (and narrowed) polarization hysteresis loops of two VDF/TrFE/CTFE terpolymers in accordance with the invention (prepared in accordance with Examples 2 and 8, respectively), compared to the wider hysteresis loop of a VDF/TrFE copolymer having a 55/45 mole ratio. The decreased width of the observed hysteresis loops is due to the incorporation of bulky monomer units into the terpolymer. The narrow hysteresis loop for the VDF/TrFE/CTFE terpolymer (Example 8) at ambient temperature, which exhibits a broad dielectric constant having a peak that shifts to a higher temperature as the frequency increases (Figure 2), is indicative of a ferroelectric relaxor with a large electric response, which is crucial for electromechanical device applications. The associated low heat of polar-nonpolar crystalline phase transition is summarized in Table 3. In fact, no detectable Curie (polar-nonpolar crystalline phase) transition was observed for the VDF/TrFE/CTFE terpolymer (Example 8) in DSC thermograph. The crystalline domains must be very small, so that the activation energy for the crystalline phase transition is extremely small.

11

Figure 4 illustrates the longitudinal strain (in %) versus the electric field (in MV/m) for three terpolymers in accordance with the invention. The first terpolymer (described more fully in Example 1) comprises VDF/TrFE/CTFE having a mole ratio of 72.2/17.8/10, whereas the second and third terpolymers (described more fully in Examples 2 and 6) comprise VDF/TrFE/CTFE having the mole ratios of 66/22.2/11.5 and 58/33.1/8.9, respectively. As illustrated, the longitudinal strain for each terpolymer increased with increasing electric field intensity up to > 0.5 % at an electric field of 50 MV/m and up to > 2.5 % at an electric field intensity of about 100 MV/m, at ambient temperature. Moreover, it has been found that a plot of the strain (S) versus square of polarization (P^2) would be nearly a straight line. Based on the electrostrictive relationship $S=QP^2$, this equation yields the extrostrictive coefficient (Q) about -13.6 and -5.57 m^4/C^2 for terpolymers in Examples 1 and 2, respectively. Overall, the terpolymers exhibit a typical relaxor ferroelectric behavior with an exceptionally large electrostrictive strain response.

In accordance with another aspect of the invention, a novel chemistry may be used to prepare the terpolymers having a narrow composition distribution, uniform nanometer size crystalline domains and a substantial freedom from impurities. All of the above characteristics are directly responsible for the terpolymers' exceptionally large electrostrictive response. The chemistry involves a combination of a bulk polymerization process and an oxygen-activated free radical initiated process, based on the oxidation adducts of organoborane molecules. As disclosed in previous publications [T. C. Chung, W. Janvikul and H. L. Lu J. Am. Chem. Soc., 118, 705, 1996; T. C. Chung, and W. Janvikul, J. Organomet. Chem., 581, 176, 1999], certain trialkylborane molecules undergo selective oxidation reactions and form free radical initiators, in situ, for polymerization of many free radical polymerizable monomers at ambient temperature. The radical formation mechanism involves mono-oxidation of one B-C bond in a trialkylborane molecule (I) with a controlled amount of oxygen, as illustrated below.

$$(I) \quad R\!-\!B\!\!\begin{smallmatrix}R'\\R'\end{smallmatrix} \quad \xrightarrow{O_2} \quad R\text{-}O\!-\!O\text{-}B\!\!\begin{smallmatrix}R'\\R'\end{smallmatrix} \quad (II)$$

$$(III) \quad R\text{-}O^* \quad {}^*O\text{-}B\!\!\begin{smallmatrix}R'\\R'\end{smallmatrix} \quad (IV) \qquad \left({}^*O\text{-}B\!\!\begin{smallmatrix}R'\\R'\end{smallmatrix} \right)$$

$$\downarrow \quad CH_2{=}CF_2$$

$$(V) \quad \left[\; \begin{array}{c} R\text{-}O^* \quad {}^*O\text{-}B\!\!\begin{smallmatrix}R'\\R'\end{smallmatrix} \\ H\!\!\diagdown \qquad \diagup F \\ C{=}C \\ H\!\!\diagup \qquad \diagdown F \end{array} \;\right]$$

"Coordination"
Radical Additio
Process

The R-O-O-BR'$_2$ species (II) that is formed further decomposes at ambient temperature to a R-O* alkoxyl radical (III) and a *O-BR'$_2$ borinate radical (IV). The alkoxyl radical is active in initiating polymerization of fluoro monomers, such as VDF, TrFE, CTFE, HFP, etc., at ambient temperature. On the other hand, the borinate radical is too stable to initiate polymerization due to the back-donating of the free electron to the empty p-orbital of boron. However, this "dormant" borinate radical may form a reversible bond with the radical at the growing chain end to prolong the lifetime of the propagating radical. In addition, during the propagating reaction, a coordination intermediate (V) may be formed due to the B-F acid-base complex between the active site and the incoming monomer. Such an interaction may enhance the reactivity of fluoromonomer and produce fluoro terpolymers having a narrow composition distribution. Overall, the reaction process resembles a living coordination free radical polymerization, which leads to the production of linear terpolymer having a narrow composition distribution.

As the free radical polymerizable monomer to be used as the bulky monomer, those well known in the art may be used. Specific examples of suitable bulky monomers include, but are not limited to, chlorotrifluoroethylene (CTFE), hexafluoropropene (HFP), vinylidene chloride (VDC), tertrafluoroethylene (TFE), vinyl fluoride, vinyl chloride, acrylonitrile, acrylamide, methyl methacrylate, ethyl methacrylate, butyl methacrylate, octyl methacylate, methacrylic acid, methyl

acrylate, ethyl acrylate, butyl acrylate, octyl acylate, 2-hydroxyethyl acrylate, glycidyl acrylate, acrylic acid, maleic anhydride, vinyl acetate, styrene, alpha-methyl styrene, trimethoxyvinylsilane, triethoxyvinylsilane and the like. These radical polymerizable comonomers can be used either singly or as a combination of two or more comonomers. Preferably, chlorotrifluoroethylene (CTFE) and/or hexafluoropropene (HFP) will be used as the bulky, free radical polymerizable monomer.

The temperature for the radical polymerization may be in the range of from about -10° C to about 40° C, and preferably from about 0° C to 30° C. The polymerization time typically would be in the range of from about 30 minutes to 10 hours, and preferably from about 1 to 5 hours.

The homogeneous bulk polymerization conditions typically involve only monomers and a very small amount of initiator, such as a organic peroxide, and preferably a borane/oxygen adduct initiator. After the polymerization reaction, the unreacted monomers (all in gas phase) are vented under ambient temperature and pressure. When a borane/oxygen adduct is employed as the free radical polymerization initiator, any trace amount of oxidized borane/oxygen adduct is further oxidized and hydrolyzed by exposing the terpolymer product to air, and the resulting water-soluble boric acid is easily removed from the terpolymer product by water washing. Elemental analysis of the terpolymer product after the water washing step will clearly indicate that no traces of boron remain in the terpolymer product. The terpolymer composition typically would be determined by a combination of elemental analysis, ^{1}H NMR measurements and ^{19}F NMR measurements.

The terpolymers of this invention are soluble in common organic solvents, such as methylethylketone (MEK), N,N-dimethylformamide (DMF), dimethylsolfoxide (DMSO), N,N-dimethylacetamide (DMA), tetrahydrofuran (THF), and the like. The terpolymers are also melt processible at temperatures in excess of about 150° C. Furthermore, the copolymers are semicrystalline thermoplastics having a high melting temperature, a high crystallinity and a high molecular weight. Thus, typical terpolymers in accordance with the invention would exhibit a melting temperature in excess of about 100° C, for example, on the order of from about 105° C to about 145° C, a heat of fusion in excess of about 15 J/g, for example, on the order of from about 15 to about 30 J/g, and a number average molecular weight in excess of about 10,000 g/mole, for example, on the order of from about 30,000 up to about 100,000, or more.

The present invention is illustrated by following non-limiting examples.

EXAMPLE 1

Synthesis of VDF/TrFE/CTFE Terpolymer

In a 75-ml stainless steel autoclave, 0.1g (0.5×10^{-3} moles) of tributylboron initiator was added under the argon atmosphere. The autoclave was then cooled from outside by liquid nitrogen and 16.7g (0.26 moles) of vinylidene fluoride (VDF), 7.6 g (0.09 moles) of trifluoroethylene (TrFE) and 1.7 g (0.015 moles) of chlorotrifluoroethylene (CTFE) were distilled into the autoclave. After the monomers and tributylborane had been added to the autoclave, 0.025×10^{-3} moles of oxygen was introduced into the autoclave and the autoclave was warmed to ambient temperature. The bulk polymerization was continued at ambient temperature for 5 hours before vacuum-distilling any unreacted monomers. The resulting terpolymer (6.5 g) was recovered, washed with methanol, and dried. According to chlorine analysis and ^{1}H NMR measurements, the terpolymer composition comprised 72.2 mole % VDF, 17.8 mole % TrFE and 10.0 mole % CTFE. The terpolymer had a peak melting temperature of 107.8 °C, based on DSC measurements (Perkin-Elmer DSC-7), and an intrinsic viscosity (MEK, 35° C) of 0.38.

EXAMPLES 2-14

Synthesis of VDF/TrFE/CTFE Terpolymers

Following the general procedures described in Example 1, several VDF/TrFE/CTFE terpolymers were prepared using the various monomer feed ratios and reaction conditions indicated in Table 1. The resulting VDF/TrFE/CTFE terpolymers were analyzed by elemental analysis, ^{1}H NMR, DSC (Perkin-Elmer DSC-7), and intrinsic viscosity (MEK, 35° C). The resulting VDF/TrFE/CTFE terpolymer compositions and the thermal properties thereof are summarized in Table 1.

TABLE 1

Ex. No.	Rxn time (Hrs.)	Monomer feed ratio (mol%)			Polymer composition (mol%)			Melting Temperature		Curie temperature		[η] (MEK) (35°C)
		VDF	TrFE	CTFE	VDF	TrFE	CTFE	Tm (°C)	ΔH (J/g)	Tc (°C)	ΔH (J/g)	
1	5	71	25	4	72.2	17.8	10	107.8	17.8	25.0	0.4	0.38
2	5	71	27	2	66	22.5	11.5	117.2	21.6	25.2	1.7	0.42
3	5	70	27	3	66.1	21.4	12.5	115.6	20.5	25.8	1.8	0.42
4	5	64	32	4	63.1	25.4	11.5	113.7	18.5	none	none	0.49
5	5	63.5	31.5	5	61.4	25.3	13.3	111.3	17.8	19.1	1.5	0.69
6	5	54	42.5	3.5	58	33.1	8.9	130.0	21.3	31.6	2.5	0.63
7	4	50	47	3	53.3	38	8.7	123.4	24.2	none	none	0.49
8	5	50	47	3	55.6	36.1	8.3	124.6	21.2	none	none	0.54
9	4	71	27	2	70	21.8	8.2	119.2	24.1	none	none	0.48
10	3	71	26	3	73.2	17.8	9.0	110.5	18.3	38.5	1.3	0.72
11	1.5	71	26	3	68.8	21.7	9.5	109.6	20.8	28.5	1.5	0.37
12	3	49	47	4	57.9	35.4	6.7	127.3	20.8	33.8	1.4	0.75
13	4	54	42.5	3.5	60.0	35.1	6.9	126.6	20.9	33.5	1.6	0.73
14	3	54	42.5	3.5	59.9	32.8	7.3	125.0	19.9	33.9	1.7	0.70

None: Undetectable

EXAMPLE 15

Synthesis of VDF/TrFE/HFP Terpolymer

Into a 75-ml stainless steel autoclave that was previously cooled down to the temperature of liquid nitrogen, there was injected 5 ml of a 10 wt. % solution of trichloroacetyl peroxide initiator dissolved in chloroform (1.5×10^{-3} moles of trichloroacetyl peroxide). The solvent was then vacuum evaporated to dryness at -30° C., whereafter a monomer mixture comprising 0.15 moles (9.6 g) of vinylidene fluoride (VDF), 0.10 moles (8.2 g) of trifluoroethylene (TrFE), and 0.018 moles (2.7 g) of hexafluoropropene (HFP) was condensed into the autoclave at the liquid nitrogen temperature. The autoclave was then rapidly warmed in an ice-water bath to 0° C, and was held in the ice-water bath for 5 hrs. Next, any unreacted monomers were released from the autoclave to terminate the polymerization. The resulting polymer was washed with methanol and dried to give a white powder. The polymer composition was analyzed by ^{19}F NMR and was observed to comprise 52.6 mole % VDF, 46.6 mole % TrFE and 0.8 mole % HFP. The melting temperature was determined to be 139.3° C, based on a Perkin-Elmer DSC-7 test device.

EXAMPLES 16-18

Synthesis of VDF/TrFE/HFP Terpolymers

Following the general procedures described in Example 15, several VDF/TrFE/HFP terpolymers were prepared using the monomer feed ratios indicated in Table 2. The resulting terpolymers were analyzed by ^{1}H and ^{19}F NMR, DSC (Perkin-Elmer DSC-7), and intrinsic viscosity (MEK, 35° C). The composition and thermal properties of the resulting VDF/TrFE/HFP terpolymers are summarized in Table 2.

TABLE 2

Ex. No.	Monomer feed (mol)			Polymer composition (mole %)			Tm (peak)	Tc (peak)	Mw $\times 10^{-4}$
	VDF	TrFE	HFP	VDF	TrFE	HFP	(° C)	(° C)	
16	0.15	0.13	0.018	63.4	35.8	0.8	139.7	42.4	18.2
17	0.15	0.12	0.044	60.5	37.2	2.3	131.5	42.4	5.2
18	0.2	0.18	0.071	55.2	42.3	2.5	129.1	35.6	17.2

EXAMPLE 19

Electrostrictive Response of VDF/TrFE/CTFE Terpolymer

A 25 μm thick polymer film was prepared from a sample of the VDF/TrFE/CTFE terpolymer of Example 1 by solution casting from a 10 wt % solution of the terpolymer in N, N-dimethylformamide at 70° C. After being formed, the film was annealed at 85° C for 7 hrs. For electric measurement, a generally circular electrode (area of 7.07 mm^{2}) was formed on both major surfaces of the film by sputtering the film with gold. The dielectric constant of the terpolymer was 56.0 at 1 KHz; 25" C, as determined by an HP 4284A Impedance Analyzer. The electric field induced strain was measured at ambient temperature in the field range of 0-150 MV/m using a bimorph-based strain sensor, which consisted of a piezoelectric bimorph-based cantileverdilatometer with a lock-in amplifier (Stanford Research System SR830 DSP) and a high voltage source (KEPCO-BOP 1000M). The electrostrictive strain was observed to be 3.04 % and 4.1 % at 100 and 150 MV/m, respectively. The polarization hysteresis loop of the terpolymer was obtained at ambient temperature using a Sawyer Tower circuit at the frequency

of 1 Hz. The terpolymer had a coercive field of 19.6 mC/m², and had a maximum polarization of 82 MV/m at ambient temperature and electric field of 100 MV/m.

EXAMPLE 20

Electrostrictive Response of VDF/TrFE/CTFE Terpolymer

A 25 μm thick polymer film was prepared from a sample of the terpolymer of Example 2 by melt pressing powdered terpolymer at 180° C. The resulting film was annealed at 85° C for 7 hrs. For electric measurement, a circular electrode (area of 7.07 mm²) was made by sputtering with gold on both surfaces of the annealed film. The terpolymer was found to have a dielectric constant of 62.0 at 1 KHz; 25° C, as determined using a HP 4284A Impedance Analyzer. The electric field induced strain was measured at ambient temperature in the field range of 0-150 MV/m using a bimorph-based strain sensor, which consisted of a piezoelectric bimorph-based cantileverdilatometer with a lock-in amplifier (Stanford Research System SR830 DSP) and a high voltage source (KEPCO-BOP 1000M). The terpolymer exhibited a 3.3 % electrostrictive strain at 100 MV/m. The polarization hysteresis loop of the terpolymer was obtained at ambient temperature using a Sawyer Tower circuit at the frequency of 1 Hz. The terpolymer had a coercive field of 24.1 mC/m², and had a maximum polarization of 78 mC/m² at ambient temperature and electric field of 100 MV/m.

EXAMPLES 21-32

Electric Properties of VDF/TrFE/CTFE Terpolymers

Films (30μm thick) were prepared from samples of the VDF/TrFE/CTFE terpolymers of Examples 3-14 and were subjected to electric measurements. The polymer films were prepared by melt pressing at 180° C, and were annealed at 85° C for 7 hrs. A circular electrode (area of 7.07 mm²) was made on each film by sputtering with gold on both major surfaces. Table 3 summarizes the polarization hysteresis loop of the terpolymers (obtained at ambient temperature using a Sawyer Tower circuit at the frequency of 1 Hz), as well as the terpolymers' dielectric constant and dielectric loss at 1 KHz; 25° C (measured by HP 4284A Impedance Analyzer).

TABLE 3

Example No.	polymer	Pmax (MV/m)	Ec (mC/m^2)	Dielectric constant	Dielectric loss
		100 MV/m, 25°C		1 KHz, 25 °C	
21	Example 3	-	-	64.0	0.05
22	Example 4	76	19.8	61.3	0.07
23	Example 5	75	33.7	58.8	0.06
24	Example 6	63	16.4	100	0.05
25	Example 7	65	31.8	41.6	0.06
26	Example 8	36	7.6	42.4	0.05
27	Example 9	90	24.9	40.8	0.05
28	Example 10	85	27.6	58.9	0.04
29	Example 11	120	32.6	45.5	0.05
30	Example 12	-	-	68.9	0.07
31	Example 13	-	-	56.9	0.07
32	Example 14	-	-	65.3	0.07

EXAMPLE 33

Electrostrictive Response of VDF/TrFE/HFP Terpolymer

A film having a thickness of about 25μm was prepared from a 10 wt% solution of the VDF/TrFE/HFP terpolymer of Example 18 dissolved in N, N-dimethylformamide. The polymer film was stretched to 4 times its original length at the ambient temperature and was annealed at 110° C for 7 hrs. A circular electrode (area 3.14 mm^2) was prepared by evaporating gold on both polymer film surfaces. The polarization hysteresis loop of the terpolymer film was obtained at the ambient temperature using a Sawyer Tower circuit at the frequency of 1 Hz. The coercive field of the terpolymer was determined to be 27 mC/m^2, and the maximum polarization was 60 MV/m. The electric field induced strain was determined at 50° C using a bimorph-based strain sensor, which consisted of a piezoelectric bimorph-based cantilever dilatometer with a lock-in amplifier (Stanford Research System SR830 DSP) and a high voltage source (KEPCO-BOP 1000M). The terpolymer showed an electrostrictive strain of 2.5 % at 50 MV/m.

What is claimed is:

Claim 1.   A melt and solution processible, semicrystalline ferroelectric terpolymer comprising from 50 – 80 mole % vinylidene fluoride, from 15 – 40 mole % trifluoroethylene, and from 2 – 20 mole % of at least one bulky monomer that is capable of being incorporated into the terpolymer by means of a free radical process, wherein said terpolymer has been prepared by a combination of bulk polymerization and free radical polymerization using oxygen and trialkylborane as reactants to form, in situ, an oxygen/trialkylborane adduct as the initiator for said free radical polymerization, and wherein said terpolymer exhibits (i) a narrow composition distribution and substantially uniform crystalline domains, (ii) a molecular weight in excess of about 10,000 grams/mole, (iii) a Curie transition temperature of from about 15 to about 40° C, (iv) a dielectric constant of at least about 40 and up to about 100 at 1 kHz, 25° C, and (v) an electrostrictive response of at least 0.5 % at 50 MV/m and at least 2.5 % at 100 MV/m at ambient temperature, whereby said terpolymer functions as a ferroelectric relaxor exhibiting rapid crystal (polar-nonpolar) phase transition at ambient temperature under an electric field.

Claim 2.   The terpolymer according to Claim 1, wherein said bulky monomer is chlorotrifluoroethylene.

Claim 3.   The terpolymer according to Claim 1, wherein said bulky monomer is hexafluoropropylene.

Claim 4.   The terpolymer according to Claim 1, wherein said bulky monomer is selected from the group consisting of chlorotrifluoroethylene, hexafluoropropylene, vinylidene chloride, tetrafluoroethylene, vinyl fluoride, vinyl chloride, acrylonitrile, acrylamide, methyl methacrylate, ethyl methacrylate, butyl methacrylate, octyl methacylate, methacrylic acid, methyl acrylate, ethyl acrylate, butyl acrylate, octyl acylate, 2-hydroxyethyl acrylate, glycidyl acrylate, acrylic acid, maleic anhydride, vinyl acetate, styrene, alpha-methyl styrene, trimethoxyvinylsilane, triethoxyvinylsilane and mixtures thereof.

Claim 5.   The terpolymer according to Claim 1, wherein said terpolymer is processible in melt or solution into the form of a ferroelectric film.

Claim 6.   A ferroelectric film prepared from the semicrystalline, ferroelectric terpolymer according to Claim 1, wherein said film has been heat treated at a temperature of from about 80 to about 110° C under vacuum for 5 hrs.

Claim 7.   A ferroelectric film prepared from the semicrystalline, ferroelectric terpolymer according to Claim 1, wherein said film has been radiation treated under an inert atmosphere with a dosage in the range of 5 to 30 Mrad irradiation.

Claim 8.   A ferroelectric film prepared from the semicrystalline, ferroelectric terpolymer according to Claim 1, wherein said film has been stretched to at least two times its original length.

Abstract

A new class of ferroelectric terpolymers having an exceptionally large electrostrictive response (> 3%) induced by external electric field at ambient temperature comprise 50-80 mole % of vinylidene fluoride (VDF), 15-40 mole % of trifluoroethylene (TrFE) and 2-20 mole % of at least one bulky monomer, such as chlorotrifluoroethylene (CTFE) or hexafluoropropene (HFP). These semicrystalline terpolymers behave like a ferroelectric relaxor having a rapid electric field-induced mechanical response, due to a low Curie temperature (phase transition between polar and nonpolar crystalline domains at or near ambient temperature) and high dielectric constant. A combination of bulk polymerization and free radical polymerization using oxidation adducts of an organoborane as the free radical initiator may be used to prepare the terpolymers, such that the terpolymers are characterized by good processibility, high purity and uniform molecular structure.

Figure 1
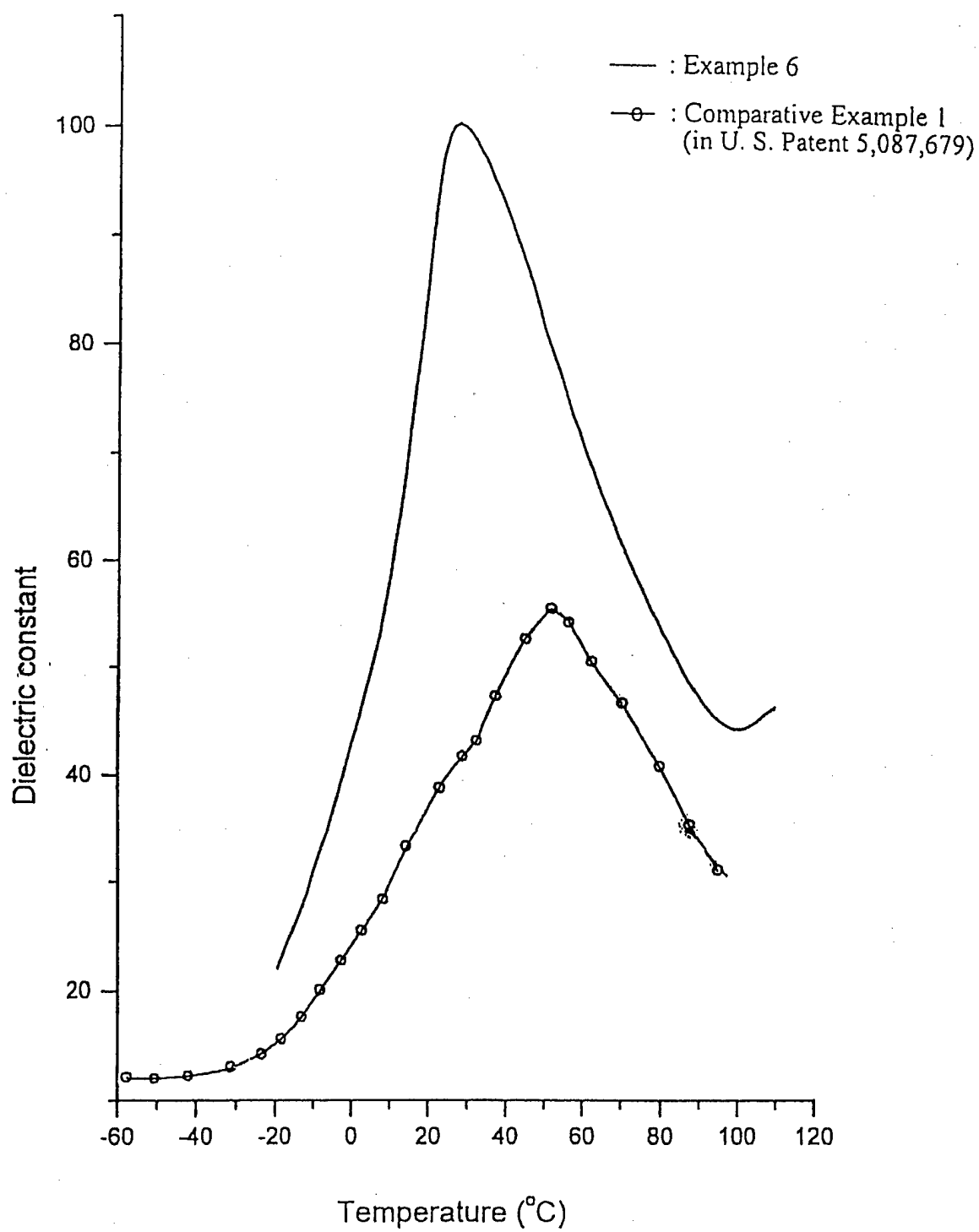
Figure 2
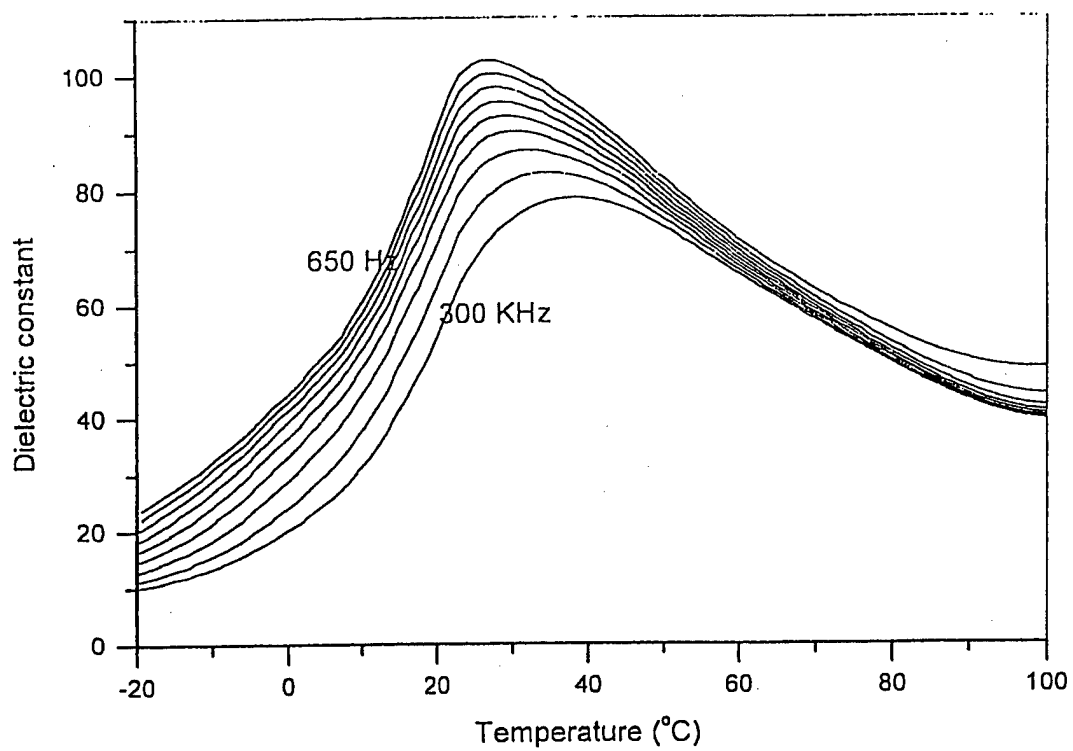
Figure 3
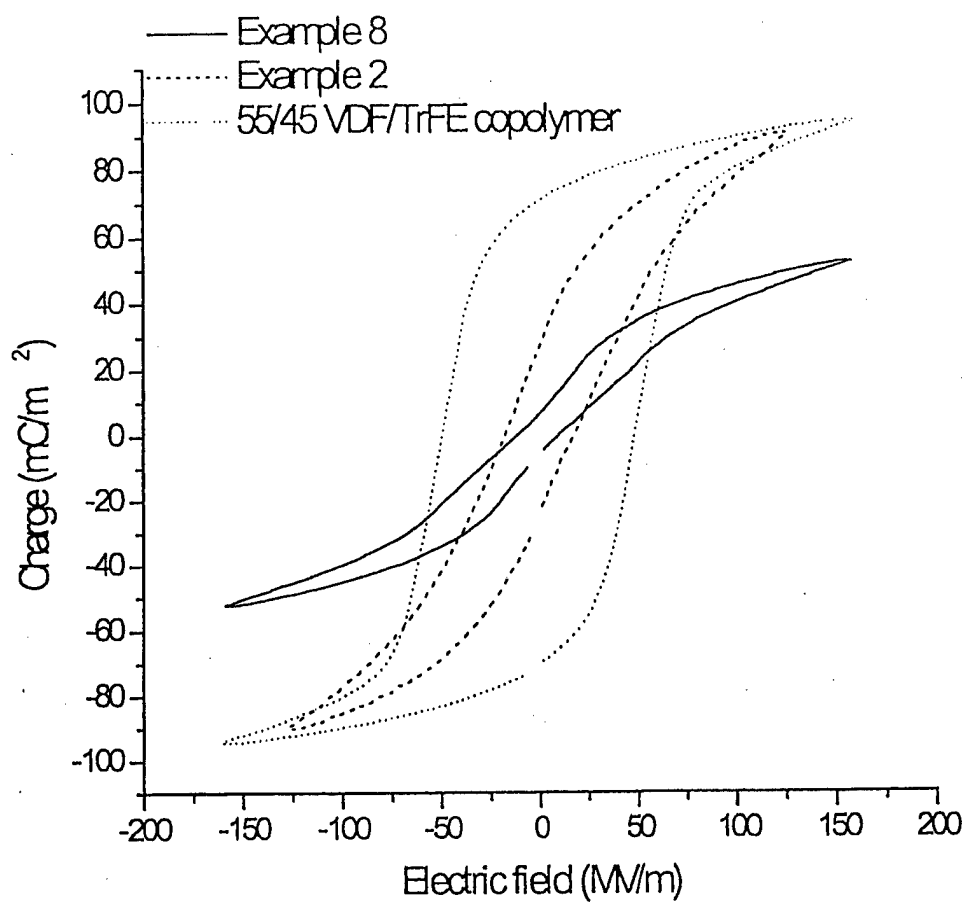
Figure 4
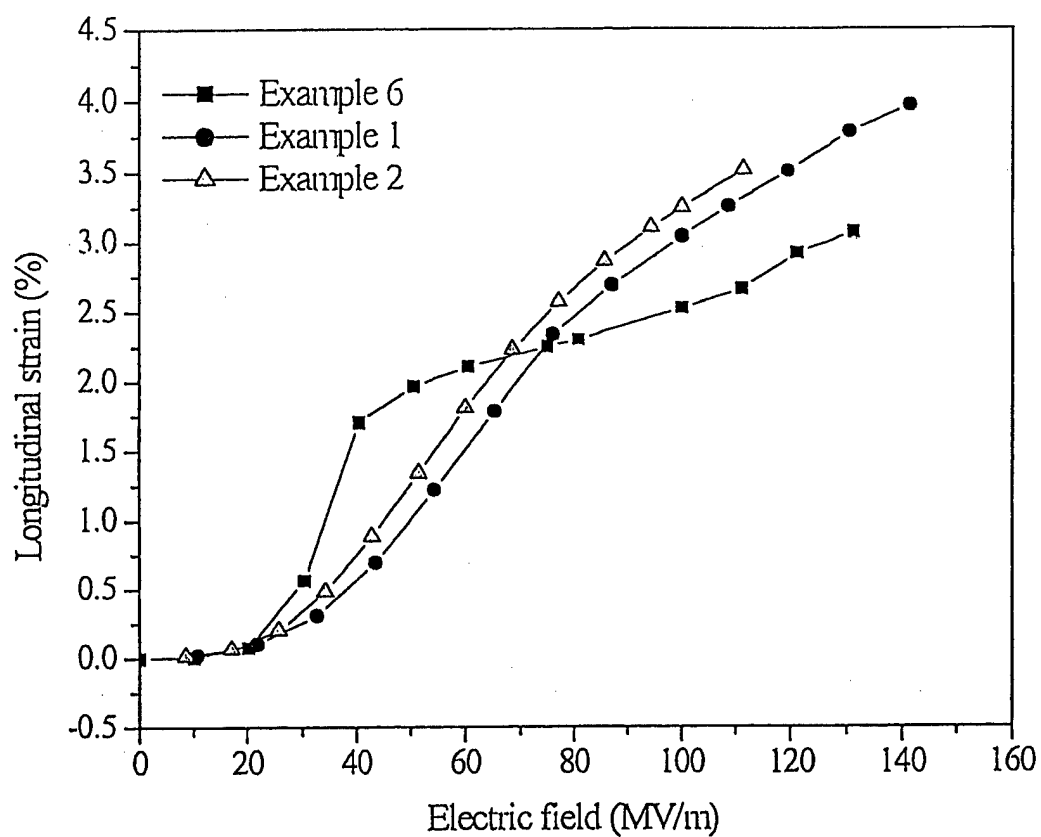
SYNTHESIS AND ELECTRIC PROPERTY OF
VDF/TrFE/HFP TERPOLYMERS

A. Petchsuk, T. C. Chung
Department of Material Science and Engineering, The Pennsylvania State University, University Park, PA 16802

ABSTRACT

This paper focuses on the molecular structure-electric property relationships of VDF/TrFE/HFP terpolymers, containing vinylidene difluoride (VDF), trifluoroethylene (TrFE) and hexafluoropropene (HFP) units. Several terpolymers were synthesized and evaluated with the corresponding VDF/TrFE copolymers. In general, a small amount of bulky HFP units in the polymer chain prevents the long sequence of crystallization and results in smaller ferroelectric (polar) micro-domains, which show the improved electric properties. The resulting terpolymer possesses a interesting combined properties with good processibility, low Curie transition temperature and high dielectric constant, narrow polarization hysteresis loop, and high strain response (2.5%) at relatively low electric field (50 MV/m).

INTRODUCTION

In the past decade, many research activities in ferroelectric fluorocarbon polymer have been focussing on VDF/TrFE copolymer with a general goal of reducing the energy barrier for ferroelectric-paraelectric (Curie) phase transition and generating large and fast electric-induced mechanical response at ambient temperature. Although VDF/TrFE copolymer exhibits a high piezoelectric and high pyroelectric constant [1], the response of the dipoles to the electric field is very slow at the ambient temperature, the polarization hysteresis loop of the copolymer is very large. The close connection between the crystalline structure and electric properties led to many attempts to alter copolymer morphology by mechanical deformation [2], electron-radiation [3], crystallization under high pressure [4], crystallization under high electric field [5], etc.

Zhang et al. [6] at Penn State University recently perfect the electron-radiation process with systematical study of the radiation conditions, such as dosage, temperature, inert atmosphere, stretching sample, etc. They revealed an exceptionally high electrostrictive response (> 4%) of the irradiated copolymer that behaves like a relaxor ferroelectric. The polarization hysteresis loop became very slim at room temperature, comparing with that of the sample before irradiation. However, the polarization was also significantly reduced and the sample became intractable because of the crosslinking. The increase of hardness of the copolymer sample was also revealed in its electric response, very high electric field was required (150 MV/m) for the irradiated sample to get a high strain response. It appears that the radiation process not only reduces the polar crystalline domain size but also involves some undesirable side reactions that increases the amorphous phase and diminishes the processibility of sample.

Another method of altering the morphology of VDF/TrFE copolymer is to introduce third (bulky) comonomer, such as hexafluoropropene (HFP), into the polymer chain. Freimuth et al. [7] studied VDF/TFE/HFP terpolymer. They concluded that the incorporation of HFP did not affect the crystalline structure, but strongly reduced the degree of crystallinity. The terpolymer exhibited thermal behavior similar to those observed in copolymer. Tajitsu et al. [8] reported the switching phenomena in VDF/TrFE/HFP terpolymers having a low HFP content (< 2.5 mol%).

Although there are experimental results on switching time, little information is available on the structure and the piezoelectric and pyroelectric properties of the VDF/TrFE/HFP terpolymers. It is very interesting to understand their structure-property relationship, especially the sample containing only a very small content of HFP termonomer (enough to reduce the size of polar crystalline domains, but not the overall crystallinity). The interested terpolymers have the VDF/TrFE mole ratio between 50/50 and 70/30, that provide high polarization at low Curie temperature (~ 60 °C). In this study, we will investigate their thermal and electrical properties, such as dielectric constant, polarization hysteresis loop, and electrostrictive response.

RESULTS AND DISCUSSION

Table 1 summarizes several VDF/TrFE/HFP terpolymers that were prepared by borane/O_2 or trichloroacetyl peroxide initiators at low temperature. Two commercial copolymers with VDF/TrFE mol% of 50/50, and 62/38 were also investigated for comparison.

Table 1 A Summary of VDF/TrFE/HFP Co- and Ter-polymers.

Run No.	Polymer Comp.(%)			Tm (°C)	ΔHm (J/g)	Tc (°C)	ΔHc (J/g)	Mw (x10^{-4})
	VDF	TrFE	HFP					
50/50	50	50	-	158.2	28.1	63.8	6.3	19.67
62/38	62	38	-	152.0	32.7	103.1	22.7	34.30
103	54.3	43.8	1.83	128.3	18.0	40.6	4.1	3.40
104	69.2	30.0	0.84	137.9	25.1	44.8	7.4	3.35
106	65.9	33.4	0.71	139.6	28.8	61.2	15.3	3.43
108	59.7	38.2	2.1	138.4	19.6	40.9	4.7	3.36
112	73.3	26.5	0.14	143.0	27.5	55.6	13.3	11.3
113	57.7	41.96	0.3	142.0	25.7	45.5	5.7	8.89
114	52.59	46.63	0.8	139.3	23.2	49.5	9.3	8.61
115	63.4	35.8	0.8	139.7	22.7	42.4	4.6	18.20
119	60.49	37.2	2.3	131.5	20.9	42.4	4.8	5.19
121	55.17	42.35	2.46	129.1	15.6	35.6	2.6	17.20

Thermal Properties

DSC measurement was used to investigate the thermal behaviors of the terpolymers. Figure 1 compares three terpolymers having VDF/(TrFE+HFP) mole ratio in the vicinity of 55/45 (run no. 114,103, 121) with the copolymer having VDF/TrFE 50/50 mole ratio. It is very clear that as the HFP molar content increased the Curie and melting temperatures of the terpolymer

decreased. The Curie temperature decreased from 63 °C (commercial VDF/TrFE 50/50 copolymer) to 49.5, 40.6, 35.6°C (our VDF/TrFE/HFP terpolymers with 0.18, 1.8, 2.46 mol%HFP, respectively). The bulky HFP units clearly effect the crystalline domains. The smaller polar domains may result in the lower energy for the conformation transition, hence the Curie transition temperature decreases. In addition, the bulky groups may also reduce the intermolecular interaction between the polymer chains.
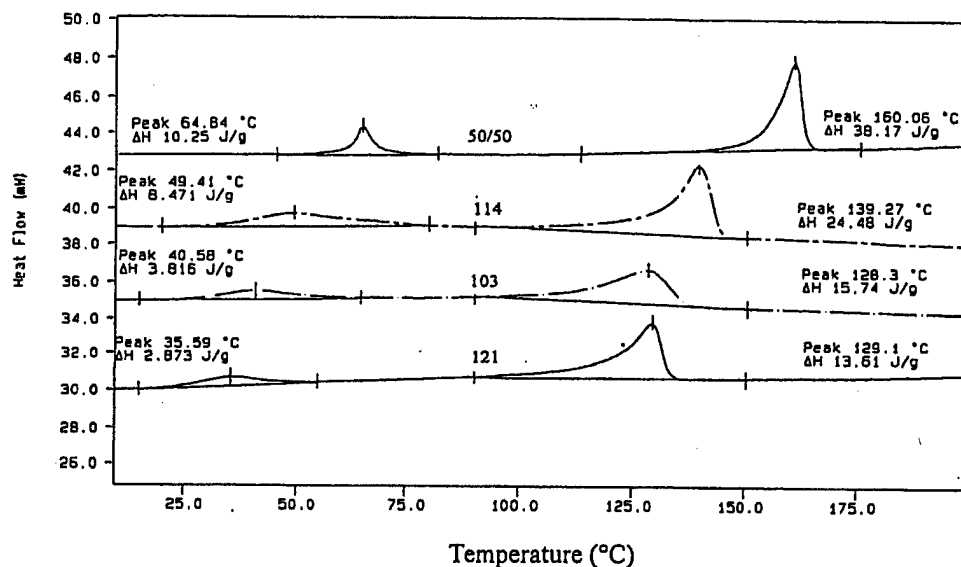

Figure 1. Comparison of DSC thermograms of VDF/TrFE/HFP terpolymer (run no. 114,103, 121) with the copolymer having VDF/TrFE 50/50 mole ratio.
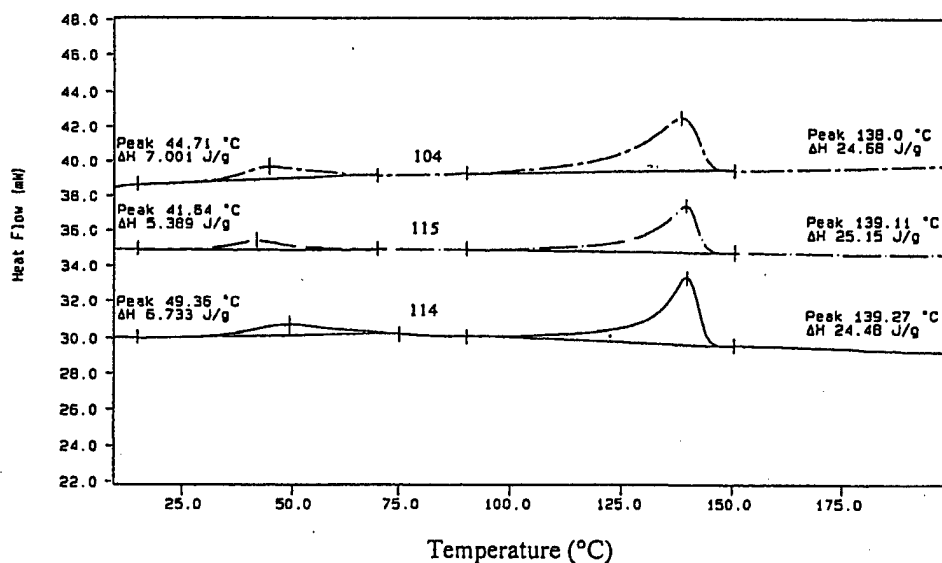
Figure 2. Comparison of DSC thermograms of VDF/TrFE/HFP terpolymers having about 0.8 mol% HFP and the TrFE content, 30 (104), 35.8(115), and 46.6 (114) mol%, respectively.

Figure 2 compares DSC curves of the terpolymers having about 0.8 mol% HFP and the TrFE content, 30, 35.8, 46.6 mol% respectively. Both Tm and Tc are not very sensitive to the TrFE contents. VDF and TrFE units in the terpolymer must co-crystallize well in the lattice, and the crystal structure and polar domain size maintains invariable despite the change of the VDF/TrFE mole ratio. Comparing with the corresponding VDF/TrFE copolymers, it appears that a small amount (< 1 mol%) of bulky HFP in VDF/TrFE/HFP terpolymers may only reduce the polar domain size, but not overall crystallinity and the magnitude of the dipole.
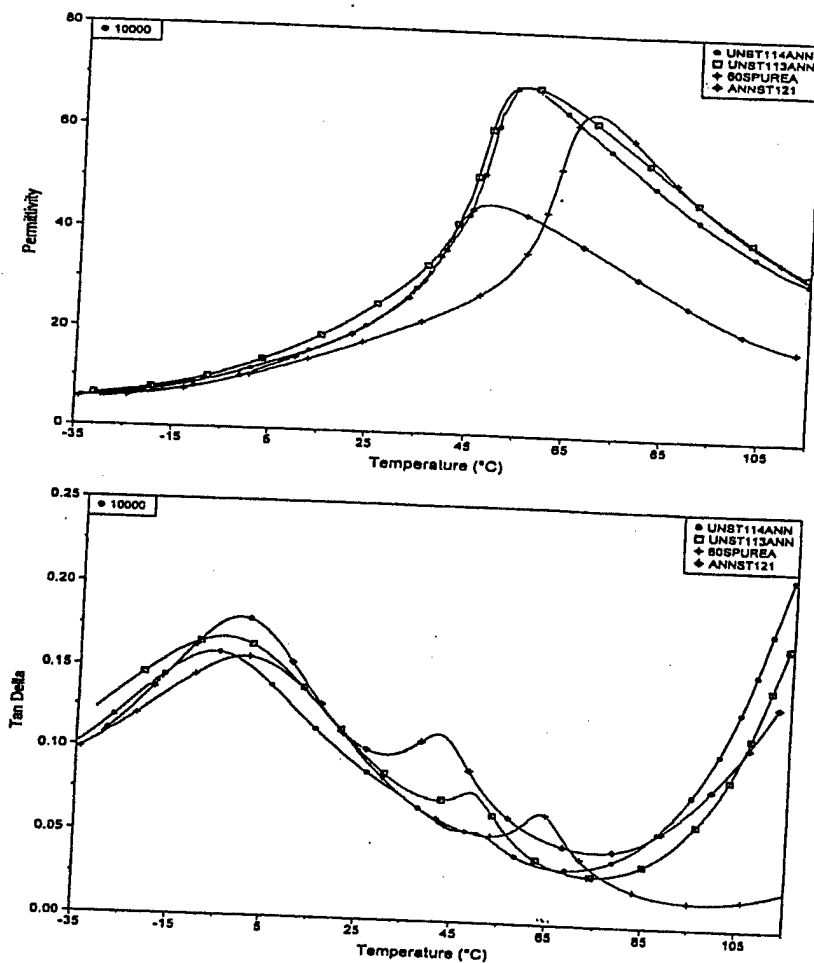
Figure 3. The comparison of dielectric constant (top) and dielectric loss (bottom) of three terpolymers with HFP content of, 0.3, 0.8, 2.46 mol%, designated as □, •, ♦, respectively, and the commercial copolymer, P(VDF/TrFE) 55/45, ✧

Dielectric Properties

Figures 3 compares permittivity and dielectric loss at 10,000 Hz, respectively, of three unstretched and annealed VDF/TrFE/HFP terpolymers containing 0.3, 0.8, 2.46 mol% HFP (run no. 113, 114, 121)and a VDF/TrFE copolymer. All polymers have a similar VDF/TrFE mol

ratio 55/45. The results clearly show a significant permittivity dependence on the HFP content. The correlated Tg (at γ relaxation) of the polymer, associated with the amorphous phase, almost no change in dielectric loss with small amount of HFP units. However, small quantity of HFP units in the crystalline domains has a large impact to the crystallization process of the polar domains. The Curie transition temperature shifts to the lower temperature as the HFP content increases. It is worth noting that the dielectric constant values of the terpolymers are about the same as comparing with copolymer. This result indicates the fact that the introduction of HFP units into polymer do not alter the conformation of the polymer chain (polymer chains still possess an all-trans ferroelectric conformation at the room temperature). Indeed, it facilitates the rotation of the dipoles upon heating by presumably breaking up the large polar domain size into microdomains. The small ferroelectric domain only need a small amount of energy to change the polymer conformation from polar to non-polar.

Ferroelectricity

Figure 4 compares the electric displacement vs. electric field of three terpolymers (run no. 115, 108, 119) with similar VDF/TrFE (~ 60/38) and different HFP content, 0.8, 2.1, 2.3 mol % HFP, respectively. As HFP content increases, the coercive field decreases as well as the polarization. For the terpolymer, the coercive field (Ec) required to change the direction of dipoles is much lower comparing with those of the commercial copolymer. Coercive field of the terpolymer is in the range of 20-30 MV/m while the coercive field of the commercial copolymer is in the range of 50-60 MV/m. This is presumably due to HFP termonomer breaks large polar domain size into smaller domain size, and allows reversal of the dipoles at lower field.
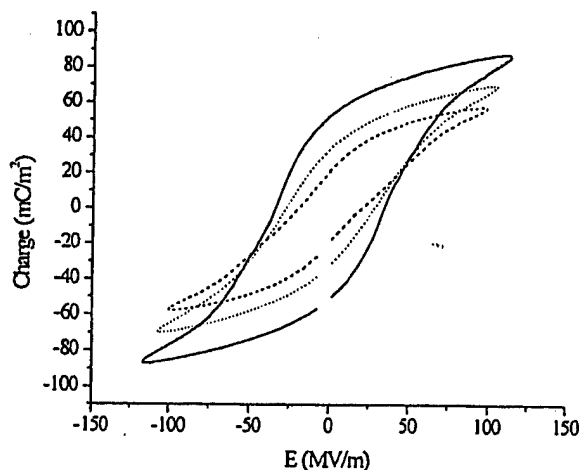
Figure 4. Comparison of electric displacement vs. electric field at 22°C of unstretched VDF/HFP/TrFE terpolymers with various HFP contents, 0.8, 2.1, 2.3 mol % HFP, designated as ——, ..., ----, respectively.

It is interesting to note that polarization of terpolymer is also dependent on the relative amounts of α- and β-phase. [12] For some terpolymers with relatively low TrFE contents, the

remnant polarization of the stretched polymer film increases dramatically compared to that of unstretched film. Mechanical drawing clearly increases the relative amount of β-phase by increasing the amount of oriented dipoles resulting in an increase in the remnant polarization.

Figure 5 compares the coercive field and the polarization of VDF/TrFE/HFP (55.17/42.35/2.46) terpolymer 121 under various temperatures. As the temperature increased from 21°C to 42°C, the coercive filed reduce since the higher temperature facilitate the change of the direction of the dipoles. As the temperature increased to 50°C, the coercive field slightly increased arising from space charge trapped in samples. As the temperature increases further beyond the Curie transition temperature, the hysteresis loop obtained was very large with "rounding" at the ends indicative of conduction losses. The ability of switching the direction of the dipoles is reduced as the temperature goes beyond the phase transition temperature.
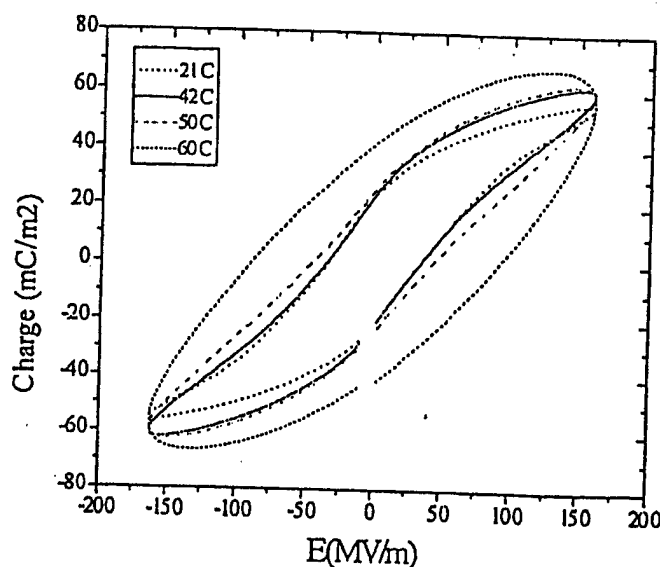
Figure 5. Comparison of polarization hysteresis loop of stretched VDF/TrFE/HFP (55.17/42.35/2.46) terpolymer 121 under various temperatures.

Piezoelectricity

One of the most desirable properties of the eletroactive polymer is to possess large mechanical deformation at low external field. Figure 6 shows the deformation of the VDF/TrFE/HFP (55.17/42.35/2.46) terpolymer under electric field at various temperatures. The deformation of the terpolymer has a highest value at 50°C, near the Curie temperature (40°C). As the temperature increases further, the deformation drops at low field. After the temperature increases beyond the Curie transition temperature, the polymer chains lose the piezoelectric properties. Consequently, the deformation drops.

It is very interesting to quantify the effect of HFP content to the strain. Figure 7 compares a deformation under electric field of stretched VDF/TrFE/HFP (55.17/42.35/2.46) terpolymer with that of the irradiated VDF/TrFE copolymer at Curie temperature. The deformation of the terpolymer indeed is higher than that of the irradiated sample at low field. Never before has the strain of almost 2.5% been achieved at 50 MV/m. It should be noted that

the high strain response of the terpolymer was obtained at 50°C because the Curie temperature of the terpolymer is still above room temperature.
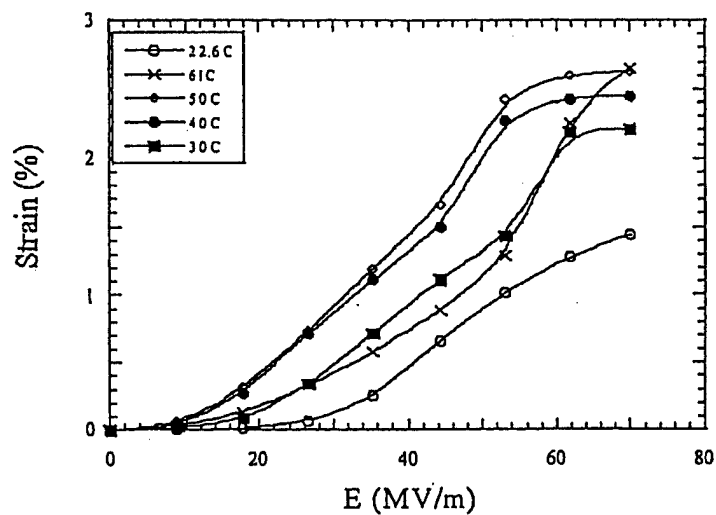

Figure 6. The dependence of the strain response of the stretched VDF/TrFE/HFP (55.17/42.35/2.46) terpolymer on the temperature.
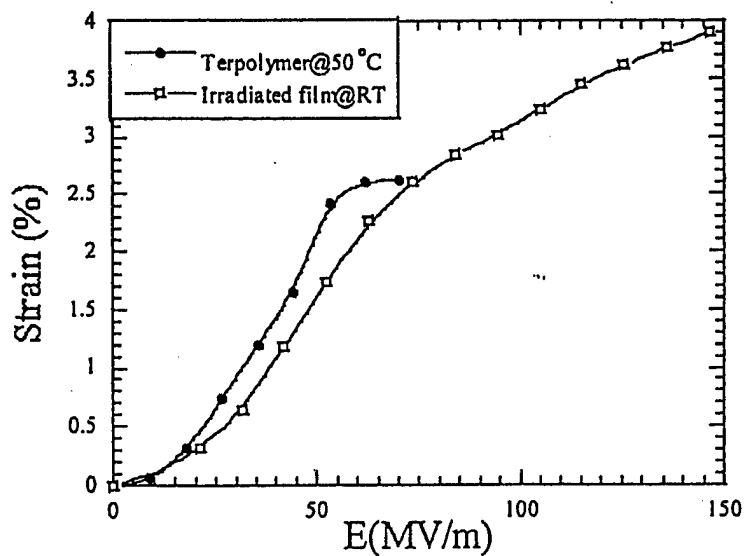

Figure 7. Comparison of the strains of stretched VDF/TrFE/HFP terpolymers measured at the Curie temperature with that of irradiated VDF/TrFE copolymer at room temperature* (*data are reproduced from ref. 6).

CONCLUSIONS

All the experimental results of VDF/TrFE/HFP terpolymers consistently show that a small amount of HFP units have a significant effect to the polymer morphology and electric properties. Few bulky groups effectively reduce the size of polar crystalline domains, but not the overall crystallinity and conformation of the polymer. The flexible dipoles in the smaller polar domains reflect in the piezoelectric property. A highest value of strain (about 2.5%) at very low field (50 MV/m) was observed in the terpolymer, which is significantly higher than that of the irradiated copolymer sample under the same conditions.

ACKNOWLEDGMENTS

REFERENCES

1. K. Koga, and H. Ohigashi, J. Appl. Phys., **59**, 2142 (1986).
2. K. Tashiro, S. Nishimura, and M. Kobayashi, Macromolecules, **21**, 2463 (1988), and **23**, 2802 (1990).
3. B. Daudin, and M. Dubus, J. Appl. Phys., **62**, 994 (1987).
4. T. Yuki, S. Ito, T. Koda, and S. Ikeda, Jpn. J. Appl. Phys., **37**, 5372 (1998).
5. S. Ikeda, H. Suzaki, and S. Nakami, Jpn. J. Appl. Phys., **31**, 1112 (1992).
6. Q. M. Zhang, V. Bharti, and X. Zhao, Science, **280**, 2102 (1998).
7. H. Freimuth, C. Sinn, and M. Dettenmaier, Polymer, **37**, 832 (1996).
8. Y. Tajitsu, A. Hirooka, A. Yamagish, and M. Date, Jpn. J. Appl. Phys., **36**, 6114 (1997).
9. T. C. Chung, and W. Janvikul, J. Organomet. Chem., **581**, 176 (1999).
10. J. E. Leffler, and H. H. Gibson, jr., J. Amer. Chem. Soc., **90**, 4117 (1968).
11. P. K. Isbester, J. L. Brandt, T. A. Kestner, and E. J. Munson, Macromolecules, **31**, 8192 (1998).
12. B. A. Newman, C. H. Yoon, K. D. Pae, And J. I. Scheinbeim, J. Appl. Phys, **50**, 6095 (1979).

FERROELECTRIC POLYMERS WITH LARGE ELECTROSTRICTION; BASED ON SEMICRYSTALLINE VDF/TrFE/CTFE TERPOLYMERS

T. C. CHUNG* and A. PETCHSUK
Department of Materials Science and Engineering, The Pennsylvania State University, University Park, PA 16802

Abstract This paper discusses a new ferroelectric polymer with large electrostrictive response (~4%) at ambient temperature, which is based on a processable semicrystalline terpolymer comprising vinylidene difluoride (VDF), trifluoroethylene (TrFE), and chlorotrifluoroethylene (CTFE). This VDF/TrFE/CTFE terpolymer was prepared by a combination of bulk polymerization process and a borane/oxygen initiator at ambient temperature. The incorporated bulky CTFE units in the terpolymer seem to reduce the crystalline domain size and move the ferroelectric-paraelectric (F-P) phase transition to near ambient temperature with a very small energy barrier. Some terpolymers exhibited common ferroelectric relaxor behaviors with a broad dielectric peak that shifted toward higher temperatures as the frequency increased, and a slim polarization hysteresis loop at near the dielectric peak (around ambient temperature) that gradually evolved into a normal ferroelectric polarization hysteresis loop with reduced temperature.

INTRODUCTION

Ferroelectric polymers that generate mechanical actuation have attracted a great deal of attention due to their many desirable properties, such as flexibility, light weight, high mechanical strength, ease of processability in large area films, and ability to be molded into a desirable configuration.[1-3] Despite these advantages, most ferroelectric polymers have the disadvantages of low electric field sensitivity in terms of their dielectric constant, piezoelectric coefficient, electromechanical coupling coefficient, and field induced strain, which limit their applications. In the past decade, most research activities in ferroelectric polymers have been focused on ferroelectric fluorocarbon polymers,[4-6] especially semicrystalline VDF/TrFE copolymers.[7-9] Many projects have been devoted to the general goal of reducing the F-P phase transition temperature[10-13] and generating large electric-induced mechanical response at ambient temperature. Although VDF/TrFE copolymer exhibits a high piezoelectric constant ($d_{31} = 15\text{-}30$ pC/N),[14] the response of the dipoles to the electric field is very low at ambient temperature. The slow response to the electric field is also revealed in a large polarization hysteresis loop (in the frequency range of 1-10 Hz)[13], due to the high energy barrier of switching the dipole direction at ambient temperature. The direct correlation between the reduced polar domain size and lower energy barrier, shown in ferroelectric ceramic materials,[15-17] led to many attempts

to alter copolymer morphology by creating non-equilibrium states that produced some improved electric responses. The methods include mechanical deformation,[18] electron-irradiation,[19] uniaxial drawing,[20] crystallization under high pressure,[21] and crystallization under high electric field.[22]

Zhang et al.[23, 24] recently perfected the electron-irradiation process with a systematic study of the radiation conditions, such as dosage, temperature, inert atmosphere, stretching sample, etc. Some irradiated VDF/TrFE copolymers showed an exceptionally high electrostrictive response (~4%) at ambient temperature and behaved like a relaxor ferroelectric. The polarization hysteresis loop became very slim at room temperature compared with that of the sample before irradiation. However, the polarization was also significantly reduced and the sample became completely insoluble because of the severe crosslinking side reaction during the high-energy radiation. The increase in the hardness of the copolymer sample due to crosslinking was also revealed in its electric response. A very high electric field was required (150 MV/m) for the irradiated sample to get a high strain response. It appears that the radiation process not only reduces the polar crystalline domain size, it also produces many undesirable side reactions that increase the amorphous phase and diminish the processability of the sample.

In this paper, we discuss a new chemical approach of altering crystalline domains and creating relaxor ferroelectric behavior of VDF/TrFE copolymer. The chemistry involves homogeneous incorporation of a small amount of bulky ter-monomer units, such as chlorotrifluoroethylene (CTFE), into a VDF/TrFE copolymer chain. The resulting VDF/TrFE/CTFE terpolymers are completely solution and melt processable, and exhibit high electrostrictive response. Prior to our research, there were some reports[25, 26] discussing the dielectric constant of several VDF/TrFE/CTFE terpolymers that were prepared by conventional free radical emulsion polymerization at elevated temperatures.

EXPERIMENTAL

The VDF/TrFE/CTFE terpolymers were prepared by a combination of the bulk polymerization process and an oxygen-activated free radical initiator, based on the oxidation adducts of the organoborane molecule,[26,27] at ambient temperature. This chemistry produces terpolymers that have relatively uniform molecular structure, high molecular weight, and few impurities (boric acid and butanol) that can be easily removed by methanol. In a typical example, 0.1 g of tributylboron initiator was added into a 75-ml autoclave under argon atmosphere. The reactor was then cooled from outside by liquid nitrogen and 16.7 g of VDF, 7.6 g of TrFE, and 1.7 g of CTFE were distilled into the reactor. After introducing a known amount of oxygen (0.5: 1 of boron: oxygen), the reactor was warmed to ambient temperature. The bulk polymerization took place at this temperature for 5 hours before vacuum-distilling the unreacted monomers. The resulting terpolymer (6.5 g) was recovered, washed with methanol, and dried. The combination of

chlorine analysis and ^{1}H NMR spectra indicates that the mole ratio of VDF/TrFE/CTFE = 72.2/17.8/10.0 (sample 1 in Table 1).

RESULTS AND DISCUSSION

Table 1 summarizes several VDF/TrFE/CTFE terpolymers prepared by the same method. All terpolymers are high molecular weight (>20,000 g/mole) polymers with a good solubility in common organic solvents and melt processable at >150° C.

TABLE 1. A summary of VDF/TrFE/CTFE terpolymers prepared by borane/oxygen initiator and bulk process

Sample No.	Terpolymer mole ratio			Melting temperature		Phase transition temperature		[η] (MEK)
	VDF	TrFE	CTFE	Tm (°C)	ΔHm (J/g)	Tc (°C)	ΔHc (J/g)	(35°C)
1	72.2	17.8	10.0	107.8	17.8	25.0	0.4	0.38
2	66.0	22.5	11.5	117.2	21.6	25.2	2.5	0.42
3	66.1	21.4	12.5	115.6	20.5	25.8	1.8	0.42
4	63.1	25.4	11.5	113.7	18.5	none	none	0.49
5	61.4	25.3	13.3	111.3	17.8	15.6	1.5	0.69
6	58.0	33.1	8.9	130.0	21.3	31.6	2.5	0.63
7	60.0	36.0	4.0	140.9	25.7	43.8	6.5	0.58
8	55.6	36.1	8.3	124.6	21.2	none	none	0.54

MEK: methylethylketone.   none: no observable

Despite having relatively high concentrations of CTFE units, all the terpolymers are still semicrystalline thermoplastics with melting temperatures >100° C, and a crystallinity of ΔH>17 J/g. Figure 1 compares the DSC curves of three VDF/TrFE/CTFE terpolymers (samples 2, 5, and 8 in Table 1) and a VDF/TrFE (55/45) copolymer that has the lowest F-P transition temperature. The relatively well-defined melting and crystalline phase transition temperatures imply a relatively uniform molecular structure and polymer morphology. These results are consistent with the molecular structure analysis in the uniform terpolymer specimen sampled during the polymerization process, which will be discussed in a future publication. In general, the incorporation of CTFE ter-monomers significantly reduced the melting and phase transition temperatures, but still maintained a high degree of crystallinity in the terpolymer. It is interesting to note that the effect of incorporated CTFE units resembles that seen from crosslinking in irradiated VDF/TrFE samples. The CTFE units may not affect the crystal unit cell of VDF/TrFE segments, and instead serve as a defect (by introducing a gauche bond) to prevent the extension of crystallization, which presumably may result in the reduction of the lamella thickness of the crystal. The detailed studies of the molecular structure and the crystal polar domain size are under investigation.
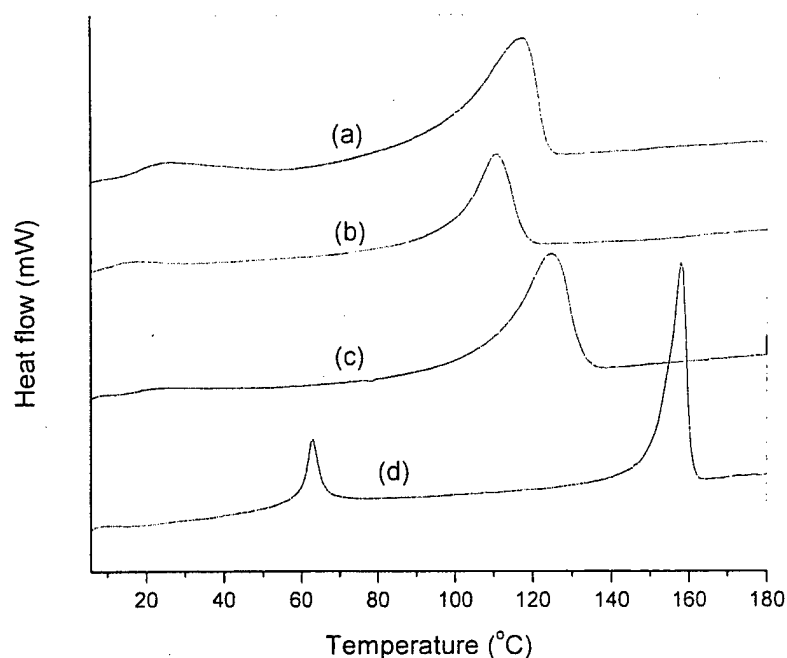
FIGURE 1. DSC comparison of three VDF/TrFE/CTFE terpolymers with (a) 66/22.5/11.5 (sample 2), (b) 61.4/25.3/13.3 (sample 5), (c) 55.6.1/36.1/8.3 (sample 8) mole ratios, and (d) a VDF/TrFE (55/45) copolymer.

As shown in Figure 1, phase transition temperatures of VDF/TrFE/CTFE terpolymers shifted to near ambient temperature (25.2 and 15.6° C) for (a) and (b), and become broader; whereas the transition temperature in (c) almost disappears, which indicates a very small energy barrier in the phase transition and implies a smaller crystalline domain. The results are consistent with the electric responses of the terpolymer under an electric field.

For electrical measurements, polymer films (~30 μm thickness) were prepared either by solution casting on a glass slide from N, N-dimethylformamide solution containing 8-10 wt% polymer or melt-pressing polymer powder at 200° C. The polymer films were annealed at 110° C under vacuum for 5 hours. Gold (<1 μm thickness) was sputtered on both surfaces of the polymer film. The dielectric constant was measured by a HP multifrequency LCR meter equipped with a temperature chamber. Figure 2 shows the dielectric constant of 55.6/36.1/8.3 in the VDF/TrFE/CTFE terpolymer (sample 8) during the heating-cooling cycles.
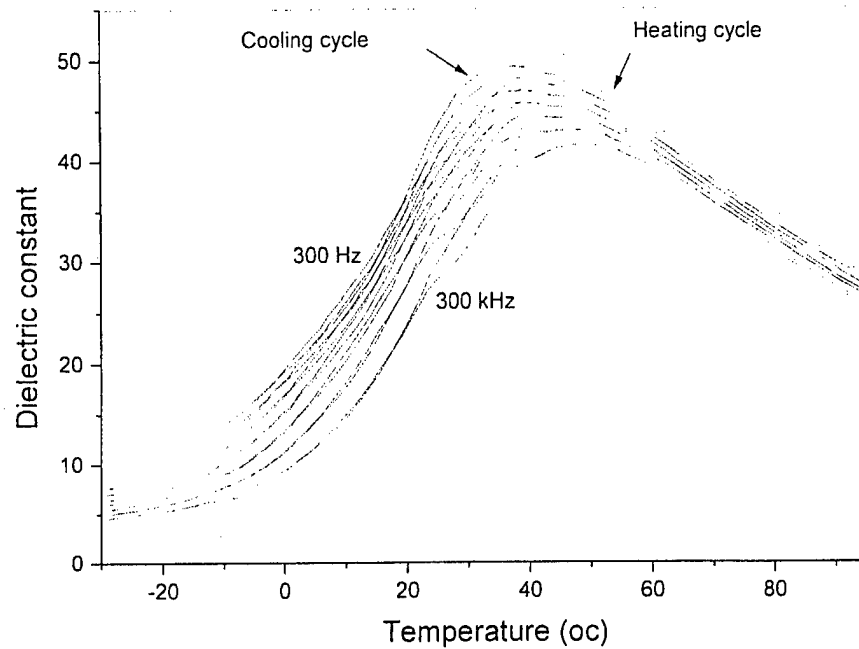
FIGURE 2. Temperature dependence of dielectric constant in a 55.6/36.1/8.3 VDF/TrFE/CTFE terpolymer (sample 8) during heating-cooling cycles. The frequencies from top to bottom of the dielectric curve range from 300 Hz to 300 kHz.

TABLE 2. A summary of electric properties for the VDF/TrFE/CTFE terpolymers shown in Table 1.

Samples No.	Pmax (mC/m^2)	Ec (MV/m)	Dielectric constant[*]	Dielectric loss
	100 MV/m, 10 Hz, 22° C		1 KHz, 22° C	
1	82	19.6	27.0	0.04
2	78	24.1	22.4	0.03
3	-	-	40.9	0.04
4	76	19.8	53.5	0.06
5	75	33.7	53.1	0.06
6	63	16.4	33.0	0.05
7	87	21.8	26.4	0.04
8	36	7.6	42.4	0.07

* based on heating cycle

In general, the dielectric constant hysteresis during the heating-cooling cycles is very small, and the dielectric peak appears near the ambient temperature-well below the

dielectric peak observed in 55/45 VDF/TrFE copolymer (>60° C) with a big hysteresis loop. Diffuse dielectric peaks and peaks shifting toward higher temperatures as the frequency increases are common features of relaxor ferroelectrics. Aging, as evidenced by the development of a local maxima at room temperature in the heating curve is also noted in some relaxor ferroelectrics.[28].

Table 2 summarizes the dielectric constants of the terpolymers, which were estimated from the heating cycles. Most of the terpolymers show high dielectric constants at ambient temperature. Samples 4 and 5 exhibit dielectric constants as high as 53.5 and 53.1 (1 kHz), respectively, at 22° C. In sharp contrast, the prior research[29] reported that high dielectric constants (>25) only existed in the VDF/TrFE/CTFE terpolymers with a narrow range (18 to 22%) of TrFE content. In addition, the mechanical stretching of the polymer film, usually very important for increasing the dielectric constant in VDF/TrFE copolymers, is not necessary in these terpolymers. The effective orientation of dipoles under an electric field may be attributed to the low phase transition energy, which occurs at near ambient temperature.

The polarization hysteresis loop was measured by a Sawyer-Tower circuit with a frequency range between 1 and 10 Hz. Figure 3 compares the polarization hysteresis loops of two terpolymers (samples 2 and 8) and a VDF/TrFE (55/45) copolymer.
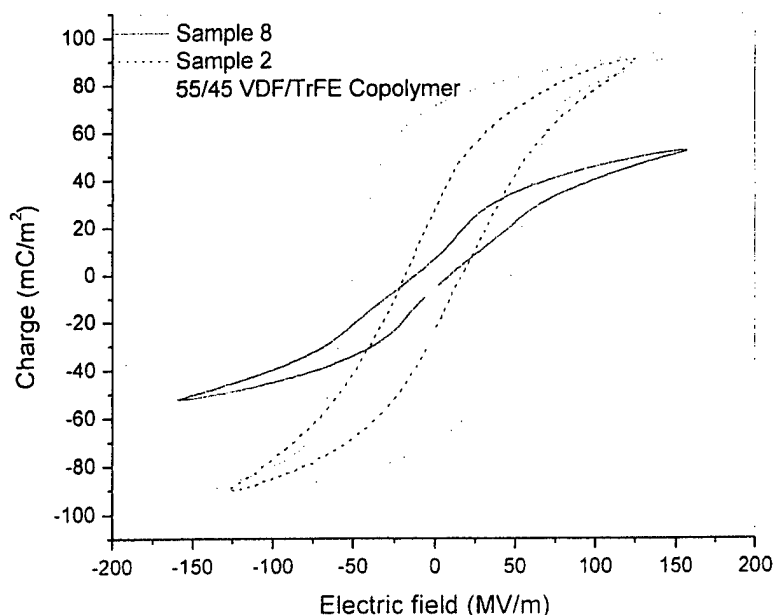

FIGURE 3. The comparison of polarization hysteresis loops between two VDF/TrFE/CTFE terpolymers (samples 2 and 8) with 66/22.5/11.5 and 55.6/36.1/8.3 mole ratios, respectively, and a VDF/TrFE (55/45) copolymer.

FERROELECTRIC POLYMERS WITH LARGE ELECTROSTRICTION

Both terpolymers show significantly smaller hysteresis than the copolymer (55/45) that has the narrowest polarization hysteresis loop observed in the copolymer samples. Sample 2 (with VDF/TrFE/CTFE = 66/22.5/11.5 mole ratio) still maintains a high polarization level (Pmax = 78 mC/m^2 at E=100MV/m) and reduces both coercive field (17.3 MV/m at P=0) and remanent polarization (25.2 mC/m^2 at E=0). Sample 8 (with VDF/TrFE/CTFE = 55.6/36.1/8.3 mole ratio) exhibits a very slim loop with very small coercive field and remanent polarization, as well as an overall reduced polarization level. These results indicate that the VDF/TrFE crystalline defects introduced by the incorporated CTFE termonomer units cannot be recovered by the application of a high electric field. It is interesting to note that the polarization hysteresis loop of sample 8 gradually appeared with reduced temperatures (<0° C), another feature common to all relaxor ferroelectrics.

The electric field-induced strain was measured at ambient temperature in the field range of 0-150 MV/m using a bimorph-based strain sensor, which consists of a piezoelectric bimorph-based cantilever dilatometer with a lock-in amplifier (Stanford Research System SR830 DSP) and a high voltage source (KEPCO-BOP 1000M). Figure 4 shows two typical samples 1 and 2, having VDF/TrFE/CTFE mole ratios of 72.2/17.8/10 and 66/22.2/11.5, respectively.
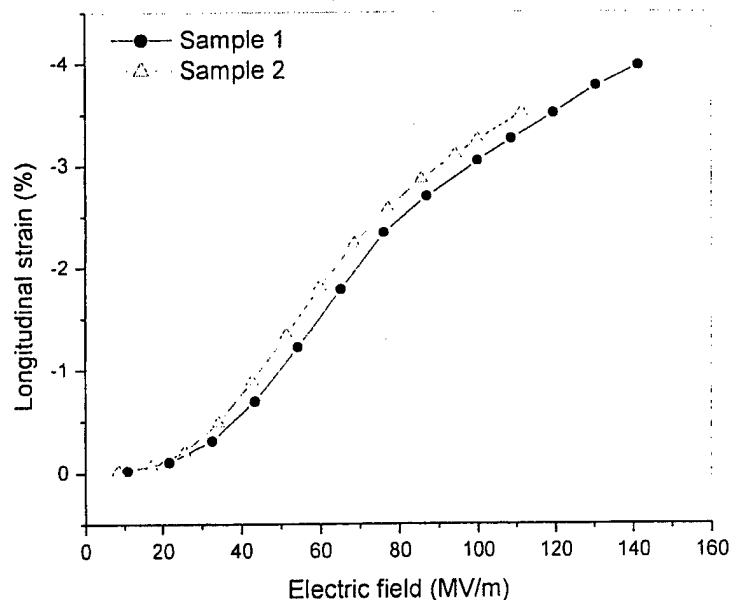

FIGURE 4.   Electric field induced strain under electric field measured at electric field from 0-150 MV/m of two VDF/TrFE/CTFE terpolymers (samples 1 and 2).

At ambient temperature, the longitudinal strain reached about 4% and 3% for samples 1 and 2 under an electric field of 150 and 100 MV/m, respectively. As shown in Figure 5, a nearly straight line of S vs. P^2 for sample 2 indicates the electrostrictive

response in the VDF/TrFE/CTFE terpolymer. Based on the electrostrictive relationship $S=QP^2$, this equation yields the electrostrictive coefficient (Q) of about -5.57 m^4/C^2.
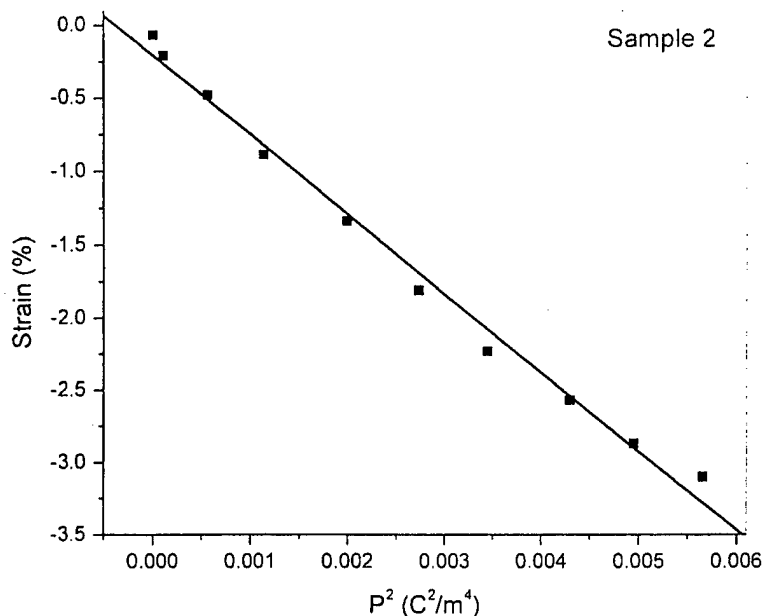

FIGURE 5.   Electrostrictive relationship between strain and polarization square measured at electric field from 0-100 MV/m of the VDF/TrFE/CTFE terpolymers (sample 2).

SUMMARY

The experimental results demonstrated that VDF/TrFE/CTFE terpolymers exhibit several common features of a typical relaxor ferroelectric behavior, such as diffuse phase transition, slim polarization hysteresis loop, high dielectric constant at ambient temperature, and dielectric relaxation (large frequency dependence). The homogeneous incorporation of a controlled amount of bulky CTFE units into the VDF/TrFE copolymer reduces the thickness of ferroelectric crystalline domains without destroying the overall crystallinity, which results in a low F-P phase transition temperature with a low energy barrier. Consequently, the large expansion and contraction of these smaller crystalline domains under an external electric field, coupled with the large difference in the lattice strain between the polar and nonpolar crystal phases, generates a large electrostrictive strain response.

ACKNOWLEDGMENT

FERROELECTRIC POLYMERS WITH LARGE ELECTROSTRICTION

REFERENCES

1. H. S. Nalwa, Recent developments in ferroelectric polymers, <u>J. Macromol. Sci. Review. Macromol.Chem.Phys.</u>, C31 (4), 341 (1991).
2. T. T. Wang, J. M. Herbert, and A. M. Glass, <u>The applications of ferroelectric polymers</u> (Glasgow : New York : Blackie; Chapman and Hall, 1988).
3. M. Zhenyi, J. I. Scheinbeim, J. W. Lee, and B. A. Newman, <u>J. Polym. Sci.: Polym. Phys., 32</u>, 2721 (1994).
4. H. Kawai, <u>Jpn. J. Appl. Phys., 8</u>, 875 (1969).
5. J. B. Lando, H. G. Olf, and A. Peterlin, <u>J. Polym. Sci., Part A-1, 4</u>, 941 (1966).
6. A. J. Lovinger, <u>Development in crystalline polymers</u> (Applied Science, London, 1982), p. 52.
7. J. B. Lando and W. W. Doll, <u>J. Macromol. Sci. Phys., B2</u>, 205 (1968).
8. Y. Higashihata, J. L. Sako, and T. Yagi, <u>Ferroelectrics, 32</u>, 85 (1981).
9. T. Yagi and T. Tatemoto, <u>Polym. J., 11</u>, 429 (1979).
10. B. Daudin and M. Dubus, <u>J. Appl. Phys., 62</u>, 994 (1987).
11. A. Odajima, Y. Takasa, T. Ishibashi, K. Yuasa, <u>Jpn. J. Appl. Phys., 24</u>, 881 (1985).
12. F. Macchi, B. Daudin, and J. F. Legrand, <u>Nucl. Instr. And Meth., B46</u>, 324 (1990).
13. Y. Higashihata, J. Sako, and T. Yagi, <u>Ferroelectrics, 32</u>, 85 (1981).
14. K. Koga and H. Ohigashi, <u>J. Appl. Phys., 59</u>, 2142 (1986).
15. K. Uchino, L. E. Cross, R. E. Newnham, and S. Nomura, <u>J. Phase Transition, 1</u>, 333 (1980).
16. G. A. Smolensky, V. A. Isupov, A. I. Agranovskaya, and S. N. Popov, <u>Sov. Phys.-Solid State, 2</u>, 2584 (1961).
17. M. L. Mulvihill, L. E. Cross, and K. Uchino, <u>Proc. 8th European Mtg. Ferroelectricity</u>, Nijmegen (1995).
18. K. Tashiro, S. Nishimura, and M. Kobayashi, <u>Macromolecules, 21</u>, 2463 (1988), and <u>23</u>, 2802 (1990).
19. A. J. Lovinger, <u>Macromolecules, 18</u>, 910 (1985).
20. T. Furukawa and N. Seo, <u>Jpn. J. Appl. Phys., 29</u>, 675 (1990).
21. T. Yuki, S. Ito, T. Koda, and S. Ikeda, <u>Jpn. J. Appl. Phys., 37</u>, 5372 (1998).
22. S. Ikeda, H. Suzaki, and S. Nakami, <u>Jpn. J. Appl. Phys., 31</u>, 1112 (1992).
23. Q. M. Zhang, V. Bharti, and X. Zhao, <u>Science, 280</u>, 2102 (1998).
24. V. Bharti, H. S. Xu, G. Shanthi, and Q. M. Zhang, <u>J. Appl. Phys., 87</u>, 452 (2000).
25. T. Sakagami, N. Arakawa, Y. Teramoto, and K. Nakamura, <u>U.S. Patent</u> 4,554,335.
26. T. C. Chung, H. L. Lu, and W. Janvikul, <u>J. Am. Chem. Soc., II 8</u>, 705 (1996).
27. T. C. Chung and W. Janvikul, <u>J. Organomet. Chem., 581</u>, 176 (1999).
28. W. A. Schulze and K. Ogino, <u>Ferroelectrics, 87</u>, 361 (1988).
29. H. Inukai, N. Kawai, T. Kitaliara, S. Kai, and M. Kubo, <u>U.S. Patent</u> 5,087,679.

Ferroelectric VDF/TrFE/CTFE terpolymers;
Synthesis and Electric Properties

T. C. Chung* and A. Petchsuk
Department of Materials Science and Engineering
The Pennsylvania State University
University Park, PA 16802

ABSTRACT

This paper discusses a new ferroelectric polymer with high dielectric constant (>50 at 1K-1M Hz) and large electrostrictive response (~5%) at ambient temperature, which is based on a processable semicrystalline terpolymer comprising vinylidene difluoride (VDF), trifluoroethylene (TrFE), and chlorotrifluoroethylene (CTFE). This VDF/TrFE/CTFE terpolymer was prepared by a combination of a borane/oxygen initiator and bulk polymerization process at ambient temperature. The control of monomer addition affords the terpolymers with high molecular weight and relatively narrow molecular weight and composition distributions. The incorporated bulky CTFE units homogeneously distributed along the polymer chain seem to reduce the thickness of ferroelectric crystalline domains without destroying the overall crystallinity. This nano-size semicrystalline morphology results in the reduction of ferroelectric-paraelectric (F-P) phase transition to near ambient temperature with a very small energy barrier. Some terpolymers exhibited common ferroelectric relaxor behaviors with a broad dielectric peak that shifted toward higher temperatures as the frequency increased, and a slim polarization hysteresis loop at near the dielectric peak (around ambient temperature) that gradually evolved into a normal ferroelectric polarization hysteresis loop with reduced temperature.

Keywords: ferroelectric polymer, electroactive polymer, poly(vinylidene difluoride), VDF/TrFE/CtFE terpolymer, dielectric constant, actuator, sensor, electrostriction.

1. INTRODUCTIONI

Ferroelectric polymers that generate mechanical actuation have attracted a great deal of attention due to their many desirable properties, such as flexibility, light weight, high mechanical strength, ease of processability in large area films, and ability to be molded into a desirable configuration.[1-3] Despite these advantages, most ferroelectric polymers have the disadvantages of low electric field sensitivity in terms of their dielectric constant, piezoelectric coefficient, electromechanical coupling coefficient, and field induced strain, which limit their applications. In the past decade, most research activities in ferroelectric polymers have been focused on ferroelectric fluorocarbon polymers,[4-6] especially semicrystalline VDF/TrFE copolymers.[7-9] Many projects have been devoted to the general goal of reducing the F-P phase transition temperature[10-13] and generating large electric-induced mechanical response at ambient temperature. Although VDF/TrFE copolymer exhibits a high piezoelectric constant ($d_{31} = 15$-30 pC/N),[14] the response of the dipoles to the electric field is very low at ambient temperature. The slow response to the electric field is also revealed in a large polarization hysteresis loop (in the frequency range of 1-10 Hz.)[13], due to the high energy barrier of switching the dipole direction at ambient temperature. The direct correlation between the reduced polar domain size and lower energy barrier, shown in ferroelectric ceramic materials,[15-17] led to many attempts to alter copolymer morphology by creating non-equilibrium states that produced some improved electric responses. The methods include mechanical deformation,[18] electron-irradiation,[19] uniaxial drawing,[20] crystallization under high pressure,[21] and crystallization under high electric field.[22]

Zhang et al.[23, 24] recently perfected the electron-irradiation process with a systematic study of the radiation conditions, such as dosage, temperature, inert atmosphere, stretching sample, etc. Some irradiated VDF/TrFE copolymers showed an exceptionally high electrostrictive response (~4%) at ambient temperature and behaved like a relaxor ferroelectric. The polarization hysteresis loop became very slim at room temperature compared with that of the sample before irradiation. However, the polarization was also significantly reduced and the sample became completely insoluble

because of the severe crosslinking side reaction during the high-energy radiation. The increase in the hardness of the copolymer sample due to crosslinking was also revealed in its electric response. A very high electric field was required (150 MV/m) for the irradiated sample to get a high strain response. It appears that the radiation process not only reduces the polar crystalline domain size, it also produces many undesirable side reactions that increase the amorphous phase and diminish the processability of the sample.

In this paper, we will discuss a new chemical approach of altering crystalline domains and creating relaxor ferroelectric behavior of VDF/TrFE copolymer. The chemistry involves homogeneous incorporation of a small amount of bulky ter-monomer units, such as chlorotrifluoroethylene (CTFE), into a VDF/TrFE copolymer chain. The resulting VDF/TrFE/CTFE terpolymers are completely solution and melt processable, and exhibit high electrostrictive response. Prior to our research, there were some reports[25, 26] discussing the dielectric constant of several VDF/TrFE/CTFE terpolymers that were prepared by conventional free radical emulsion polymerization at elevated temperatures.

2. EXPERIMENTAL

The VDF/TrFE/CTFE terpolymers were prepared by a combination of the bulk polymerization process and an oxygen-activated free radical initiator, based on the oxidation adducts of the organoborane molecule,[27,28] at ambient temperature. This chemistry produces terpolymers that have relatively uniform molecular structure, high molecular weight, and few impurities (boric acid and butanol) that can be easily removed by methanol. In a typical example, 0.1 g of tributylboron initiator was added into a 75-ml autoclave under argon atmosphere. The reactor was then cooled from outside by liquid nitrogen and 16.7 g of VDF, 7.6 g of TrFE, and 1.7 g of CTFE were distilled into the reactor. After introducing a known amount of oxygen (0.5: 1 of boron: oxygen), the reactor was warmed to ambient temperature. The bulk polymerization took place at this temperature for 5 hours before vacuum-distilling the unreacted monomers. The resulting terpolymer (6.5 g) was recovered, washed with methanol, and dried. The combination of chlorine analysis and ^{1}H NMR spectra indicates that the mole ratio of VDF/TrFE/CTFE = 72.2/17.8/10.0 (sample 1 in Table 1).

3. RESULTS AND DISCUSSION

Table 1 summarizes several VDF/TrFE/CTFE terpolymers prepared by the same method. All terpolymers are high molecular weight (>20,000 g/mole) polymers with a good solubility in common organic solvents and melt processable at >150° C.

Table1. A summary of VDF/TrFE/CTFE terpolymers prepared by borane/oxygen initiator and bulk process

Sample No.	Terpolymer mole ratio			Melting temperature		Phase transition temperature		[η] (MEK) (35°C)
	VDF	TrFE	CTFE	Tm (°C)	ΔHm (J/g)	Tc (°C)	ΔHc (J/g)	
1	72.2	17.8	10.0	107.8	17.8	25.0	0.4	0.38
2	66.0	22.5	11.5	117.2	21.6	25.2	2.5	0.42
3	66.1	21.4	12.5	115.6	20.5	25.8	1.8	0.42
4	63.1	25.4	11.5	113.7	18.5	none	none	0.49
5	61.4	25.3	13.3	111.3	17.8	15.6	1.5	0.69
6	58.0	33.1	8.9	130.0	21.3	31.6	2.5	0.63
7	60.0	36.0	4.0	140.9	25.7	43.8	6.5	0.58
8	55.6	36.1	8.3	124.6	21.2	none	none	0.54
9*	60.0	35.1	6.9	126.6	20.9	33.5	1.6	0.78
10*	59.3	32.9	7.8	125.1	20.3	24.8	1.4	0.80
11*	57.3	31.2	11.5	111.1	14.8	None	None	0.75

* Control monomer feed ratio during the polymerization. MEK: methylethylkerone. none: no observable.
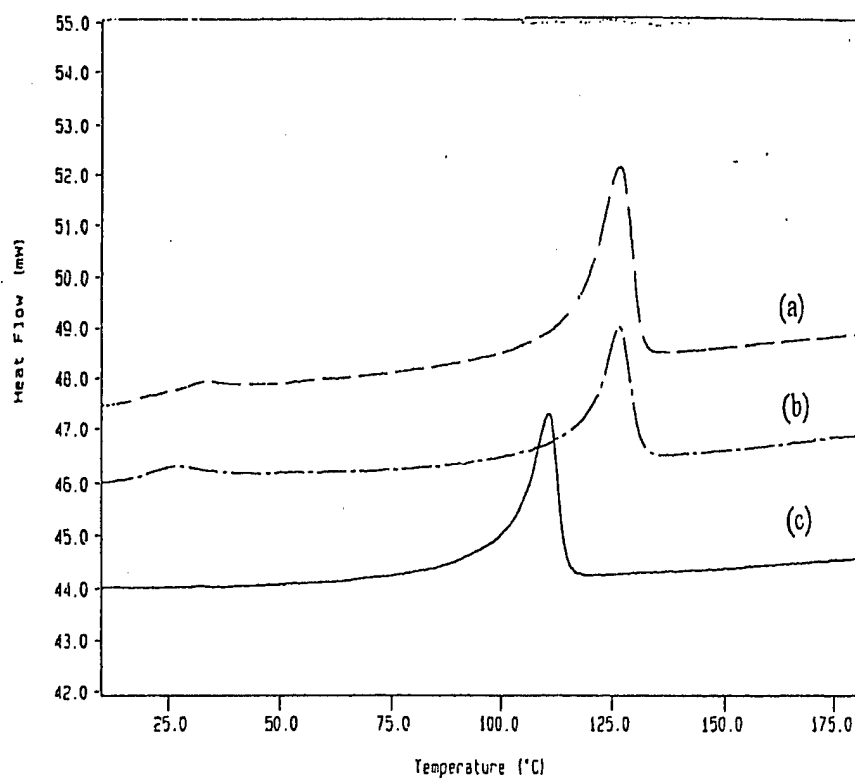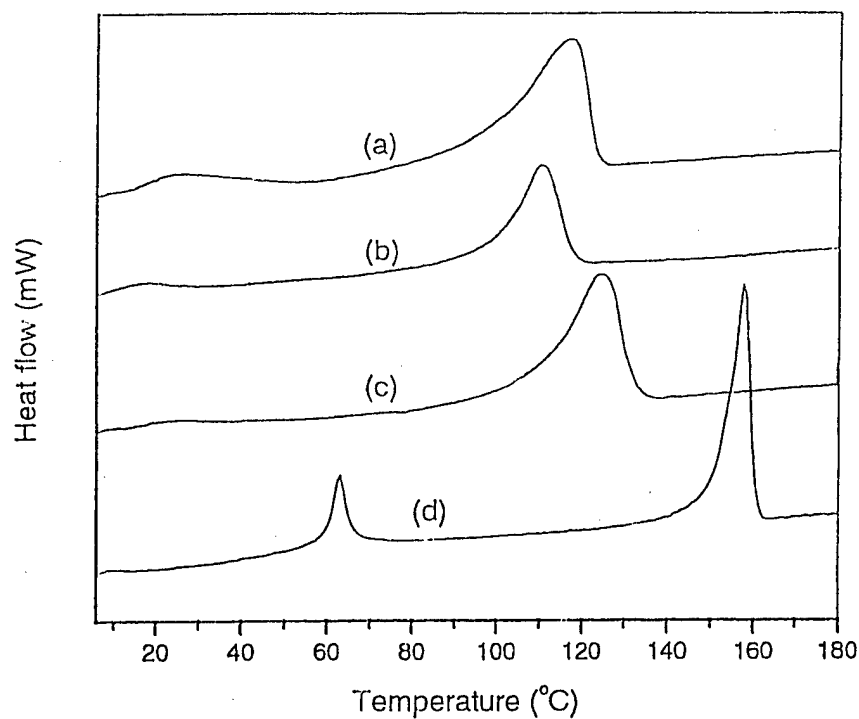
Figure 1: (top) DSC comparison of three VDF/TrFE/CTFE terpolymers with (a) 66/22.5/11.5 (sample 2), (b) 61.4/25.3/13.3 (sample 5), (c) 55.6.1/36.1/8.3 (sample 8) mole ratios, and (d) a VDF/TrFE (55/45) copolymer. (bottom) DSC curves of (a) sample 9, (b) sample 10, and sample 11 in Table 1.

Despite having relatively high concentrations of CTFE units, all the terpolymers are still semicrystalline thermoplastics with melting temperatures >100° C, and a crystallinity of ΔH>17 J/g. Figure 1 (top) compares the DSC curves of three VDF/TrFE/CTFE terpolymers (samples 2, 5, and 8 in Table 1) and a VDF/TrFE (55/45) copolymer that has the lowest F-P transition temperature of all copolymers. Figure 1 (bottom) shows the DSC curves of samples 9, 10, and 11, prepared by maintaining constant monomer feed ratio throught the terpolymerization.The relatively well-defined melting and crystalline phase transition temperatures (especially in samples 9-11) imply a relatively uniform molecular structure and polymer morphology. In general, the incorporation of CTFE ter-monomers significantly reduced the melting and phase transition temperatures, but still maintained a high degree of crystallinity in the terpolymer. It is interesting to note that the effect of incorporated CTFE units resembles that seen from crosslinking in irradiated VDF/TrFE samples. The CTFE units may not affect the crystal unit cell of VDF/TrFE segments, and instead serve as a defect (by introducing a gauche bond) to prevent the extension of crystallization, which results in the reduction of the lamella thickness of the crystal. The detailed studies of the molecular structure and the crystal polar domain size are under investigation.

In general, the third CTFE monomer units in VDF/TrFE/CTFE terpolymers shift (and broader) the phase transition to lower temperatures, at near ambient temperature for samples 1, 2, 3, and 10, and almost disappeared for samples 4, 8, and 11. That indicates a very small energy barrier in the phase transition and implies a smaller crystalline domain. The results are consistent with the electric responses of the terpolymer under an electric field.
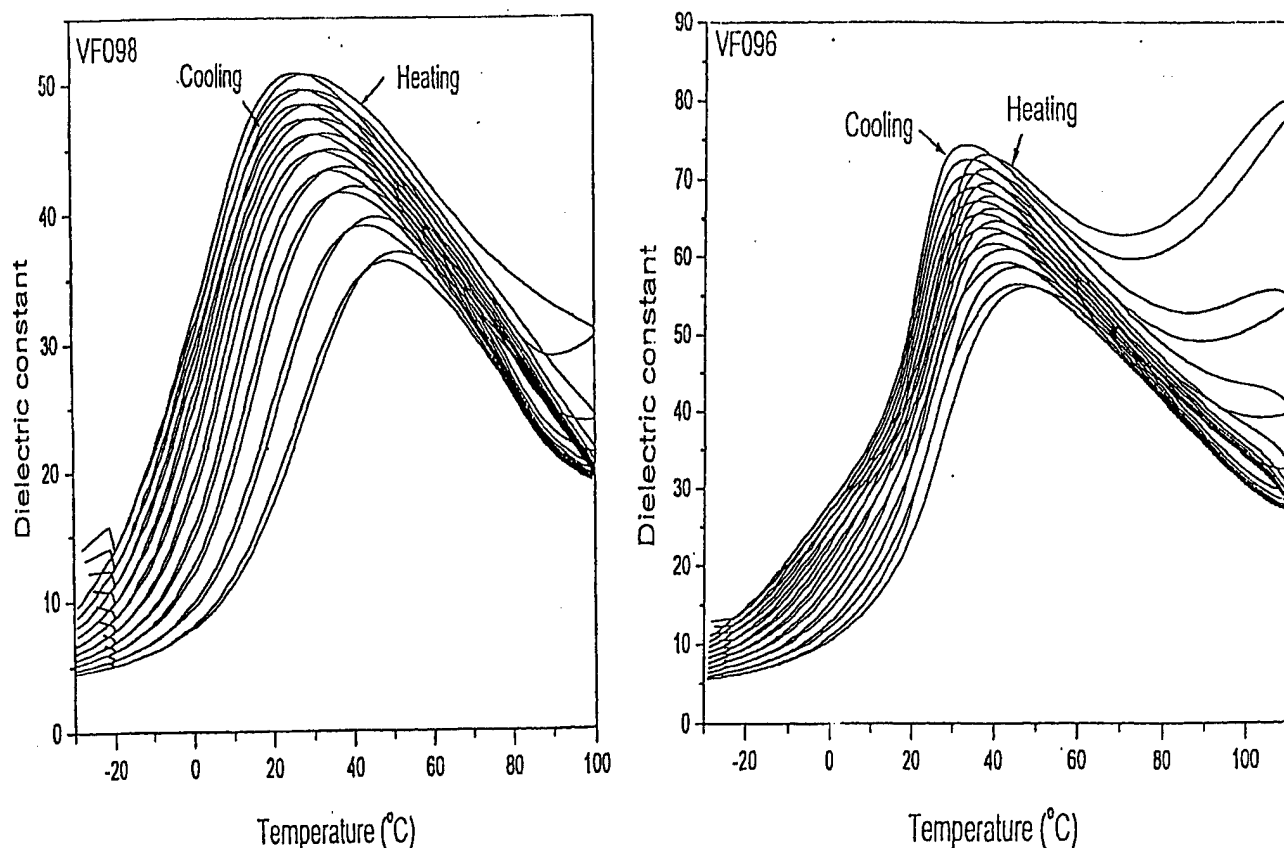

Figure 2: Temperature dependence of dielectric constant in two terpolymers, (right) sample 10 (VDF/TrFE/CTFE= 59.3/32.9/7.8) and (left) sample 11 (VDF/TrFE/CTFE= 57.3/31.2/11.5) during heating-cooling cycles. The frequencies from top to bottom of the dielectric curve range from 1 kHz to 300 kHz.

For electrical measurements, polymer films (~30 μm thickness) were prepared either by solution casting on a glass slide from N, N-dimethylformamide solution containing 8-10 wt% polymer or melt-pressing polymer powder at 200° C. The polymer films were annealed at 110° C under vacuum for 5 hours. Gold (<1 μm thickness) was sputtered on both surfaces of the polymer film. The dielectric constant was measured by a HP multifrequency LCR meter equipped with a temperature chamber. Figures 2 shows the dielectric constant of 59.3/32.9/7.8 in the VDF/TrFE/CTFE terpolymer (sample 10) and 57.3/31.2/11.5 in the VDF/TrFE/CTFE terpolymer (sample 11) during the heating-cooling cycles.

In general, the dielectric constant hysteresis during the heating-cooling cycles is very small, and the dielectric peak appears near the ambient temperature-well below the dielectric peak observed in 55/45 VDF/TrFE copolymer (>60° C) with a big hysteresis loop. Diffuse dielectric peaks and peaks shifting toward higher temperatures as the frequency increases are common features of relaxor ferroelectrics.

Table 2 summarizes the dielectric constants of the terpolymers, which were estimated from the heating cycles. Most of the terpolymers show high dielectric constants at ambient temperature. Samples 4 and 5 exhibit dielectric constants as high as 53.5 and 53.1 (1 kHz), respectively, at 22° C. In sharp contrast, the prior research[26] reported that high dielectric constants (>25) only existed in the VDF/TrFE/CTFE terpolymers with a narrow range (18 to 22%) of TrFE content. In addition, the mechanical stretching of the polymer film, usually very important for increasing the dielectric constant in VDF/TrFE copolymers, is not necessary in these terpolymers. The effective orientation of dipoles under an electric field may be attributed to the low phase transition energy, which occurs at near ambient temperature.

Table 2, A summary of electric properties for the VDF/TrFE/CTFE terpolymers shown in Table 1.

Samples No.	Pmax (mC/m^2)	Ec (MV/m)	Dielectric constant[*]	Dielectric loss
	100 MV/m, 10 Hz, 22° C		1 KHz, 22° C	
1	82	19.6	27.0	0.04
2	78	24.1	22.4	0.03
3	-	-	40.9	0.04
4	76	19.8	53.5	0.06
5	75	33.7	53.1	0.06
6	63	16.4	33.0	0.05
7	87	21.8	26.4	0.04
8	36	7.6	42.4	0.07
9	110	55.9	52.7	0.07
10	70	11.5	51.0	0.07
11	45	39.4	50.5	0.06

[*] based on heating cycle

The polarization hysteresis loop was measured by a Sawyer-Tower circuit with a frequency range between 1 and 10 Hz. Figure 3 compares the polarization hysteresis loops of two terpolymers (samples 2 and 8) and a VDF/TrFE (55/45) copolymer. Both terpolymers show significantly smaller hysteresis than the copolymer (55/45) that has the narrowest polarization hysteresis loop observed in the copolymer samples. Sample 2 (with VDF/TrFE/CTFE = 66/22.5/11.5 mole ratio) still maintains a high polarization level (Pmax = 78 mC/m^2 at E=100MV/m) and reduces both coercive field (17.3 MV/m at P=0) and remanent polarization (25.2 mC/m^2 at E=0). Sample 8 (with VDF/TrFE/CTFE = 55.6/36.1/8.3 mole ratio) exhibits a very slim loop with very small coercive field and remanent polarization, as well as an overall reduced polarization level. These results indicate that the VDF/TrFE crystalline defects introduced by the incorporated CTFE termonomer units cannot be recovered by the application of a high electric field. It is interesting to note that the polarization hysteresis loop of sample 8 gradually appeared with reduced temperatures (<0° C), another feature common to all relaxor ferroelectrics.
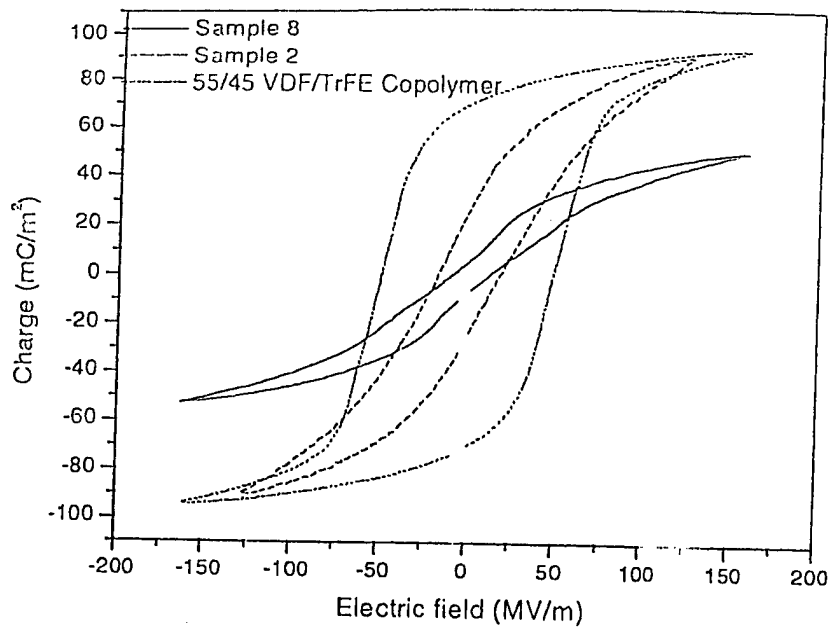
Figure 3: The comparison of polarization hysteresis loops between two VDF/TrFE/CTFE terpolymers (samples 2 and 8) with 66/22.5/11.5 and 55.6/36.1/8.3 mole ratios, respectively, and a VDF/TrFE (55/45) copolymer.
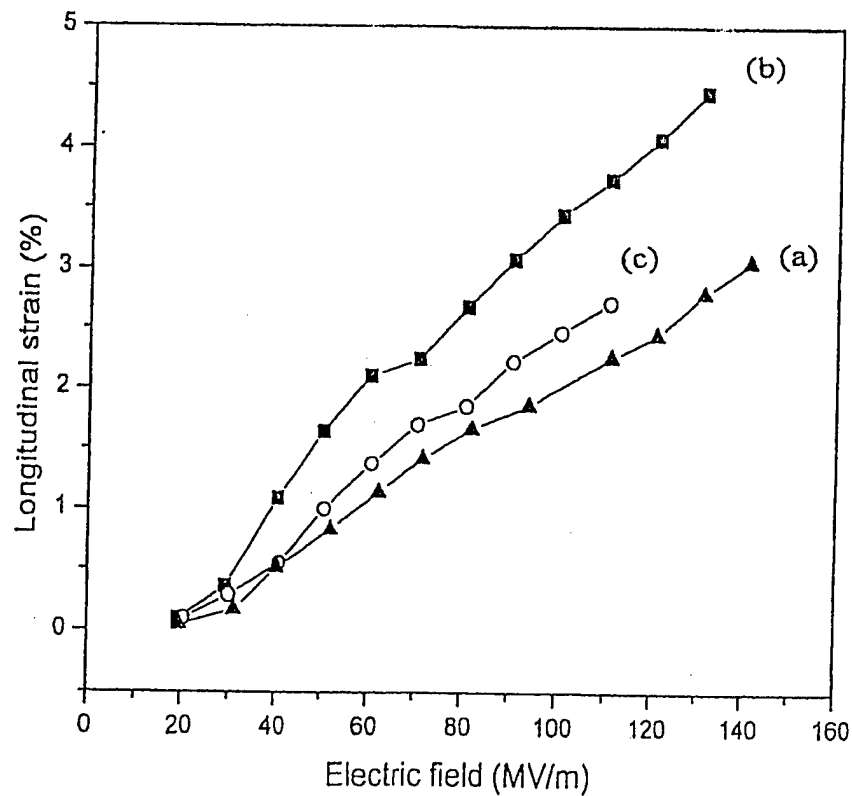

Figure 4: Electric field induced strain under electric field measured at electric field from 0-150 MV/m of three VDF/TrFE/CTFE terpolymers, samples 9 (a), 10 (b) and 11 (c).

The electric field-induced strain was measured at ambient temperature in the field range of 0-150 MV/m using a bimorph-based strain sensor, which consists of a piezoelectric bimorph-based cantilever dilatometer with a lock-in amplifier (Stanford Research System SR830 DSP) and a high voltage source (KEPCO-BOP 1000M). Figure 4 shows three samples 9, 10, and and 11, having VDF/TrFE/CTFE mole ratios of 60.0/35.1/6.9, 59.3/32.9/7.8, and 57.3/31.2/11.5, respectively.

At ambient temperature, the longitudinal strain reached about 4.5% for samples 10 under an electric field of 130 MV/m. A nearly straight line of S vs. P^2 for sample 10 indicates the electrostrictive response in the VDF/TrFE/CTFE terpolymer. Based on the electrostrictive relationship $S=QP^2$, this equation yields the electrostrictive coefficient (Q) of about $-5.57 \, m^4/C^2$.

4. SUMMARY

The experimental results demonstrated that VDF/TrFE/CTFE terpolymers exhibit several common features of a typical relaxor ferroelectric behavior, such as diffuse phase transition, slim polarization hysteresis loop, high dielectric constant at ambient temperature, and dielectric relaxation (large frequency dependence). The homogeneous incorporation of a controlled amount of bulky CTFE units into the VDF/TrFE copolymer reduces the thickness of ferroelectric crystalline domains without destroying the overall crystallinity, which results in a low F-P phase transition temperature with a low energy barrier. Consequently, the large expansion and contraction of these smaller crystalline domains under an external electric field, coupled with the large difference in the lattice strain between the polar and nonpolar crystal phases, generates a large electrostrictive strain response.

ACKNOWLEDGMENT

REFERENCES

1. H. S. Nalwa, Recent developments in ferroelectric polymers, J. Macromol. Sci. Review. Macromol.Chem.Phys., C31 (4), 341, 1991.
2. T. T. Wang, J. M. Herbert, and A. M. Glass, The applications of ferroelectric polymers, Blackie; Chapman and Hall, Glasgow and New York, 1988.
3. M. Zhenyl, J. I. Scheinbeim, J. W. Lee, and B. A. Newman, J. Polym. Sci.: Polym. Phys., 32, 2721, 1994.
4. H. Kawai, Jpn. J. Appl. Phys., 8, 875, 1969.
5. J. B. Lando, H. G. Olf, and A. Peterlin, J. Polym. Sci., Part A-1, 4, 941, 1966.
6. A. J. Lovinger, Development in crystalline polymers, P. 52, Applied Science, London, 1982.
7. J. B. Lando and W. W. Doll, J. Macromol. Sci. Phys., B2, 205, 1968.
8. Y. Higashihata, J. L. Sako, and T. Yagi, Ferroelectrics, 32, 85, 1981.
9. T. Yagi and T. Tatemoto, Polym. J., 11, 429, 1979.
10. B. Daudin and M. Dubus, J. Appl. Phys., 62, 994, 1987.
11. A. Odajima, Y. Takasa, T. Ishibashi, K. Yuasa, Jpn. J. Appl. Phys., 24, 881, 1985.
12. F. Macchi, B. Daudin, and J. F. Legrand, Nucl. Instr. And Meth., B46, 324, 1990.
13. Y. Higashihata, J. Sako, and T. Yagi, Ferroelectrics, 32, 85, 1981.
14. K. Koga and H. Ohigashi, J. Appl. Phys., 59, 2142, 1986.
15. K. Uchino, L. E. Cross, R. E. Newnham, and S. Nomura, J. Phase transition, 1, 333, 1980.
16. G. A. Smolensky, V. A. Isupov, A. I. Agranovskaya, and S. N. Popov, Sov. Phys.-solid state, 2, 2584, 1961)
17. M. L. Mulvihill, L. E. Cross, and K. Uchino, Proc. 8th European Mtg. Ferroelectricity, Nijmegen, 1995.
18. K. Tashiro, S. Nishimura, and M. Kobayashi, Macromolecules, 21, 2463, 1988, and 23, 2802 , 1990.
19. A. J. Lovinger, Macromolecules, 18, 910, 1985.
20. T. Furukawa and N. Seo, Jpn. J. Appl. Phys., 29, 675, 1990.
21. T. Yuki, S. Ito, T. Koda, and S. Ikeda, Jpn. J. Appl. Phys., 37, 5372, 1998.
22. S. Ikeda, H. Suzaki, and S. Nakami, Jpn. J. Appl. Phys., 31, 1112, 1992.
23. Q. M. Zhang, V. Bharti, and X. Zhao, Science, 280, 2102, 1998.

24. V. Bharti, H. S. Xu, G. Shanthi, and Q. M. Zhang, J. Appl. Phys., 87, 452, 2000.
25. T. Sakagami, N. Arakawa, Y. Teramoto, and K. Nakamura, U.S. Patent 4,554,335.
26. H. Inukai, N. Kawai, T. Kitaliara, S. Kai, and M. Kubo, U.S. Patent 5,087,679.
27. T. C. Chung, H. L. Lu, and W. Janvikul, J. Am. Chem. Soc., 118, 705, 1996.
28. T. C. Chung and W. Janvikul, J. Organomet. Chem., 581, 176, 1999.
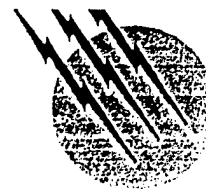
Polymers, Ferroelectric

T. C. Mike Chung

Pennsylvania State University

GLOSSARY

Actuator Transducer capable of transducing an input energy into mechanical output energy (displacement/force).

Dielectric constant The relative permittivity (compared with vacuum) that represents the charge-storing capacity of a dielectric material in the presence of an external electric field.

Electroactive polymer Polymer whose shape can be changed under an electric field to perform energy conversion between the electric form and the mechanical form.

Electrostriction Phenomenon in all dielectric materials which gives rise to a strain that is proportional to the square of the applied electric field.

Ferroelectric polymer Polymer whose direction of spontaneous polarization can be reversed under an electric field.

Poly(vinylidene fluoride) Polymer consisting of vinylidene fluoride monomer units.

Sensor A detection device that produces a measurable response to a change in a physical condition, such as temperature or pressure.

VDF/TrFE/CTFE terpolymer A random copolymer consisting of three different monomers: vinylidene fluoride, trifluoroethylene, and chlorotrifluoroethylene.

STRONG INTEREST has been generated in recent decades regarding the development of ferroelectric, piezoelectric, and magnetostrictive materials with high performance for such applications as electromechanical transducers, actuators, and sensors. However, many traditional electroactive materials (piezoceramic and magnetostrictive materials) have been found to suffer from low strain response (<1%), despite their high dielectric constant, low hysteresis, and fast speed. Developing new ferroelectric, piezoelectric, and magnetostrictive materials with high strain, high elastic density, and high electromechanical coupling has been a scientific and technological challenge. Recently, polymeric materials have received much more

extensive attention as new ferroelectric or piezoelectric materials. Compared to current ceramic-based materials, polymeric materials could offer many unique features, such as light weight, low cost, great mechanical strength, easy processability into thin and flexible films of various shapes and sizes, high reliability, large strain, and, most importantly, flexible architecture design via molecular tailoring.

It was not until 1969 that Kawai demonstrated the significant increase of piezoelectricity in poly(vinylidene fluoride); pyroelectricity and ferroelectricity were reported in 1971. Since then, tremendous growth in the new field of ferroelectric polymers has occurred. The exploration of the chemistry, physics, and technology of poly(vinylidene fluoride) led to the search for other classes of novel ferroelectric polymers, such as its copolymers, odd-numbered polyimides, cyanopolymers, polyureas, polythioureas, biopolymers (including polypeptides), and ferroelectric liquid crystal polymers. Significant progress has been made both in finding new materials and in better understanding structure–property relationships.

In this review, the primary goals are to update current research in ferroelectric polymers and provide a fundamental understanding of ferroelectric physics. Since many extensive reviews of poly(vinylidene fluoride) and its copolymers already exist in great detail, only a brief summary is given of their chemical synthesis, structure-electrical property relationships, and applications. Some emphasis will be on the newly developed VDF/TrFE/CTFE terpolymers containing vinylidene difluoride (VDF), trifluoroethylene (TrFE), and chlorotrifluoroethylene (CTFE) units. These processable terpolymers show high dielectric constants, narrow polarization hysteresis loops, and large electrostrictive responses at ambient temperature. The last section will cover some other novel ferroelectric polymers, such as polyimides, polyurethanes, and polyureas. No attempt is made to discuss ferroelectric biopolymers and ferroelectric liquid crystal polymers, comprehensive reviews of which are available elsewhere.

I. DEFINITION OF PIEZO-, PYRO-, AND FERROELECTRICS

It is well established that electrical properties such as piezoelectricity and pyroelectricity can only exist in materials lacking a center of symmetry. In fact, among the 32 classes of the crystal point symmetry group, only 20 can exhibit piezoelectric and pyroelectric effects. A piezoelectric material is one that develops electric polarization only when mechanical stress is applied. Pyroelectric materials possess a permanent polarity (spontaneous polarization)

which responds not only to stress, but also to temperature change. Pyroelectric crystals whose spontaneous polarization can be reversed by an external electric field are called ferroelectrics.

A. Piezoelectric d Constant

The magnitude of the induced strain x by an external field E or the dielectric displacement D by a stress X is represented in terms of the piezoelectric d constant (an important parameter for acoustic applications)

$$x = dE \tag{1a}$$

$$D = dX. \tag{1b}$$

The effect in Eq. (1b) is the direct piezoelectric effect, where the induced charge is proportional to the mechanical stress, whereas the effect in Eq. (1a) is the converse piezoelectric effect. Extending Eqs. (1a) and (1b) with the use of the linear elastic (Hooke's law) and dielectric equations, and writing the results in matrix notation form yields

$$x_i = s_{ij}^E X_j + d_{mi} E_m, \tag{2a}$$

$$D_m = d_{mi} X_i + \varepsilon_{mk}^X E_k, \tag{2b}$$

where s_{ij}^E is the elastic compliance, ε_{ik}^X is the dielectric permittivity, $i, j = 1, 2, \ldots, 6$, and m, $k, = 1, 2, 3$. The superscripts refer to the conditions under which these quantities are measured, that is, compliance is measured under constant electric field, and permittivity is measured under constant stress. ε_0 is the vacuum dielectric permittivity (=8.85 × 10^{-12} F/m).

B. Piezoelectric g Constant

The induced electric field E is related to an external stress X through the piezoelectric voltage constant g, which is an important parameter for sensor applications:

$$E = gX. \tag{3}$$

Taking into account $D = dX$, we obtain

$$g = \frac{d}{\varepsilon \varepsilon_0}. \tag{4}$$

C. Field-Related and Charge-Related Electrostrictive Coefficients

Generally, there are two phenomenologies used to describe the electric field-induced strain: the electrostrictive and piezoelectric effects. The piezoelectric effect is a primary electromechanical coupling effect in which the

strain is proportional to the electric field, whereas the electrostrictive effect is a secondary effect in which the strain is proportional to the square of the electric field (this effect exists in any polymer). Electrostriction can be expressed as

$$x = ME^2, \tag{5}$$

$$x = QP^2. \tag{6}$$

where $P = \varepsilon\varepsilon_0 E$ in the *paraelectric* phase and $P = P_s + \varepsilon\varepsilon_0 E$ in the *ferroelectric* phase. The electric field-related electrostrictive coefficient M and charge-related electrostrictive coefficient Q are related to each other through $M = Q\varepsilon_0^2\varepsilon^2$.

For an isotropic polymer,

$$x_{33} = Q_{33}P^2, \qquad x_{31} = Q_{31}P^2. \tag{7}$$

where the two numerals in the subscripts refer to the electric field direction and the measured polarization direction, respectively. Therefore, x_{33} and x_{31} are strains parallel to and perpendicular to the polarization direction, known as longitudinal and transverse strains, respectively. For isotropic polymers, both experimental and theoretical data show that $Q_{11} < 0$, $Q_{13} > 0$, $M_{33} < 0$, and $M_{13} > 0$, hence the polymer will contract along the polarization direction as the polarization increases. In other words, the polymer will contract along the thickness direction and will expand along the film direction when an electric field is applied across the thickness.

It should be noted that most polymers exhibit nonlinear dielectric behavior and deviate from Eq. (5) in a high field, where the field-induced strain will be saturated.

D. Electromechanical Coupling Factor K

The electromechanical coupling factor K is related to the conversion rate between electrical energy and mechanical energy; K^2 is the ratio of stored mechanical energy to input electrical energy, or the ratio of stored electrical energy to input mechanical energy.

When an electric field E is applied to a piezoelectric material, K^2 can be calculated as

$$K^2 = d^2/\varepsilon\varepsilon_0 s. \tag{9}$$

There are many electromechanical coupling factors corresponding to the direction of the applied electric field and to the mechanical strain (or stress) direction. For instance, in cases where a polymer actuator is made with the electric field along the 3-direction, the mechanical coupling factor is longitudinal to the electromechanical coupling factor K_{33}, which can be related to the Eq. (9) as

$$K_{33}^2 = d_{33}^2/\varepsilon_{33}^X \varepsilon_0 s_{33}^E. \tag{10}$$

E. Acoustic Impedance Z

The acoustic impedance Z is a parameter used for evaluating the acoustic energy transfer between two materials. It is defined as $Z^2 = \text{pressure/volume} \cdot \text{velocity}$. In solid material,

$$Z = \sqrt{\rho \cdot c} \tag{11}$$

where ρ is the density and c is the elastic stiffness of the material.

Piezoelectric ferroelectrics fall into four classes: optical active polymers, poled polar polymers, ferroelectric polymers, and ceramic/polymer composites. *The poling procedure involves the application of an external field to a ferroelectric to induce a cooperative alignment of constituent dipoles.* Most polymers in the first group are biological materials, such as derivatives of cellulose, proteins, and synthetic polypeptides. The origin of piezoelectricity in these polymers is attributed to the internal rotation of the dipoles of asymmetric carbon atoms, which gives rise to optical activity. The second class of piezoelectric polymers includes polyvinyl chloride (PVC), polyvinyl fluoride (PVF), polyacrylonitriles (PAN), odd-numbered nylons, and copolymers of vinylidene cyanide. The piezoelectricity in these polymers is caused by the trifluoroethylene (TrFE) or tetrafluoroethylene (TFE). Recently, other polymers were found to show ferroelectric behavior, such as copolymers of vinylidene cyanide, odd-numbered nylons, and polyureas, in which piezoelectricity arises from the functional polar groups in the polymer molecules. In the fourth class (polymer/ceramic composites), the piezoelectric activity comes from the intrinsic piezoelectricity of ceramics. Physical properties of these composites can be controlled by the choice of the ferroelectric ceramics and the polymer matrix. They have a combination of high piezoelectric activity from the ferroelectric ceramics and flexibility from the polymer matrix.

Table I compares the piezoelectric properties of the ferroelectric ceramics and polymers. The piezoelectric strain constant d_{31} of polymers is relatively low compared to that of ceramics. However, the piezoelectric voltage constant g_{31} is larger. In addition, polymers have a high electromechanical coupling factor and low acoustic impedance, which permit their use in ultrasonic transducer applications and medical instrumentation. The combination of these properties with their flexibility, light weight, toughness, and availability in large-area sheets has led to tremendous growth in research on novel ferroelectric polymers.

TABLE I Typical Physical, Piezoelectric, and Pyroelectric Properties of Various Materials

Material[a]	Density ρ (g/cm³)	Modulus C_{11} (GN/m²)	d_{31} (pC/N)	e_{31} (pC/N)	g_{31} (mV·m/N)	Pyroelectric constant (μC/K·m²)	Dielectric constant (ε_r)	Coupling factor k_{31}	Acoustic impedance (Gg/m²·sec)
			Piezoelectric constants						
PVDF	1.78	1–3	20	6.0	174	30–40	10–15	0.1	2–3
P(VDF/TrFE)	~1.9	1.2	15–30	2–3	100–160	30–40	15–30	0.2	
PVF	1.4	1	1			10			
PVC	1.5	4	1			1–3	3		
Nylon-11	1.1	1.5	3	6.2		3	4	0.1–0.15	
Nylon-11/PVDF Laminate film		2.3	41	109			13.8		
P(VDCN/VAc)	1.2	4.5	6	2.7	169		4.5	0.06	
PTUFB						3.0	20–30		
PVDF/PZT	5.3	3.0	20	6.0	19		120	0.07	
Rubber/PZT	5.6	0.04	35	1.4	72		55	0.01	
POM/PZT	4.5	2.0	17	3.4	20		95	0.08	
Quartz	2.65	77.2	2	15.4	50		4.5	0.09	
PZT	7.5	83.3	110	920	10		1200	0.31	

[a] PVDF, poly(vinylidene fluoride); P(VDF/TrFE), poly(vinylidene fluoride-co-trifluoroethylene); PVF, polyvinyl fluoride; PVC, polyvinyl chloride; P(VDCN/Vac), poly(vinylidene cyanide-co-vinyl acetate); PTUFB, polyurea-formaldehyde; PZT, lead zirconate titanate.

II. CONVENTIONAL PIEZOELECTRIC POLYMERS: POLY(VINYLIDENE FLUORIDE) AND ITS COPOLYMERS

A. Poly(vinylidene fluoride)

1. Synthesis

Poly(vinylidene fluoride) (PVDF) is commercially produced by free radical polymerization of 1,1-difluoroethylene ($CH_2=CF_2$) at high temperature (50–150°C) and high pressure (10–300 atm). The most common polymerization process is emulsion or suspension using water as a reaction medium. The catalysts used in these processes are either inorganic (persulfate) or organic peroxides. Since the monomer units of PVDF have a directionality (CH_2 is denoted the "head" and CF_2 the "tail"), typically 5% of the monomer units enter the growing chain with a reverse orientation, leading to head-to-head and tail-to-tail defects. These defects cause a reduction of the average dipoles by 6–10%. Polymers with defect concentrations ranging from 0.2% to 23.5% have been synthesized and the effect of defects on crystal structure has been studied.

2. Molecular and Crystal Structure

PVDF ($-CH_2-CF_2-$) has a chemical structure in between those of PE ($-CH_2CH_2-$) and PTFE ($-CF_2CF_2-$). Unlike PTFE, which has a helical conformation due to the steric hindrance of the fluorine atom, or PE, which takes

the most stable conformation (all-*trans* conformation due to low rotational barrier), PVDF can take several conformations. The three known conformations are tg^+tg^-, all-*trans*, and $tttg^+tttg^-$. The first two conformations are the most common and important ones, and are schematically drawn in Fig. 1.

The C—F bond is a polar bond (dipole moment $\mu = 6.4 \times 10^{-30}$ C-m), and contributes to the polar conformation. The all-*trans* conformation has the highest dipole moment ($\mu = 7.0 \times 10^{-30}$ C-m/repeat) due to the alignment of all dipoles in the same direction. The tg^+tg^- conformation is also polar, but the net dipoles that are perpendicular and parallel to the chain are approximately the same, giving rise to lower net dipole.

The packing of these polar chains in a crystal adopts several distinct morphologies in PVDF. At least four are known, the α, β, γ, and δ phases, which can easily be transformed into one another. The most common one is the α phase, which may be obtained by crystallization from the melt. As depicted in Fig. 1, the unit cell of the α phase consists of two tg^+tg^- chain conformations whose dipole components normal to the chain are antiparallel and neutral to each other. Thus the α phase is a nonpolar phase. The polar analog δ phase can be obtained by poling under a high electric field. The lattice dimensions of these two phases are essentially the same: $a = 4.96$ Å, $b = 9.64$ Å, and $c = 4.96$ Å.

The β phase is the most highly polar and important phase, and is typically prepared by stretching polymer film at room temperature or by crystallization from the melt
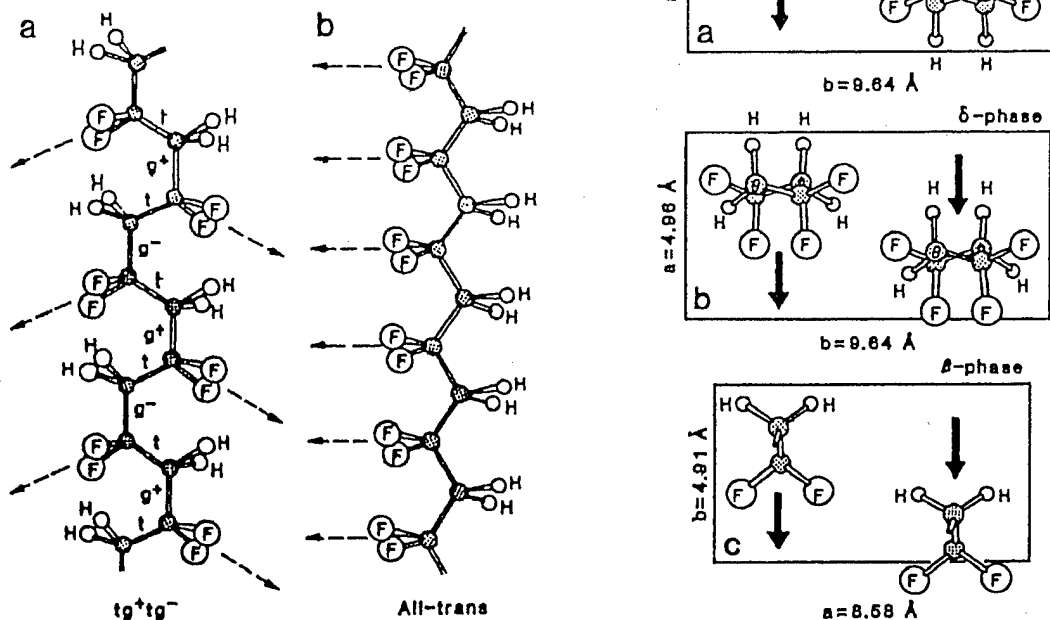
FIGURE 1 (Left) Schematic depiction of the two most common chain conformations in PVDF: (a) $tg^+ tg$ and (b) all-*trans*. (Right) Unit cells of (a) α phase, (b) δ phase, and (c) β phase of PVDF in projection parallel to the chain axis.

under high pressure or epitaxial technique. The unit cell of the β phase contains two all-*trans* chain conformations in orthorhombic symmetry with the lattice with $a = 8.45$ Å, $b = 4.88$ Å, and $c = 2.55$ Å. The dipole components normal to the chain (b axis) are parallel. Thus, the β phase is a polar phase that possesses spontaneous polarization and exhibits piezoelectricity as well as pyroelectricity.

The γ phase contains two $tttg^+tttg^-$ chain conformations that are packed in a polar fashion. It has unit cell dimensions of $a = 4.96$ Å, $b = 9.58$ Å, and $c = 9.23$ Å. This phase may be obtained by the crystallization of a molten sample at high temperature or solution cast from dimethylacetamide (DMA) or dimethylformamide (DMF).

3. Morphology of PVDF

The crystallization of PVDF from the melt results in spherulitic morphologies in which the lamella stacks have a periodicity of about 10 nm and have no net dipoles. A number of papers have reported on the morphology of melt-solidified PVDF. There are two types of spherulites grown from the melt at high temperature (up to 60°C). The most common is a spherulite from the nonpolar phase

(α form), which is larger and has high birefringence and tightly spaced concentric bonding. The second type is smaller and has less birefringence, and comes from the γ phase. The morphology of PVDF has recently been investigated as a function of head-to-head defects and crystallization temperature for a wide range of temperatures.

4. Ferroelectricity and Related Properties of PVDF

Although the β and δ phases are known to be polar since the components of their dipoles are arranged in the same direction, the β phase has stronger pyroelectric and piezoelectric coefficients than the other phase. Therefore, to obtain a useful PVDF as a transducer material, a polymer film must be oriented and polarized. The orientation or stretching can be performed between the glass temperature T_g and melting temperature T_m by stretching a polymer film to several times its original length. Poling can be accomplished either at room temperature with a high electric field or at high temperature with a low field. For conventional thermal poling, a polymer film is stretched, annealed, electroded on both surfaces, and subjected to
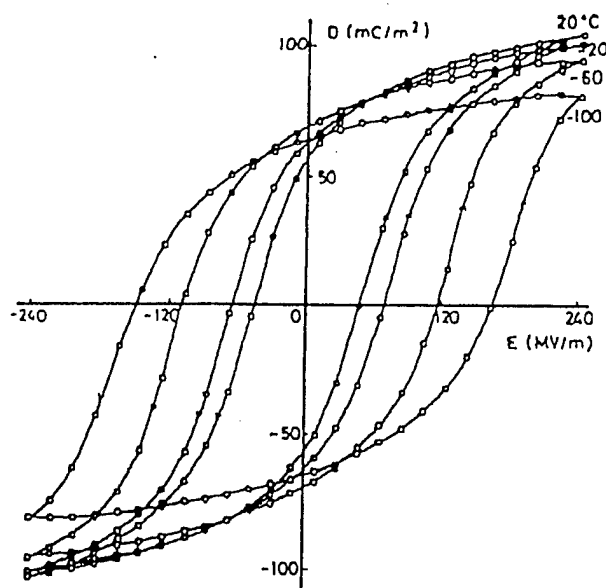
FIGURE 2 The D–E hysteresis loops of PVDF at various electric fields.

an electric field of about 0.5 MV/cm at high temperature (80–100°C), followed by cooling in the presence of the applied field. Other methods of poling include corona discharge, plasma, and poling during orientation.

For many years, there was debate over the origins of the piezoelectric and pyroelectric properties in PVDF. The arguments seem to have reached the conclusion that the properties primarily arise from the dipole orientation, rather than from trapped space charge. The discovery of the enhancement of piezoelectric activity in PVDF by Kawai led to the revelation of others properties, such as pyroelectricity and ferroelectricity. Although there is no obvious evidence of a Curie transition in PVDF, the existence of polarization loops together with polarization reversal and the switching phenomenon is generally accepted as proof of ferroelectricity in PVDF. Figure 2 shows the D–E hysteresis loops at various temperatures. Even at $-100°C$ a square-shape hysteresis loop is clearly observed with a remanent polarization P_r about 60 mC/m², which does not change with temperature. However, the coercive field E_c, which is the electric field used for neutralizing polarization in the material, is temperature-dependent. The value is about 50 MV/m at room temperature and remains almost constant above the glass transition temperature ($-50°C$), but increases sharply at lower temperatures.

The remanent polarization P_r, which is the polarization after the field has been removed, is dependent on the crystallinity. For PVDF, the calculated macroscopic polarization for 100% alignment of all dipoles is 130 mC/m², and the measured polarization of 60 mC/m² is consistent with about 50% crystallinity and perfect alignment. The

direction of P_r can be reversed by subsequent application of the field in the opposite direction. This phenomenon, called ferroelectric switching, has been investigated extensively to elucidate the mechanism of polarization reversal.

Although PVDF exhibits strong piezoelectric and pyroelectric properties, it is necessary that the polymer film be subjected to mechanical stretching and electrical poling to get the β phase. Such procedures include, for example, subjecting the ferroelectric polymer to mechanical deformation, electron irradiation, uniaxial drawing, crystallization under high pressure, and crystallization under high electric field. It is tempting to speculate about how much improvement of the dielectric, piezoelectric, and pyroelectric properties may yet be achieved by modification of the chemical structure of the polymer. Some improvement has been achieved by synthesizing copolymers of vinylidene fluoride with trifluoroethylene (TrFE), tetrafluoroethylene (TFE), or vinyl fluoride (VF), and, indeed, some of these copolymers exhibit even higher piezoelectric and pyroelectric properties that will be discussed in the next section.

B. Poly(vinylidene fluoride–trifluoroethylene) (VDF/TrFE) Copolymer

P(VDF/TrFE) is the most studied copolymer. Lando *et al.* and Yagi *et al.* initially studied the properties and structure of this copolymer. The randomly distributed VDF and TrFE units form the cocrystalline phase in the whole composition range of the copolymers. The greater proportion of bulky trifluorine atoms in PVDF prevents the molecular chains from accommodating the $tg^{+}tg^{-}$ conformation. Therefore, copolymers crystallize at room temperature into a ferroelectric phase with the extended planar zigzag (all-*trans*) conformation, whose crystalline phase is similar to the β phase of PVDF homopolymer.

1. Ferroelectric–Paraelectric Phase Transition

Probably the solid evidence for the ferroelectricity in this copolymer is the existence of the ferroelectric to paraelectric (F–P) phase transition or Curie temperature T_c. The Curie temperature of synthetic polymer was discovered in 1980. At this temperature, the dielectric constant shows a maximum value, the polarization and piezoelectric constants go down to zero, and the Young's modulus and elastic constant decrease. The phase transition of copolymers has been found to be affected by several factors, especially the VDF content. As shown in Fig. 3, copolymers with VDF content below 82 mol% exhibit a phase transition below the melting point.

The lowest Curie temperature of the copolymer is about 60°C, and this phase temperature increases linearly with
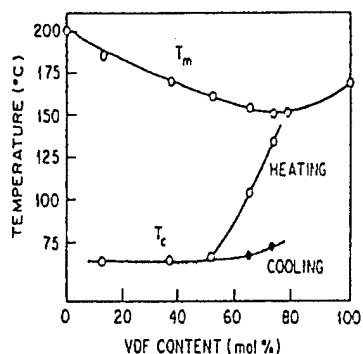
FIGURE 3 The thermal transition temperature in VDF/TrFE copolymers.

increasing VDF content, which allows an extrapolation of the Curie transition temperature of PVDF homopolymer to about 215°C. Other widely studied factors that affect the Curie transition are hydrostatic pressure, tensile stress, external electric field, annealing temperature and time, mechanical drawing, poling, irradiation, solution history, thermal history, and crystallization conditions.

2. Crystal Structures

A number of experimental techniques such as differential scanning calorimetry (DSC), dielectric constant determination, ferroelectric measurement, and X-ray diffraction have been employed to investigate structural change during the phase transition. It is not clear whether the double peak at the ferroelectric transition of 70/30 VDF/TrFE copolymer is associated with the formation of different sizes of ferroelectric domains or the two-step phase transformation. Tashiro suggested the existence of two types of ferroelectric phases: a low-temperature phase (LT) consisting of a parallel arrangement of dipoles in planar zigzag (all-*trans*) chain (as seen in the β phase of PVDF homopolymer) and the cooled phase (CL) consists of long *trans* segments connected by irregular *gauche* linkages along the chain axis (depending on the VDF content of the copolymer as well as the sample preparation conditions).

The transition behavior of the copolymer change with change in the VDF content in the copolymer. For instance, in a copolymer with a VDF content of 70–80 mol%, a first-order transition between the LT and HT phases at high temperature is observed, whereas a second-order transition between the CT and HT phases occurs in copolymer with a VDF content of <50 mol%. The 50–60% VDF samples show more complicated transitional behavior. The *trans* zigzag chains transform to the irregular *trans* form of the LT phase, which easily changes to the random *gauche* conformation. Recently, the phase transition from the LT to CL phases has been confirmed.

During the transition from the ferroelectric to the para-electric phase, structural changes in the crystal lattice and the domain size are clearly demonstrated. The phase transition occurs through the *trans–gauche* conformational change, where all-*trans* molecular chains change their conformation to a disordered sequence of conformation isomers (tg^+, tg^-, tt), resulting in the nonpolar unit cell structure of hexagonal packing, with unit cell dimensions of $a = 9.96$ Å, $b = 4.96$ Å, and $c = 4.64$ Å.

Interestingly, during the phase transition, there is large strain change associated with the phase transformation. For 65/35 mol% VDF/TrFE copolymers, respective lattice strains as high as 10% and 7% in the crystalline phase along (001 reflection) and perpendicular to (200, 110 reflections) the polymer chain have been detected during the phase transition. Therefore, for a high-crystalline (>50% crystallinity) copolymer, these strains can be transformed into macroscopic strains; indeed, a thermal strain of more than 6% in 65/35 copolymer has been observed. More importantly, for a ferroelectric polymer, the phase transformation can be controlled by an external electric field, hence the high-field induced strain can be achieved by exploring the lattice strain at the phase transition.

3. Ferroelectricity and Related Properties

Copolymers were demonstrated to possess ferroelectricity over a wide composition range. Piezoelectric and pyroelectric properties of these copolymers have also been reported. Since the electrical properties originate from the crystal units, chain orientation by drawing, crystallization by annealing, and CF_2 dipole orientation by poling are important for achieving high piezoelectric and pyroelectric constants. The dipole orientation can result in a change of chain conformation, chain packing, crystallinity, and crystal size. Recently, the structural and crystal changes of copolymers have been reported as functions of poling conditions and high-pressure crystallization. The polarization reversal of copolymers strongly depends on their thermal and mechanical treatment. The polarization reversal of quenched copolymers proceeds over several decades if annealed above the Curie temperature T_C, whereas it is completed within one decade if annealed below T_C.

The phase transition T_C of all VDF/TrFE copolymers occurs at high temperatures (>60°C) and the transition is relatively sharp. In addition, the early experimental results showed a large hysteresis at the phase transition, which is not desirable for practical applications. Therefore, many attempts have been devoted to broadening and reducing the phase transition to room temperature and minimizing or eliminating the hysteresis. Zhang *et al.* found that by systematic study of the irradiation conditions of the copolymer, high electromechanical response

can be achieved. The longitudinal strain S_3 measured at room temperature and 1 Hz frequency reaches -4% at 150 MV/m. The irradiation significantly reduces the hysteresis in the polarization loop. However, the polarization was also significantly reduced, and the sample becomes completely insoluble in common solvent because of a severe crosslinking side reaction during the high-energy irradiation.

The increase in hardness of the copolymer due to crosslinking was also revealed in the electromechanical response. A very high field was required to get high strain response. It appears that the irradiation process produces many undesirable side reactions that increase the amorphous phase content and diminish the processability of the sample.

C. Poly(vinylidene fluoride–tetrafluoroethylene) (VDF/TFE) Copolymer

The second mostly studied copolymer is the VDF/TFE random copolymer, which can be viewed as a PVDF polymer containing an increased amount of head-to-head and tail-to-tail defects. The steric hindrance created by the TFE unit effectively stabilizes the *trans* conformer of the VDF chain. As the content of TFE units increases, the *trans* conformation is stabilized overwhelmingly and the generation of the *gauche* bonds is suppressed. The copolymers of VDF/TFE with at least 7% are crystallized in the β form. The Curie transition was clearly observed in 18–23 mol% TFE. The crystal structure and phase transition behavior of copolymers have been studied by X-ray, IR, and Raman spectroscopies.

Piezoelectric and pyroelectric studies of VDF/TFE copolymers showed highly inhomogeneous polarization across the thickness of the copolymer films. Ferroelectric studies revealed a hysteresis loop, but no Curie transition in the temperature-dependent dielectric curve. However, there was some evidence showing that the Curie transition occurs in the vicinity of the melting temperature.

III. NEW PIEZOELECTRIC VDF/TRFE/CTFE TERPOLYMERS

In our laboratory, we have adopted a new chemical strategy of altering crystalline domains and creating relaxor ferroelectric behavior of VDF/TrFE copolymer, with the objective of achieving a processable polymer with controllable phase transition temperature, high dielectric constant, and fast and large electromechanical response at ambient temperature. The chemistry involves homogeneous incorporation of a small amount of bulky ter-monomer units, such as chlorotrifluoroethylene (CTFE), as the crystalline

defects into a VDF/TrFE copolymer chain. The resulting VDF/TrFE/CTFE terpolymers are completely solution and melt processable, and exhibit high dielectric constant and electrostrictive response at ambient temperature.

A. Synthesis

Prior to our research, there were some reports discussing the terpolymerization reactions involving VDF, TrFE, and a small amount of termonomer, such as hexafluoropropene (HFP), chlorotrifluoroethylene (CTFE), or tetrafluoroethylene (TFE), by conventional free radical polymerization processes. The ter-polymerization was usually carried out in the emulsion or suspension process using inorganic or organic peroxides as initiator at elevated temperatures.

Recently, we have developed a bulk (room temperature) polymerization process initiated by the oxidation adducts of the organoborane molecule, as illustrated in Fig. 4.

Upon exposure to a controlled quantity of oxygen, asymmetrical alkylborane (I) is selectively autoxidized at the linear alkyl group to produce ethylperoxylborane (II). The peroxyborane (II) behaves very differently from regular benzoyl peroxides and consequently decomposes to alkoxy radical (C—O$*$) and a borinate radical (B—O$*$) (III) that is relatively stable due to the back-donating of electron density to the empty p orbital of boron. In the presence of fluro-monomers, the homolytic cleavage of peroxide occurs even at very low temperatures ($-30°C$). The alkoxyl radical is very reactive and initiates the radical polymerization at ambient temperature. On the other hand, the borinate radical forms a weak and reversible bond with the growing chain end, which assures the "stable" radical polymerization. During the propagating reaction, a coordination intermediate (IV) may form due to the B—F acid–base complex between the active site and the incoming monomer. Such an interaction
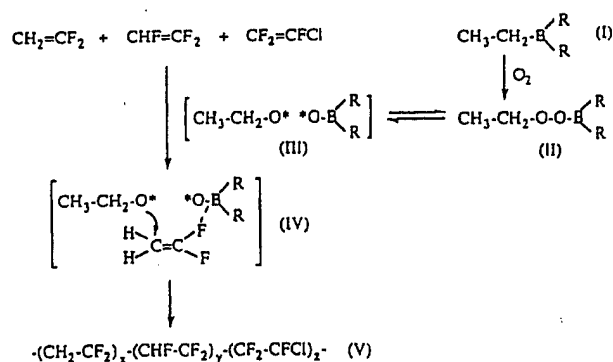

FIGURE 4 An equation showing selective auto-oxidation of organoborane and terpolymerization of VDF, TrFE, and CTFE monomers.

TABLE II A Summary of VDF/TrFE/CTFE Terpolymers Prepared by Borane/Oxygen Initiator[a]

Sample no.	Terpolymer mole ratio			Melting temperature		Phase transition temperature		$[\eta]$ (MEK)[b] (35°C)	P_{max} (mC/m²)	E_c (MV/m)	Dielectric constant[c]	Dielectric loss
	VDF	TrFE	CTFE	T_m (°C)	ΔH_m (J/g)	T_C (°C)	ΔH_C (J/g)					
1	72.2	17.8	10.0	107.8	17.8	25.0	0.4	0.38	82	19.6	27.0	0.04
2	66.0	22.5	11.5	117.2	21.6	25.2	2.5	0.42	78	24.1	22.4	0.03
3	66.1	21.4	12.5	115.6	20.5	25.8	1.8	0.42	—	—	40.9	0.04
4	63.1	25.4	11.5	113.7	18.5	None[d]	None	0.49	76	19.8	53.5	0.06
5	61.4	25.3	13.3	111.3	17.8	15.6	1.5	0.69	75	33.7	53.1	0.06
6	58.0	33.1	8.9	130.0	21.3	31.6	2.5	0.63	63	16.4	33.0	0.05
7	60.0	36.0	4.0	140.9	25.7	43.8	6.5	0.58	87	21.8	26.4	0.04
8	55.6	36.1	8.3	124.6	21.2	None	None	0.54	36	7.6	42.4	0.07
9[e]	60.0	35.1	6.9	126.6	20.9	33.5	1.6	0.78	110	55.9	52.7	0.07
10[e]	59.3	32.9	7.8	125.1	20.3	24.8	1.4	0.80	70	11.5	51.0	0.07
11[e]	57.3	31.2	11.5	111.1	14.8	None	None	0.75	45	39.4	50.5	0.06

[a] P_{max} and E_c at 100 MV/m, 10 Hz. 22°C. Dielectric constant and dielectric loss at 1 KHz, 22°C.
[b] MEK, methylethylketone.
[c] Value measured in the heating cycle.
[d] None: no observable.
[e] Sample prepared by constant monomer feed ratio during the polymerization.

will regulate the insertion of monomers in a preferred head-to-tail sequence. No chain transfer and termination reactions are expected during the propagating process, which will lead to a linear polymer structure with relatively narrow molecular weight and composition distributions. Figure 5 shows that the VDF/TrFE/CTFE terpolymer increases in molecular weight with the conversion of monomers.

In addition, this chemistry produces terpolymers that have relatively uniform molecular structure and few
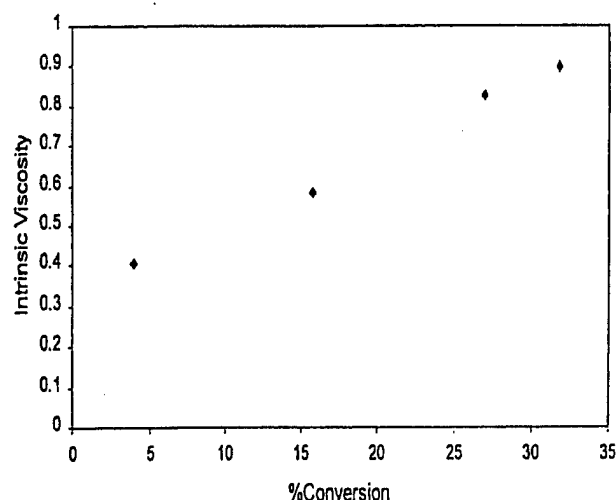

FIGURE 5 Intrinsic viscosity of VDF/TrFE/CTFE terpolymer versus monomer conversion.

impurities (boric acid and butanol), which can be easily removed by methanol. Table II summarizes several VDF/TrFE/CTFE terpolymers prepared by the same method. All terpolymers are high-molecular-weight (>20,000 g/mole) polymers with good solubility in common organic solvents and are melt processable at >150°C.

B. Thermal Properties

Despite having relatively high concentrations of CTFE units, all the terpolymers are still semicrystalline thermoplastics with melting temperatures >100°C and a crystallinity of $\Delta H > 17$ J/g. Figure 6 compares the DSC curves of three VDF/TrFE/CTFE terpolymers (samples 9, 10, and 11). The relatively well-defined melting and crystalline phase transition temperatures imply a relatively uniform molecular structure and polymer morphology. In addition to the reduction of melting temperature, the incorporated CTFE units also significantly reduced the F–P phase transition temperature. It is interesting to note that the effect of incorporated CTFE units resembles that seen from crosslinking in irradiated VDF/TrFE samples. The CTFE units may not affect the crystal unit cell of VDF/TrFE segments, and instead serve as a defect (by introducing a gauche bond) to prevent the extension of crystallization, which results in the reduction of the lamella thickness of the crystal. Detailed studies of the molecular structure and the crystal polar domain size are underway.

In general, the third CTFE monomer units in VDF/TrFE/CTFE terpolymers shift (and broaden) the phase
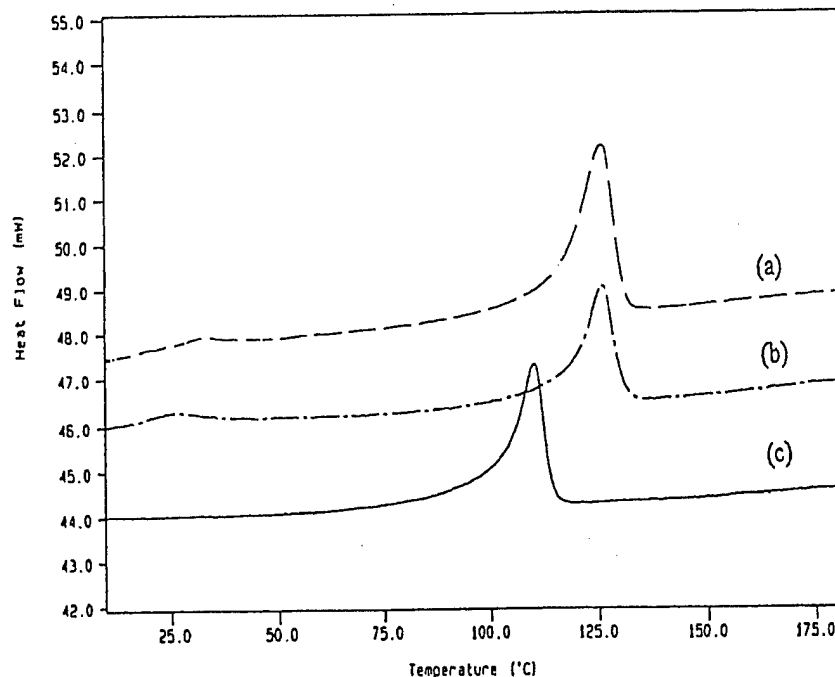
FIGURE 6 DSC comparison of three VDF/TrFE/CTFE terpolymers: (a) sample 9, (b) sample 10, and (c) sample 11 in Table II.

transition to lower temperatures, to near ambient temperature for samples 1, 2, 3, and 10, and almost disappearing for samples 4, 8, and 11. That indicates a very small energy barrier in the phase transition and implies a smaller crystalline domain. The results are consistent with the electric responses of the terpolymer under an electric field.

C. Electric Properties

For electrical measurements, polymer films ($\sim$30 μm thickness) were prepared either by solution casting on a glass slide from N,N-dimethylformamide solution containing 8–10 wt% polymer or melt-pressing polymer powder at 200°C. The polymer films were annealed at 110°C under vacuum for 5 hr. Gold (<1μm thickness) was sputtered on both surfaces of the polymer film. The dielectric constant was measured by an HP multifrequency LCR meter equipped with a temperature chamber. Figure 7 shows the dielectric constant of 59.3/32.9/7.8 VDF/TrFE/CTFE terpolymer (sample 10) and 57.3/31.2/11.5 VDF/TrFE/CTFE terpolymer (sample 11) during the heating–cooling cycles.

In general, the dielectric constant hysteresis during the heating–cooling cycles is very small, and the dielectric peak appears near the ambient temperature, well below the dielectric peak observed in 55/45 VDF/TrFE copolymer (>60°C) with a big hysteresis loop. Diffuse dielectric

peaks and peaks shifting toward higher temperatures as the frequency increases are common features of relaxor ferroelectrics.

As shown in Table II, most of the terpolymers show high dielectric constants at ambient temperature. Samples 4 and 5 exhibit dielectric constants as high as 53.5 and 53.1 (1 kHz), respectively, at 22°C. In sharp contrast, prior research reported that high dielectric constants (>25) only existed in the VDF/TrFE/CTFE terpolymers with a narrow range (18–22%) of TrFE content. In addition, the mechanical stretching of the polymer film, usually very important for increasing the dielectric constant in VDF/TrFE copolymers, is not necessary in these terpolymers. The effective orientation of dipoles under an electric field may be attributed to the low phase transition energy which occurs at near-ambient temperature.

The polarization hysteresis loop was measured by a Sawyer–Tower circuit with a frequency range between 1 and 10 Hz. Figure 8 compares the polarization hysteresis loops of two terpolymers (samples 2 and 8) and a 55/45 VDF/TrFE copolymer. Both terpolymers show significantly smaller hysteresis than the 55/45 copolymer, which has the narrowest polarization hysteresis loop observed in the copolymer samples. Sample 2 (VDF/TrFE/CTFE = 66/22.5/11.5 mole ratio) maintains a high polarization level ($P_{max} = 78$ mC/m^2 at $E = 100$ MV/m) and reduces both a coercive field (17.3 MV/m at $P = 0$) and remanent polarization (25.2 mC/m^2 at $E = 0$). Sample 8
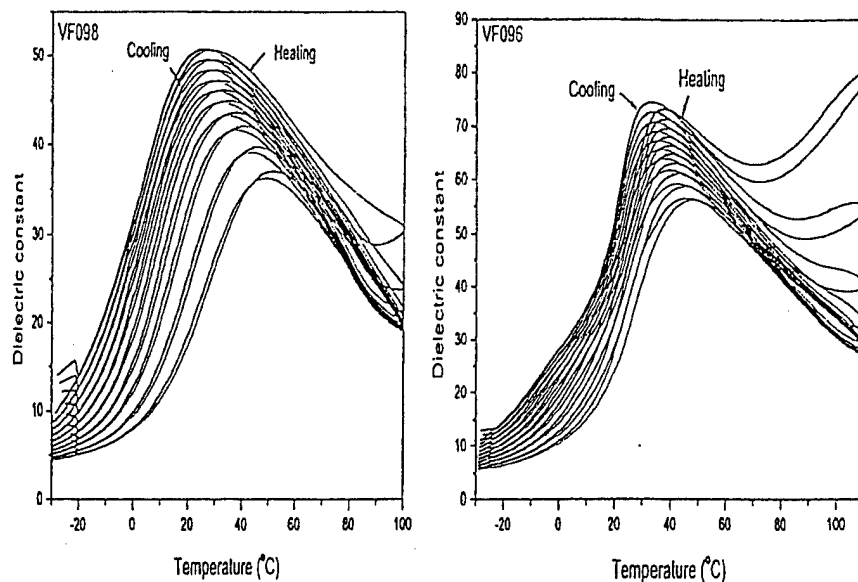
FIGURE 7 Temperature dependence of dielectric constant in two terpolymers: (right) sample 10 (VDF/TrFE/CTFE = 59.3/32.9/7.8) and (left) sample 11 (VDF/TrFE/CTFE = 57.3/31.2/11.5) during heating–cooling cycles. The frequencies from top to bottom of the dielectric curve range from 1 to 300 kHz.

(VDF/TrFE/CTFE = 55.6/36.1/8.3 mole ratio) exhibits a very slim loop with very small coercive field and remanent polarization, as well as an overall reduced polarization level. These results indicate that the VDF/TrFE crystalline defects introduced by the incorporated CTFE termonomer units cannot be recovered by the application of a high

electric field. It is interesting to note that the polarization hysteresis loop of sample 8 gradually appears with reduced temperature ($<0°C$), another feature common to all relaxor ferroelectrics.

The electric field-induced strain was measured at ambient temperature in the field range of 0–150 MV/m
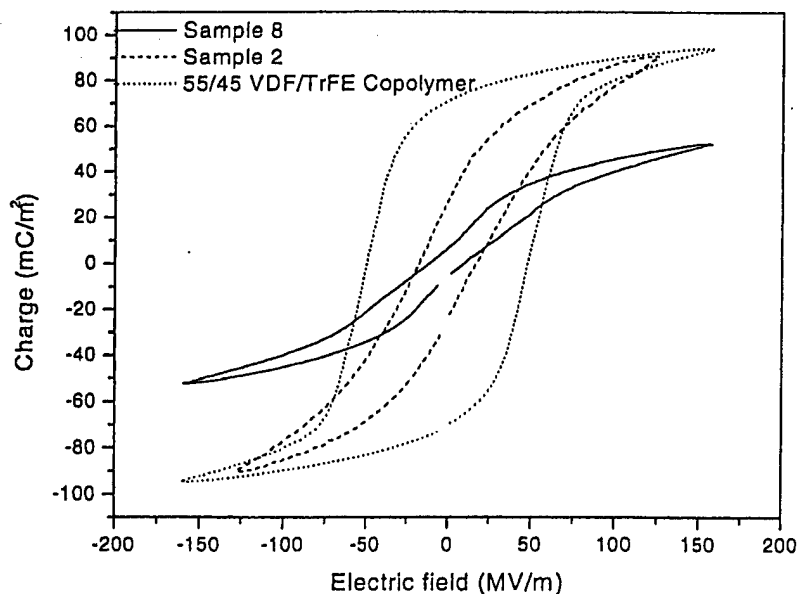
FIGURE 8 The comparison of polarization hysteresis loops between two VDF/TrFE/CTFE terpolymers (samples 2 and 8) with 66/22.5/11.5 and 55.6/36.1/8.3 mole ratios, respectively, and a VDF/TrFE (55/45) copolymer.
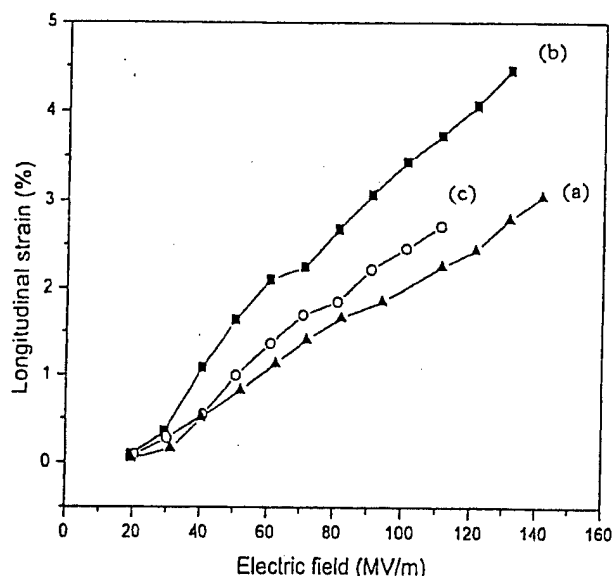
FIGURE 9 Electric field-induced strain of three VDF/TrFE/CTFE samples 9–11.

using a bimorph-based strain sensor. Figure 9 shows three samples, 9–11, having VDF/TrFE/CTFE mole ratios of 60.0/35.1/6.9, 59.3/32.9/7.8, and 57.3/31.2/11.5, respectively. At ambient temperature, the longitudinal strain was about 4.5% for samples 10 under an electric field of 130 MV/m. A nearly straight line of S versus P^2 for sample 10 indicates the electrostrictive response in the VDF/TrFE/CTFE terpolymer. Based on the electrostrictive relationship $S = QP^2$, this yields an electrostrictive coefficient Q of about -5.57 m^4/C^2.

IV. OTHER FERROELECTRIC POLYMERS

A. Ferroelectric Nylon

1. Polymeric and Crystal Structure

The discoveries of piezoelectric and pyroelectric properties in PVDF polymer led to the search for other classes of novel ferroelectric polymeric materials. Recently, odd-numbered nylons have emerged as a new class of ferroelectric polymer similar to PVDF. These materials have attracted much interest in the past two decades because of the stability of their electroactive properties at relatively high temperatures and relatively high electromechanical coupling coefficient.

Polyamides, commonly known as nylons, have molecular repeated units of $(-HN(CH_2)_xCO-)$. Generally, nylons are named after the number of carbon in the repeating unit of the polymer backbone. For example if $x = 5$, the corresponding nylon is identified as nylon-5.

Nylons with an odd number of carbon atoms are called "odd nylons" and nylons with an even number of carbon atoms are called "even nylons." Other categories of polyamides having molecular repeating units of $[-HN(CH_2)_xNHOC(CH_2)_yCO-]$ are termed odd–odd nylons if the numbers of carbon atoms in the repeating units (x and y) are both odd numbers. Nylons are prepared by melt polymerization solution and interfacial polymerization, ring-opening polymerization, and anionic polymerization. The morphology and degree of crystallinity of the nylons depend on the basic structure of their chemical linkages. Strong interactions between the amide group of neighboring chains account for the unique physical properties of nylons, such as toughness, stiffness, high melting points, and low coefficients of friction.

Odd nylons and odd–odd nylons are important classes of ferroelectric polymers. Nylons crystallize in all-*trans* conformation and are packed so as to maximize the hydrogen bonds between the adjacent amine and carbonyl groups, as seen in Fig. 10. The dipoles of odd nylons are aligned in the same direction and give rise to a large dipole moment and spontaneous polarization in the unit cell of the crystalline phase, whereas the dipole components of even nylons cancel each other out. The density
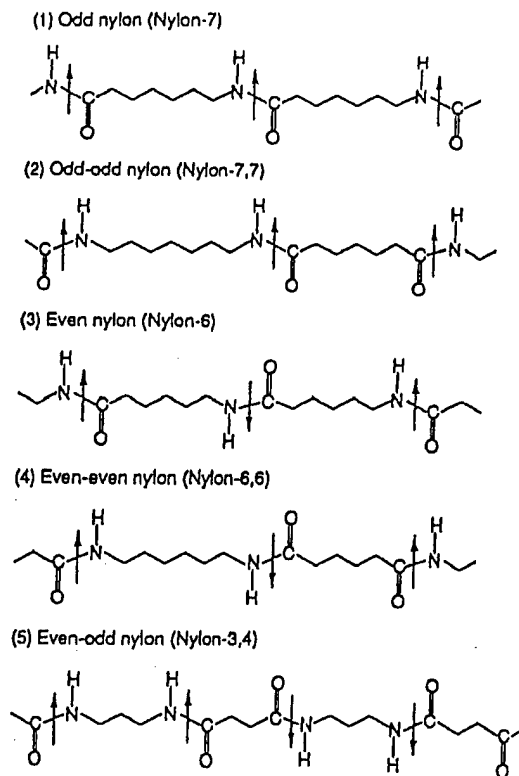

FIGURE 10 All-*trans* conformation of odd-numbered and even-numbered nylons. Arrows indicate the dipole direction.

of NH···C=O dipoles per unit volume of nylon is larger for lower-numbered nylons; thus nylon-5 is expected to possess a larger dipole moment (i.e., remnant polarization) than nylon-7, nylon-9, and nylon-11. Indeed, the experimental results show that the remnant polarization of nylon-5 is ~135 mC/m^2. Odd-numbered nylons have polymorphs. Nylon-11 has at least five different crystal structures: triclinic α form I, monoclinic form II, pseudo-hexagonal γ form III, δ' phase, γ' and phase. The α form of nylon-11 is polar in nature, with dipoles that are hydrogen-bonded and aligned in the same direction, whereas the γ form is nonpolar and has amide groups that lie in the plane perpendicular to the chain axis. The crystal phase transformation of nylon-11 occurs between a triclinic α form and a pseudo-hexagonal γ form at high temperature (>90°C) through the randomization of the hydrogen bonding. Polymorphs of nylon-9, nylon-5,7, and nylon-7,7 have also been prepared. The α form seems to be the most common polymorph in many odd-numbered nylons.

2. Ferroelectricity and Related Properties

Nylons exhibit very interesting dielectric behavior in that the dielectric constant changes significantly with changes in temperature and frequency. The dielectric constants of poled and annealed nylons are relatively low (about 2.5–3) at various frequencies below 0°C, and increase rapidly above the glass transition. The peak position, magnitude of dielectric constant, and relaxation process in nylons change with poling conditions and the presence of absorbed water. Several articles have been focused on the high-frequency properties that are of interest for ultrasonic transducers.

The pyroelectricity and piezoelectricity of the α and γ phases of nylon-11 films with variation of poling conditions have been reported. The γ phase nylon films show much higher piezoelectric response than α-phase films under the same poling conditions. This characteristic difference was interpreted as the breaking and re-forming of hydrogen bonds under a high electric field. The γ phase has a more regular arrangement of dipoles and has stronger hydrogen bonding, and thus is more strongly influenced by an applied electric field. However, it is found that a mixture of α phase and γ phase, rather than pure α phase or γ phase, has the highest piezoelectric constants. The piezoelectricity and pyroelectricity of odd nylons were also affected by anisotropy, absorbed water, orientation, and annealing temperature.

Ferroelectric properties of nylons have been investigated by several research groups. Polarization reversal was found to be complete in a few tens of milliseconds under 140 MV/m at 20°C. This fast polarization reversal and the rectangular D–E hysteresis loop are evidence of the

dipoles' origin. The effect of annealing on the ferroelectric behavior of nylon-11 and nylon-7 has been investigated. The remanent polarization decreases with increasing annealing temperature and disappears at an annealing temperature of 185°C, whereas the coercive field increases as annealing temperature increases, indicating the rearrangement of the hydrogen bonding structure. The mechanism of ferroelectric polarization in odd nylons has not been addressed, except for nylon-11. The ferroelectricity of poled nylon-11 is related to the hydrogen bond breaking, followed by the reorientation of the amide groups toward the electric field's direction and the re-forming of hydrogen bonds in a new direction. The orientation is retained in the glassy state below T_g even after the electric field is removed. Ferroelectricity has also been observed in polyamides containing m-xylylenediamine, aliphatic dicarboxylic acids, and fluorinated odd–odd nylons.

Ferroelectricity in aliphatic odd nylons has been reported recently. Unlike nylons with ring systems, in which the ferroelectric nature arises from the orientation of the amide dipoles in the amorphous region, the ferroelectric polarization of aliphatic odd nylons originates from the crystalline phases. A slightly higher density of amide dipoles contributes to a larger value for the remanent polarization, as seen in other nylon systems. Recently, a new class of ferroelectric and piezoelectric polymers, nylon-11/PVDF laminated films prepared by a co-melt-pressing method, has been reported. The laminated films exhibit a typical ferroelectric hysteresis loop with high remanent polarization, higher than that observed in PVDF homopolymers or nylon-11 under the same measurement conditions. The film's piezoelectric stress constant ($d_{31} = 41$ pC/N) and piezoelectric strain constant ($e_{31} = 109$ mC/m^2) are significantly higher than those of PVDF and nylon-11. Another new class of ferroelectric polyamides recently reported is the ferroelectric polyamide blends. The D–E hysteresis curves were observed in all blends of nylon 6I/6T copolymers (6 = hexamethylenediamine, I = isophthalic acid, T = terephthalic acid) and m-xylylenediamine-6 (MXD6). It was concluded that the intermolecular exchange of hydrogen bonding in the amide groups is responsible for the ferroelectricity.

B. Cyanopolymers

Cyanopolymers discussed here include polyacrylonitriles (PAN), poly(vinyl cyanide), and cyanocopolymers. The cyano group (C—CN) has the unique feature of a large dipole moment (3.5 D) and the ability to form complexes with transition metals. The polymerization can occur through free radical and ionic polymerization, leading to nonstereoregular (atactic) cyano groups in the polymer structure. Thus, cyanopolymers have no clear melting

temperature because of their high cohesive force and low thermal stability. It has been accepted that the strong interaction and repulsion of the cyano groups force polymer chains to adopt a helical conformation. However, the all-*trans* conformation is more stable.

The ferroelectricity of poled and annealed PAN has been studied by X-ray and IR spectroscopy. It is believed that the ferroelectricity of PAN is related to the dipole orientation and kinking of the chain above the glass transition temperature. The piezoelectric and pyroelectric properties of PAN were initially studied by Ueda and Carr, and were proved by Von Berlepsch using copolymer with methylacrylate. The $D-E$ hysteresis loop of a stretched film of this copolymer has been measured at 68°C, which is below the glass transition temperature. The copolymer showed very low remanent polarization and high coercive field at low temperature. However, an alternating copolymer of PAN, poly(allycyanide[35%]/acrylonitrile[65%]), showed very high remanent polarization, 200–700 mC/m^2 at 105°C.

Another alternating copolymer that has received more attention as an amorphous copolymer is vinylidene cyanide/vinyl acetate copolymer. The dipole moment of the repeating unit is 4.5 D in *trans* conformation, thus contributing to a large piezoelectric constant after poling. The piezoelectricity (d_{31}) of drawn and poled films is comparable to that of PVDF in the temperature range 20–100°C. Interestingly, this copolymer shows a very large dielectric strength of more than 100, one of the largest values among polymers. It is concluded that the large dielectric relaxation strength originates from the cooperative motion of 10 or more CN dipoles. The exceptionally high dielectric peaks occur near the glass transition temperature, similar to a ferroelectric transition. A most unique feature of this copolymer is its low density, which results in low acoustic impedance, close to the levels seen in water and the human body. This makes this copolymer very useful in medical applications.

C. Polyureas and Polythioureas

Polyureas and polythioureas are amino resins, and are thermosetting polymers. They are usually synthesized by condensation polymerization, and their products are mostly in the form of powder. The preparation of thin films was not possible due to their insolubility until a technique of vapor deposition polymerization was developed. The synthesis and characterization of different kinds of thin-film polyureas have been reported. A typical polymerization consists in vapor deposition of monomers onto the surface of a substrate in a vacuum chamber. The monomers diffuse on the surface and react with each other to form urea bonds between an amino (NH$_2$) group and an iso-

cyanate (CNO) group. The urea bond (NHCONH) has a dipole moment of 4.9 D and is responsible for high piezoelectric and pyroelectric properties.

The dielectric constants of aromatic polyureas [P(4,4'-diphenylmethane diisocyanate (MDI)/4,4'-diamino diphenylmethane (MDA)] have been reported. The dielectric constant of MDA-rich films of poled and annealed P(MDA/MDI) are relatively constant up to 200°C, whereas the MDI-rich films have a low dielectric constant but show good stability up to 200°C. The dielectric constants of the balanced stoichiometric films increase with increasing temperatures above 100°C. Pyroelectric and piezoelectric constants are also large for the balanced composition films. This is due to the fact that a crosslinked network structure does not form in balanced film the way it does in unbalanced films. The high-molecular-weight molecules are oriented or crystallized in a local region under a high poling field and form a semicrystalline structure; thus, stabilized residual polarization is produced and gives rise to high piezoelectric and pyroelectric constants.

The pyroelectric and piezoelectric properties of aliphatic polyureas display similar features to those seen in nylons, i.e., there is no observation of these activities if the number of carbon atoms between the urea bond is even. This is because alternating urea bond dipoles arrange in antiparallel direction, and the dipole moments cancel out. Strong hydrogen bonds are possible in cases where the parallel orientation of dipoles in a planar zigzag chain gives rise to high glass transition and melting temperatures. Dielectric peaks above 125°C have been observed in poly(heptamethylene/nanomethyleneurea). The relatively large dielectric constant is believed to be related to the crystal transition from the mobile dipole state to the rigid dipole state corresponding to the different hydrogen bonding states. The value of remanent polarization obtained from $D-E$ hysteresis of the same sample is as high as 200–440 mC/m^2 at 90°C, which may be attributed to the effect of the ionic currents of impurities. The remanent polarization disappears above 110°C, which suggests the rearrangement of the hydrogen bonding at this temperature.

Polythioureas are known pyroelectric, pyroelectric, and ferroelectric polymers. Their chemical structure is H$_2$N—CS—NH$_2$. Ferroelectric thiourea polymers have been prepared by condensation reaction of thiourea and formaldehyde under different conditions. Thiourea [SC(NH$_2$)$_2$] has a large dipole moment of 5.4 D. Ferroelectricity in polythioureas was initially studied in 1978. The sharp dielectric constant of thiourea-formaldehyde (PTUBFB) observed at 145°C is as high as 320. Recently, an odd-numbered aliphatic polythiourea, polythiourea-9, has been synthesized. The odd number of carbons was chosen to ensure a polar chain and polar packing. Large

dielectric relaxation as well as a large dielectric constant were observed in the glass transition region. According to the theoretical data of Meakins *et al.*, the dielectric relaxation and dielectric loss increase with any increase in hydrogen bonding. As a result, the hydrogen-bonded thiourea dipoles in the intermolecular chains are easily rotated under an electric field above the glass transition. The ferroelectric transition in thiourea is essentially due to both crystalline domains and an "incommensurate phase," which are due to both hydrogen bonding and dipole interactions. The $D-E$ hysteresis was first observed in drawn polythiourea-9 above T_g. The remanent polarization is very small. This may be due to the fact that only a small amount of chains can form hydrogen bonding. Therefore, the remanent polarization stabilized by hydrogen bonding is small.

D. Polyurethane

Polyurethanes have emerged as nonlinear optic, ferro-electric, and piezoelectric materials in which molecular structures can be tailored for specific applications. Polyurethanes have the chemical structure [$-(CH_2)_x OC(O)NH(CH_2)_y NHCO(O)-$]. The dipole moment of the urethane group is 2.8 D. Polyurethanes are usually composed of a polyester or polyether soft segment and a diisocyanate-based hard segment. From the viewpoint of the chemical structure of the hard segments, polyurethanes can be classified into urethane polymers (PU), which are formed by extending a diisocyanate with low-molecular-weight diols, and urethane–urea polymers (PUU), which are formed by extending a diisocyanate with low-molecular-weight diamine. Polyurethanes undergo microphase separation due to the immiscibility of the hard-segment and soft-segment. The hard segment domain acts as the physical crosslink as well as the filler particles for the soft-segment matrix. The driving force of the domain formation is the strong intermolecular interaction of the hydrogen bondings between the hard–hard segments and the urea/urethane linkages.

Both the temperature dependence and pressure–temperature effects on the dielectric constant and relaxation processes of aliphatic polyurethanes have been studied. The relaxation times for both the I process, associated with the molecular motion in hard segments, and the α process, associated with the glass transition temperature, increase with pressure, and that these shifts are much more pronounced for the I process. Dielectric properties of polyurethanes were also studied as a function of drawing and poling effects.

The $D-E$ hysteresis of polyurethanes can be obtained above the glass transition temperature (at 70°C). Ferro-electricity originated from the crystal region by control-

ling the hydrogen bonding. Recently, there was a report on the origin of ferroelectricity that suggested it derives from the amorphous region above the glass transition temperature. The electrostrictive responses, which are proportional to the square of the electric field, have been investigated in polyurethane. The field-induced strain was found to be very sensitive to the processing conditions and the thickness of the specimen. The increase of the strain response as the sample thickness is reduced is suggested to be caused by a nonuniform electric field across the thickness direction. In nonpiezoelectric materials, the field-induced strain can be caused by the electrostrictive and also the Maxwell stress effects. Experimental results show that the Maxwell stress can significantly contribute to the strain response at temperatures higher than the glass transition temperature, and that the electrostrictive coefficient is much higher than those of other materials.

V. APPLICATIONS

In recent years, many kinds of piezoelectric devices have been developed from organic polymer materials and widely used in industrial settings as well as in medical instruments. These device applications can be grouped into sensors, medical instrumentation, robotics, low- or audiofrequency transducers, ultrasonic and underwater transducers, electroacoustic transducers, electromechanical transducers, actuators, pyroelectric devices, and optical devices. The pyroelectric, biomedical, and robotic applications and the optical devices will not be discussed here.

The first commercial application of piezoelectric polymer film was in audio transducers (tweeters) and loudspeakers. The merits of ferroelectric polymers for piezoelectric devices over ferroelectric ceramics is their softness, light weight, toughness, flexibility, and ability to be fabricated into large sheets. In addition to these traits, they have a good electromechanical coupling factor and much lower acoustic impedance (this property is proportional to the product of density and stiffness) than ferroelectric ceramics. Therefore, they are suitable for acoustic applications in media such as air, water, and human tissue. Such applications include audio transducers (headphones, microphones, loudspeakers.), underwater acoustic hydrophones, and biomedical transducers (sensors and probes, imaging systems, and acoustic sources). Another merit of polymer piezoelectrics is their thin-film-forming ability. This could lead to very promising applications, such as ultrasonic transducers or paperlike speakers for the future's thin TVs, decorations, and interiors. The main disadvantages of polymer piezoelectrics are

their relatively low piezoelectric constant and relatively poor dimensional stability.

Devices based on the conversion of a mechanical input (stress or strain) into an electrical output signal are often used as sensors to detect displacement, stress, vibration, and sound. Typical sensors are hydrophones, blood pulse counters, blood pressure meters, pressure sensors, acceleration sensors, shock sensors, vibration sensors, touch sensors, microphones, antinoise sensors, and keyboards. Reverse devices, in which the input is an electrical signal and the output is a mechanical signal, include position controls, acoustic systems, and actuators.

BIBLIOGRAPHY

Brown, L. F., Scheinbeim, J. I., and Newman, B. A. (1995). *Ferroelectrics* 171, 321.

Chung, T. C., and Janvikul, W. (1999). *J. Organomet. Chem.* 581, 176.

Cross, L. E. (1996). *Ceram. Trans.* 68, 15.

Furukawa, T., Date, M., Fukada, E., Tajitsu, Y., and Chiba, A. (1980). *Jpn. J. Appl. Phys.* 19, L109.

Kawai, H. (1969). *Jpn. J. Appl. Phys.* 8, 1975.

Lovinger, A. J. (1982). "Poly(vinylidene Fluoride)." *In "Developments in Crystalline Polymers,"* Vol. 1, pp. 195–273 (Basett, D.C., ed.). Applied Science. London.

Lovinger, A. J. (1983). *Science* 220, 1115.

Nalwa, H. S. (1991). *J. Macromol. Sci. Rev. Macromol. Chem. Phys.* C-31, (4), 341.

Nalwa, H. S. (ed.). (1995). "Ferroelectric Polymers." Marcel Dekker. New York.

Ueda, H., and Carr, S. H. (1984). *Polymer J.* 16, 661.

Von Berlepsch, H., Kunstler, W., and Danz, R. (1988). *Ferroelectrics* 81, 353.

Wang T. T., Herbert, J. M., and Glass A. M. (eds.). (1988). "The Applications of Ferroelectric Polymers," Blackie. Chapman and Hall, Glasgow.

Zhang, Q. M., Bharti, V., and Zhao, X. (1998). *Science* 280, 2102.

Synthesis of Syndiotactic Polystyrene (s-PS) Containing a Terminal Polar Group and Diblock Copolymers Containing s-PS and Polar Polymers

Guangxue Xu and T. C. Chung*

Department of Material Science and Engineering, The Pennsylvania State University, University Park, Pennsylvania 16802

Scheme 1

One of the major advantages of metallocene technology is in the preparation of syndiotactic polystyrene (s-PS),[1] which is a semicrystalline polymer with a high melting temperature (>270 °C). Despite the unique thermal properties, the s-PS polymer resembles regular atactic polystyrene (a-PS) prepared by free radical or anionic initiators in that it has a very poor impact strength and a low surface energy. The absence of polar groups in hydrophobic polystyrene restricts their end uses, especially where adhesion to substrates (metals, ceramics, glass, etc.) and compatibility[2] with polar polymers are desired. So far, there are only few reports discussing the functionalized s-PS polymer, including sulfonated s-PS[3] and hydroxylated s-PS[4] prepared via a poly(styrene-*co*-4-*tert*-butyldimethylsilyloxystyrene) precursor.

The in situ chain transfer reaction to the molecule containing the heteroatom during the transition metal coordination polymerization of α-olefins presents a very convenient method of preparing polyolefins containing a terminal polar group. A couple of years ago, Marks et al.[5] reported that some organosilanes having Si–H groups are effective chain transfer agents in metallocene-mediated polymerizations that result in silane-terminated polyolefins and copolymers. Recently, we reported a new organoborane chain transfer agent[6] containing a B–H group, such as a 9-borabicyclo[3.3.1]nonane (9-BBN), that can also effectively engage in chain transfer reaction during zirconocene-catalyzed ethylene polymerizations. The resulting borane-terminated polyethylene is a very versatile intermediate in the preparation of poly(ethylene-*b*-methyl methacrylate) diblock copolymer.

In this communication, we will explore this B–H chain transfer reaction in titanocene-catalyzed styrene polymerizations for the preparation of two new types functionalized s-PS polymers, including a s-PS having a terminal polar group and a diblock copolymer containing a s-PS and a polar polymer. The reaction scheme is illustrated in Scheme 1.

With the appropriate choice of reaction conditions and catalyst systems to prevent potential side reactions, such as hydroboration of styrene and reaction between borane and cocatalyst, the ligand exchange reaction takes place between B–H and Ti–polymer chain during the syndiospecific styrene polymerization to obtain the borane-terminated syndiotactic polystyrene (s-PS-t-B). The borane terminal group can be easily interconverted to a hydroxy group under mild reaction conditions, or spontaneously transformed to a peroxide (B–O–O–C)
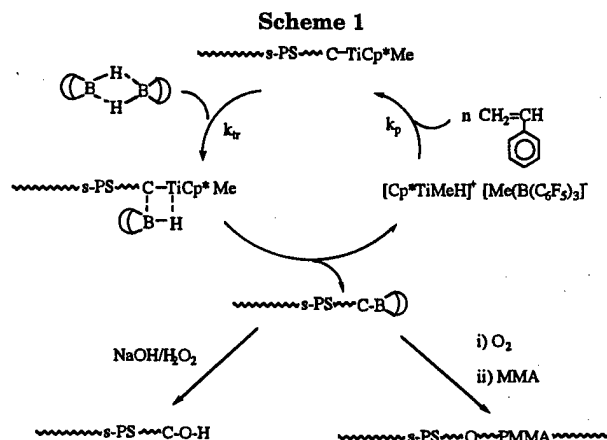
species by oxidation with oxygen. The B–O–O–C species formed will further decompose to a stable polymeric (C–O*) radical and a borinate radical (B–O*). The alkoxyl radical is active in initiating polymerization of functional monomers.[7] On the other hand, the borinate radical (B–O*) is too stable to initiate polymerization due to the back-donating of electrons to the empty p-orbital of boron. However, this "dormant" borinate radical may form a reversible bond with the radical at the growing chain end to prolong the lifetime of the propagating radical.[8] Overall, the reaction process resembles a transformation reaction from metallocene coordination polymerization to living free radical polymerization via a borane group at the polymer chain end. Since the reaction only involves one borane group per polymer chain, the whole reaction process provides an ultimate test for examining the effectiveness of borane chain transfer agents and the efficiency of the borane reagent in the chain extension process.

A metallocene polymerization with in situ chain transfer reaction was conducted in an autoclave reactor by mixing the designated quantities (shown in Table 1) of styrene, 9-BBN, toluene, and a [Cp*TiMe₂]⁺[MeB(C₆F₅)₃]⁻ complex, under rigorously anhydrous/anaerobic conditions. To minimize mass transfer and to maintain the constant 9-BBN/styrene ratio, the reactions were carried out by rapid mixing and with a short reaction time.

After 3 min of reaction time, the polymer solution was quenched with anhydrous/anaerobic MeOH, and the resulting borane-terminated s-PS (s-PS-t-B) was washed with anhydrous/anaerobic THF to remove excess 9-BBN. The s-PS-t-B was then dried at 50 °C on a high-vacuum line. Some of the s-PS-t-B polymer was oxidized by NaOH/H₂O₂ reagents at 40 °C for 6 h to form a hydroxy-terminated polymer (s-PS-t-OH). For the ¹H NMR study, the terminal hydroxy group was further reacted with Cl–Si(CH₃)₃ to form silane-terminated s-PS (s-PS-t-O–Si(CH₃)₃). Figure 1a shows the ¹H NMR spectra of a s-PS-t-O–Si(CH₃)₃ sample with a molecular weight of about 15 000.

There are two sets of major peaks at 1.45 and 2.10 ppm, corresponding to the CH₂ and CH protons in the s-PS backbone, and at 6.82 and 7.21 ppm, corresponding to the protons of the phenyl groups that have a syndiotactic arrangement. In addition, two minor peaks at 0.15 and 3.81 ppm correspond to the protons of the –O–Si-

* To whom all correspondence should be addressed

Table 1. Metallocene-Activated Styrene Syndiospecific Polymerization in the Presence of 9-BBN as Chain Transfer Agent[a]

run	amt of 9-BBN (μmol)	reacn time (min)	yield (g)	catalyst activity[b]	syn.[c] (%)	T_m (°C)	$[\eta]$	$M_w{}^d$
1	25	3	1.3	2600	97.0	270	1.270	460 000
2	50	3	1.4	2800	96.2	271	0.806	240 000
3	100	3	1.3	2600	95.8	270	0.580	150 000
4	150	3	1.1	2200	95.2	271	0.373	80 000
5	200	3	0.8	1600	93.4	270	0.340	70 000
6	300	3	0.5	1000	94.7	272	0.188	30 000
7	400	3	0.3	600	95.0	270	0.116	15 000
8	500	3	0.1	200	93.2	270	0.087	10 000

[a] Styrene = 10 mL. Catalyst = $[Cp^*TiMe_2]^+[Me(B(C_6F_5)_3]^-$; catalyst concentration = 10 μmol. [b] Catalyst activity = kg of s-PS/mol of Ti·h. [c] Syndiotactic index was determined by ^{13}C NMR. [d] Molecular weight was determined from the intrinsic viscosity in o-dichlorobenzene at 135 °C: $[\eta] = 1.38 \times 10^{-4}M_w{}^{0.7}$.

Figure 2. Plot of average molecular weight of s-PS-t-B vs 1/[9-BBN].

Figure 1. ^1H NMR spectrum of (a) s-PS-t-O−Si(CH₃)₃ and the corresponding diblock copolymers, (b) s-PS-*b*-PMMA and (c) s-PS-*b*-PBMA. (solvent, $C_2D_2Cl_4$; temperature, 110 °C).

$(CH_3)_3$ and $-CH(Ph)-OSi(CH_3)_3$ groups, respectively. The combination of peak intensity ratio between silane and phenyl groups and the molecular weight of polymer
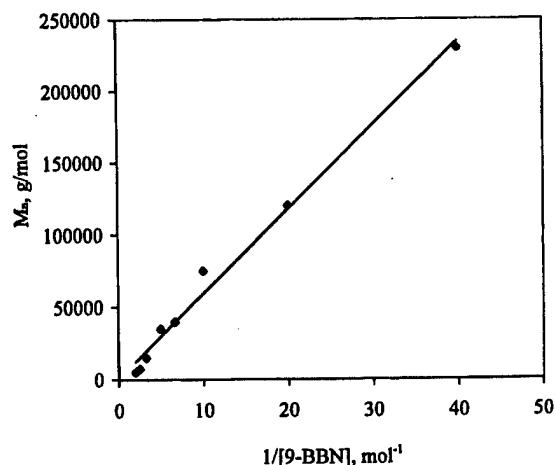
indicates that most of the s-PS polymers contain a terminal silane group. The silane terminal group in each s-PS polymer implies the effective in situ chain transfer reaction as well as the oxidation and silation reactions, despite of the heterogeneous reaction conditions. Most of the borane and silane terminal groups are located in the amorphous phases, and are readily accessible for the reaction.

The effects of the chain transfer reaction are further revealed by the reduction of polymer molecular weight in the presence of 9-BBN. Figure 2 shows the plot of polymer molecular weight vs the 1/[9-BBN] for the comparative runs 1−8 in Table 1.

Basically, the higher the concentration of 9-BBN chain transfer agent used, the lower the molecular weight of the resulting polystyrene. The catalyst activity was somewhat depressed if a high concentration of 9-BBN was presented in the system, which may reflect the competitive coordination at the titanocene active sites between monomers and chain transfer agents. The polymer molecular weight is almost linearly proportional to 1/[9-BBN]. It is clear that the chain transfer reaction to 9-BBN is the dominant termination process. It is very interesting to note that all s-PS-t-B polymers have similar syndiotacticity and melting temperature (shown in Table 1) to those of s-PS polymer. The 9-BBN chain transfer agent did not interfere the regio- and stereoselective insertion process.

Most of the s-PS-t-B polymer was suspended in benzene and subjected to the oxidation reaction by oxygen in the presence of free radical polymerizable monomers, i.e., methyl methacrylate (MMA) and n-butyl methacrylate (BMA). As illustrated in Scheme 1, the borane-terminated s-PS was selectively oxidized and transformed to a stable polymeric radical for polymerization of MMA and BMA. The resulting reaction mixture was carefully fractionated by Soxhlet extraction using boiling THF to remove any PMMA or PBMA homopolymers. In most cases, only a very small amount (about 10%) of homopolymer was present and which may have been initiated by the radical in a bicyclic ring, instead of a polymeric radical, due to the nonselective oxidation reaction of alkyl-9-BBN. The insoluble fraction is primarily s-PS-*b*-PMMA or s-PS-*b*-PBMA diblock copolymer. Parts b and c of Figure 1 show the ^1H NMR spectra of the s-PS-*b*-PMMA and s-PS-*b*-PBMA copolymers, respectively. The new peak at 3.78 ppm is

Table 2. Summary of SPS-*b*-PMMA and SPS-*b*-PBMA Diblock Copolymers

| run | T (°C) | sPS-t-B (g) | O_2 (mL) | polar monomer | | reacn time (h) | yield (g) | polystyrene block | | p-MMA block | |
				monomer	concn (M)			$10^{-3}M_n$	M_w/M_n	$10^{-3}M_n{}^a$	unit ratio
1	25	5	1.9	MMA	1.87	3	5.43	15.0	2.2		
2	25	5	1.9	MMA	1.87	6	6.25	15.0	2.2	2.0	100:14
3	25	5	1.9	MMA	1.87	12	7.56	15.0	2.2	5.0	100:35
4	25	5	1.9	MMA	1.87	24	9.98	15.0	2.2	14.0	100:97
5	25	3	1.5	MMA	1.87	6	4.25	10.0	2.4	1.7	100:18
6	40	3	1.5	MMA	1.87	12	5.56	10.0	2.4	4.1	100:43
7	60	3	1.5	MMA	1.87	24	7.23	10.0	2.4	10.5	100:109
8	25	7	2.4	MMA	1.87	6	7.56	70.0	2.1	3.0	100:4.5
9	25	7	2.4	MMA	1.87	12	8.13	70.0	2.1	8.0	100:12
10	25	7	2.4	MMA	1.87	24	8.98	70.0	2.1	17.0	100:25
11	25	5	1.9	BMA	1.87	10	6.72	15.0	2.2	7.1	100:35
12	25	5	1.9	BMA	1.87	20	7.56	15.0	2.2	15.0	100:72
13	25	5	1.9	BMA	1.87	24	8.94	15.0	2.2	18.3	100:89

[a] Determined by ^{1}H NMR with reference to M_n values of the initial polystyrene.
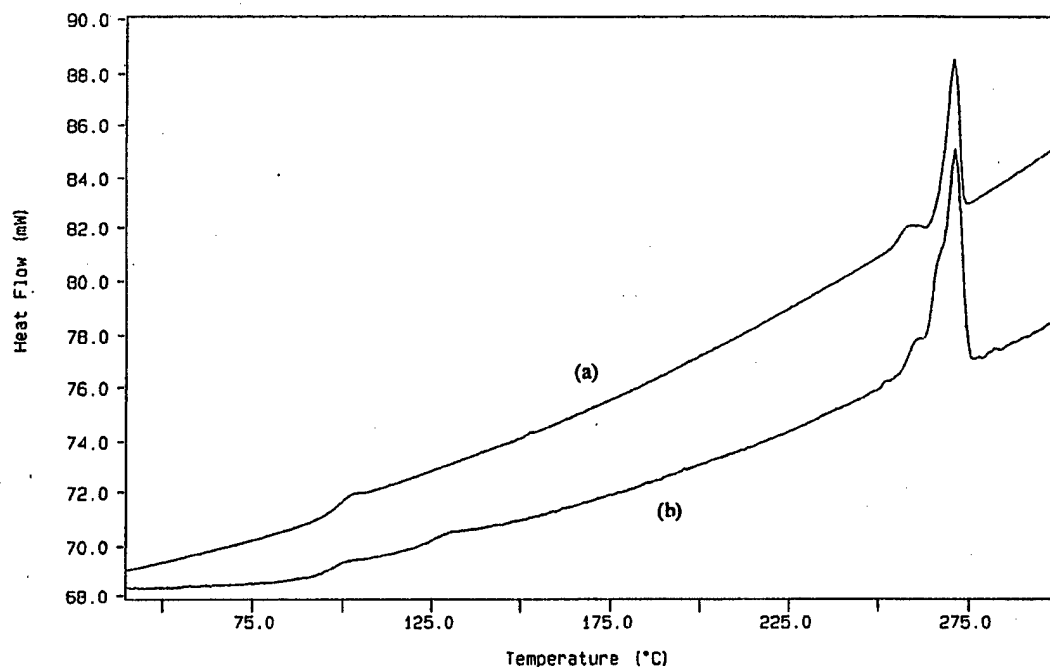
Figure 3. DSC curve comparison between (a) s-PS-t-OH polymer and (b) the corresponding s-PS-*b*-PMMA.

assigned to the methoxyl groups (OCH_3) in the PMMA block, and the peak at 4.15 ppm is assigned to the methylene groups (OCH_2) in the PBMA block. Apparently, a very high concentration of polar polymer blocks can be incorporated in the s-PS diblock copolymers.

Table 2 summarizes the reaction conditions and results of the diblock copolymers.

In general, both PMMA and PBMA blocks increase with increased the reaction time, and chain extension reactions continue even after 12 h. Diblock copolymers with a nearly 1/1 mole ratio of [styrene]/[MMA] or [styrene]/[BMA] have been prepared, despite the heterogeneous reaction conditions. These effective and long-life chain extension reactions provide strong evidence of the borane group existence at the s-PS chain end and imply the living free radical chain extension process. Figure 3 compares two DSC curves of s-PS-t-B (run 7 in Table 1) and the corresponding s-PS-*b*-PMMA (run 4 in Table 2).

Two identical thermal transition temperatures, including a T_m near 270 °C and a T_g near 100 °C for the s-PS polymer, were observed in both samples. A clear new T_g at about 130 °C (corresponding to the high

molecular weight PMMA polymer[7]) was shown in Figure 3b. Both polymer segments in the s-PS-*b*-PMMA copolymer must have long consecutive (undisturbed) sequences to form separate domains.

In summary, this research clearly demonstrates a novel method that can be used to prepare new functionalized s-PS polymers, namely s-PS containing a terminal polar group and a s-PS diblock copolymer containing a s-PS and a polar polymer blocks. The in situ chain transfer reaction to borane (B—H) during titanocene-catalyzed styrene polymerization provides a convenient and effective route for preparing borane-terminated s-PS that is a very valuable intermediate for preparing functionalized s-PS with a polar end group or diblock copolymer containing a polyolefin and functional (polar) polymer segments.

Supporting Information Available: Text giving experimental details for this work, including instrumentation and

materials and syntheses. This material is available free of charge via the Internet at http://pubs.acs.org.

References and Notes

(1) (a) Ishihara, N.; Seimiya, T.; Kuramoto, M.; Uoi, M. *Macromolecules* **1986**, *19*, 2464. (b) Thayer, A. M. Metallocene Catalysts Initiate New Era In Polymer Synthesis. *Chem. Eng. News* **1995**, *11*, 1–20. (c) Campbell, R. E., Jr.; Hefner, J. G. Int. Pat. Appl. WO88-10276, 1988. (d) Chien, J. C. W.; Salajka, Z. *J. Polym. Sci., Part A* **1991**, *29*, 1253. (e) Xu, G. *Macromolecules* **1998**, *31*, 586.

(2) (a) Lee, S. H.; Li, C. L.; Chung, T. C. *Polymer* **1994**, *35*, 2980. (b) Xu, G.; Lin, S. *J. Macromol. Sci.—Rev. Macromol. Chem. Phys.* **1994**, *C34*, 555.

(3) Orler, E. B.; Moore, R. B. *Macromolecules* **1994**, *27*, 4774.

(4) Kim, K. H.; Jo, W. H.; Kwak, S.; Kim, K. U.; Kim, J. *Macromol. Rapid Commun.* **1999**, *20*, 175.

(5) (a) Fu, P.-F.; Marks, T. J. *J. Am. Chem. Soc.* **1995**, *117*, 10747. (b) Koo, K.; Marks, T. J. *J. Am. Chem. Soc.* **1998**, *120*, 4019. (c) Koo, K.; Fu, P.-F.; Marks, T. J. *Macromolecules* **1999**, *32*, 981.

(6) Xu, G.; Chung, T. C. *J. Am. Chem. Soc.* **1999**, *121*, 1.

(7) (a) Chung, T. C.; Jiang, G. J. *Macromolecules* **1992**, *25*, 4816. (b) Chung, T. C.; Janvikul, W.; Bernard, R.; Jiang, G. J. *Macromolecules* **1994**, *27*, 26. (c) Lu, B.; Chung, T. C. *Macromolecules* **1998**, *31*, 5943.

(8) Chung, T. C.; Lu, H. L.; Janvikul, W. *J. Am. Chem. Soc.* **1996**, *118*, 705.

Synthesis of Syndiotactic Polystyrene Derivatives Containing Amino Groups

Guangxue Xu and T. C. Chung*

*Department of Materials Science and Engineering, The Pennsylvania State University,
University Park, Pennsylvania 16802*

Received February 18, 2000; Revised Manuscript Received May 31, 2000

ABSTRACT: This paper discusses a new family of syndiotactic polystyrene (s-PS) derivatives containing the amino group, including poly(4-aminostyrene), poly(4-aminomethylstyrene), and poly(4-aminoethyl-styrene). These semicrystalline polymers exhibit high melting temperatures (350 °C) and relatively fast crystallization rates. These functional syndiotactic polymers are prepared in two steps. Syndiospecific polymerization of a styrene derivative containing a masking *N,N*-bis(trimethylsilyl)amino group is achieved by using a half-sandwich titanocene/perfluoroborane catalyst system. This study focused on the catalyst system (catalyst and cocatalyst) that can polymerize functional monomers with high catalyst activity and syndiotacticity. Acid hydrolysis leads to the complete recovery of primary amino groups in s-PS derivatives.

Introduction

One of the most interesting features of metallocene catalysis is the preparation of syndiotactic polystyrene (s-PS) by half-sandwich titanocene catalysts,[1] such as CpTiCl₃/MAO and [Cp*Ti(CH₃)₃/B(C₆F₅)₃]. The s-PS polymers with high crystallinity exhibit many unique properties, superior to traditional atactic polystyrene (a-PS) prepared by anionic or free radical initiators and isotactic polystyrene (i-PS) prepared by heterogeneous Ziegler–Natta catalyst. The combination of high melting temperature (270 °C) with relatively high crystallization rate, low dielectric constant, high chemical resistance, and low specific gravity makes s-PS an attractive material for many applications in the electronic, packaging, and automotive industries.

Despite some unique properties, s-PS polymer resembles a-PS polymer with poor impact strength and low surface energy. The absence of polar groups in hydrophobic polystyrene restricts their end uses, especially where adhesion to substrates (metals, ceramics, glass, etc.) and compatibility[2] with polar polymers are desired. So far, there are only few reports discussing functionalized s-PS copolymers, including sulfonated s-PS,[3] hydroxylated s-PS[4] prepared via poly(styrene-*co*-4-*tert*-butyldimethylsilyloxystyrene) precursor, and s-PS-*b*-PMMA prepared via borane-terminated s-PS.[5]

It has been a long-standing scientific challenge and industrially interesting subject to prepare poly(R-olefin)s containing functional (polar) groups,[6] such as alcohol, amine, ether, ester, etc., by Ziegler–Natta (Z–N) polymerization. The facile acid–base interaction between catalytic sites (Lewis acid) and functional groups (Lewis base) usually prohibits the polymerization reaction. Two general approaches of preventing catalyst poisoning include the protection of functional groups by bulky substituents[7] (masking groups) and precomplexation of the functional group with Lewis acids, such as the alkylaluminum cocatalyst.[8] Many attempts in conventional Ziegler–Natta systems, containing group III or IV transition metal halides and alkylaluminum cocata-

lysts, showed only very limited success. Most of these efforts were in the copolymerization reactions of R-olefins with a small amount of protected functional comonomers.

Recently, interest in the functionalization approach has been renewed by using metallocene catalysts. Zirconocene/methylaluminoxane (MAO) catalysts were used in copolymerization[9] of ethylene and propylene with a small amount of comonomers that have large spacers between the olefin and the functional group, including 1-hydroxy-10-undecene,[9] 1-chloro-10-undecene,[10] *N,N*-bis(trimethylsilyl)-1-amino-10-undecene,[11] and *o*-heptenylphenol.[12] It is believed that MAO (in large excess) may serve as an in-situ protection agent to prevent catalyst deactivation. In fact, the pretreatment of functional monomer with MAO before initiation significantly increases the catalyst activity. Similar pretreatment using trimethylaluminum (TMA)[13] also showed good copolymerization results between R-olefins and hydroxy- and amino-containing monomers using zirconocene/MAO catalysts. It is interesting to note that the benefit of TMA-protected functional monomers in the copolymerizations[15] is also extended to the less oxophilic late transition metal catalysts.

Waymouth et al.[14] reported the advantage of perfluoroborane cocatalysts (replacing MAO in the metallocene catalyst) that were compatible with the protected functional groups. They successfully demonstrated the homopolymerization of several masked monomers, i.e., 5-(*N,N*-diisopropylamino)-1-pentene and 4-trimethylsiloxy-1,6-heptadiene, in good yields using zirconocene/perfluoroborane catalysts. However, stereospecific polymerization of functional olefin monomers with metallocene catalysts, especially titanocene systems, is an open research area. Detailed experimental results are needed to understand the effects of protected functional group on catalyst activity, stereoselectivity, and polymer molecular weight.

Results and Discussion

In this paper, we will discuss stereospecific homopolymerization of functional styrene derivatives, containing amino groups, using half-sandwich titanocene cata-

* To whom all correspondence should be addressed.

Scheme 1

n : 0, 1, and 2.

G: Si(CH$_3$)$_3$ masking group.
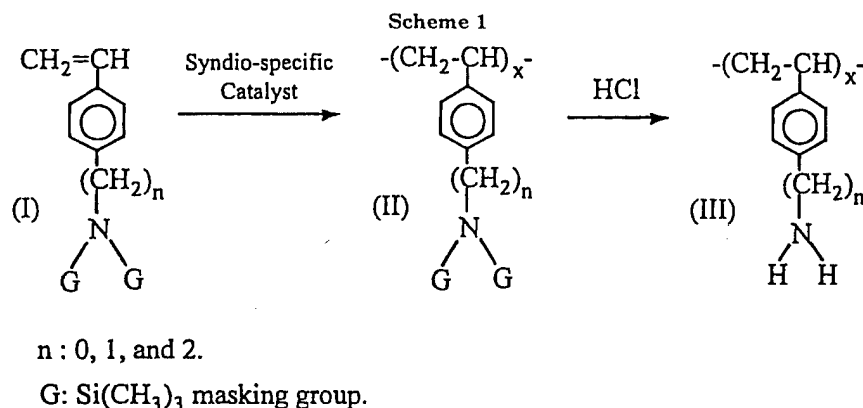
lysts. The chemistry affords a new family of functional s-PS homopolymers with high syndiotacticity, including syndiotactic poly(4-aminostyrene), poly(4-aminomethylstyrene), and poly(4-aminoethylstyrene). The research plan was formulated with several intriguing questions and objectives in mind. (i) Because the titanocene cation is generally more oxophilic than the corresponding zirconocene ion, is it still possible to homopolymerize the protected functional monomers in such an environment with high functional group concentration? (ii) How does the bulky protected functional group in the monomer affect the stereoselectivity of active site? (iii) Is it possible to manipulate active site with bulky ligands in the catalyst and/or cocatalyst to prevent acid–base complexation further and therefore enhance catalyst activity, polymer molecular weight, and syndiotacticity of the polymer? (iv) The resulting new syndiotactic functional s-PS homopolymers containing primary amino groups may be very interesting materials in terms of high surface energies, high melting temperatures, and fast crystallization rates due to strong hydrogen bonding.

The preparation of syndiotactic functional polystyrene homopolymers involves a two-step process as illustrated in Scheme 1. After polymerization of the styrene derivatives (I) containing the protected amino group, the resulting s-PS derivatives (II) were then deprotected by acid hydrolysis to recover primary amino groups along the polymer chain (III).

All polymers formed were analyzed by ¹H, ¹³C NMR, DSC, GPC, and intrinsic viscosity to determine their molecular structures.

Syndiotactic Polystyrene Derivatives Containing Masked Amino Groups. As discussed, the polymerization study focused on suitable masking groups, initiators, and co-initiators that afford syndiotactic polystyrene derivatives with high syndiotacticity and catalyst activity. Two masking groups, including methyl and trimethylsily groups, were evaluated in the polymerization reaction along with several half-sandwich titanocene catalysts, including Cp*TiMe$_3$, Cp*TiCl$_3$, IndTiMe$_3$, [2-Me-Benz[e]Ind]TiMe$_3$, and [2-Ph-Phen[e]-Ind]TiMe$_3$, and co-initiators, including MAO, B(C$_6$F$_5$)$_3$, [Ph$_3$C]⁺[B(C$_6$F$_5$)$_4$]⁻, [HNMe$_2$Ph]⁺[B(C$_6$F$_5$)$_4$]⁻, and tris-(2,2′,2″-nonafluorobiphenyl)borane (PBB). In addition, a control polymerization of styrene was carried out under the same reaction conditions to understand the effect of the protected functional group on the polymerization reaction.

Figure 1 shows the ¹H NMR spectrum of three trimethylsilyl protected polymers prepared from 4-(*N,N*-bis(trimethylsilyl)amino)styrene, 4-(*N,N*-bis(trimethylsilyl)aminomethyl)styrene, and 4-(*N,N*-bis(trimethylsilyl)aminoethyl)styrene monomers.

There are five common peaks in all three spectra, the peak at 0.15 ppm, corresponding to Si(CH$_3$)$_3$ protons of the masking group, two aliphatic proton peaks at 1.5 and 2.0 ppm, corresponding to the CH$_2$ and CH protons in the polymer backbone, and two distinctive aromatic peaks around 7 ppm, corresponding to two sets of aromatic protons in the para-substituted phenyl groups that have a syndiotactic arrangement along the polymer chain. The detailed analysis of syndiotacticity will be discussed in further ¹³C NMR studies. In
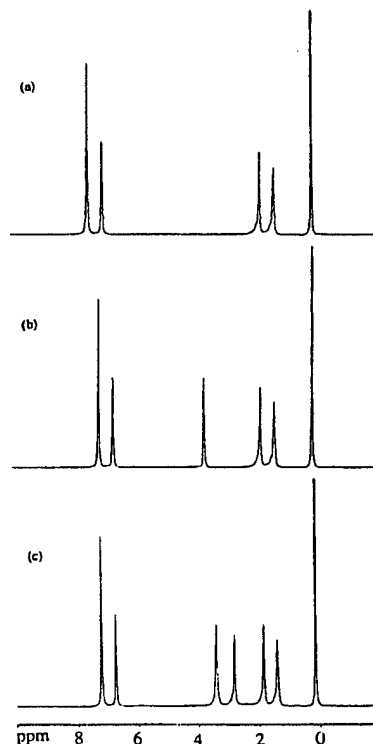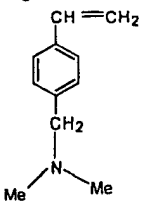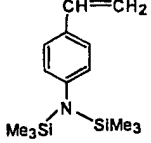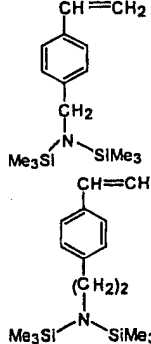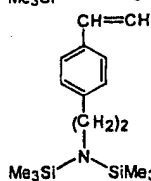

Figure 1. ¹H NMR spectra of (a) poly(4-(*N,N*-bis(trimethylsilyl)amino)styrene), (b) poly(4-(*N,N*-bis(trimethylsilyl)aminomethyl)styrene), and (c) poly(4-(*N,N*-bis(trimethylsilyl)aminoethyl)styrene.

Table 1. Polymerization of Styrenic Monomers Using $Cp^*TiMe_3/B(C_6F_5)_3$ Catalyst[a]

monomer	[catalyst] (mM)	[monomer] (M)	conversion (wt %)	activity[b] ($\times 10^{-6}$)	syndiotactic[c] (%)	T_g^d (°C)	T_m^d (°C)	$[L]_{inh}^e$ (dL/g)
styrene (CH=CH₂ on benzene)	0.6	1.28	96.5	11.15	97.1	100	270	0.75
4-(dimethylaminomethyl)styrene	9.5	1.30	8.5	0.10	35.8	115	278 (weak)	0.04
4-(N,N-bis(trimethylsilyl)amino)styrene	5.0	1.27	45.0	1.58	76.5	157	325	0.12
4-(N,N-bis(trimethylsilyl)aminomethyl)styrene	5.0	1.30	80.2	2.97	85.2	152	330	0.29
4-(N,N-bis(trimethylsilyl)aminoethyl)styrene	2.5	1.28	90.1	7.00	90.5	138	320	0.45

[a] Polymerization conditions: at 35 °C for 60 min, $Cp^*TiMe_3/B(C_6F_5)_3$) 1, toluene solvent) 15 mL. [b] Activity in units of g of polymer/ (mol of Ti) (mol of monomer) (h). [c] Portion of syndiotactic polymer, insoluble in 2-butanone and determined by ^{13}C NMR. [d] Determined by DSC at a heating rate of 10 °C/min. [e] Inherent viscosity, [L], determined in 1,2,4-trichlorobenzene at 130 °C.

addition, one peak at 3.75 ppm in Figure 1b is assigned to the protons of the -CH₂-N group and two peaks at 2.88 and 3.45 ppm in Figure 1c are assigned to the protons of the -CH₂-CH₂-N group. The good agreement between expected and measured peak intensity ratios for the protons in each group indicates, within the experimental error, that all three reaction products are clean.

Table 1 compares the polymerization results of styrene derivatives containing masked amino groups and styrene (control reaction) using $Cp^*TiMe_3/B(C_6F_5)_3$ catalyst under similar reaction conditions.

Homopolymerization of 4-(dimethylaminomethyl)styrene gave a very low polymer yield, with less than 1% of catalyst activity compared to that of styrene. The poor catalyst activity may due to the inadequate steric protection of the amino group by the two methyl groups. On the other hand, all three trimethylsilyl protected monomers, i.e., 4-(N,N-bis(trimethylsilyl)amino)styrene, 4-(N,N-bis(trimethylsilyl)aminomethyl)styrene, and 4-(N,N-bis(trimethylsilyl)aminoethyl)styrene, exhibited good catalyst activities. Especially, 4-(N,N-bis(trimethylsilyl)aminoethyl)styrene, having a spacer of two methylene groups between styrene and the protected amino group, showed close to 70% of the reactivity of styrene. A relatively weak interaction between the protected functional group and active sites may still exist, and locating the functional group further away from the

olefin unit is clearly advantageous in minimizing the acid-base complexation.

The influence of the functional group on the polymerization reaction was also evident in the polymer structure. Both polymer molecular weight and syndiotacticity paralleled catalyst activity. About 90% of poly-(4-(N,N-bis(trimethylsilyl)aminoethyl)styrene) obtained was syndiotactic polymer with high molecular weight (M_w) 10.5 $\times 10^4$; M_n) 4.6 $\times 10^4$ g/mol), determined by gel permeation chromatography (GPC). The narrow molecular distribution (M_w/M_n) 2.3), similar to s-PS homopolymer, strongly indicates the negligible effect of functional group on the catalytic site during the polymerization reaction.

Because the masking amino group in 4-(N,N-bis-(trimethylsilyl)amino)styrene has some effects on the polymerization, it was very interesting to study this system further in terms of the nature of the catalytic site, especially the relationship between bulky ligands in the catalyst and/or cocatalyst and the catalyst activity and syndiotacticity of the resulting polymer. Table 2 summarizes the results for 4-(N,N-bis(trimethylsilyl)-amino)styrene using various half-sandwich titanocene catalyst systems.

Comparing the first four polymerization reactions, using the same Cp^*TiMe_3 catalyst and four different borane cocatalysts, the bulky tris(2,2',2''-nonafluorobiphenyl)borane (PBB) shows significantly higher catalyst

Table 2. Syndiospecific Polymerization of 4-(N,N-Bis(trimethylsilyl)amino)styrene with Titanocene Catalysts[a]

catalyst + cocatalyst	[catalyst] (mM)	[monomer] (M)	conversion (wt %)	activity[b] (10^6)	syndiotactic[c] (%)	T_g (°C)[d]	T_m (°C)[d]	[L] (dL/g)[e]
Cp*TiMe₃ + B(C₆F₅)₃	5.0	0.95	44	2.32	76.5	160	325	0.12
Cp*TiMe₃ + [Ph₃C]⁺[B(C₆F₅)₄]⁻	5.0	0.95	65	3.42	78.2	158	325	0.14
Cp*TiMe₃ + [HNMe₂Ph]⁺[B(C₆F₅)₄]⁻	5.0	0.96	40	2.11	67.8	157	324	0.07
Cp*TiMe₃ + PBB	3.0	0.94	90	7.90	94.5	160	325	0.28
IndTiMe₃ + B(C₆F₅)₃	5.0	0.95	40	2.11	70.6	158	323	0.14
[2-Me-Benz[e]Ind]TiMe₃ + B(C₆F₅)₃	3.0	0.95	75	6.59	85.7	160	326	0.24
[2-Me-Cp[l]Phen]TiMe₃ + B(C₆F₅)₃	3.0	0.95	86	7.55	90.2	159	327	0.38
Cp*TiMe₃ + MAO (100)	10.0	0.95	5	0.13				
Cp*TiCl₃ + MAO (1000)	10.0	0.96	10	0.26	46.7	158	318	0.08

[a] Polymerization conditions: at 35 °C for 60 min, toluene) 10 mL, [catalyst]/[cocatalyst]) 1 except MAO cases. [b] Activity in units of g of polymer/(mol of Ti) (mol of monomer) (h). [c] Portion of syndiotactic polymer, insoluble in 2-butanone and determined by ^{13}C NMR. [d] Determined by DSC at a heating rate of 10 °C/min. [e] Inherent viscosity, [L], determined in 1,2,4-trichlorobenzene at 130 °C.

activity (more than 2–3 times higher than the others) and the highest content (94.5%) of syndiotactic polymer. The large (PBB–CH₃)⁻ anion, associated with the half-sandwich titanocene cation, apparently prevents any acid–base interaction between the active sites and the silane-protected amino groups. In addition, it does not reduce the coordination capacity or insertion of R-olefin. In fact, both catalyst activity and syndiotactic polymer content surpasses the levels for 4-(N,N-bis(trimethyl-silyl)aminoethy)styrene) as shown in Table 1. Similar steric effects were also observed in the catalyst itself. In a second set of comparative reactions, using various titanocene catalysts and the same B(C₆F₅)₃ cocatalyst, significantly higher catalyst activity and content of syndiotactic polymer were observed in the polymerization using ([2-Me-Cp[l]Phen]TiMe₃/B(C₆F₅)₃ catalyst with a bulky ligand. It is interesting to note that all catalyst systems using MAO cocatalyst produced very low yields of polymer, which may be associated with the interaction between MAO and the silane-protected functional group. Overall, the experimental results clearly show the advantages of combined protection mechanisms, including masking group, spacer, and bulky ligands in catalyst and cocatalyst. All of them appear to have no effect on the syndiospecific polymerization of styrene derivatives.

Syndiotactic Polystyrene Derivatives Containing Primary Amino Groups. The trimethylsilyl protected amino groups in polymer II were converted to primary amino groups by hydrolysis followed by neutralization. The complete removal of trimethylsilyl groups was evidenced by ¹H NMR spectra (Figure 2). Three resulting polymers, i.e., poly(4-aminostyrene), poly(4-methyleneaminostyrene), and poly(4-ethylene-aminostyrene), were prepared from the three corresponding protected polymers shown in Figure 1.

The silane groups, with a chemical shift near 0.15 ppm, were removed to beyond the detectable level in all samples. New chemical shifts appear at 3.95 ppm (Figure 2a) and 2.47 ppm (Figure 2b), corresponding to -NH₂ and -CH₂NH₂ in poly(4-aminostyrene) and poly-(4-aminomethylstyrene), respectively. The chemical shift for -CH₂-CH₂NH₂ in poly(4-aminoethylstyrene) (Figure 2c) appears at 3.45 ppm, which almost overlaps with the peak at 3.40 ppm, corresponding to -CH₂-CH₂NH₂. The rest of resonances for aliphatic and aromatic protons remain unchanged, indicating a clean and selective deprotection reaction. It is very interesting to note that two sharp aromatic resonances, compared with those of the corresponding atactic polystyrene derivatives[16] prepared by living anionic polymerization, imply the steric regularity along the polymer chain.
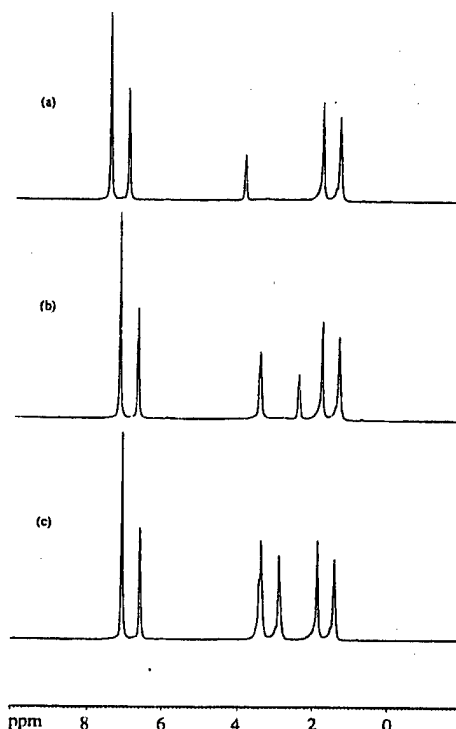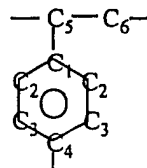

Figure 2. ¹H NMR spectra of (a) poly(4-aminostyrene), (b) poly(4-aminomethylstyrene), and (c) poly(4-aminoethylstyrene).

Stereostructure of polymer was further examined by ¹³C NMR. Figure 3 shows ¹³C NMR spectra of poly(4-aminostyrene), poly(4-aminomethylstyrene), and poly-(4-aminoethylstyrene).

All peaks are sharp and assigned to the corresponding carbon atoms in the polymer structures. The presence of a single resonance for the quaternary C₁ carbon in phenyl groups (at 140.2 ppm in Figure 3a, 142.1 ppm in Figure 3b, and 142.5 ppp in Figure 3c) shows that these polymers are highly syndiotactic.

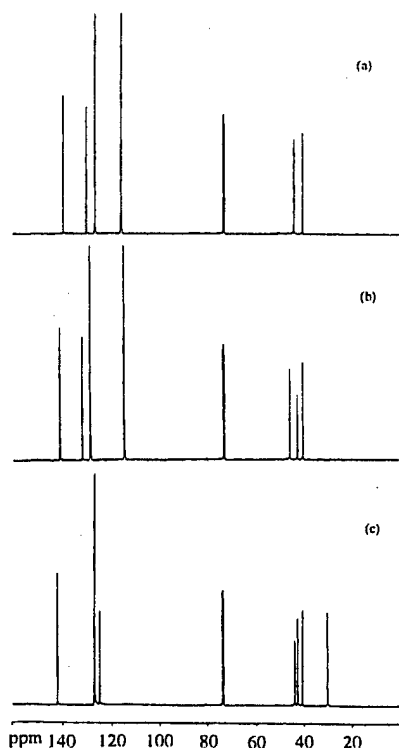
The same conclusion can be reached by considering two

Figure 3. ^{13}C NMR spectra of (a) poly(4-aminostyrene), (b) poly(4-aminomethylstyrene), and (c) poly(4-aminoethylstyrene).

Figure 4. DSC curves of (a) poly(4-(N,N-bis(trimethylsilyl)-amino)styrene), (b) poly(4-(N,N-bis(trimethylsilyl)aminomethyl)styrene), and (c) poly(4-(N,N-bis(trimethylsilyl)aminoethyl)-styrene.

Figure 5. DSC curves of (a) poly(4-aminostyrene), (b) poly-(4-aminomethylstyrene), and (c) poly(4-aminoethylstyrene).

C_5 and C_6 aliphatic carbons in the polymer backbone. Figure 3a shows two sharp resonances at 45.0 and 41.5 ppm, corresponding to methine C_5 and methylene C_6 in a highly stereoregular environment. In Figure 3b, in addition to C_5 and C_6 carbons (peaks at 43.8 and 41.5 ppm, respectively), a new resonance at 47.0 ppm corresponds to the methylene carbon atom in the –CH_2–NH_2 group. In Figure 3c, two C_5 and C_6 carbon resonances (peaks at 43.2 and 41.0 ppm, respectively) are accompanied by two new resonances at 44.4 and 30.2 ppm, corresponding to –CH_2–CH_2–NH_2 and –CH_2–CH_2–NH_2, respectively. It is interesting to note that the sharp resonance feature resembles those of syndiotactic polystyrene but is very different from several reported atactic polystyrene derivatives containing chloro and methoxy groups[17] prepared with other catalyst systems.

After deprotection, the molecular weight distribution of the polymer remains narrow (M_w/M_n) 2.4) with an expected reduction in polymer molecular weight (M_w) 8.4 10^4; M_n) 3.5 10^4 g/mol), estimated by standard polystyrene calibration.

DSC Studies. Differential scanning calorimetry (DSC) was used to measure the melting temperature of new polymers. Figures 4 and 5 show DSC curves of two sets of samples studied in Figures 1 and 2, respectively.

All samples were measured under the same thermal treatment, and the curves were recorded in the second heating cycle. In general, every sample shows a melting endotherm, indicative of semicrystalline morphology. Their melting temperatures are significantly higher than that of s-PS (270 °C). In Figure 4, three silane-protected polymers show melting points around 320 °C. In Figure 5, after deprotection the melting point in-
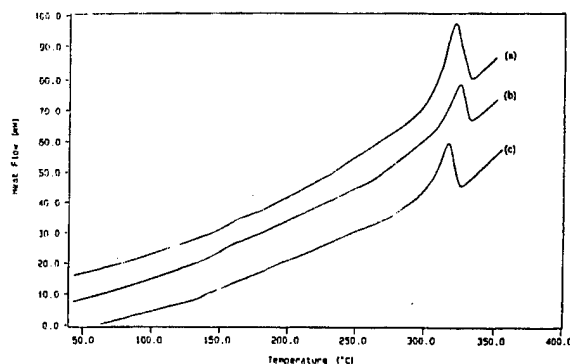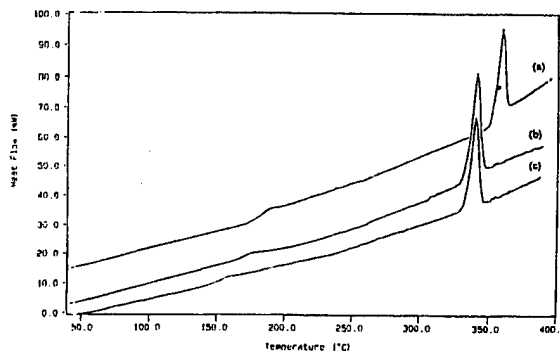
creases to about 340 °C for poly(4-aminomethylstyrene) and poly(4-aminoethylstyrene) and about 360 °C for poly(4-aminostyrene). It is very interesting to note that the endothermic peak becomes very sharp in all three NH_2-containing polymers, implying well-organized and uniform crystalline structure. The hydrogen bonding between NH_2 groups may also enhance the crystallization rate.

Experimental Section

All manipulations of air- and moisture-sensitive chemicals were performed with the rigorous exclusion of oxygen and moisture in flamed Schlenk-type glassware on a dual manifold Schlenk line or interfaced to a high-vacuum (10^{-6} Torr) line or in a argon-filled glovebox with a high-capacity recirculator (< 1 ppm of O_2).

Materials. Anhydrous hexane, tetrahydrofuran (THF), heptane, pentane, diethyl ether, and toluene were purified by refluxing over Na–K alloy/benzophenone ketyl under nitrogen for at least a week followed by distillation. Styrene, 4-aminostyrene, 4-chlorostyrene, N-(4-vinylbenzyl)-N,N-dimethylamine, and 4-vinylbenzyl chloride were purchased from Aldrich or Fisher Scientific and dried over calcium hydride for 5 h at room temperature and distilled under reduced pressure prior to use. Trimethylsilyl chloride (Aldrich) was distilled from CaH_2 and degassed before use. Cp*TiCl$_3$ (Cp*) $\L^5$-C_5Me_5), IndTiCl$_3$, B(C_6F_5)$_3$, Cp$_2$ZrMe$_2$, Cp*$_2$ZrMe$_2$ hexamethyldisilazane, ethylmagnesium bromide, benzylmagnesium chloride, lithium bis(trimethylsilyl)amide, and chloromethyl methyl ether were purchased from Aldrich and used without further purification. (2-Methylbenz[e]indenyl)trichlorotitanium ([2-Me-Benz[e]Ind]TiCl$_3$),[18] 2-methylcyclopenta-[l]-phenanthrene titanium trichloride ([2-Me-Cp[l]Phen]TiCl$_3$),[19]

[Ph$_3$C]$^+$ [B(C$_6$F$_5$)$_4$]$^-$,[20] [HNMe$_2$Ph]$^+$ [B(C$_6$F$_5$)$_4$]$^-$,[21] Cp*TiMe$_3$,[22] tris(2,2′,2″-nonafluorobiphenyl)borane (PBB),[23] *N,N*-bis(tri-methylsilyl)methoxymethylamine,[24] 4-(*N,N*-bis(trimethylsilyl)-amino)styrene,[25] 4-[*N,N*-bis(trimethylsilyl)aminomethyl]sty-rene,[26] and 4-[2-*N,N*-bis(trimethylsilyl)amino]ethyl]styrene[26] were prepared according to literature procedures.

Synthesis of IndTiMe$_3$. IndTiCl$_3$ (0.93 g, 3.46 mmol) was mixed with 40 mL of hexane in a 100 mL Schlenk tube in a drybox. The flask, equipped with a septum and a stir bar, was removed from the drybox, cooled to – 78 °C, and allowed to stir for 10 min. Three equivalents of MeLi was added as a 1.6 M solution in diethyl ether (6.5 mL, 10.4 mmol). The resultant red/orange solution was allowed to stir at this reduced tem-perature for 30 min before it was warmed to room temperature and allowed to stir for 4 h. The reaction mixture became a yellow suspension. Upon filtration of LiCl through a medium glass frit packed with Celite and elimination of the solvent under reduced pressure, 0.68 g (90% yield) of yellow IndTiMe$_3$ was obtained as a microcrystalline solid. Recrystallization from pentane at – 78 °C gave the product as yellow prisms that were sensitive to moisture and air. ^{1}H NMR (CDCl$_3$):   7.81 (m, 2H, arom H), 7.52 (m, 2H, arom H), 7.15 (d, 2H, CpH), 7.10 (t, 1H, CpH), 0.68 (s, 9H, Ti-Me).

Synthesis of [2-Me-Benz[*e*]Ind]TiMe$_3$ and [2-Me-Cp[*l*]-Phen]TiMe$_3$. Similar procedures (in the previous section) were followed for the addition of 3 equiv of MeLi to [2-Me-Benz[*e*]Ind]TiCl$_3$ (1.05 g, 3.14 mmol) solution to yield a orange solution. After stirring the solution overnight at room tem-perature, a white/yellow suspension was observed. Filtration and crystallization produced 0.73 g (85% yield) of yellow/beige microcrystalline [2-Me-Benz[*e*]Ind]TiMe$_3$ solid. The structure was confirmed by ^{1}H NMR (CDCl$_3$):   8.20- 8.25 (m, 1H, arom H), 7.55- 7.82 (m, 5H, arom H), 7.45 (d, 1H, CpH), 7.10 (d, 1H, CpH), 2.65 (s, 3H, CH$_3$), 0.75 (s, 9H, Ti- Me).

In the preparation of [2-Me-Cp[*l*]Phen]TiMe$_3$, MeMgCl (8.7 mmol) in THF was added to [2-Me-Cp[*l*]Phen]TiCl$_3$ solution. The resulting red/orange solution turned yellow after stirring overnight at room temperature. Filtration and crystallization produced 0.42 g (49% yield) of a yellow [2-Me-Cp[*l*]Phen]TiMe$_3$ powder. The structure was confirmed by ^{1}H NMR (CDCl$_3$): 8.55 (d, 2H, arom H), 8.17 (d, 2H, arom H), 7.70- 7.60 (m, 4H, arom H), 7.45 (s, 2H, CpH), 2.75 (s, 3H, CH$_3$), 0.77 (s, 9H, Ti- Me).

Polymerization. A 100 mL glass reactor equipped with a magnetic stirrer was attached to a high-vacuum line and then sealed under nitrogen. The reactor was then placed in a bath at the desired temperature. Freshly distilled anhydrous/anaerobic toluene was introduced through a syringe, followed by addition of anhydrous/anaerobic styrene monomers. A prescribed amount of the mixture of catalyst and cocatalyst in toluene was then quickly syringed into the rapidly stirred reaction system through an Ar-purged gastight syringe. After a measured time interval, the reaction was quenched with 10% HCl in methanol, filtered, and dried overnight in a vacuum oven at 80 °C. The polymer was then extracted with 2-bu-tanone for 48 h in a Soxhlet extractor to remove any atactic polymer. The percent of syndiotactic polymer was determined as the amount of polymer insoluble in 2-butanone and con-firmed by the ^{13}C NMR spectra.

Deprotection of Amino-Functionalized Syndiotactic Polystyrenes. Syndiotactic poly[4-(*N,N*-bis(trimethylsilyl)-amino)]styrene (2.0 g) was dissolved in *o*-dichlorobenzene (50 mL) at 110 °C and then cooled to 80 °C. To this solution was added dropwise 2 N methanolic hydrogen chloride solution. The mixture was stirred for 2.5 h at 80 °C, and the pH of the system was controlled between 3 and 5 during the reaction. The reaction mixture was then added slowly to 1 N methanolic KOH solution. The neutralized poly(4-aminostyrene) was collected and washed with 1 M aqueous ammonia and water under a nitrogen atmosphere. After the solution was removed, the polymer was dried overnight at 40 °C in a vacuum. The polymer yield was quantitative. Similarly, both syndiotactic poly(4-aminomethylstyrene) and poly(4-aminoethylstyrene) were obtained in almost quantitative yields.

Measurements. The inherent viscosity of the polymers was determined in 1,2,4-trichlorobenzene solutions at 135 °C. DSC curves were recorded with a Perkin-Elmer DSC-7 system at a heating rate of 10 °C/min. The melting temperature of the polymers was determined from the second heating scan. Both ^{1}N NMR and ^{13}C NMR spectra were recorded in 1,1,2,2-tetrachloroethane-*d$_2$* at 110 °C on a Bruker PX-300 spectrom-eter. The molecular weight and molecular weight distribution of polymers were determined by gel permeation chromatog-raphy (GPC) using a Waters 150 C instrument with a refrac-tive index (RI) detector and a set of u-Styragel HT columns of 10^6, 10^5, 10^4, and 10^3 pore size in series. The measurements were taken at 140 °C using 1,2,4-trichlorobenzene (TCB) as solvent and mobile phase at a flow rate of 0.7 mL/min. Polystyrene samples were used as standards for calibration.

Conclusion

In this work, a new family of syndiotactic styrenic polymers containing primary amino groups, including poly(4-aminostyrene), poly(4-aminomethylstyrene), and poly(4-aminoethylstyrene), has been described. With the combination of trimethylsilane masking group and a selective catalyst system, the styrene derivatives con-taining amino groups were homopolymerized to high polymers with high catalyst activity and high syndio-tactic polymer content (similar to s-PS). The effective removal of the masking group affords the desired polymers with high melting temperature and relatively fast crystallization rate.

References and Notes

(1) (a) Ishihara, N.; Seimiya, T.; Kuramoto, M.; Uoi, M. *Macro-molecules* **1986**, *19*, 2464. (b) Thayer, A. M. Metallocene Catalysts Initiate New Era In Polymer Synthesis. *Chem. Eng. News* **1995**, *11*, 1. (c) Ishihara, N.; Kuramoto, M.; Uoi, M. Eur. Patent, EP 210615, 1987; Chem. Abst. 106:177084P. (d) Chien, J. C. W.; Salajka, Z. *J. Polym. Sci., Part A* **1991**, *29*, 1253. (e) Xu, G. *Macromolecules* **1998**, *31*, 586.

(2) (a) Lee, S. H.; Li, C. L.; Chung, T. C. *Polymer* **1994**, *35*, 2980. (b) Xu, G.; Lin, S. *J. Macromol. Sci., Rev. Macromol. Chem. Phys.* **1994**, *C34* (4), 555.

(3) Orler, E. B.; Moore, R. B. *Macromolecules* **1994**, *27*, 4774.

(4) Kim, K. H.; Jo, W. H.; Kwak, S.; Kim, K. U.; Kim, J. *Macromol. Rapid Commun.* **1999**, *20*, 175.

(5) Xu, G.; Chung, T. C. *Macromolecules* **1999**, *25*, 8689.

(6) (a) Chung, T. C. *Macromolecules* **1988**, *21*, 865. (b) Chung, T. C.; Rhubright, D. *Macromolecules* **1993**, *26*, 3019.

(7) (a) Langer, A. W. U.S. Patent 3,755,279, 1973. (b) Purgett, M. D.; Vogl, O. *J. Polym. Sci., Part A: Polym. Chem.* **1988**, *26*, 677. (c) Wilen, C. E.; Auer, M.; Nasman, J. H. *J. Polym. Sci., Part A: Polym. Chem.* **1992**, *30*, 1163. (d) Bertolini, G.; Lanzini, L.; Marchese, L.; Roggero, A.; Lezzi, A.; Costanzi, S. *J. Polym. Sci., Part A: Polym. Chem.* **1994**, *32*, 961.

(8) (a) Clark, K. J.; City, W. G. U.S. Patent 3,949,277, 1970. (b) Schulz, D. N.; Kitano, K.; Burkhardt, T. J.; Langer, A. W. U.S. Patent 4,518,757, 1984; Chem. Abst. 103:73252P.

(9) (a) Aaltonen, P.; Lofgren, B. *Macromolecules* **1995**, *28*, 5353. (b) Aaltonen, P.; Fink, G.; Lofgren, B.; Seppala, J. *Macro-molecules* **1996**, *29*, 5255.

(10) Bruzaud, S.; Cramail, H.; Duvignac, L.; Deffieux, A. *Macro-mol. Chem. Phys.* **1997**, *198*, 291.

(11) Schneider, M. J.; Schafer, R.; Mulhaupt, R. *Polymer* **1997**, *38*, 2455.

(12) Wilen, C. E.; Nasman, J. H. *Macromolecules* **1994**, *27*, 4051.

(13) Marques, M. M.; Correia, S. G.; Ascenso, J. R.; Ribeiro, A. F. G.; Gomes, P. T.; Dias, A. R.; Foster, P.; Rausch, M. D.; Chien, J. C. W. *J. Polym. Sci., Part A: Polym. Chem.* **1999**, *37*, 2457.

(14) (a) Kesti, M. R.; Coates, G. W.; Waymouth, R. M. *J. Am. Chem. Soc.* **1992**, *114*, 9679. (b) Stehling, U. M.; Stein, K. M.; Kesti, M. R.; Waymouth, R. M. *Macromolecules* **1998**, *31*, 2019.

(15) Correia, S. G.; Marques, M. M.; Ascenso, J. R.; Ribeiro, A. F. G.; Gomes, P. T.; Dias, A. R.; Blais, M.; Rausch, M. D.; Chien, J. C. W. *J. Polym. Sci., Part A: Polym. Chem.* **1999**, *37*, 2471.

(16) Suzuki, K.; Yamaguchi, K.; Hirao, A.; Nakahama, S. *Macromolecules* **1989**, *22*, 2607.

(17) Grassi, A.; Longo, P.; Proro, A.; Zambelli, A. *Macromolecules* **1989**, *22*, 104.

(18) Foster, P.; Chien, J. C. W.; Rausch, M. D. *Organometallics* **1996**, *15*, 2404.

(19) Schneider, N.; Prosenc, M. H.; Brintzinger, H. H. *J. Organomet. Chem.* **1997**, *545*, 291.

(20) Chien, J. C. W.; Tsai, W. M.; Rausch, M. D. *J. Am. Chem. Soc.* **1991**, *113*, 8570.

(21) Stehling, U. M.; Stein, K. M.; Kesti, M. R.; Waymouth, R. M. *Macromolecules* **1998**, *31*, 2019.

(22) Mena, M.; Royo, P.; Serrano, R.; Pellinghelli, M. A.; Tiripicchio, A. *Organometallics* **1989**, *8*, 476.

(23) Chen, Y. X.; Metz, M. V.; Li, L.; Stern, C. L.; Marks, T. J. *J. Am. Chem. Soc.* **1998**, *120*, 6287.

(24) (a) Bestmann, H. J.; Wolfel, G. *Angew. Chem., Int. Ed. Engl.* **1984**, *23*, 53. (b) Morimoto, T.; Takahashi, T.; Sekiya, M. *J. Chem. Soc., Chem. Commun.* **1984**, 794.

(25) Suzuki, K.; Yamaguchi, K.; Hirao, A.; Nakahama, S. *Macromolecules* **1989**, *22*, 2607.

(26) Suzuki, K.; Hirao, A.; Nakahama, S. *Makromol. Chem.* **1989**, *190*, 2893.

JOURNAL
OF THE
AMERICAN
CHEMICAL
SOCIETY

A Novel Consecutive Chain Transfer Reaction to p-Methylstyrene and Hydrogen during Metallocene-Mediated Olefin Polymerization

T. C. Chung* and J. Y. Dong

*Contribution from the Department of Materials Science and Engineering,
The Pennsylvania State University, University Park, Pennsylvania 16802*

Received November 10, 2000

Abstract: This paper describes the first example of consecutive chain transfer reaction, first to p-methylstyrene (or styrene) and then to hydrogen, during metallocene-catalyzed propylene polymerization by rac-Me$_2$Si[2-Me-4-Ph(Ind)]$_2$ZrCl$_2$/MAO complex. The PP molecular weight is inversely proportional to the molar ratio of [p-methylstyrene]/[propylene] and [styrene]/[propylene] with the chain transfer constants of $k_{tr}/k_p = 1/6.36$ and $1/7.5$, respectively. Although hydrogen does not influence the polymer molecular weight, it greatly affects the catalyst activity. Each PP chain formed contains a terminal p-methylstyrene (or styrene) unit. The terminal p-MS unit can be metalated to form a stable polymeric anion for living anionic polymerization to prepare new PP diblock copolymers, such as PP-b-PS, which are very difficult to prepare by other methods. The overall process resembles a transformation reaction from metallocene to living anionic polymerization.

Introduction

The in situ chain transfer reaction during polymerization presents a very convenient route for introducing a reactive terminal group to the polymer chain end. It also offers an opportunity for the preparation of diblock copolymers by using the reactive terminal group as the linkage between two distinctive polymer blocks. This approach is particularly interesting in polyolefins[1] since the lack of functionality and poor compatibility with any other materials has imposed limitations on the application of polyolefins in many areas, such as in polymer blends and composites. The diblock copolymer is known to be the most effective compatibilizer[2] for improving the interfacial interaction between polymer and other materials.

So far, there are only a few reports describing the introduction of a reactive terminal group to polyolefin through a chain transfer reaction with chain transfer agents. Marks[3] first showed that some organosilanes having Si–H groups are effective chain transfer agents in metallocene-mediated polymerizations that result in silane-terminated polyolefins. In our laboratory, we observed that organoboranes having B–H groups are very effective chain transfer agents for forming borane-terminated polyolefins.[4] The terminal borane group transforms to a stable free radical initiator for chain extension that results in polyolefin diblock copolymers. Hessen[5] studied thiophene as a chain transfer agent in ethylene polymerization using a neutral lanthanum catalyst system. In general, the polymerization was sluggish with very low catalyst activity. Kim[6] also observed various modes of chain transfer reactions in the copolymeriza-

* To whom all correspondence should be addressed.

(1) (a) Chung, T. C.; Rhubright, D. *Macromolecules* **1991**, *24*, 970. (b) Chung, T. C.; Rhubright, D.; Jiang, G. J. *Macromolecules* **1993**, *26*, 3467. (c) Chung, T. C.; Lu, H. L.; Janvikul, W. *J. Am. Chem. Soc.* **1996**, *118*, 705. (d) Chung, T. C.; Lu, H. L.; Ding, R. D. *Macromolecules* **1997**, *30*, 1272. (e) Lu, H. L.; Hong, S.; Chung, T. C. *Macromolecules* **1998**, *31*, 2028.

(2) (a) Riess, G.; Periard, J.; Bonderet, A. *Colloidal and Morphological Behavior of Block and Graft Copolymers*; Plenum: New York, 1971. (b) Lohse, D.; Datta, D.; Kresge, E. *Macromolecules* **1991**, *24*, 561. (c) Lu, B.; Chung, T. C. *Macromolecules* **1999**, *32*, 2525. (d) Chung, T. C.; Rhubright, D. *Macromolecules* **1994**, *27*, 1313.

(3) (a) Koo, K.; Marks, T. J. *J. Am. Chem. Soc.* **1998**, *120*, 4019. (b) Fu, P.-F.; Marks, T. J. *J. Am. Chem. Soc.* **1995**, *117*, 10747. (c) Koo, K.; Fu, P.-F.; Marks, T. J. *Macromolecules* **1999**, *32*, 981.

(4) (a) Xu, G.; Chung, T. C. *J. Am. Chem. Soc.* **1999**, *121*, 6763. (b) Xu, G.; Chung, T. C. *Macromolecules* **1999**, *32*, 8689.

(5) Ringelberg, S. N.; Meetsma, A.; Hessen B.; Teuben, J. H. *J. Am. Chem. Soc.* **1999**, *121*, 6082.

(6) (a) Byun, D. J.; Kim S. Y. *Macromolecules* **2000**, *33*, 1921. (b) Byun, D. J.; Shin, D. K.; Kim S. Y. *Macromol. Rapid Commun.* **1999**, *20*, 419.

4872 *J. Am. Chem. Soc., Vol. 123, No. 21, 2001*

Chung and Dong

tion of ethylene and allylbenzene using the zirconocene/MAO catalyst system. When highly substituted catalysts were used, chain transfer to aluminum was preferred rather than β-hydride elimination. The suppression of β-hydride elimination was attributed to the unfavorable β-agostic interaction at the propagating active site having an allylbenzene end unit.

Results and Discussion

In this paper, we report a novel chain transfer reaction involving a combination of a styrenic molecule, including *p*-methylstyrene (*p*-MS) and styrene (S), and hydrogen during metallocene-catalyzed propylene polymerization. The research stemmed from several intriguing observations[7] during the copolymerization of propylene and *p*-MS using the *rac*-SiMe$_2$[2-Me-4-Ph(Ind)]$_2$ZrCl$_2$/MAO complex. The reaction was completely stalled in the very beginning of the copolymerization process. The catalyst's deactivation was speculated to be due to a steric jamming during the consecutive insertion of 2,1-inserted *p*-MS and 1,2-inserted propylene (k_{21} reaction), as illustrated in eq 1.

(III)

k_{21}
(very slow reaction) | 1,2-insertion
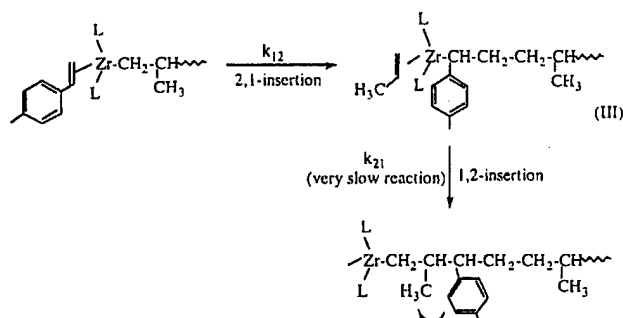
The combination of unfavorable 1,2-insertion of propylene (k_{21}) and lack of *p*-MS homopolymerization (k_{22} reaction) at the propagating site (III) drastically reduces catalyst activity. This hypothesis was supported by the effect[7] of a small amount of ethylene dramatically improving the catalyst activity. The sluggish propagating chain end (III) (which poses a difficulty in both the k_{21} and k_{22} reactions) allows the insertion of ethylene, which reenergizes the propagation process.

If the above hypothesis of catalyst deactivation proves correct, we might be able to take advantage of the dormant propagating site (III) to react with hydrogen, which not only recovers the catalytic site but also produces PP polymer with a terminal *p*-MS group. Equation 2 illustrates a general reaction scheme.
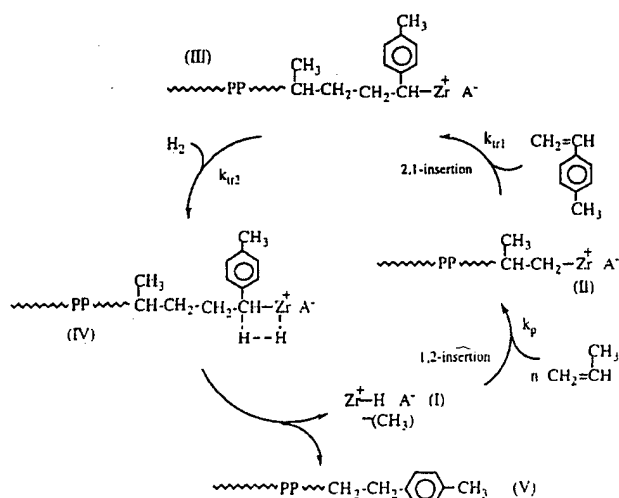
During the polymerization of propylene (with the 1,2-insertion method) the propagation Zr−C site (II) can also react with *p*-MS (with the 2,1-insertion method) to form a dormant propagating site (III) at the terminal *p*-MS unit. Although the catalytic Zr−C site in compound (III) becomes inactive to both propylene and *p*-MS, the dormant Zr−C site (III) can react with hydrogen to form *p*-MS terminated polypropylene (PP-*t*-*p*-MS) (V) and regenerate a Zr−H species (I) that is capable of reinitiating the polymerization of propylene and of continuing the polymerization cycles. In other words, the ideal chain transfer reaction will not significantly affect the rate of polymerization, but it reduces the molecular weight of the resulting polymer. The molecular weight of PP-*t*-*p*-MS will be linearly proportional to the molar ratio of [propylene]/[*p*-MS], and basically independent of the [propylene]/[hydrogen] ratio.

PP-*t*-S and PP-*t*-*p*-MS Polymers. This consecutive chain transfer reaction will be applicable to many α-olefin and styrenic molecules if several conditions are met to avoid undesirable side reactions, namely the copolymerization of α-olefin with styrenic molecules and several direct chain transfer reactions from the propagating olefinic chain end (II) to hydrogen, monomer, and β-hydride elimination. To this end, the *rac*-Me$_2$-Si[2-Me-4-Ph(Ind)]$_2$ZrCl$_2$/MAO catalyst is an excellent candidate[8] that produces highly regio and styrenic regular PP polymers with high molecular weight, and which exhibits no copolymerization activity with styrenic monomers and low undesirable chain transfer activity. The regioselective 1,2-insertion[9] of propylene is known to be the key factor to reduce the chain transfer reactions. As shown in two control reactions (3 and 4 in Table 1), this bridged catalyst system is quite insensitive to hydrogen, even in large dosages. Tables 1 and 2 summarize two systematic studies of propylene polymerization by using a *rac*-Me$_2$Si[2-Me-4-Ph(Ind)]$_2$ZrCl$_2$/MAO catalyst in the presence of *p*-methylstyrene/hydrogen and styrene/hydrogen chain transfer agents, respectively. The reactions resulted in *p*-MS terminated PP (PP-*t*-*p*-MS) and styrene-terminated PP (PP-*t*-S), respectively. In general, both systems showed very similar results. The in situ chain transfer reaction to *p*-MS/hydrogen in *rac*-Me$_2$Si[2-Me-4-Ph(Ind)]$_2$ZrCl$_2$/MAO catalyzed polymerization of propylene is evidenced by its comparison with two control reactions that were carried out under similar reaction conditions: without chain transfer agent (control 1) and with *p*-MS only (control 2). A small amount of *p*-MS effectively stops the polymerization of propylene. The introduction of hydrogen restores the catalyst activity, as shown in run A-1, which exhibits about 85% of the catalytic activity of control 1 (without chain transfer agents). Hydrogen is clearly needed to complete the chain transfer cycle during the polymerization. Comparing runs from A-1 to E−1 by altering *p*-MS concentration, we note that the higher the concentration of the *p*-MS, the lower the molecular weight of the resulting polymer. Polymer with very low molecular weight (just a few thousand) has been obtained, and the molecular weight distribution is generally narrow, which is consistent with single site polymerization processes. The catalyst activity was also proportionally depressed with the concentration of *p*-MS, which reflects the

(7) Lu, H. L.; Chung, T. C. *J. Polym. Sci. Part A: Polym. Chem.* **1999**, *37*, 2795.

(8) Spaleck, W.; Kuber, F.; Winter, A.; Rohrmann, J.; Bachmann, B.; Antberg, M.; Dolle, V.; Paulus, E. F. *Organometallics* **1994**, *13*, 954.

(9) (a) Chadwick, J. C.; Miedema, A.; Sudmejer, O. *Macromol. Chem. Phys.* **1994**, *195*, 167. (b) Chadwick, J. C.; van Kessel, G. M. M.; Sudmejer, O. *Macromol. Chem. Phys.* **1995**, *196*, 1431. (c) Jüngling, S.; Mülhaupt, R.; Stehling, U.; Brintzinger, H. H.; Fischer, D.; Langhauser, F. *J. Polym. Sci., Part A* **1995**, *33*, 1305. (d) Busico, V.; Cipullo, R.; Talarico, G. *Macromolecules* **1998**, *31*, 2387. (e) Lin, S.; Waymouth, R. M. *Macromolecules* **1999**, *32*, 8283.

Table 1. Comparison of the Experimental Results in the *rac*-Me$_2$Si[2-Me-4-Ph(Ind)]$_2$ZrCl$_2$/MAO Catalyzed Polymerization[a] of Propylene with *p*-MS/Hydrogen Chain Transfer Agents

run	*p*-MS (M)	H$_2$ (psi)	cat. activity[b]	*p*-MS in PP (mol %)	*p*-MS conversion (%)	M_n (×10^3)	PDI (M_w/M_n)	T_m (°C)
control 1	0	0	86 208	0		77.6	2.9	159.6
control 2	0.0305	0	0					
control 3	0	6	88 576	0		74.5	2.6	160.1
control 4	0	12	95 616	0		66.0	2.4	159.1
A-1	0.0305	28	73 760	0.15	50.51	56.1	1.9	159.3
A-2	0.0305	20	68 430	0.15	48.53	54.8	1.9	159.2
A-3	0.0305	16	52 536	0.14	38.78	53.6	1.9	159.7
A-4	0.0305	12	38 528	0.15	28.19	55.4	1.9	159.2
A-5	0.0305	6	25 728	0.15	18.83	54.8	2.0	159.2
A-6	0.0305	2	12 160	0.14	8.30	55.5	1.9	159.6
B-1	0.076	35	33 664	0.41	26.86	25.8	2.3	158.2
B-2	0.076	20	28 192	0.43	23.65	20.5	2.4	158.9
B-3	0.076	12	5 408	0.41	4.33	25.9	2.3	157.9
B-4	0.076	6	2 912	0.40	2.33	27.6	2.1	158.1
C-1	0.153	35	14 112	0.63	8.67	9.7	1.9	154.1
C-2	0.153	20	12 192	0.61	7.26	11.7	2.0	154.3
C-3	0.153	12	1 120	0.66	0.72	10.0	2.3	155.0
D-1	0.305	35	6 720	1.43	4.69	4.6	1.7[c]	152.9
D-2	0.305	20	4 704	1.47	3.28	4.4	1.8[c]	153.4
E-1	0.458	35	2 912	2.16	2.05	1.8	1.4[c]	145.6
E-2	0.458	20	1 728	2.24	1.22	1.8	1.4[c]	143.2

[a] Reaction conditions: 50 mL of toluene, propylene (100 psi), [Zr] = 1.25 × 10^{-6} mol/L, [MAO]/[Zr] = 3000, temperature = 30 °C, time = 15 min. [b] Catalyst activity = kg of PP/mol of catalyst·h. [c] Product distribution narrowed may be due to loss of GPC sensitivity for low molecular weight oligomers.

Table 2. Comparison of the Experimental Results in the *rac*-Me$_2$Si[2-Me-4-Ph(Ind)]$_2$ZrCl$_2$/MAO Catalyzed Polymerization[a] of Propylene

example	styrene (M)	H$_2$ (psi)	cat. activity[b]	styrene in PP (mol %)	styrene conversion (%)	M_n (×10^{-3})	PDI (M_w/M_n)	T_m (°C)
control 1	0	0	86 208	0		77600	2.9	159.6
control 2	0.0865	0	~0		0			
A'-1	0.0346	20	74 176	0.11	35.1	53.4	2.0	159.0
B'-1	0.0865	20	28 512	0.33	16.9	26.1	1.7	157.2
C'-1	0.173	20	12 224	0.77	8.1	9.8	1.6	153.3
D'-1	0.346	20	6 720	1.45	4.1	4.6	1.5[c]	153.1
E'-1	0.519	20	3 328	2.11	2.0	1.8	1.5[c]	143.2
A'-2	0.0346	6	27 392	0.12	14.14	55.2	2.1	159.2
A'-3	0.0346	2	15 648	0.12	8.08	54.8	2.2	159.3
B'-2	0.0865	12	15 008	0.33	8.78	25.9	1.7	158.4
B'-3	0.0865	6	9 216	0.34	5.39	25.3	1.7	158.1
D'-2	0.346	35	11 392	1.41	6.97	4.6	1.5[c]	152.1
D'-3	0.346	12	2 848	1.42	1.74	4.7	1.6[c]	152.7

[a] Reaction conditions: 50 mL of toluene, propylene (100 psi), [Zr] = 1.25 × 10^{-6} mol/L, [MAO]/[Zr] = 3000, temperature = 30 °C, time = 15 min. [b] Catalyst activity = kg of PP/mol of catalyst·h. [c] Product distribution narrowed may be due to loss of GPC sensitivity for low molecular weight oligomers.

competitive coordination at metallocene active sites between monomer and chain transfer agents.

It is very interesting to quantify the hydrogen concentration needed in the chain transfer reaction. Three comparative reaction sets (including runs from A-1 to A-6, runs from B-1 to B-4, and runs from C-1 to C-3) were conducted under the same reaction conditions except for varying the hydrogen pressure. In contrast with the results from the *p*-MS chain transfer agent, the change of hydrogen concentration does not affect the polymer molecular weight and molecular weight distribution, but has a profound effect on the catalyst activity. Therefore, hydrogen does not engage in the initial chain transfer reaction, but rather assists in the completion of the reaction cycle (as shown in eq 2). A sufficient quantity of hydrogen, proportional to the *p*-MS concentration, is needed to maintain high catalyst activity and *p*-MS conversion.

Similar effects of styrene and hydrogen were observed in the *rac*-Me$_2$Si[2-Me-4-Ph(Ind)]$_2$ZrCl$_2$/MAO catalyzed polymerization of propylene. As summarized in Table 2, all four comparative reaction sets show that hydrogen is necessary to complete the chain transfer reaction to styrene during the propylene

polymerization. Hydrogen concentration does not affect the molecular weight and molecular weight distribution of the resulting PP-*t*-S polymers. However, a sufficient quantity of hydrogen, increasing along with [styrene], is needed to maintain high catalyst activity. Figure 1 shows the GPC curves of PP-*t-p*-MS polymers (control 1, B-1, C-1, D-1, and E-1 in Table 1) prepared by *rac*-Me$_2$Si[2-Me-4-Ph(Ind)]$_2$ZrCl$_2$ mediated propylene polymerization in the presence of *p*-MS/hydrogen. The polymer's molecular weight clearly decreased with the increase in *p*-MS concentration. It is interesting to note that the polymer's molecular weight distribution stayed relatively narrow (M_w/M_n = ~2), indicating a single site polymerization with a clean chain transfer (termination) reaction. Similar GPC curves of PP-*t*-S polymers were also observed, with progressive reduction of polymer molecular weight and narrow molecular weight distribution while the styrene concentration was increased. Figure 2 shows the plot of the polymer molecular weight (M_n) versus the mole ratios of [propylene]/[*p*-MS] and [propylene]/[styrene]. There is a linear proportionality between the polymer molecular weight and molar ratio of [propylene]/[*p*-MS] or [propylene]/[styrene]. It is clear that the chain transfer
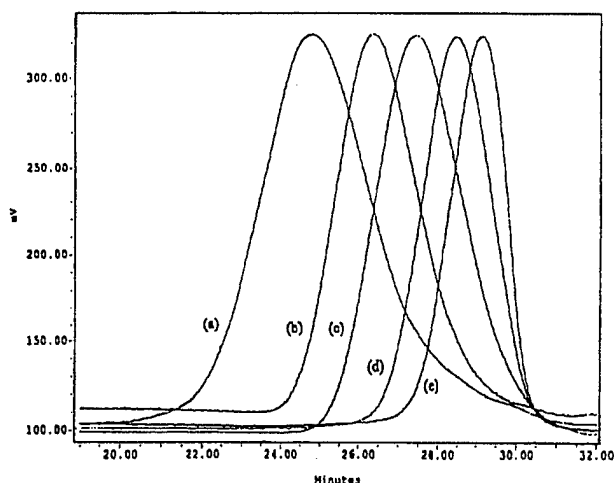
4874   *J. Am. Chem. Soc., Vol. 123, No. 21, 2001*

Chung and Dong

Figure 1. GPC curves of (a) PP (control 1) and several PP-*t*-*p*-MS polymers, (b) B-1, (c) C-1, (d) D-1, and (e) E-1 (in Table 1).
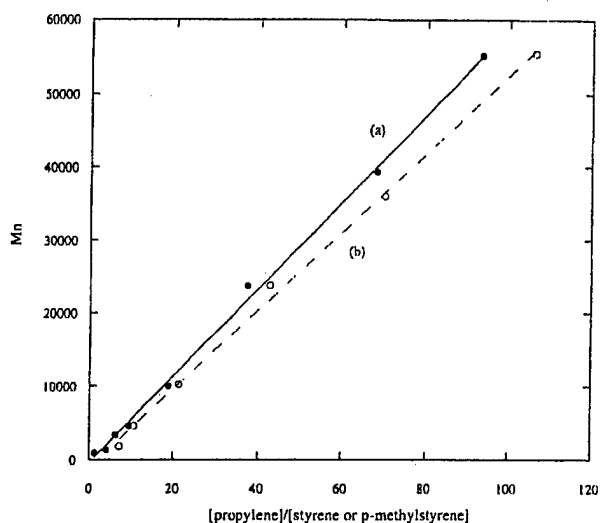

Figure 2. The plots of number average molecular weights (Mn) of (a) PP-*t*-S and (b) PP-*t*-*p*-MS polymers versus the mole ratios of [propylene]/[styrene] and [propylene]/[*p*-MS], respectively.
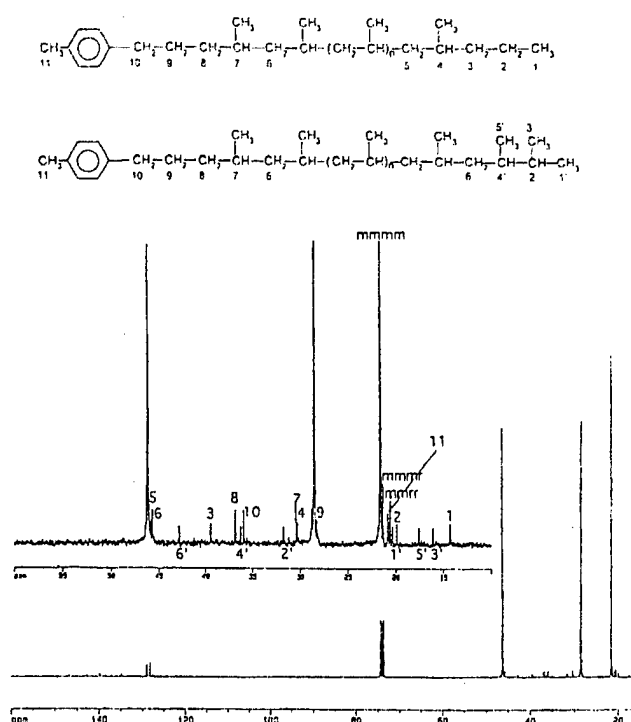

Figure 3. ^{13}C NMR spectra of PP-*t*-*p*-MS sample ($M_n = 4600$ g/mol; $M_w/M_n = 1.7$)
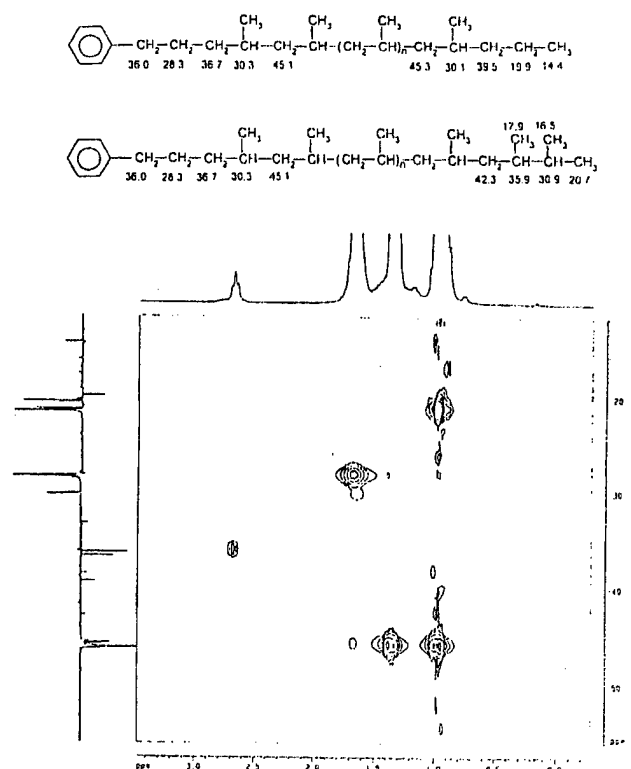
Figure 4. 2-D ^{1}H and ^{13}C (DEPT-135) NMR spectrum of the PP-*t*-S polymer (sample E-1).

reaction to styrenic molecule (with rate constant k_{tr}) is the dominant termination process, and that it competes with the propagating reaction (with rate constant k_p). The degree of polymerization (X_n) follows a simple comparative equation $X_n = k_p[\text{olefin}]/k_{tr}[\text{styrenic molecule}]$ with the chain transfer constant $k_{tr}/k_p \sim 1/6.36$ and $1/7.5$ for *p*-methylstyrene and styrene, respectively. The fact of the cationic nature of the catalyst site is reflected in its higher reactivity to *p*-methylstyrene than styrene during the chain transfer reactions.

End Group Analysis. End group structures at both polymer chain ends provide direct evidence of the chain transfer reaction. This analysis was greatly benefited by the low molecular weight polymers. Figure 3 shows its ^{13}C NMR spectrum of PP-*t*-*p*-MS sample ($M_n = 4600$ g/mol; $M_w/M_n = 1.7$), with an inset of the expanded aliphatic region. In addition to three major peaks ($\delta = 21.6, 28.5,$ and 46.2 ppm) corresponding to the CH$_3$(mmmm), CH, and CH$_2$ groups in the PP backbone, the spectrum exhibits all of the carbon chemical shifts associated with both chain ends. Two types of polymer structures at the beginning of polymer chain are due to the initiation reaction of Zr$^+$–H (**I**) with 1,2- (top) and 2,1- (bottom) insertions[10] of propylene. Although both

insertion modes are allowed in the initiation step, it is generally accepted that isotactic polypropylene polymerization with zirconocene catalysts takes place by a regioselective 1,2-insertion[8] of the propylene monomer at the Zr$^+$–C (**II**) active center. The peak intensity ratio indicates both polymer chain ends (–CH$_2$–C$_6$H$_4$–CH$_3$ and –CH$_3$) with about a 1/1 mole ratio, and the PP-*t*-*p*-MS molecular weight estimated from the chain end and GPC curve is in good agreement. It is important

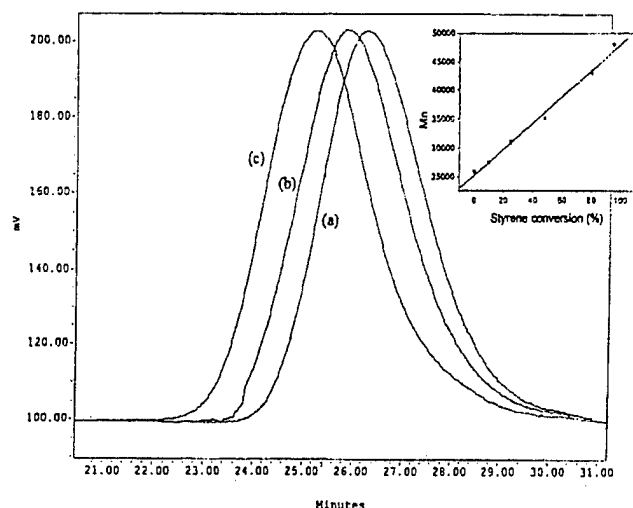(10) Moscardi, G.; Piemontesi, F.; Resconi, L. *Organometallics* **1999**, *18*, 5264.

Figure 5. The GPC curve comparison between (a) PP-*t*-*p*-MS (M_n = 25.8 × 10^3 g/mol; M_w/M_n = 2.3) and two PP-*b*-PS diblock copolymers with (b) M_n = 34.1 × 10^3 and M_w/M_n = 2.4 and with (c) M_n = 48 × 10^3 g/mol and M_w/M_n = 2.5 (solvent, trichlorobenzene; temperature, 135 °C) (Inset: molecular weight of PP-*b*-PS vs styrene monomer conversion).

to note that there is no detectable vinyl group associated with the conventional chain transfer process (via β-H elimination), nor any chemical shifts for $-CH-C_6H_4-CH_3$ associated with the copolymerization reaction.

Figure 4 shows the aliphatic region of the 2-D ^{1}H and ^{13}C (DEPT-135) NMR spectrum of a PP-*t*-S polymer (sample E-1 in Table 1; M_n = 1800 g/mol; M_w/M_n = 1.5). In addition to three major proton chemical shifts (δ = 0.95, 1.35, and 1.65 ppm) corresponding to CH_3, CH_2, and CH groups in the PP backbone and minor peaks (between 7.2 and 7.4 ppm) corresponding to ϕ-H (not shown in this spectra), there is only a triplet proton chemical shift (at 2.67 ppm) corresponding to the end group CH_2-ϕ. Furthermore, all the observed C chemical shifts associated with the aliphatic groups of both chain ends are in good agreement with the calculated ones (shown in Figure 4).

PP-*b*-PS Diblock Copolymers. The existence of a terminal *p*-MS unit in PP is further supported by a chain extension reaction. The terminal *p*-MS group was selectively metalated by *s*-BuLi/TMEDA reagent[11] and transformed to a stable polymeric anion for living anionic polymerization[12] of styrene as illustrated in eq 3. The resulting PP-*b*-PS diblock copolymer
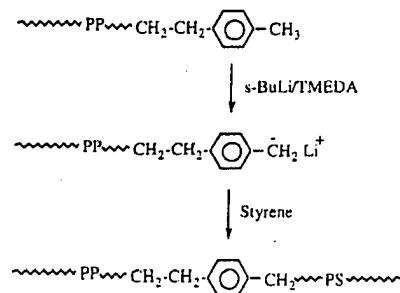
was subjected to Soxhlet extraction by boiling THF to gain no detectable soluble PS homopolymer. The insoluble fraction (soluble in 1,1,2,2-tetrachloroethane at elevated temperatures) is PP-*b*-PS diblock copolymer. Figure 5 compares the GPC curves of the starting PP-*t*-*p*-MS polymer (M_n = 25.9 × 10^3; M_w/M_n = 2.3) with two PP-*b*-PS diblock copolymers (M_n = 34.1 × 10^3 and 47.5 × 10^3, respectively) sampled after 1 and
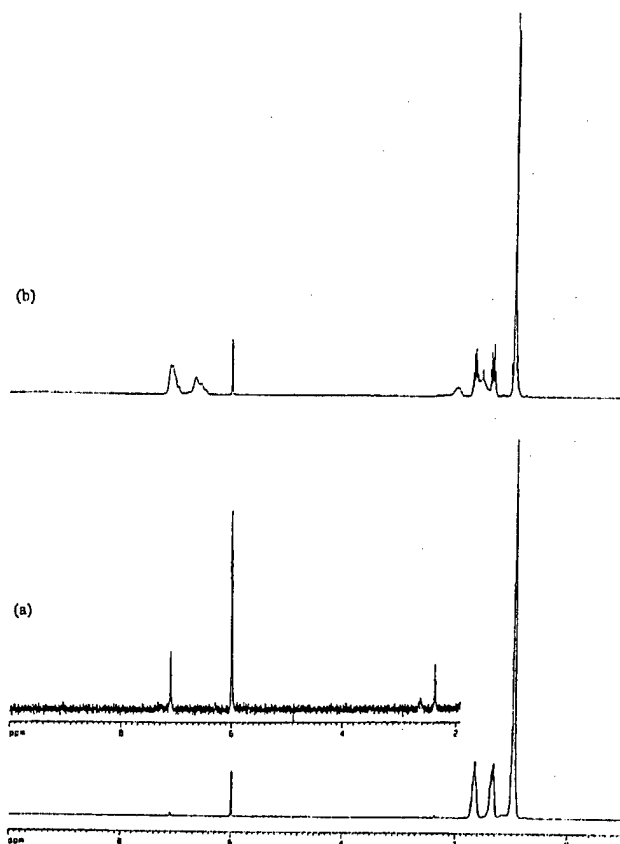

Figure 6. ^{1}H NMR spectra of (a) PP-*t*-*p*-MS (M_n = 25.8 × 10^3 g/mol; M_w/M_n = 2.3) and (b) PP-*b*-PS diblock copolymer (M_n = 48 × 10^3 g/mol; M_w/M_n = 2.5) (solvent, $C_2D_2Cl_4$; temperature, 110 °C).

5 h reaction time. The inset plots the polymer molecular weight vs monomer conversion during the chain extension process. The polymer linearly increased its molecular weight with the consumption of styrene monomers, an indication of the living anionic polymerization process. Despite the heterogeneous reaction condition, most of the styrene monomers were incorporated into diblock copolymer within 5 h. This combination of a monochromatic increase of the copolymer molecular weight (with only a slight broadening in the molecular weight distribution) and no detectable PP homopolymer clearly points to the existence of a *p*-MS group at each PP chain end. Figure 6 shows the ^{1}H spectra of PP-*t*-*p*-MS polymer (M_n = 25.9 × 10^3; M_w/M_n = 2.3) and the corresponding PP-*b*-PS diblock copolymer (M_n = 48 × 10^3; M_w/M_n = 2.5). New resonances at chemical shifts between 6.4 and 7.3 ppm in Figure 6b correspond to aromatic protons of the PS block. An about 1/1 mole ratio of [propylene]/[styrene] in the PP-*b*-PS copolymer is consistent with the polymer molecular weight estimated by GPC measurement.

Conclusion

In summary, this research clearly demonstrates a new in situ chain transfer reaction, first to the styrenic molecule (*p*-methylstyrene or styrene) and then to hydrogen, in metallocene-catalyzed propylene polymerization. With the proper choice of reaction conditions and catalyst system, it is very effective for preparing polyolefin polymer with a terminal styrenic unit. The *p*-MS terminal group provides an efficient route for preparing

(11) Lu, H. L.; Chung, T. C. *J. Polym. Sci. Part A: Polym. Chem.* **1999**, *37*, 4176.

(12) (a) Helary, G.; Fontanille, M. *Eur. Polym. J.* **1978**, *14*, 345. (b) Young, R. N.; Quirk, R. P.; Fetters, L. J. *Adv. Polym. Sci.* **1984**, *56*, 1.

polyolefin diblock copolymers, such as PP-*b*-PS, that would be very difficult to obtain using other existing methods.

Experimental Details:

Instrumentation and Materials. All ^{1}H and ^{13}C NMR spectra were recorded on a Bruker AM 300 instrument in 1,1,2,2-tetrachloroethane-d_2 at 110 °C. The molecular weight and molecular weight distribution of the polymers were determined by Gel Permeation Chromatography (GPC) using a Waters 150 C with a refractive index (RI) detector and a set of u-Styragel HT columns of 10^6, 10^5, 10^4, and 10^3 pore size in series. The measurements were taken at 140 °C using 1,2,4-trichlorobenzene (TCB) as solvent and a mobile phase of 0.7 mL/min flow rate. Narrow molecular weight PS samples were used as standards for calibration. The melting temperatures of the polymers were measured by Differential Scanning Calorimetry (DSC) using a Perkin-Elmer DSC-7 instrument controller. The DSC curves were recorded during the second heating cycle from 30 to 180° C with a heating rate of 20 °C/min.

All O$_2$ and moisture sensitive manipulations were carried out inside an argon filled Vacuum Atmosphere drybox. Toluene, cyclohexane, and *p*-methylstyrene (Wiley Organics) were distilled over CaH$_2$ under argon. High purity grade propylene (MG Industries), methanol, *N,N,N',N'*-tetramethyethylenediamine (TMEDA), *s*-BuLi (Aldrich), and methylaluminoxane (MAO) (Ethyl) were purchased and used as received. The *rac*-Me$_2$Si[2-Me-4-Ph(Ind)]$_2$ZrCl$_2$ catalyst was prepared by the published procedures.[8]

Chain Transfer Reaction in Metallocene-Mediated Propylene Polymerization. In a typical reaction (run A-1 in Table 1), a Parr 450 mL stainless autoclave equipped with a mechanical stirrer was charged with 50 mL of toluene and 1.5 mL of MAO (30 wt % in toluene) before purging with hydrogen (28 psi). The reactor was then injected with 0.2 g (0.0305 M) of *p*-methylstyrene and charged with 100 psi (3.24 M)[13] of propylene to a total pressure of 128 psi at ambient

temperature. About 1.25×10^{-6} mol of *rac*-Me$_2$Si[2-Me-4-Ph-(Ind)]$_2$ZrCl$_2$ in toluene solution was then syringed into the rapidly stirring solution under propylene pressure to initiate the polymerization. Additional propylene was fed continuously into the reactor to maintain a constant pressure (128 psi) during the course of the polymerization. To minimize mass-transfer and to maintain the constant feed ratio, the reactions were carried out by rapid mixing and short reaction time. After 15 min of reaction at 30 °C, the polymer solution was quenched with methanol. The resulting *p*-MS-terminated polypropylene (PP-*t*-*p*-MS) was washed with THF to remove excess styrene and then vacuum-dried at 50 °C. About 23.25 g of PP-*t*-*p*-MS polymer was obtained with a catalytic activity of 73 760 kg of PP/mol of Zr·h.

Synthesis of PP-*b*-PS Diblock Copolymer. The first reaction step is a lithiation reaction of PP-*t*-*p*-MS polymer. In an argon filled drybox, 5 g of PP-*t*-*p*-MS (sample B-1 in Table 1) was suspended in 80 mL of cyclohexane in a 250 mL air-free flask with a magnetic stirrer bar. Next, 1 mL (1.3 mmol) of 1.3 M *s*-BuLi solution and 0.2 mL (1.3 mmol) of TMEDA were added to the flask, and the flask was brought out of the drybox and heated to 60 °C for 4 h under N$_2$. The reaction was then cooled to room temperature and moved back to the drybox. The resulting lithiated PP-*t*-*p*-MS polymer was filtered and washed with cycohexane a few times to remove excess *s*-BuLi and TMEDA.

The lithiated PP-*t*-*p*-MS polymer (3 g) was then again suspended in 100 mL of anhydrous cyclohexane, and the anionic polymerization was carried out at ambient temperature in a slurry solution by introducing 5 mL of styrene. After 5 h, 10 mL of methanol was added to terminate the reaction. The precipitated polymer was filtered and then subjected to fractionation. A good solvent (THF) for PS side chain polymers was used in a Soxhlet apparatus under N$_2$ for 24 h, resulting in almost no soluble fractions. The THF-insoluble fraction was a PP-*b*-PS diblock copolymer that was completely soluble in 1,1,2,2-tetrachloroethane at elevated temperatures.

---

(13) (a) Plocker, U.; Knapp, H.; Prausnitz, J. *Ind. Eng. Chem. Proc. Des. Dev.* **1978**, *17*, 324. (b) Tyvina, T. N.; Efremova, G. D.; Pryanikova, R. O. *Russ. J. Phsy. Chem.* **1973**, *47*, 1513.

Synthesis of functional polyolefin copolymers with graft and block structures

T.C. Chung[*]

Department of Materials Science and Engineering, The Pennsylvania State University, University Park, PA 16802, USA

Abstract

This paper reviews a very useful approach in the preparation of polyolefin graft and block copolymers, containing both polyolefin block (PE, PP, *s*-PS, EP, etc.) and functional polymer block (acrylic and methacrylate polymers), with good control of molecular structure. The chemistry involves polyolefin 'intermediates' containing reactive borane, *p*-methylstyrene, and divinylbenzene units in the side chains or at the chain end, which are prepared by the combination of metallocene catalysts and reactive comonomers and chain transfer agents. The incorporated borane and *p*-MS groups can be transformed into 'living' radical and anion, respectively, for initiating graft-from polymerization. On the other hand, the incorporated DVB unit resembles to a styrene monomer that can involve the subsequent polymerization reactions. A broad range of polyolefin graft and block copolymers have been prepared, which have high functional (polar) group concentration without compromising the desirable polyolefin properties, such as crystallinity, melting temperature, elasticity, etc. They are very effective interfacial agents to improve compatibility of polyolefin in polymer blends and composites. © 2001 Elsevier Science Ltd. All rights reserved.

Contents

* Tel.: +1-814-863-1394; fax: +1-814-865-2917.
  E-mail address: chung@ems.psu.edu (T.C. Chung).

1. Introduction

Polyolefin — including polyethylene (PE), polypropylene (PP), poly(4-methyl-1-pentene), ethylene–propylene elastomer (EPR), and ethylene–propylene–diene rubber (EPDM) — is the most widely used commercial polymer family, with over 53 billion pounds (24 million tons) [1] US annual production (about 40% worldwide) in 1999, or close to 60% of the total polymer produced. They are greatly influencing our day-to-day life, and range from common items like bread and garbage bags, milk jugs, bottles, containers, hoses, outdoor-indoor carpets, tires, bumpers and trims to bullet-proof jackets. The excellent combination of chemical and physical properties [2–4] along with low cost, superior processability and recyclability has positioned itself as the most preferred choice among commercial polymers.

Despite the great successes, there are some inherent shortfalls in polyolefin materials that prevent their even wider usage in many areas currently occupied by other polymers that are much more expensive and less environmentally friendly materials. The major stumbling block has been the poor adhesion and incompatibility between polyolefin and other materials, such as pigments, glass fibers, clays, metals, carbon black, fillers and most polymers. Due to lack of chemical functionality (polar groups) and semi-crystalline morphology (in PE, PP, etc.), polyolefin naturally exhibits low surface energy. For examples, polyolefin is most commonly used for films and molded articles where single polyolefin is required, and it is inadequate for polymer blends and composites, those in which adhesion and compatibility with other materials is paramount.

Since the discovery of HDPE and PP about a half century ago, functionalization of polyolefin has been a scientifically challenging and industrially important area [5–8]. The constant interest, despite the lack of effective functionalization chemistry, is obviously due to the strong desire to improve polyolefin's poor interactive properties and broaden polyolefin applications to higher value products, especially in polymer blend and composite areas. With the recent decade of fierce worldwide competition in single site transition metal (metallocene and non-metallocene) coordination catalysis [9–15], defined polymerization mechanisms, many research activities were geared toward the preparation of functional polyolefin copolymers.
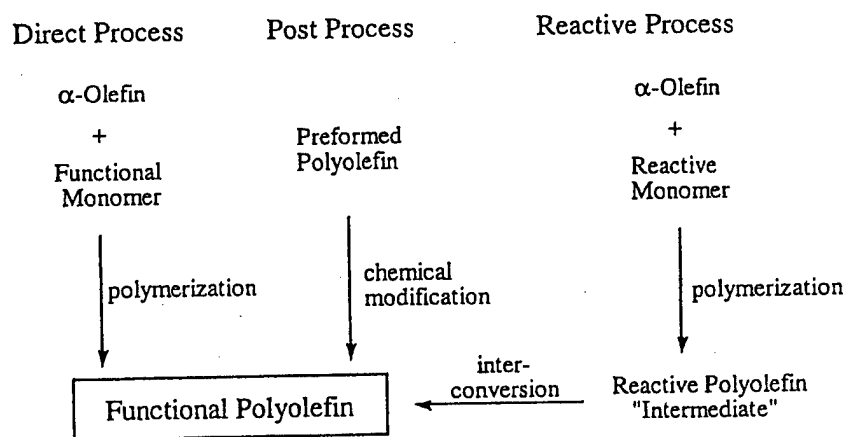
2. General functionalization approaches

Theoretically, there are three possible approaches to the functionalization of polyolefin, as illustrated in Scheme 1. They include (a) direct copolymerization of α-olefin with functional monomer, (b) chemical modification of the preformed polymer, and (c) reactive copolymer approach by incorporating reactive comonomers that can be selectively and effectively interconverted to functional groups.

The first two approaches are more obvious and naturally have enjoyed the most attention. In the past, they were referred to as direct and post-polymerization processes, respectively. The direct process could be an ideal one (one-step reaction) if the copolymerization reaction with functional monomers would be as effective and straightforward as the corresponding homopolymerization reaction. Unfortunately, some fundamental chemical difficulties, namely catalyst poisoning and other side reactions, have prevented serious consideration of the direct process for commercial application. The Lewis acid components (Ti, Zr, Hf, V and Al) of the catalyst will tend to complex with non-bonded electron pairs on N, O, and X (halides) of functional monomers in preference to react with the π-electrons of the double bonds. The net result is the deactivation of the active polymerization sites by formation of stable complexes between catalysts and functional groups, thus inhibiting polymerization.

So far, most research activities in this direct process have been focused on the prevention of catalyst poison by (i) protecting sensitive functional group from poisoning catalyst [16–20], or (ii) employing catalysts that are less oxophilic and more stable to heteroatoms [14,15,21]. In general, both methods have their own concerns and limitations. Some protected functional groups, via acid-base complexization, reduces the solubility of the propagating polymer chain, which in turn reduces catalyst efficiency. On the other hand, in steric protection cases it is very important to choose the bulky protecting group that can not only prevent catalyst poisoning, but also can be effectively deprotected. However, the expensive protection and deprotection reactions, with some environmental concerns due to by-products, prohibit any large-scale commercialization.

In recent years, some very interesting results were reported by using less oxophilic late transition metal catalysts, such as Fe, Ni, Co and Pd complexes, in the copolymerization of α-olefins and acrylate monomers. The combination of a less oxophilic catalyst and an electronic-protected functional group significantly increases catalyst activity, indicating that the lone pair electrons in the heteroatom (such as

Direct Process   Post Process   Reactive Process

α-Olefin   α-Olefin

+   +

Functional   Preformed   Reactive
Monomer   Polyolefin   Monomer

↓ polymerization   ↓ chemical modification   ↓ polymerization

Functional Polyolefin ←— inter-conversion — Reactive Polyolefin "Intermediate"

Scheme 1.

O and N) still compete with the olefin insertion during the late transition metal polymerization [21]. The polymer produced usually contains a branched molecular structure with relatively low (or no) melting temperature and crystallinity. There is no example of steric-specific polymerization of α-olefin by using late transition metal catalysts. It is very challenging to prepare functionalized *i*-PP or *s*-PS polymers by this route.
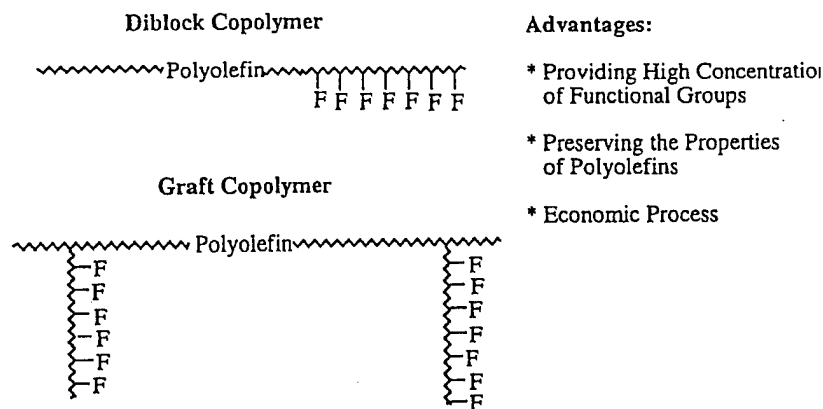
Currently, most of the commercial functionalization processes are based on post-polymerization process [22–26]. Chemical modification of the pre-formed polyolefin homopolymers has been usually carried out in situ during the fabrication process to reduce the production cost, as well as to relieve the significant concern (in many cases) of reducing processibility of polyolefin after functionalization reaction. However, the combination of the inert nature of polyolefin (requiring highly energetic reaction conditions) and a very short reaction time (during the processing) causes a great deal of difficulties in controlling polymer composition and structure. There is no facile reaction site in the saturated PE, PP and EP polymers. The only way is to activate the polymer by breaking some stable C–H bonds and forming free radicals along the polymer chain. The resulting polymeric radicals then undertake chemical reactions with some chemical reagents, such as maleic anhydride. However, this functionalization reaction is usually accompanied with many undesirable side reactions (crosslinking and degradation) and by-products. Overall, the current commercial process is far from the ideal one.

The third functionalization approach is a relatively new one (mostly developed in our laboratory) [27–32]. The basic idea is to circumvent the chemical difficulties in both direct and post-polymerization processes by designing a reactive copolymer 'intermediate' that can be effectively synthesized and subsequently interconverted to functional polymer. This approach has benefited greatly from metallocene technology, especially due to its superior capability in the copolymerization and chain transfer reactions. As will be discussed later, several new reactive comonomers can be effectively incorporated into polyolefins in the side chains or at the chain end. In turn, these reactive groups incorporated in polymer open up a lot of possibility to produce new polyolefin products, including functional graft and block copolymers, that would be very difficult to prepare by other methods.

3. Functional polyolefins with graft and block structures

One of the major concerns in the functionalization of polyolefin (PE or PP) is the alternation of some desirable polyolefin properties, such as melting temperature, crystallinity, etc. which are essential for an effective compatibilizer in polymer blends and composites. However, the introduction of high concentration of functional groups along the polymer chain (such as PE and PP) will inevitably reduce its crystallinity and melting temperature, as well as its co-crystallization ability with pure PE or PP polymer (in matrix).

Functional polyolefin with block and graft structures (illustrated in Scheme 2) are the most desirable material, which not only offer large quantity of functional groups, but also preserve the original polyolefin properties. As the established technique for improving the interfacial interaction, block and graft copolymers are the ideal compatibilizers [33–35] that can dramatically increase the adhesion of polyolefin. In the ideal polyolefin blends and composites, the graft/block copolymers are located at the interfaces, the functional polymer segments provide good adhesion to the polar surfaces, and the polyolefin segments can interpenetrate (with entanglements or/and co-crytallization) into pure polyolefin homopolymer domains.

Diblock Copolymer

Advantages:

* Providing High Concentratior of Functional Groups

* Preserving the Properties of Polyolefins

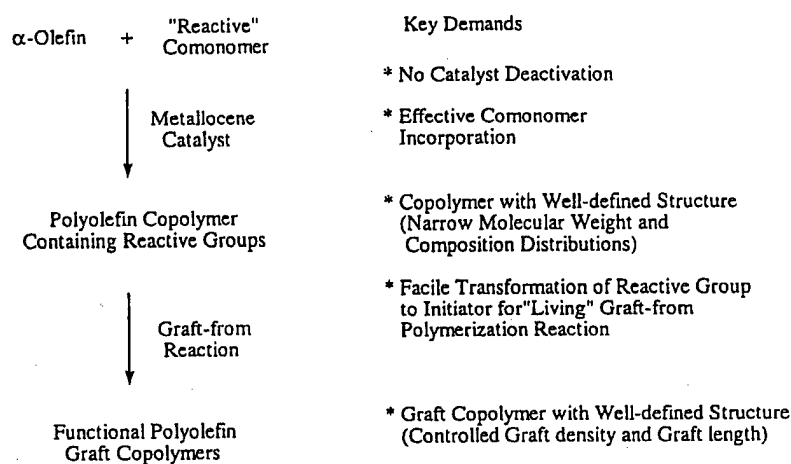* Economic Process

Graft Copolymer

Scheme 2.

In terms of the feasibility of mass-producing polyolefin block and graft copolymers, only a very few linkages (chemical bonds) exist for connecting polymer segments. In other words, the ideal chemical process only requires a few active sites in the polyolefin chain. With the appropriate choice of reactive comonomer or chain transfer agent, it is very possible to produce both block and graft copolymers in an economical fashion.

4. Reactive polyolefin approach

As discussed, both direct and post-polymerization processes have only achieved very limited successes in the functionalization of polyolefins. It is very interesting to explore the alternative routes to prepare functional polyolefins, especially those having block and graft structures. In the past decade, our group has been focusing on a reactive polyolefin approach. As illustrated in Scheme 3, the reactive polyolefin can be prepared by the copolymerization reaction of α-olefin and a selected 'reactive'

α-Olefin + "Reactive" Comonomer

Key Demands

* No Catalyst Deactivation

* Effective Comonomer Incorporation

| Metallocene Catalyst

Polyolefin Copolymer Containing Reactive Groups

* Copolymer with Well-defined Structure (Narrow Molecular Weight and Composition Distributions)

* Facile Transformation of Reactive Group to Initiator for"Living" Graft-from Polymerization Reaction

| Graft-from Reaction

Functional Polyolefin Graft Copolymers

* Graft Copolymer with Well-defined Structure (Controlled Graft density and Graft length)

Scheme 3.

comonomer using metallocene catalyst. The formed reactive polyolefin copolymer serves as the intermediate for the preparation of graft copolymers.

Obviously, the key factor in this approach is the design of a comonomer containing a reactive group that can simultaneously fulfill the following requirements. First, the reactive group must be stable to metallocene catalysts and soluble in hydrocarbon polymerization media. Second, the reactive monomer should have good copolymerization reactivity with α-olefins. Third, the reactive group must be facile in the subsequent interconversion reaction to form a stable initiator for the polymerization of functional monomers. In other words, each incorporated reactive group can produce a functional polymer chain containing hundreds of functional groups.

As will be discussed, three reactive comonomers — including borane monomers [36–41], p-methylstyrene (p-MS) [42–48], and divinylbenzene (DVB) [49] — have been effectively incorporated into polyolefinns with narrow molecular weight and composition distributions.

$$
\begin{array}{ccc}
CH_2=CH & CH_2=CH & CH_2=CH \\
(CH_2)_4 & \bigcirc & \bigcirc \\
B & CH_3 & CH=CH_2 \\
\bigcirc & & \\
\end{array}
$$
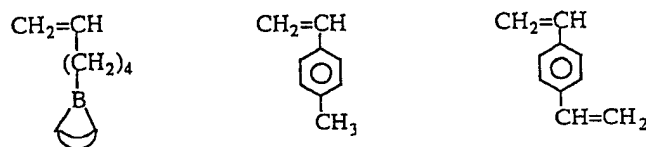
All three reactive sites, i.e. borane, benzylic protons, and styrene units, pending along the polyolefin backbone are very versatile in the subsequent graft reactions. The graft reactions are selectively taken place at the reactive sites, and the concentration of functional groups is basically proportional to the concentration of the reactive sites and functional monomers. As will be discussed later, three reactive comonomers provide complemental coverage of the most desirable functional polyolefin compositions and structures.
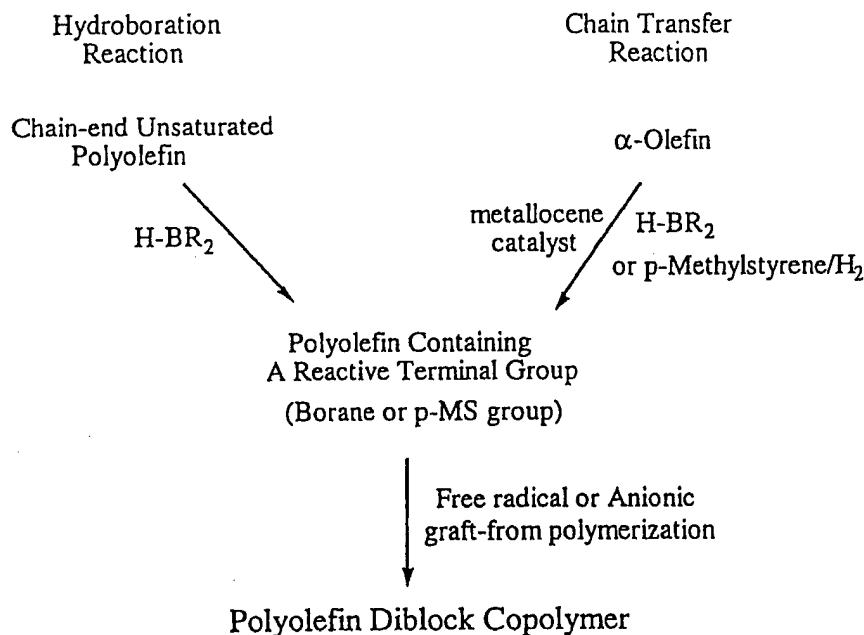
It is very interesting to note that the reactive polyolefin approach has also been extended to the preparation of polyolefin containing a reactive terminal group (borane or p-methylstyrene) and polyolefin diblock copolymers [50–52]. One example is illustrated in Scheme 4.

As will be discussed, the combination of chain transfer and hydroboration reactions provides a convenient route to prepare a broad range of polyolefins containing a reactive terminal group, which include all commercial polyolefins (PE, PP, s-PS, and their co- and ter-polymers). In turn, the terminal reactive group (borane or p-methylstyrene) can be transformed to living free radical or anionic initiator, respectively, for chain extension reaction to form diblock copolymers. The overall reaction process resembles a transformation from metallocene polymerization to living free radical polymerization via a borane terminal group or to living anionic polymerization via a p-methylstyrene terminal group.

5. Synthesis of polyolefin containing reactive groups

5.1. Polyolefins containing borane side groups

Copolymerization of α-olefin and borane monomer (a high α-olefin containing a borane moiety) is a very convenient way to prepare borane-containing polyolefin. Due the unique features of borane moiety, including good stability to metallocene catalyst and good solubility [8] in organic solvents used in the polymerization, borane monomer generally behaves similarly to the corresponding high α-olefin. In other words, we could treat the borane monomer as a high α-olefin in the copolymerization reaction and expect similar copolymer structure that is governed by the reactivity ratios of two comonomers under

Hydroboration
Reaction

Chain Transfer
Reaction

Chain-end Unsaturated
Polyolefin

α-Olefin

H-BR$_2$

metallocene
catalyst

H-BR$_2$
or p-Methylstyrene/H$_2$

Polyolefin Containing
A Reactive Terminal Group

(Borane or p-MS group)

Free radical or Anionic
graft-from polymerization

Polyolefin Diblock Copolymer

Scheme 4.

each set of the catalyst system. In the Ziegler–Natta heterogeneous catalyst system, the reactivity of monomer is dramatically dependent on the size of the monomer — the bigger the size of the monomer, the lower the reactivity. Ethylene is generally five times more reactive than propylene, and the reactivity becomes more constant in high α-olefins. It could be predicted that the copolymerization of ethylene with borane monomer would be very difficult in Ziegler–Natta heterogeneous catalyst system [39]. The borane monomer may have a better chance to be incorporated with propylene [40,41] and high α-olefins, such as 1-butene and 1-octene [38]. On the other hand, the use of a homogeneous metallocene catalyst with constrained ligand geometry (having an open active site) could significantly improve the copolymerization ability of borane monomers with ethylene.

The copolymerization reaction between ethylene and 5-hexenyl-9-BBN [39] is the best testing ground for studying the copolymerization ability of borane monomer, especially in terms of its dependence on the Ziegler–Natta and metallocene catalysts. Eq. (1) shows the copolymerization of ethylene and a borane monomer, such as 5-hexenyl-9-BBN, by various catalyst systems. The reactions were carried out in a Parr reactor under N$_2$ atmosphere.

x CH$_2$=CH$_2$ + y CH$_2$=CH
(CH$_2$)$_4$
B

Catalyst*

Catalysts: Et(Ind)$_2$ZrCl$_2$/MAC
Cp$_2$ZrCl$_2$/MAO
TiCl$_4$/EtAlCl$_2$

-(CH$_2$-CH$_2$)$_x$-(CH$_2$-CH)$_y$-
(CH$_2$)$_4$
B

(1)

Table 1
A summary of copolymerization reactions between ethylene (m_1) and 5-Hexenyl-9-BBN (m_2)

Run number	Catalyst type[a]	Comonomers m_1/m_2 (psi)[b]/ (g)	Reaction temperature/time (°C/min)	Catalyst activity (Kg/mol hr)	Borane in copolymer (mol%)
A-1	I	45/0	30/60	644	0
A-2	I	45/0.56	30/30	1469	1.25
A-3	I	45/1.52	30/30	2020	2.15
A-4	I	45/2.10	30/30	2602	2.30
B-1	II	45/0	30/70	337	0
B-2	II	45/5	30/70	643	1.22
C-1	III	80/10	60/110	4.0	0

[a] Catalysts: Et(Ind)$_2$ZrCl$_2$/MAO (I), Cp$_2$ZrCl$_2$/MAO (II) and TiCl$_3$·AA/Et$_2$AlCl (III), solvent: 100 ml toluene.
[b] Corresponding to 0.38 mol/l.

Three catalyst systems, including two homogeneous metallocene Et(Ind)$_2$ZrCl$_2$ and Cp$_2$ZrCl$_2$ with MAO catalysts and one heterogeneous TiCl$_3$·AA/(Et)$_2$AlCl catalyst, were evaluated in the copolymerization reactions. Usually, the reaction was initiated by charging the catalyst solution into the mixture of ethylene and 5-hexenyl-9-BBN, and a constant ethylene pressure was maintained throughout the polymerization process. Almost immediately, white precipitate was observed at the beginning of the reaction. After a specific reaction time, the copolymerization was terminated by addition of IPA.

Table 1 summarizes the experimental results. Overall, the homogeneous metallocene catalysts, especially Et(Ind)$_2$ZrCl$_2$/MAO with stained ligand geometry and an open active site, show satisfactory copolymerization results at ambient temperature. Comparing runs A-1–A-4, the concentration of borane groups in PE is basically proportional to the concentration of borane monomer feed. About 50–60% of borane monomers was incorporated into the PE copolymers after about a half hour. It was very unexpected that the catalyst activity systematically increased with the concentration of borane monomer in the Et(Ind)$_2$ZrCl$_2$/MAO catalyst system. Obviously, no retardation due to the borane groups is shown in these cases. The copolymerization of borane monomers in Cp$_2$ZrCl$_2$/MAO system (shown in run B-2) is significantly more difficult — only 1.22 mol% of borane monomer incorporated in PE copolymer even high concentration of borane monomer used. On the other hand, the heterogeneous TiCl$_3$·AA/Et$_2$AlCl catalyst shows no detectable amount of borane group in the copolymer as shown in run C-1.

Fig. 1 shows the GPC curves of poly(ethylene-co-5-hexenyl-9-BBN) copolymers containing 0.5 and 1.2 mol% of 5-hexenyl-9-BBN, respectively. Due to the air-sensitivity of the borane group, most of the analyses were carried out on the corresponding hydroxy or ester polymers after converting borane to hydroxy or ester groups. The copolymers were prepared by the Et(Ind)$_2$ZrCl$_2$/MAO catalyst. Overall, the copolymers have high molecular weight and narrow molecular weight distribution ($M_w/M_n < 3$). There is no indication of any negative influence of borane group on the metallocene polymerization.

This α-olefin/borane monomer copolymerization reaction has been applied to prepare other polyolefin co- and ter-polymers using metallocene and Ziegler–Natta catalysts. Some semicrystalline copolymers, including poly(ethylene-co-B-5-hexenyl-9-BBN), poly(propylene-co-B-5-hexenyl-9-BBN) and poly(1-butene-co-B-5-hexenyl-9-BBN), were found to contain low concentration of borane monomers (<10 mol%), and are insoluble in common organic solvents at room temperature, but soluble at higher temperatures. However, the copolymers of poly(1-octene-co-B-5-hexenyl-9-BBN) (PO-B) and terpolymers
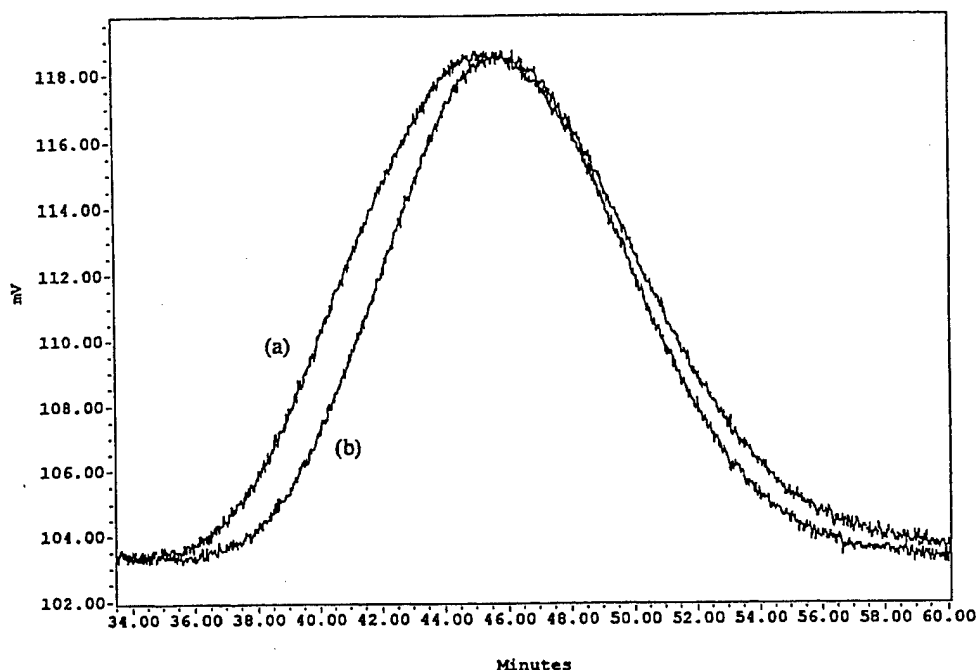
Fig. 1. GPC curves of poly(ethylene-*co*-5-hexenyl-9-BBN) copolymers containing (a) 0.5 and (b) 1.2 mol% of 5-hexenyl-9-BBN.

of poly(ethylene-*ter*-propylene-*ter*-B-5-hexenyl-9-BBN) (EP-B) were found to be soluble in most hydrocarbon solvents at room temperature.

Alternatively, borane-containing polyolefins were prepared by hydroboration of unsaturated poly-olefins, such as poly(propylene-*co*-1,4-hexadiene) [53] and poly(ethylene-*co*-propylene-*co*-1,4-hexadiene) [54]. The internal double bond was reacted by dialkylborane, such as 9-BBN. The reaction is very effective in both homogeneous and heterogenious solutions under mild reaction conditions. The concentration of borane groups in polyolefin was controlled by the amount of 9-BBN used in the hydroboration reaction and the concentration of unsaturation in the copolymers. In a typical hydrobora-tion reaction, a THF solution of the borane reagent (e.g. 9-BBN) was added to a toluene suspension of the unsaturated polymer (e.g. inhibitor-free poly(propylene-*co*-1,4-hexadiene) containing 1.7% 1,4-hexadiene units). The suspension was heated to 65°C in a flask equipped with a condenser. After stirring for 5 h, the polymer was precipitated into 150 ml dry/degassed isopropanol and isolated by filtration (in dry-box). The borane-containing polymer was then placed in a suspension of THF for further oxidation reactions.

5.2. Polyolefins containing p-methylstyrene side groups

The second reactive comonomer can be effectively incorporated into polyolefins is *p*-methylstyrene (*p*-MS), which is advantaged by its commercial availability. In general, the preparation of *p*-MS contain-ing polyolefin copolymers has been greatly enhanced by the metallocene catalyst with constrained ligand geometry, having a spatially opened catalytic site, allows the effective incorporation of styrenic

comonomers (Eq. (2)), which was almost impossible by using Ziegler–Natta catalysts:
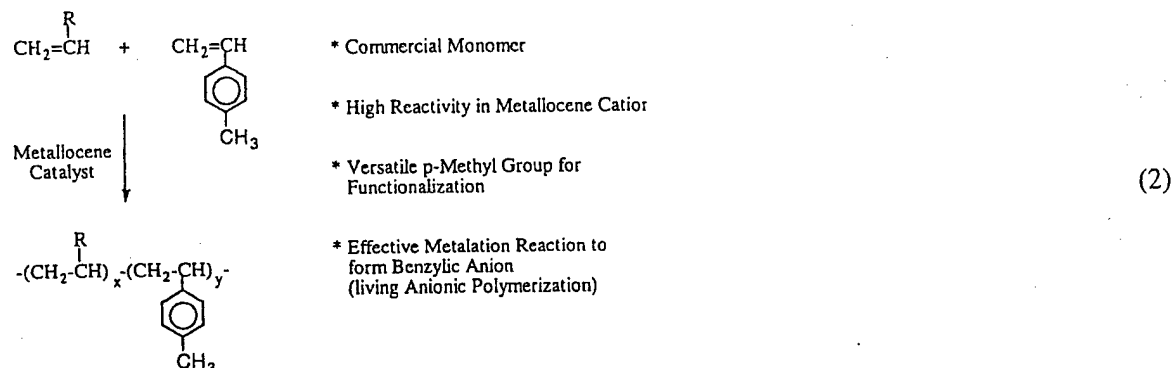

(2)

Table 2 summarizes the results by using three metallocene catalysts, including a simple Cp_2ZrCl_2 catalyst and two bridged $Et(Ind)_2ZrCl_2$ and $[C_5Me_4(SiMe_2N'Bu)]TiCl_2)$ catalysts [45,46]. The copolymerization efficiency follows the sequence of $[C_5Me_4(SiMe_2N'Bu)]TiCl_2 > Et(Ind)_2ZrCl_2 > Cp_2ZrCl_2$, which is directly relative to the spatial opening at the active site. In run P-377, about 90% of the p-MS was incorporated into the copolymer in 1 hour. In run P-383, the reaction produced copolymer containing 40 mol% of p-MS, which is close to the ideal 50 mol% (as known that the consecutive insertion of p-MS in all three catalyst systems is almost impossible).

Fig. 2 shows the typical GPC and DSC curves of the homo- and copolymers prepared by the $[C_5Me_4(SiMe_2N'Bu)]TiCl_2$ catalyst. The uniform molecular weight distribution in all samples, with $M_w/M_n = 2$–3, implies the single-site polymerization mechanism. DSC curves show that even a small amount (~1 mol%) of p-MS comonomer incorporation has a significant effect on the crystallization of PE. The melting point (T_m) and crystallinity (χ_c) of the copolymer are strongly relative to the density of the comonomer — the higher the density, the lower the T_m and χ_c. Only a single peak is observed throughout the whole composition range, and the melting peak completely disappears at ~10 mol% of p-MS concentration.

The copolymerization of propylene and p-MS was not effective in producing PP-p-MS copolymers [47], completely opposite to those observed in the corresponding ethylene/p-MS copolymerization reaction. The drastic differences are due to the steric jamming phenomenon in the cross-over k_{21} reaction (from p-MS to propylene), as illustrated in Eq. (3).

(3)
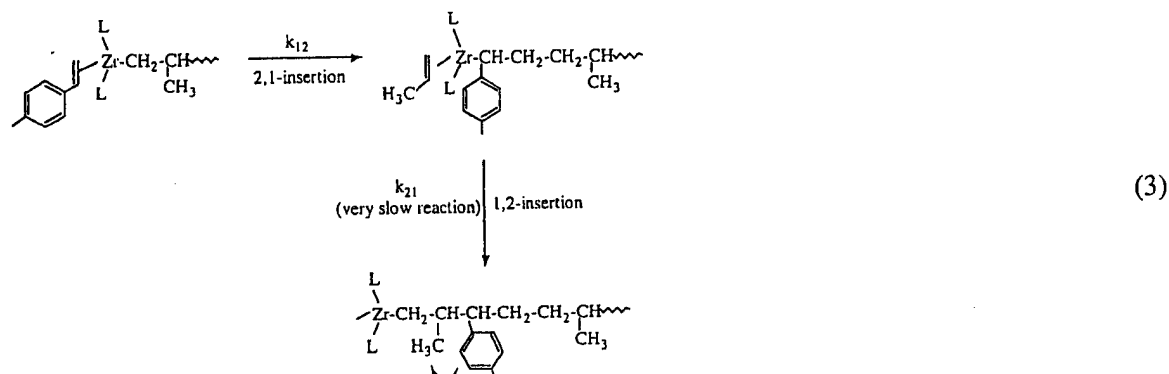
It is well known that in metallocene catalytic polymerization, the insertion of the styrene monomer is

Table 2
Summary of copolymerization reactions (45 psi ethylene ~0.309 mol/l in toluene, 0.424 mol/l in hexane at 50°C; ~0.398 mol/l in toluene, 0.523 mol/l in hexane at 30°C. 10 psi ethylene ~0.116 mol/l in hexane at 30°C) between Ethylene and p-MS

Run number	Catalyst (μmol)[a]	Ethylene/p-MS (psi/M)	Solvent/ temperature (°C)	Yield (g)	Catalyst efficiency kg P/mol Mh	p-MS in copolymer (mol%)	Conversion of p-MS (%)
p-363	I/17	45/0.678	Hexane/50	24.2	1423.5	2.2	26.2
p-365	I/17	45/0.678	Toluene/50	8.44	496.5	1.84	7.7
p-356	II/17	45/0.085	Hexane/50	6.5	382.4	1.83	47.2
p-358	II/17	45/0.678	Hexane/50	21.9	1288.2	5.16	51.1
p-361	II/17	45/1.36	Hexane/50	18.9	1111.8	7.2	29
p-371	II/17	45/2.03	Hexane/50	20.8	1223.5	8.94	25.4
p-357	II/17	45/0.085	Toluene/50	5.7	335.3	1.3	29.9
p-360	II/17	45/0.678	Toluene/50	15.1	888.2	4.76	32.8
p-362	II/17	45/1.36	Toluene/50	19.5	1147.1	6.36	27
p-375	II/17	45/2.03	Toluene/50	19.4	1141.2	8.49	22.8
p-270	III/10	45/0	Toluene/30	4.4	440	-	-
p-377	III/10	45/0.447	Hexane/30	12	1200	13.5	90.3
p-378	III/10	45/0.912	Hexane/30	15.5	1550	22.6	81.3
p-267	III/10	45/0.447	Toluene/30	13	1300	10.9	83.8
p-379	III/10	45/0.912	Toluene/30	17.4	1740	21.6	86.9
p-380	III/10	45/1.82	Toluene/30	24.2	2420	32.8	75.8
p-383	III/10	10/1.82	Hexane/30	15.9	1590	40	54.6

[a] I: Cp_2ZrCl_2/MAO; II: $Et(Ind)_2ZrCl_2$/MAO; III: $[(C_5Me_4)SiMe_2N(t\text{-}Bu)]TiCl_2$/MAO.
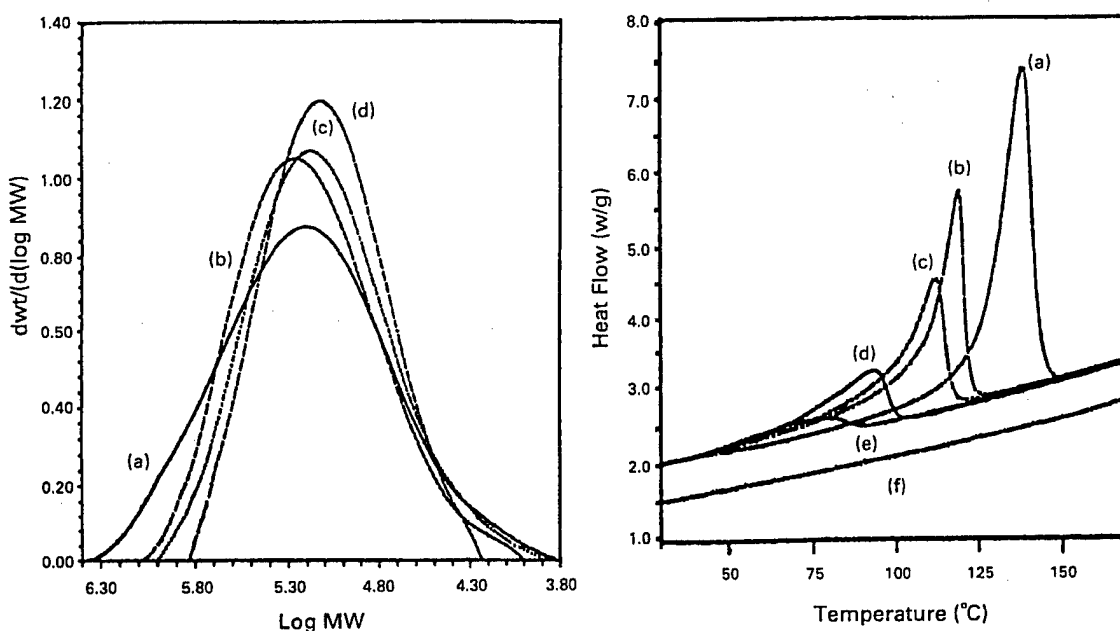
Fig. 2. Left: GPC curves of (a) PE and three PE-*p*-MS copolymers, containing (b) 1.08, (c) 9.82 and (d) 18.98 mol% of *p*-MS units; (right) DSC curves of (a) PE and PE-*p*-MS containing (b) 1.08, (c) 2.11, (d) 5.40, (e) 9.82 and (f) 18.98 mol% of *p*-MS.

predóminately secondary (2,1-insertion), while the 1,2-insertion of the propylene monomer is dominant. Once the propagating PP chain has a chance to react with the *p*-MS monomer (k_{12} reaction) via 2,1-insertion, the bulky *p*-phenyl group in the last unit of the growing chain is adjacent to the central metal atom and blocks the upcoming 1,2-insertion of a propylene unit (i.e. k_{21} reaction). Since the homo-polymerization (k_{22}) of *p*-MS via the metallocene coordination mechanism is known to be near zero, the metallocene active site at *p*-MS unit dramatically slows the propagation process. Therefore, a small amount of *p*-MS significantly reduces the catalyst reactivity.

Despite the difficulty in propylene/*p*-MS copolymerization, the terpolymerization involving ethylene was very effective, the dormant species shown in Eq. (3) reacts with ethylene to continue the reaction. Tables 3 and 4 summarize the experimental results of the terpolymerization reactions of ethylene/propylene/*p*-MS and ethylene/1-octene/*p*-MS to prepare EP-*p*-MS and EO-*p*-MS terpolymers [48], respectively. Both reactions were carried out by using [C$_5$Me$_4$(SiMe$_2$N^{t}Bu)]TiCl$_2$/MAO catalyst. Overall, the catalyst shows excellent activity in all terpolymerization reactions. The incorporation of *p*-MS seems quiet insensitive to the ethylene/propylene or ethylene/1-octene feed ratios. The molecular weight of terpolymer is quiet high ($M_w \sim 200,000$ g/mol) and is not significantly dependent on the content of *p*-MS. In addition, the molecular weight distributions (M_w/M_n) < 3, similar to most metallocene-based homo- and co-polymers, indicate single-site reaction with good comonomer reactivities

The glass transition temperature (T_g) was examined by DSC. All samples show a well-defined T_g with shape transition, indicating uniform terpolymer structures. The T_g is clearly a function of *p*-MS content. Comparing runs p-116 and p-120, both with ideal ~54 mol% ethylene content and only a very small difference in *p*-MS/propylene mole ratios (0/46 vs. 1.8/44), the T_gs are −50 and −45°C, respectively. Overall, the composition of EP-*p*-MS material with low $T_g < -45°C$ is very limited, only to the

Table 3

A summary of Terpolymerization (polymerization conditions: 100 ml toluene; [Ti] = 2.5 × 10^{-6} mol; [MAO]/[Ti] = 3000; 50°C; 15 min) of ethylene/propylene/p-MS by using [C$_5$Me$_4$(SiMe$_2$N'Bu)]TiCl$_2$/MAO (Reproduced with permission from Macromolecules 1998;31:2028. Copyright 1998 Am. Chem. Soc.)

Run number	Monomer feed [E]/[P]/[p-MS] (mol/l)	Catalyst activity kg/mol Ti h	Copolymer [E]/[P]/[p-MS] (mol%)	T_g (°C)	M_w (g/mol)	M_n (g/mol)
p-116	0.13/0.28/0	4.9 × 10^3	53.9/46.1/0	−49.4	300,400	134,300
p-117	0.12/0.35/0	4.7 × 10^3	41.8/58.2/0	−43.7	284,300	120,800
p-118	0.12/0.35/0.3	4.0 × 10^3	46.4/43.6/10.0	−20.7	198,200	74,900
p-119	0.12/0.35/0.05	4.0 × 10^3	46.1/52.3/1.6	−41.0	195,800	75,100
p-120	0.13/0.28/0.05	4.1 × 10^3	54.4/43.8/1.8	−45.8	237,700	107,500
p-127	0.13/0.28/0.03	3.8 × 10^3	50.7/48.6/0.7	−45.9	244,300	85,500
p-128	0.14/0.25/0.03	4.4 × 10^3	56.3/43.1/0.6	−48.6	269,400	104,300

polymers with <2 mol% of p-MS content. Despite the random terpolymer structure and the ideal (~55/45) ethylene/propylene ratio, a further increase of p-MS raises the T_g of the terpolymer to > − 40°C. On the other hand, the EO-p-MS sample with even up to 8 mol% of p-MS still shows T_g < −45°C, these results clearly show the advantages of the 1-octene comonomer (over propylene), which assures the formation of an amorphous polyolefin elastomer with low T_g and high p-MS content.

5.3. Polyolefins containing divinylbenzene side groups

The third reactive comonomer having been incorporated into polyolefin was divinylbenzene (DVB)

Table 4

Summary of terpolymerization (polymerization conditions (unless specified otherwise): 100 ml of toluene; [Ti] = 2.5 × 10^{-6} mol; [MAO]/Ti = 3000; 50°C; 30 min) of ethylene, 1-octene and p-MS using [C$_5$Me$_4$(SiMe$_2$N'Bu)]TiCl$_2$/MAO metallocene catalyst [306] (Reproduced with permission from Macromolecules 1998;31:2028. Copyright 1998 Am. Chem. Soc.)

Run number	Monomer concentration in feed (mol/l)			Yield (g)	Copolymer composition (mol%)			T_g (°C)	M_w (g/mol)	M_n (g/mol)	PD
	E^a	1-Oct	p-MS		[E]	[O]	[p-MS]				
p-470	0.20	0.80	0.10	7.3	54.2	43.0	2.7	−56.2	173,989	74,703	2.3
p-471	0.40	0.80	0.10	10.1	61.1	36.0	2.9	−58.1	219,752	96,802	2.3
p-472	0.40	0.80	0.20	9.8	60.3	36.3	4.4	−55.7	182,185	77,497	2.4
p-473	0.40	0.40	0.20	8.2	59.6	34.0	6.4	−50.1	208,920	86,812	2.4
p-477	0.40	0.20	0.20	6.4	80.2	14.1	5.7	−37.3	227,461	91,490	2.5
p-476	0.40	0.80	0.40	9.0	63.4	29.3	7.3	−50.3	202,085	96,035	2.1
p-475	0.40	0.60	0.40	9.1	67.2	24.7	8.1	−48.2	205,124	93,763	2.2
p-478	0.40	0.40	0.40	7.9	73.3	18.5	8.1	−44.7	246,300	122,306	2.0
p-474	0.40	0.60	0.15	9.0	64.7	31.3	4.0	−55.7	224,476	102,617	2.2

^{a} Solubility of ethylene: 0.25 mol/l for 29 psi in hexane at 60°C, 0.20 mol/l for 2 bar, 0.40 mol/l for 4 bar in toluene at 50°C. 0.52 mol/l for 45 psi in hexane at 30°C, 0.13 mol/l for 10 psi in hexane at 30°C.

[49], which results in the polyolefin copolymers with pending styrene units that can serve as the active sites for many graft reactions. The potential problem in the polymerization reaction is the double enchainment of DVB, which will lead to the crosslinked product [55]. In fact, DVB is known as a good crosslinker in many free radical polymerizations. In our laboratory, we have been investigating the metallocene catalysts that can prepare α-olefin/DVB copolymers with a linear copolymer structure, as illustrated in Eq. (4).

$$\tag{4}$$
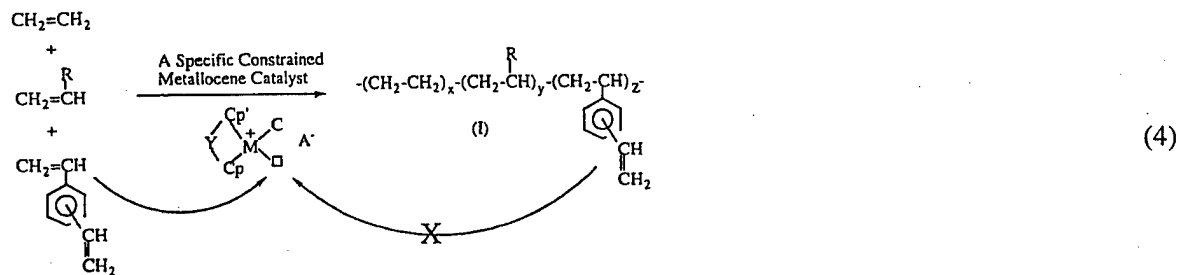
In general, the metallocene catalysts that have non-bridgeted ligand geometry, such as Cp_2ZrCl_2 with a small open active site, incorporate a very low concentration of DVB units. On the other hand, the metallocene catalysts with constrained ligand geometry, such as $[C_5Me_4(SiMe_2N^tBu)]TiCl_2$) with a large open active site, engage in serious double enchainment with both vinyl groups in the DVB monomer, which results in copolymers with branching or/and crosslinking structures. However, there is a small group of metallocene catalysts with narrowly defined openings at active sites, which can effectively incorporate DVB comonomers and produce an α-olefin/DVB copolymer with a linear copolymer structure. In other words, the catalyst can effectively incorporate DVB into the polymer through single enchainment, and no reactivity to the styrenic units already existed in the polymer.

The ideal α-olefin/DVB copolymer would have a linear polymer structure with narrow molecular weight and composition distributions, and the vinyl/phenyl (VN/PH) mole ratio in the copolymer would be nearly unity. Fig. 3 shows a ^1H NMR spectrum of two PE copolymers (PE-DVB) containing 1.5 and 7.2 mol% of DVB units. Four chemical shifts were observed at near 5.3, 5.8, 6.8, and 7.0–7.4 ppm (with the integrated peak intensity ratio near 1:1:1:4), corresponding to three individual vinyl protons and four aromatic protons in the pending styrene unit.

Table 5 summarizes the experimental results of terpolymerization reactions of ethylene, propylene, and DVB by using $Et(Ind)_2ZrCl_2/MAO$ catalyst. High DVB incorporation was observed in all reactions — up to 20 mol% of DVB units in the EP-DVB terpolymer has been prepared. In addition, all of the terpolymers were completely soluble in common organic solvents, such as hexane, toluene, and tetrahydrofuran (THF). In general, the prepared EP-DVB terpolymers have a relatively well-defined molecular structure with narrow molecular weight and composition distributionsThe intergrated peak intensity ratio indicates that the mole ratio of vinyl/phenyl moieties (UN/PH) is nearly equal.

Fig. 4 compares the GPC curves of the EP copolymer (E: 64.8 mol%, P: 35.2 mol%) and the EP-DVB terpolymer (E: 63.7 mol%, P: 33.4 mol%, DVB: 2.9 mol%) prepared under identical reaction conditions, except for the addition of the DVB monomer. Both polymers have similar molecular weight distributions ($M_w/M_n \sim 2$), indicating nearly ideal reaction conditions. The DSC results also showed a homogeneous terpolymer microstructure with no detectable melting point (T_m) and a sharp glass transition temperature (T_g) with a flat baseline in each terpolymer.
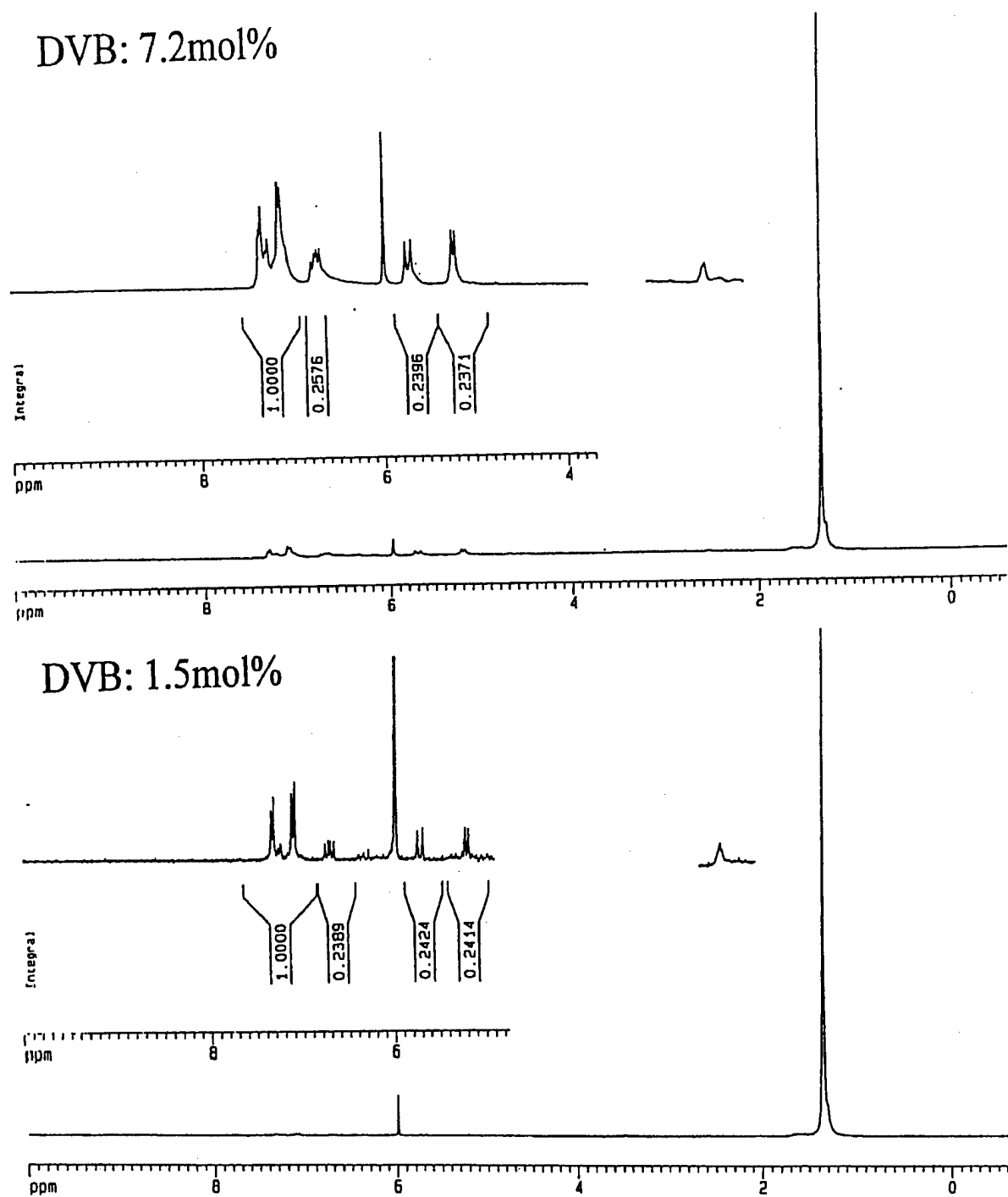
DVB: 7.2mol%

DVB: 1.5mol%

Fig. 3. ^{1}H NMR spectra of PE-DVB copolymers containing 1.5 and 7.2 mol% of DVB units.

Table 5

A Summary of terpolymerization (polymerization condition: [cat] $= 2.5 \times 10^{-6}$ mol; [MAO]/[Zr] $= 3000$; solvent: 100 ml hexane; temperature: 50°C; pressure: 30 psi; time: 15 min) of ethylene, propylene, and divinylbenzene using an Et(Ind)$_2$ZrCl$_2$/MAO catalyst

Monomer feed		Catalyst[a] activity	Terpolymer composition (mol%)				T_g (°C)
Mixed C$_2$/C$_3$ (psi)	DVB (mol/l)		C$_2$	C$_3$	DVB	VN/PH	
40/60	0.1	2780	56.4	42.5	1.1	95.0	−50.6
40/60	0.3	2000	59.3	39.0	1.7	93.2	−47.3
40/60	0.6	1650	62.4	32.9	4.7	97.0	−31.3
40/60	1.2	1230	56.0	22.9	21.1	98.0	−21.6
60/40	0.3	1810	67.8	30.6	1.6	97.0	−36.4
60/40	0.6	1710	65.3	30.3	4.4	95.2	−29.0

[a] Catalyst activity: Kg/mol Zr.h.

6. Synthesis of polyolefin containing a reactive end group

It is always a scientific challenge to prepare polymer having a terminal functional group, which offers an opportunity to serve as a building block for constructing multi-segmented polymers. In chemistry, the general method of preparing this class of polymers has been based on living polymerization [56–60] with a chemical reaction to convert living chain end to a functional group. In our laboratory, we have developed a very convenient and effective route to prepare polyolefin containing a borane or p-MS terminal group by in situ chain transfer reaction during the metallocene polymerization process. With the
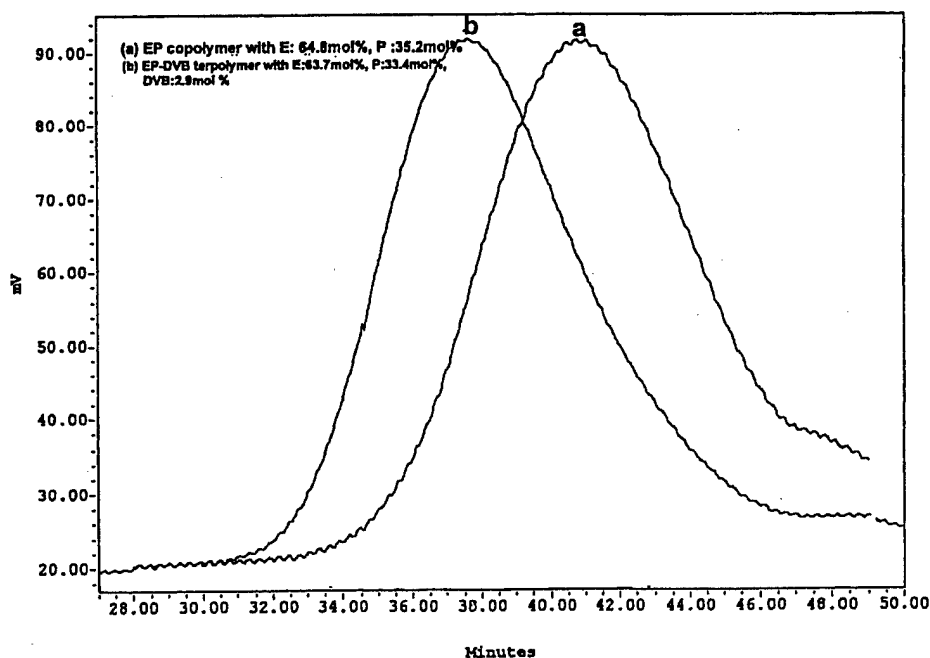

Fig. 4. GPC Curves of (a) EP copolymer and (b) EP-DVB terpolymer.

appropriate chain transfer agent (CT), it's possible to have a chain transfer reaction that in situ takes place without changing the rate of polymerization. Each catalyst can produce multiple polymer chains as usual, and the polymer chain produced has a terminal group (the residue of the chain transfer agent). Usually, the polymer's molecular weight is reversibly proportional to the [CT]/[monomer] ratio. This chemistry is a potential drop-in technology with only a small modification to current processes, and might also be applicable to all polyolefin (PE, PP, *s*-PS, etc.) cases.

6.1. Polyolefins containing a borane end group [50,51]

The application of organoboranes (containing B–H moiety) as the chain transfer agents was formulated with several intriguing questions and objectives in mind. With the knowledge of facile ligand exchange of B–H with many metal-alkyl groups, it is very possible that the B–H group has a high reactivity with M–C active sites, as illustrated in Eq. (5).

$$(5)$$
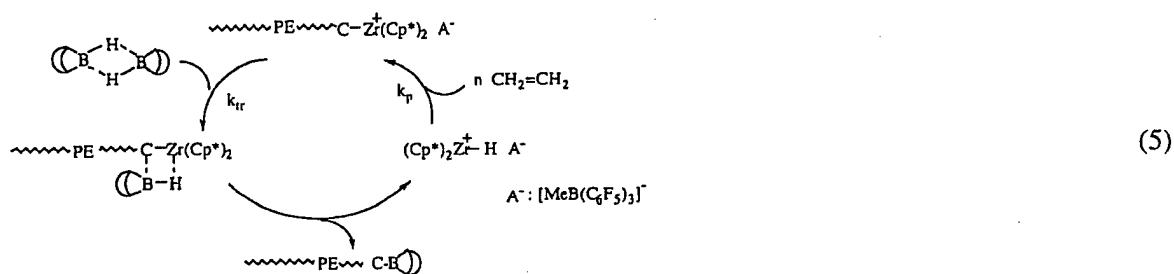
There are two concerns in the B–H chain transfer reaction, namely, hydroboration reaction of the B–H group to α-olefin monomers and ligand exchange reaction between borane and the aluminium-alkyl co-initiator. It is known that the borane compounds containing B–H groups usually form a stable dimer (unreactive to olefins) in hexane and toluene solvents that are used in metallocene polymerizations. No reaction between borane and α-olefin is expected during the polymerization. On the other hand, we can use a perfluoroborate co-initiator instead of MAO or alumium-alkyl compounds, which are stable with most alkylborane compounds. Therefore, the B–H moiety in dialkylborane can engage a chain transfer reaction by ligand exchange between B–H and M–C (M: transition metal), as illustrated in Eq. (5). Each PE chain (PE-*t*-B) will have a terminal borane group [50] if the chain transfer reaction is the dominant termination reaction, and the molecular weight of the borane-terminated polymer will be reversally proportional to the concentration of borane chain transfer agent.

Table 6 summarizes the experimental results of ethylene polymerization in the presence of 9-BBN using two metallocene catalysts, $[Cp_2^*ZrMe]^+[MeB(C_6F_5)_3]^-$ and $[Cp_2^*ZrMe]^+[B(C_6F_5)_4]^-$ ($Cp^* = \eta^5$-C_5H_5, ηs^5-Me_5C_5). To maintain the constant [borane]/[ethylene] feed ratio, the reactions were carried out with rapid mixing and a short reaction time, about a three to five minutes reaction time. Basically, higher concentrations of a 9-BBN chain transfer agent resulted in lower molecular weights of the resulting PE. The polymer molecular weight distribution is generally narrow, which is consistent with single site polymerization process. The catalyst activity was also depressed in the presence of 9-BBN, which may reflect the competitive coordination at metallocene active sites between monomer and chain transfer agents. For analytical studies, a PE-*t*-B polymer was usually oxidized by NaOH/H$_2$O$_2$ to form a hydroxy-terminated polymer (PE-*t*-OH).

Fig. 5 shows the plot of polymer molecular weight (M_n) vs. the mole ratio of ethylene/9-BBN for the

Table 6
Metallocene-activated ethylene polymerization (pressure = 1 atm; [ethylene] = 0.11 M) in the presence of 9-BBN as the chain transfer agent (Reproduced with permission from J. Am. Chem. Soc. 1999;121:6763. Copyright 1999 Am. Chem. Soc.)

Run	Catalyst	9-BBN (mM)	Time (min)	Yield (g)	Catalyst[a] activity	M_n[b] ($\times 10^{-3}$)	M_w/M_n
1	$[Cp_2^*ZrMe]^+[MeB(C_6F_5)_3]^-$	0	3	3.50	2333	85.2	2.0
2	$[Cp_2^*ZrMe]^+[MeB(C_6F_5)_3]^-$	3.0	3	2.01	1333	76.0	2.4
3	$[Cp_2^*ZrMe]^+[MeB(C_6F_5)_3]^-$	4.5	3	2.05	1366	55.5	2.9
4	$[Cp_2^*ZrMe]^+[MeB(C_6F_5)_3]^-$	7.5	3	1.45	1033	42.2	2.6
5	$[Cp_2^*ZrMe]^+[MeB(C_6F_5)_3]^-$	7.5	5	2.02	1333	45.8	2.6
6	$[Cp_2^*ZrMe]^+[MeB(C_6F_5)_3]^-$	12.0	3	1.20	800	19.4	2.7
7	$[Cp_2^*ZrMe]^+[MeB(C_6F_5)_3]^-$	18.0	3	0.75	500	8.9	3.2
8	$[Cp_2^*ZrMe]^+[MeB(C_6F_5)_3]^-$	23.4	3	0.25	167	3.7	4.0
9	$[Cp_2^*ZrMe]^+[B(C_6F_5)_4]^-$	4.5	3	2.00	1333	59.4	2.6
10	$[Cp_2^*ZrMe]^+[B(C_6F_5)_4]^-$	7.5	3	1.51	1000	46.2	2.5
11	$[(Ind)_2ZrMe]^+[MeB(C_6F_5)_3]^-$	7.5	3	1.90	1267	43.9	2.3
12	$[Cp_2ZrMe]^+[MeB(C_6F_5)_3]^-$	7.5	3	2.50	1667	46.9	2.1

[a] Catalyst activity = kg of PE/mol of catalyst.atm.h.
[b] By GPC in 1,2, 4-trichlorobenzene vs. polystyrene standards.

comparative runs 2–8 in Table 6. The polymer's molecular weight is almost linearly proportional to the molar ratio of [ethylene]/[9-BBN]. It is clear that the chain transfer reaction with 9-BBN (with rate constant k_{tr}) is the dominant termination process, and competes with the propagating reaction (with rate constant k_p). The degree of polymerization (X_n) follows a simple comparative equation $X_n = k_p[\text{olefin}]/k_{tr}[\text{9-BBN}]$ with a chain transfer constant $k_{tr}/k_p \sim 1/75$. The existence of a borane terminal group in PE was also evidenced by the NMR spectrum of a low molecular weigth PE-t-OH.

Similar B–H chain transfer reactions can be applied to other metallocene-mediated olefin polymerizations. One example is the synthesis of borane-terminated syndiotactic polystyrene (s-PS-t-B) [51]. Table 7 shows several $[Cp^*TiMe_2]^+[MeB(C_6F_5)_3]^-$ mediated polymerizations of styrene with the presence of 9-BBN. The effects of the chain transfer reaction are clearly revealed by the reduction of the polymer's molecular weight in the presence of 9-BBN. Basically, the higher the concentration of 9-BBN chain transfer agent used, the lower the molecular weight of the resulting PE. The catalyst activity was somewhat depressed if a high concentration of 9-BBN was presented in the system, which may reflect the competitive coordination at the titanocene active sites between monomers and chain transfer agents. It is very interesting to note that the syndiotacticity and melting temperatures of all s-PS-t-B polymers are similar to those of the s-PS polymer. The 9-BBN chain transfer agent did not interfere with the regio- and stereo-selective insertion process.

6.2. Polyolefins containing a p-methylstyrene end group [52]

Recently, we have also discovered a new polymerization process to prepare p-methylstyrene (p-MS) terminated polyolefins. The process involves contacting α-olefin ($>C_3$) with p-MS and hydrogen simultaneously in the presence of some metallocene catalysts containing a specific bridged Cp* ligand. Ironically, the desirable metallocene catalysts usually show very poor styrene incorporation in the copolymerization reaction between propylene and styrene. The reaction mechanism involved in forming
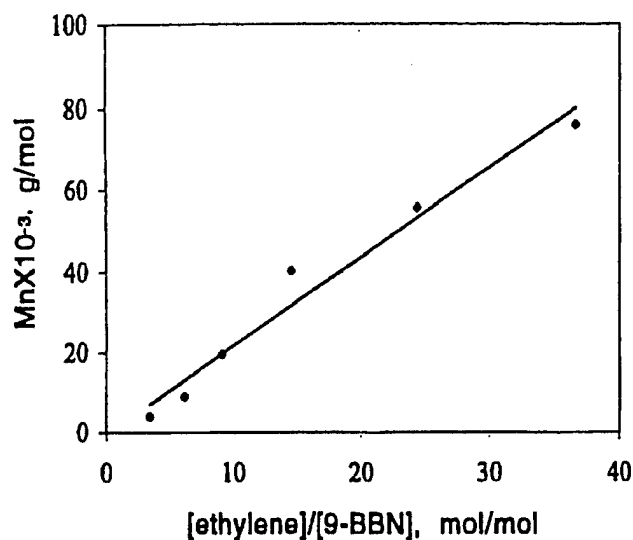
Fig. 5. A plot of the average molecular weights (Mn) of PE-t-B polymers vs. the mole ratio of [ethylene]/[9-BBN] in the feed (runs 2–8 in Table 6). (Reproduced with permission from J. Am. Chem. Soc. 1999;121:6763. Copyright 1999 Am. Chem. Soc.)

the p-MS terminated polyolefin may be exemplified by the polymerization of propylene in the presence of p-MS and H_2 chain transfer agents using a rac-Me$_2$Si[2-Me-4-Ph(Ind)]$_2$ZrCl$_2$/MAO catalyst, as illustrated in Eq. (6).

(6)
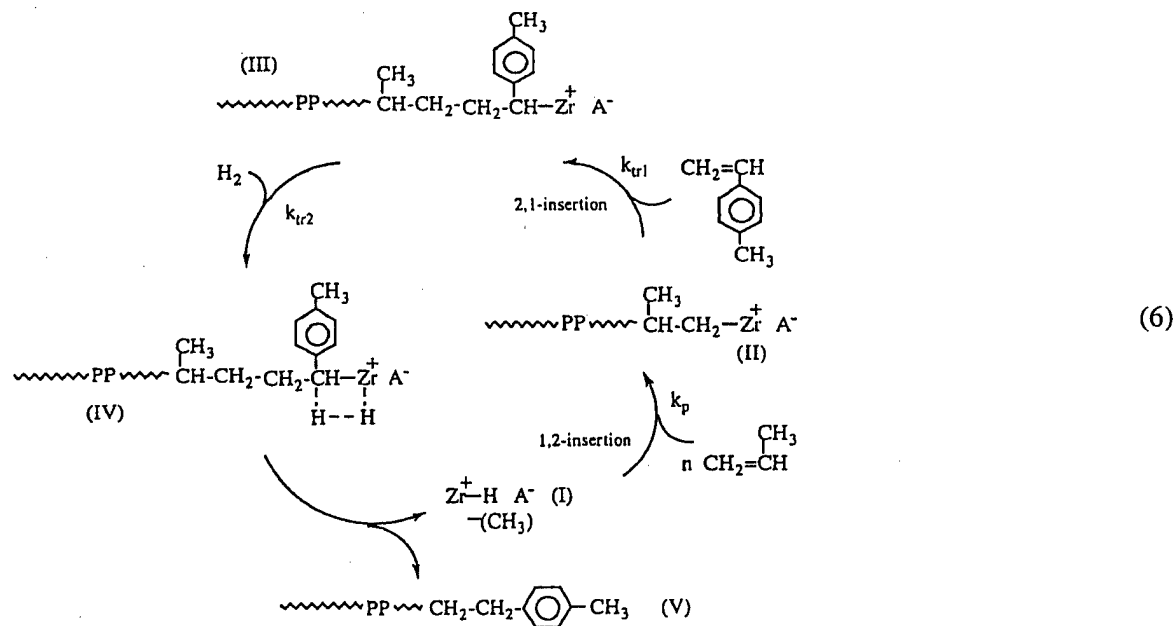
During the polymerization of propylene (with 1,2-insertion manner) the propagation Zr–C site (II) can also react with p-methylstyrene (with 2,1-insertion manner) to form p-methylstyrene terminated PP (III). The catalytic Zr–C site in compound (III) becomes inactive to both propylene and p-methylstyrene

Table 7

[Cp*TiMe$_2$]$^+$[Me(B(C$_6$F$_5$)$_3$]$^-$ — activated styrene syndiospecific polymerization in the presence of 9-BBN as a chain transfer agent (styrene = 10 ml, catalyst concentration = 10 μmol) (Reproduced with permission from Macromolecules 1999;32:8689. Copyright 1999 Am. Chem. Soc.)

Run	9-BBN (μmol)	Reaction time (min)	Yield (g)	Catalyst activity[a]	Syn.[b] (%)	T_m (°C)	[η]	M_w (g/mol)
1	25	3	1.3	2600	97.0	270	1.270	460,000
2	50	3	1.4	2800	96.2	271	0.806	240,000
3	100	3	1.3	2600	95.8	270	0.580	150,000
4	150	3	1.1	2200	95.2	271	0.373	80,000
5	200	3	0.8	1600	93.4	270	0.340	70,000
6	300	3	0.5	1000	94.7	272	0.188	30,000
7	400	3	0.3	600	95.0	270	0.116	15,000
8	500	3	0.1	200	93.2	270	0.087	10,000

[a] Catalyst activity = kg of s-PS/mol of Ti·h.
[b] Syntactic index was determined by ^{13}C NMR.

[302] due to the combination of steric hindrance between the active site (Zr–C) and the incoming monomer (propylene with 1,2-insertion), and the formation of complex between the adjacent phenyl group and the Zr$^+$ ion. On the other hand, with the presence of hydrogen the dormant Zr–C site (III) can react with hydrogen to form PP-*t*-*p*-MS (V) and regenerate a Zr–H species (I) that is capable of reinitiating the polymerization of propylene and continuing the polymerization cycle. Overall, the polymerization process resembles a sequential chain transfer reaction — first to styrene (or styrene derivative) and then hydrogen — during the metallocene mediated propylene polymerization. This process not only produces PP with a terminal *p*-MS unit, but also maintains high catalyst activity. The molecular weight of the resulting polymer is proportional to the [propylene]/[*p*-MS] ratio.

Table 8 summarizes the results of *p*-methylstyrene terminated polypropylene (PP-*t*-*p*-MS) using a rac-Me$_2$Si[2-Me-4-Ph(Ind)]$_2$ZrCl$_2$/MAO catalyst in the presence of *p*-MS and hydrogen chain transfer agents. The systematic study was conducted to evaluate the effect of hydrogen and *p*-MS concentrations on the catalyst activity and polymer molecular weight. All comparative reaction sets show that hydrogen is necessary to complete the chain transfer reaction to *p*-MS during the metallocene-mediated polymerization of propylene. In general, the change of hydrogen concentration does not affect the molecular weight and molecular weight distribution of the resulting *p*-MS terminated PP polymers. However, a sufficient quantity of hydrogen, which increases with the increasing of [*p*-MS], is needed to maintain high catalyst activity and *p*-MS conversion.

Fig. 6 (left) compares the GPC curves of PP-*t*-*p*-MS polymers with a PP homopolymer. All polymers were prepared under the same reaction conditions, except for varying the quantity of the *p*-MS chain transfer agent. An appropriate concentration of hydrogen was also introduced in each chain transfer reaction to assure the completion of the polymerization cycles. The GPC curves show the systematic reduction of the polymer molecular weight, along with the increase of the *p*-MS concentration. The low molecular weight PP-*t*-*p*-MS (M_n as low as a few thousandths) that has been prepared is a well-defined polymer with narrow molecular weight distribution (M_w/M_n ~ 1.7). In fact, the molecular weight distribution of PP-*t*-*p*-MS gradually reduced along with the reduction in the polymer molecular weight. All experimental results clearly indicate effective chain transfer reactions.

The kinetic constants during the polymerization can be obtained from Fig. 6 (right), which shows the

Table 8

A summary of PP-t-p-MS polymers prepared (reaction conditions: 50 ml toluene, propylene (100 psi), $[Zr] = 1.25 \times 10^{-6}$ mol/l, $[MAO]/[Zr] = 3000$, temperature = 30°C, time = 15 min) by the combination of a rac-Me$_2$Si[2-Me-4-Ph(Ind)]$_2$ZrCl$_2$/MAO catalyst and p-MS/hydrogen chain transfer agents

Run	p-MS (M)	H$_2$ (psi)	Yield (g)	Catalyst activity[a]	p-MS in PP (mole%)	p-MS Conversion (%)	Mn (× 10^{-3})	PDI (Mw/Mn)
Control 1	0	0	26.94	86,208	0	–	77,600	2.9
Control 2	0.0305	0	0.051	163	0.16	0.05	59,700	3.4
1	0.0305	2	3.80	12,160	0.14	8.30	55,500	2.4
2	0.0305	6	8.04	25,728	0.15	18.83	54,800	2.5
3	0.0305	12	12.04	38,528	0.15	28.19	55,400	2.3
4	0.0305	35	24.67	78,944	0.13	50.05	34,600	2.8
Control 3	0.076	0	~0	–	–	–	–	–
5	0.076	6	0.91	2912	0.40	2.33	27,600	2.1
6	0.076	12	1.69	5408	0.41	4.33	25,900	2.3
7	0.076	20	8.81	28,192	0.43	23.65	20,500	2.3
8	0.076	35	10.52	33,664	0.41	26.86	25,800	2.3
Control 4	0.153	0	~0	–	–	–	–	–
9	0.153	12	0.35	1120	0.66	0.72	10,000	2.0
10	0.153	20	3.81	12,192	0.61	7.26	11,700	2.0
11	0.153	35	4.41	14,112	0.63	8.67	9700	1.9

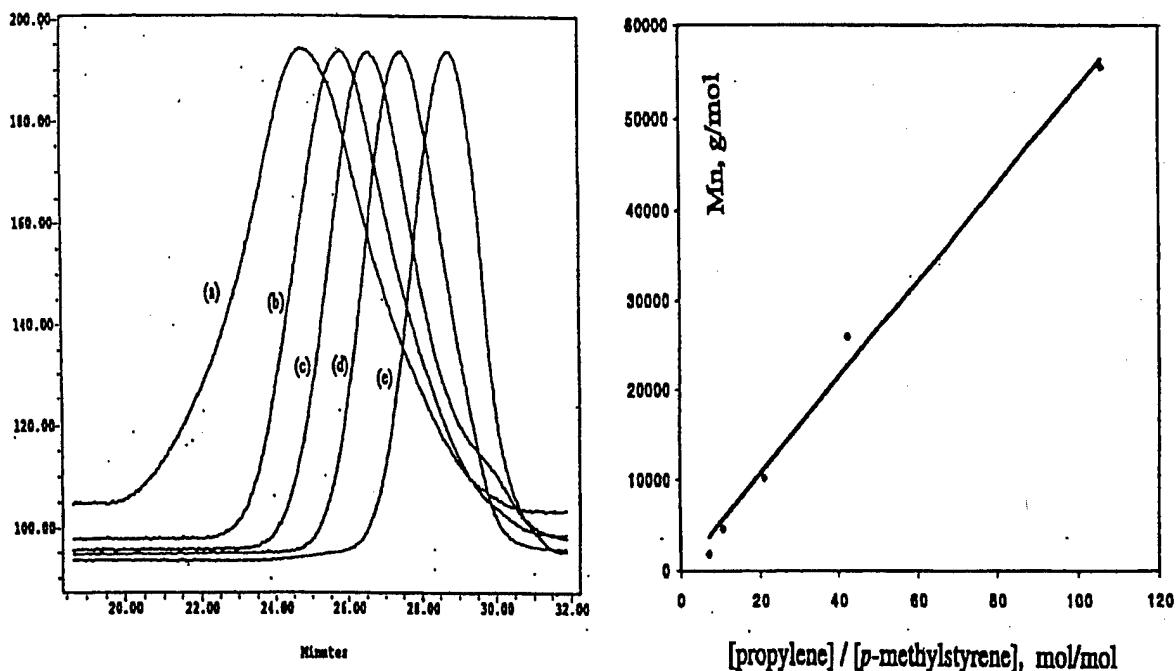[a] Catalyst activity = kg of PP/mol of catalyst.h.

Fig. 6. Left: GPC curves of (a) PP (M_n = 77.6 × 10^3) and several PP-t-p-MS polymers with M_n of (b) 54.8 × 10^3, (c) 25.9 × 10^3, (d) 10 × 10^3, and (e) 4.6 × 10^3 g/mol. Right: the plot of PP-t-p-MS molecular weight to mole ratio of [propylene]/[p-MS]. (Reproduced with permission from J. Am. Chem. Soc. 2001;123:4871. Copyright 2001 Am. Chem. Soc.)

plot of the PP-t-p-MS molecular weight to the mole ratio of [propylene]/[p-MS]. The linear relationship between M_n and [propylene]/[p-MS] clearly indicates that the chain transfer reaction to p-MS (with rate constant k_{tr}) is the dominant termination process, and competes with the propagating reaction (with rate constant k_p). The degree of polymerization (X_n) follows the equation $X_n = k_p$[propylene]/k_{tr}[p-MS] with a chain transfer constant $k_{tr}/k_p \sim$ 1/6.36. It is very interesting to note that the same chain transfer reaction scheme can be applied to many styrenic derivatives, including the ones containing masked functional group, which are very desirable in some polymer modification reactions.

7. Synthesis of polyolefin graft copolymers

As discussed, the major objective of developing reactive polyolefins is to prepare functional polyolefins with graft and block structures. These polymers, containing high concentration of functional (polar) groups and persisting the desirable polyolefin properties, are very effective interfacial agents to improve the compatibility of polyolefin with other materials.

In the graft copolymer structure, the polymer contains a polyolefin backbone and several functional polymer side chains, such as PMMA, PVA, and PCL. In general, the chemistry to prepare polyolefin graft copolymers is very limited. Numerous approaches, based on post polymerization process, have been employed in forming polyolefin graft copolymers. Ionizing radiation (X-ray, γ-rays, and e-beams) in the presence of air, ozone, UV with accelerators, and free radical initiators [61,62] have all been used

to form polymeric peroxides. When heated in the presence of monomers, some polymeric peroxides initiate graft polymerization. However, these high-energy reactions lead to many side reactions, such as crosslinking and chain cleavage. In most cases, the structure and composition of copolymers are difficult to control given the considerable amounts of ungrafted homopolymers.

By far, the most effective route for preparing functional polyolefin graft copolymers is by employing reactive polyolefin intermediates, containing borane [63–67], *p*-methylstyrene [42–44], and divinylbenzene [52] reactive side groups. The reactive groups provide the selective sites (serving as initiators, monomers, or termination agents) in the graft reaction of functional monomers. The combination of these three reactive polyolefin approaches (discussed in this section) offers a comprehensive coverage of polyolefin graft copolymers with well-defined molecular structure, i.e. controlled graft density and graft length.

7.1. Living radical graft-from polymerization via borane side groups

As illustrated in Eq. (7), the alkyl-9-BBN side groups in polyolefin (see Section 5.1) can then be spontaneously oxidized to a peroxide (B–O–O–C) moiety (I) even at very low temperature ($-65°C$). Due to the unfavorable ring strain increase by inserting oxygen into the C–B bonds in the bicyclic ring of 9-BBN, which destroys the stable double chair-form structure, the oxidation reaction selectively takes place at the C–B bond [68,69] in the linear alkyl group to produce peroxyborane (C–O–O–B) (I).

$$(7)$$
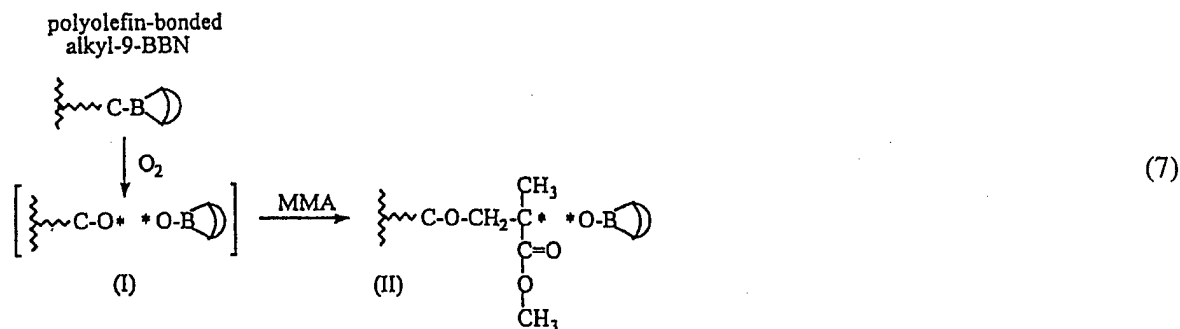
The peroxyborane (I) behaves very differently from regular benzoyl peroxides, and consequently decomposes by itself even at ambient temperature. The decomposition reaction follows the homolytical cleavage of peroxide to generate an alkoxy radical (C–O $*$) and a borinate radical (B–O $*$). The alkoxyl radical (C–O $*$) is very reactive and can then be used for the initiation of radical polymerization with the presence of free radical polymerizable monomers, such as methacrylates, vinyl acetate, acrylonitrile, etc., at ambient temperature. On the other hand, the borinate radical (B–O $*$), stabilized by the empty p-orbital of boron through back-donating electron density, is too stable to initiate polymerization. However, the borinate radical may form a weak and reversible bond with the growing chain end during the polymerization reaction. Upon the dissociation of the electron pairs in the resting state, the growing chain (II) can then react with monomers to extend the polymer chain to form graft copolymer. This living polymerization process minimizes the undesirable chain transfer reaction and termination (coupling and disproportional) reaction between the two growing chain ends, which result in the formation of homopolymers and crosslinked material. In most cases, the resulting graft copolymers are completely soluble and processible. The graft length (PMMA side chain) is basically controlled by the MMA concentration and reaction time. Some interesting graft polymers - including PE-*g*-PVA, PE-*g*-PMMA, PP-*g*-PMMA,

Table 9
A summary of PP-*g*-PMMA graft copolymers [66]

Run number	9-BBN in PP (mol%)	O_2 (ml/h)	Monomer/solvent	Reaction time (h)	MMA in PP (mol%)
1	0.5	1.5/12	MMA (neat)	48	66
2	0.5	3.0/1	MMA (neat)	2	6
3	0.5	1.4/3	MMA/THF	12	52
4	0.5	6 (at once)	MMA (neat)	48	1.5
5	0.5	Diffusion	MMA/THF	48	12

PP-*g*-PMA, PP-*g*-PVA, PP-*g*-SMA (SMA: styrene/maleic anhydride alternating copolymer), EP-*g*-PMMA, EP-*g*-SMA and Butyl-*g*-PMMA — have been synthesized with controllable compositions and molecular microstructures [63–67].

Table 9 summarizes the experimental results of PP-*g*-PMMA copolymers. The comparison among runs (A-1–A-4) shows the relationship of the addition of oxygen to the graft efficiency. Even though the final stoichiometry of oxygen to boron should be 1:1, the best results in this heterogeneous reaction system are realized when the O_2 is introduced slowly so that O ≪ B at any time. Excess O_2 is not only a poison for free radical polymerizations, but also leads to over-oxidation to boronates and borates which are poor free radical initiators at room temperature. The polarity of the solution also effects the graft reaction. THF is a very good solvent in this reaction. Non-polar solvents, such as benzene, slow down the graft-from reaction, which may be due to the solubility of O_2 in the solvent. In the run A-5, the oxygen was introduced by diffusion of air through the rubber septum that was tightly installed on the top of the reactor. The insufficient O_2 in this process leads to low percentage of PMMA formation.

Fig. 7 compares the IR spectra of three PP-*g*-PMMA graft copolymers and a corresponding PP-OH. All of them were derived from the same copolymer contained 0.5 mol% borane monomers. PP-OH polymer was obtained by converting borane groups to hydroxy groups, and all graft copolymers were prepared under the same reaction conditions expect for reaction time. The IR spectrum of PP-OH is basically indistinguishable from that of *i*-PP because of the extremely low concentration of hydroxy groups. On the other hand, the strong absorption band at 1730 cm^{-1}, corresponding to ester groups, clearly shows the existence of PMMA in the graft copolymers. A high concentration (>65 mol%) of PMMA can be incorporated into PP by a small quantity (0.5 mol%) of borane groups. The PMMA content increases with the reaction time, which indicates the living free radical polymerization process, and the graft length is basically controlled by the reaction time and monomer concentration.

Similar graft-from reactions have been extended to other polyolefins. Satisfactory results were obtained in both homogeneous (PE, PP, and PB cases) and heterogeneous (PO, EP, and Butyl rubber cases) reaction conditions [70,71]. In one homogeneous case, a commercial EPDM rubber was used to prepare EP-*g*-PMMA graft copolymers. Fig. 8 compares the ^{1}H NMR spectra of the resulting EP-*g*-PMMA copolymers and the starting EPDM rubber, poly(ethylene-*co*-propylene-*co*-1,4-hexadiene). The chemical shift at 3.6 ppm in Fig. 11(b) and (c) corresponds to the methyl groups (CH_3O) in PMMA. The chemical shifts between 2.1 and 0.7 ppm include all of the protons in EP and five of the protons in the methyl group located on the PMMA backbone. The copolymer composition was calculated by the ratio of the two integrated intensities at 3.6 and 0.7–2.1 ppm and the number of protons both chemical shifts represent. Fig. 11(b) and (c) indicate 28 and 52 mol % PMMA in EP-*g*-PMMA copolymers, respectively.

The DSC curve of the EP-*g*-PMMA copolymer (with a 50/50 composition) shows two glass transition
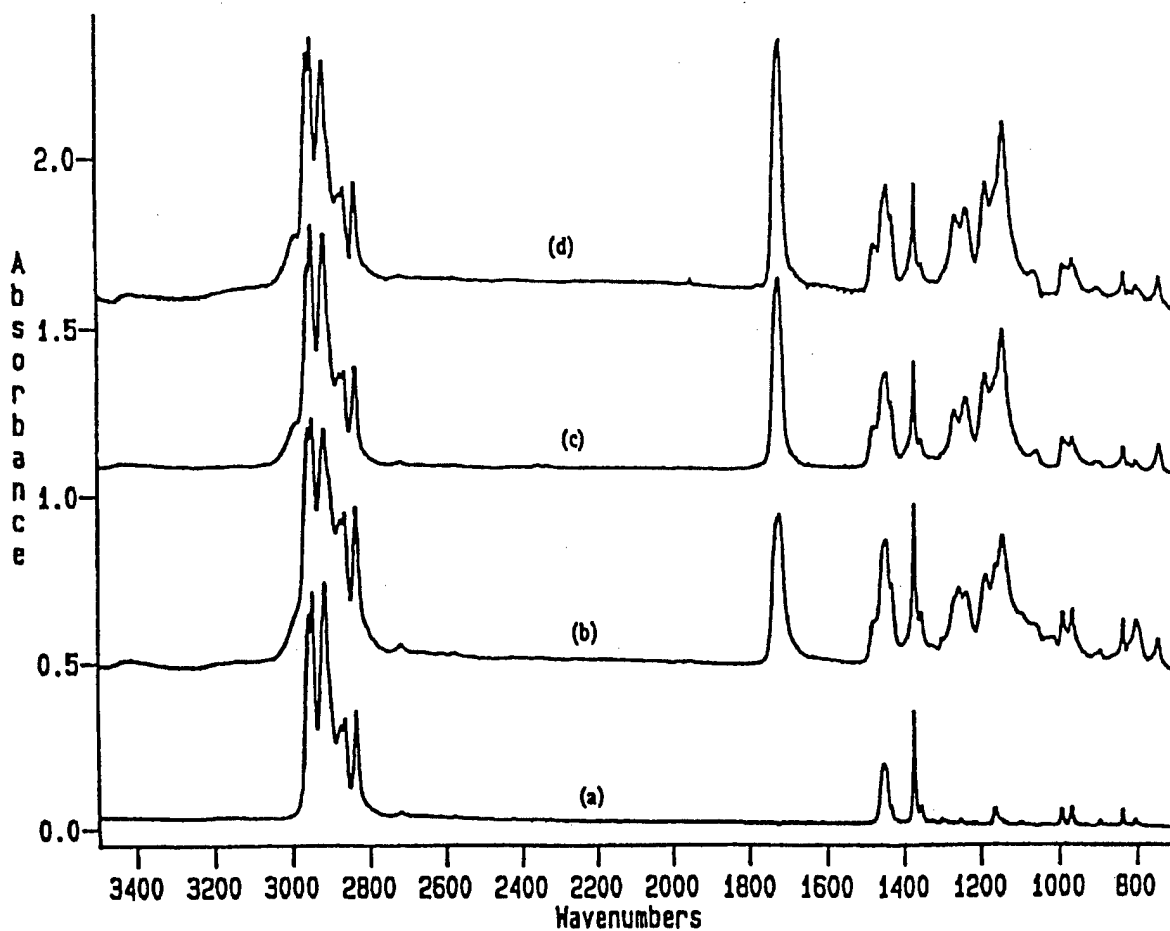
Fig. 7. IR spectra of (a) PP-OH with 0.5 mol% OH groups and three PP-g-PMMA graft copolymers containing (b) 20, (c) 52, and (c) 66 mol% MMA. (Reproduced with permission from Macromolecules 1993;26:3467. Copyright 1993 Am. Chem. Soc.)

temperatures (T_g), −47 and +130°C, corresponding to the starting EPDM rubber and PMMA homopolymer, respectively. This result indicates a clear phase separation between the EP backbone and the PMMA side chains. The copolymer backbone must have enough consecutive sequences of EP backbone units to form separate domains. The side chain must be a high molecular weight polymer with a microstructure similar to that of PMMA homopolymer. The clear phase separation with hard (polar) and soft (non-polar) domains is a very interesting molecular structure. In fact, most of the graft copolymers behave like thermoplastic elastomers.

7.2. Living anionic graft-from polymerization via p-methylstyrene side groups [72]

As discussed in Section 5.2, polyolefins containing p-MS groups have been prepared via metallocene copolymerization reactions, the copolymers cover a wide range of compositions and narrow molecular weight and composition distributions. Usually, a low concentration (<1 mol%) p-MS in the copolymer
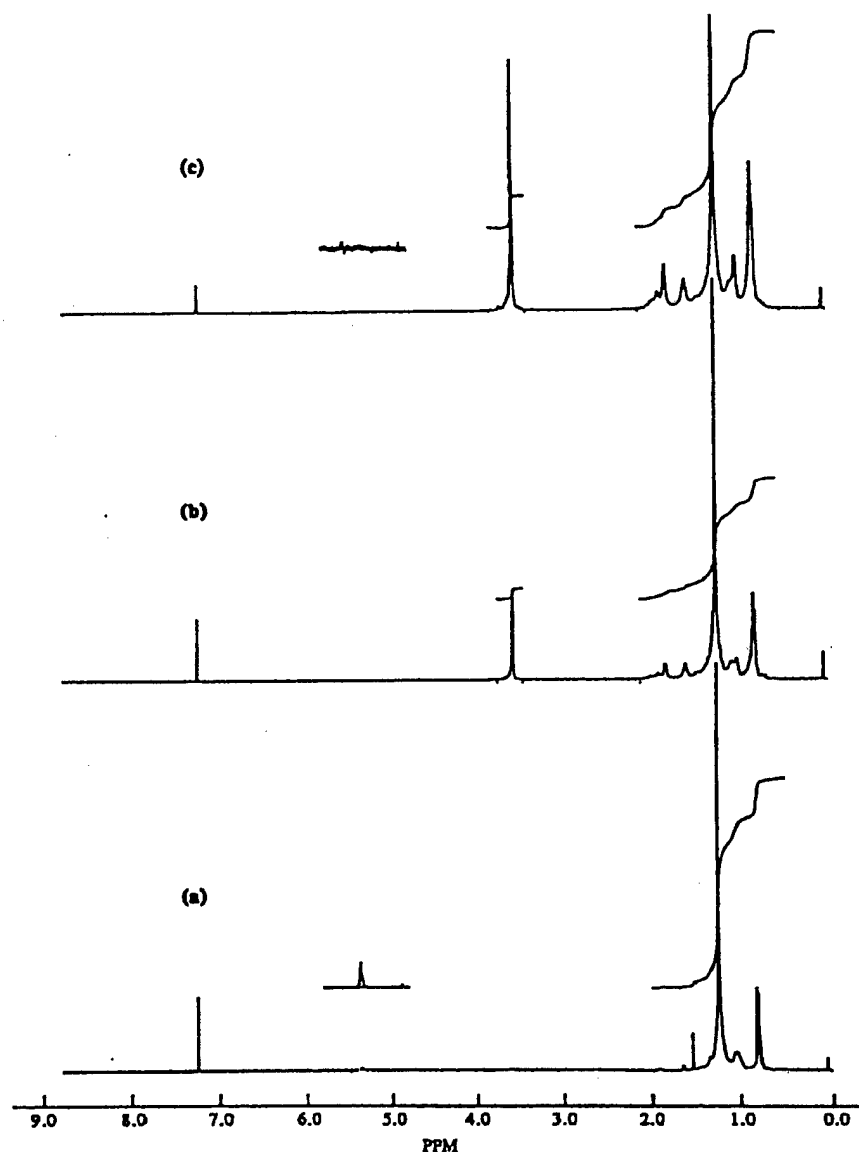
Fig. 8. Comparison of the ^{1}H NMR spectra of (a) EPDM and two resulting EP-g-PMMA copolymers containing (b) 28 and (c) 52 mol% PMMA. (Reproduced with permission from Macromolecules 1994;27:26. Copyright 1994 Am. Chem. Soc.)

is preferred for the preparation of graft copolymer because the resulting graft copolymer will have low graft density and long graft length. As illustrated in Eq. 8, the p-MS groups in PE can be effectively metallated at ambient temperature. The lithiated PE-p-MS copolymer contain several polymeric anions that are homogeneously distributed in the polymer chain. The living anionic graft-from reactions were generally carried out at ambient temperature by suspending the lithiated PE-p-MS copolymer in cyclohexane in the presence of the monomers. After the polymerization reaction, the crude product was vigorously extracted to remove any ungrafted homopolymer. In all cases, the homopolymer fraction

was negligible. The insolubility of the crystalline PE-*p*-MS copolymer at room temperature allows for maximum removal of the unreacted lithiation reagent after the metallation reaction. The combination of pure lithiated polymer and the living graft-from polymerization minimizes the formation of ungrafted homopolymer during the graft-from polymerization.
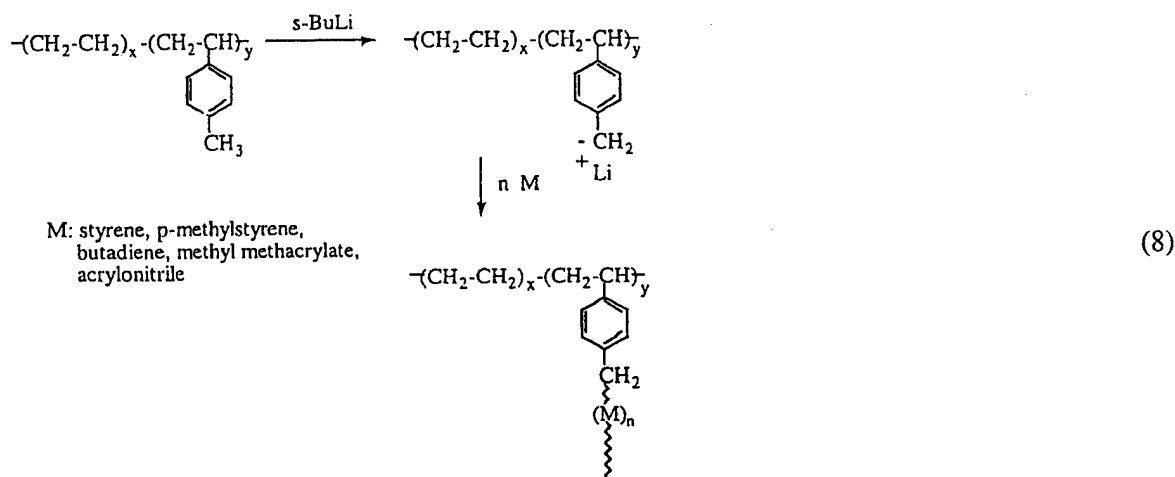
$$-(CH_2-CH_2)_x-(CH_2-CH)_y \quad \xrightarrow{\text{s-BuLi}} \quad -(CH_2-CH_2)_x-(CH_2-CH)_y$$

CH₃ → -CH₂ ⁺Li

M: styrene, p-methylstyrene,
   butadiene, methyl methacrylate,
   acrylonitrile

↓ n M

$$-(CH_2-CH_2)_x-(CH_2-CH)_y$$
CH₂
(M)ₙ

(8)

Fig. 9 shows ^{1}H NMR spectra of three resulting PE-*g*-PS graft copolymers containing 25.6, 38.1, and 43.8 mol% polystyrene, respectively. They were prepared from the same starting PE-*p*-MS polymer, containing 0.9 mol % of *p*-MS units. In contrast to the starting PE-*p*-MS, three additional chemical shifts arise in the graft copolymers at 1.55, 2.0, and 6.4–7.3 ppm corresponding to CH_2, CH, and aromatic protons in polystyrene. The quantitative analysis of the copolymer composition was calculated by the ratio of two integrated intensities between the aromatic protons ($\delta = 6.4$–7.3 ppm) in the PS side chains and the methylene protons ($\delta = 1.35$–1.55 ppm) and the number of protons both chemical shifts represent.

Table 10 summarizes the experimental conditions and results of two sets of comparative graft-from reactions, all started from the same PE-*p*-MS copolymer (containing 0.9 mol% *p*-MS) and different extend of metallation reaction. Both the yield and graft compositions (PS content) of the graft copolymer are basically proportional to the quantity of monomers used in the graft-from reaction. The good control of graft copolymer formation is obviously due to the living anionic polymerization, which effectively converts monomers to the grafted side chains. The graft density is defined as the number of grafted side chains per 1000 repeating methylene units of the PE backbone. Since this process involves living anionic polymerization and fast initiation, it is reasonable to assume that each benzylic lithium produces one PS side chain and that the side chains have a narrow molecular weight distribution. Therefore, the graft density is the same as the density of the benzylic anions. The molecular weight of the side chain is inversely proportional to the degree of metallation and proportional to the quantity of monomer used in the graft-from polymerization.

Overall, this chemistry provides a very useful route for preparing PE-*g*-PS and PE-*g*-PMS copolymers with relatively well-defined molecular structures, i.e. relatively narrow molecular weight distribution ($\bar{M}_w/\bar{M}_n = 2.5$) of the backbone and well-defined side chains. All the important factors in a graft copolymer — including graft density, graft length and copolymer composition — can be controlled during the reaction processes.
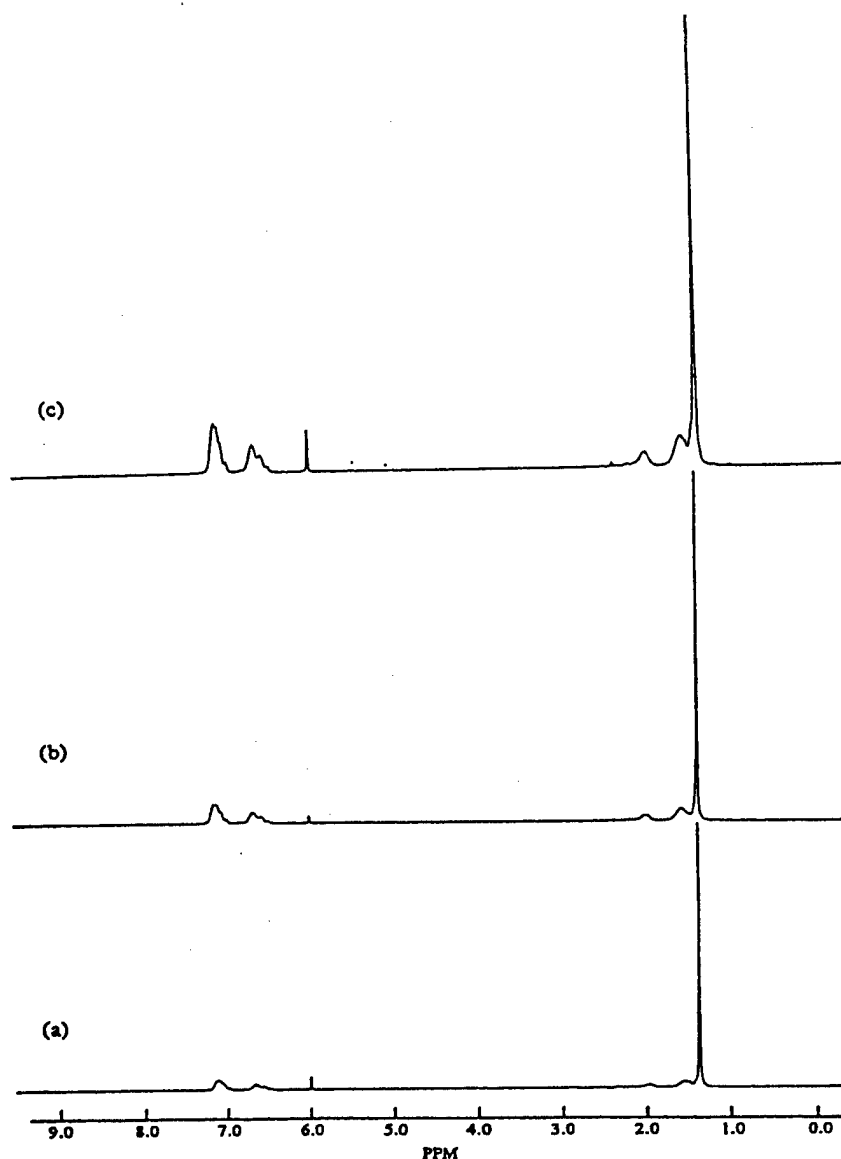
Fig. 9. ^{1}H NMR spectra of PE-*g*-PS graft copolymers with (a) 25.6, (b) 38.1, and (c) 43.8 mol% polystyrene (Reproduced with permission from Macromolecules 1997;30:1272. Copyright 1997 Am. Chem. Soc.).

It is interesting to note that as the PS graft length increases, the T_m of PE only slightly decreases. The sample B-3, containing 47.8 mol% (77.3 wt%) PS, still shows the T_m at 120.3°C. On the other hand, the heat of fusion (H_f = J/g of graft copolymer) is very dependent on the PS graft chain length. In samples B-1 and B-2, with graft chain lengths $< 12 \times 10^3$ g/mol, the heat of fusion after normalizing with the content of PE (H_f = J/g of PE) in each case is very similar to that of the pure PE sample, despite relatively high PS contents (48.9 and 58.4 wt%, respectively). The simple dilution effect seems to govern the heat of fusion in the graft copolymers. However, in samples A-1, A-2, A-3 and B-3, with the graft

Table 10

A summary of PE-*g*-PS graft copolymers (solvent: anhydrous cyclohexane (30 ml/g PE); reaction time: 1 h; temperature: 25°C)

Run number	Reaction conditions			Graft copolymers[a]						
	PE^--i^+ g	ST (g)	Yield (g)	Graft (mol%)	Graft density	Graft length	T_g (°C)	T_m (°C)	H_f J/g of graft
	Starting material[b]			0	0	0	–	127.8	199.0
A-1	1.0	1.7	2.30	25.6	0.8	23.4	103.6	121.9	60.6
A-2	1.0	2.9	3.30	38.1	0.8	41.4	103.8	120.3	41.7
A-3	1.0	4.0	3.90	43.8	0.8	52.2	103.0	120.9	31.1
B-1	1.0	1.4	2.00	20.5	2.0	6.99	84.6	126.6	99.6
B-2	1.0	2.3	2.50	27.4	2.0	10.5	91.9	123.2	80.4
B-3	1.0	4.2	4.42	47.8	2.0	23.9	103.7	120.3	25.4

[a] Graft density: # of graft/1000 carbons of backbone; graft length: 10^3 g/mol.

[b] The starting material was poly(ethylene-*co*-*p*-methylstyrene) with 0.90 mol% of *p*-MS, $\bar{M}_w = 100,000$ g/mol, $\bar{M}_w/\bar{M}_n = 2.5$.

length $>17 \times 10^3$ g/mol, the additional disorder associated with long grafted side chains becomes significant. So far, there is no theoretical explanation for the graft chain length effect on the crystallinity of the PE backbone. On the other hand, the glass transition temperature (T_g) of the PS side chains is clearly observed in DSC curves. As the molecular weight of PS increases, so does the T_g. The T_g becomes constant when the graft length exceeds 15×10^3 g/mol.

The lithiated PE-*p*-MS polymer was also used as the starting material to initiate graft-from polymerization of methyl methacrylate (MMA) and acrylonitrile (AN) in THF or cyclohexane solvents. The crude polymer products were subjected to solvent fractionation. In most cases, less than 10% of homopolymer was obtained. Table 11 summarizes the experimental results of PE-*g*-PMMA and PE-*g*-PAN. Overall, the graft-from polymerization reactions of MMA and AN are less efficient compared with those of styrene and *p*-MS. A polar solvent like THF gives poor yield at both 0 and 25°C, while a non-polar solvent such as cyclohexane gives much better results. Polar solvents may increase the nucleophilicity of the carbanion, which results in more side reactions. It is very interesting to note that the anionic polymerization of polar monomers using butyllithium as an initiator cannot achieve high

Table 11

Summary of PE-*g*-PMMA and PE-*g*-PAN Coplymers [32]

Lithiated polymer (g)	Monomer (g)	Solvent	Temperature (°C)	Time (h)	Graft copolymer (g)	PMMA or PAN content (mol%)
1.0	MMA/3.7	THF	0	1.5	1.86	20.0
1.0	MMA/3.4	THF	0	15	2.66	31.8
1.0	MMA/5.0	THF	25	5	1.90	20.1
0.8	MMA/4.0	Hexane	25	5	3.08	44.4
0.8	MMA/4.0	Hexane	0	5	2.21	33.0
1.2	AN/3.0	THF	25	1	1.60	15.0
1.2	AN/3.6	THF	25	16	2.25	32.0
1.0	AN/3.0	Hexane	25	16	2.99	51.2

polymer at ambient temperature. Usually, very low reaction temperatures ($< -20°C$) are required. In lithiated PE-*p*-MS case, the formed polymeric benzylic lithium is much more stable, and therefore minimizes the side reactions. As can be seen from Table 11, graft-from polymerization reactions of MMA and AN in the non-polar solvent cyclohexane are fairly effective and a sufficiently long graft length can be achieved even at ambient temperature. Similar graft-from polymerization of polar monomers were also observed the lithiated PP-*g*-PS polymer.

7.3. Graft-from and graft-onto polymerization involving divinylbenzene side groups

One major advantage of the α-olefin/divinylbenzene copolymers is the existence of many pending styrene groups along the backbone, which are very reactive in many chemical reactions — including free radical, cationic, anionic, and transition metal coordination processes. As illustrated in Eq. (9), the pending styrene units serve as comonomers in the graft reactions [49]. This process resembles graft-through polymerization, and the resulting graft copolymer has a polyolefin backbone and several polymer side chains that are bonded to the polyolefin at the middle of the polymer chain. The major concern of this graft reaction is the potential of crosslinking involving multiple polyolefin-bonded styrene units. Usually, the reaction has to be carried out in specific reaction conditions to obtain completely soluble graft copolymers with desirable compositions.

$$(9)$$
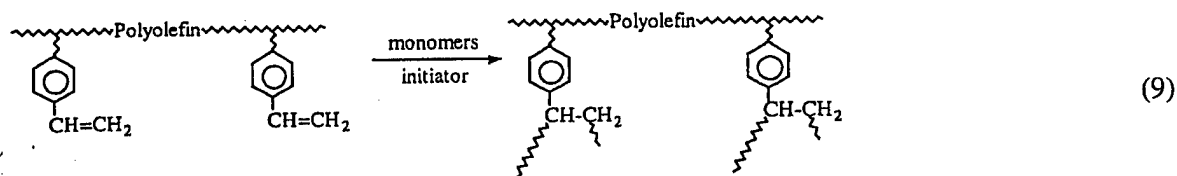
To eliminate the concerns about crosslinking reactions, it is important to design a graft reaction with the pending styrene units serving as the initiation or termination sites. In other words, the side chain polymer grafts to the backbone at its chain end, and the graft polymer basically has a similar molecular structure as those discussed in the previous sections. The following two graft reactions, involving a pending styrene unit as the anionic initiating site and metallocene terminating site, respectively, are used to illustrate the general idea.

In anionic graft-from polymerization, the process begins with a metallation reaction of DVB containing copolymer with alkyllithium (such as *n*-BuLi) to form a polyolefin containing pending benzylic anions. By limiting the alkyllithium added to the reaction to the amount required to react with all of the DVB units in the copolymer, the metallation reaction between the pending styrene unit and the alkyllithium is quantitative. In other words, no purification is needed before adding anion-polymerizable monomers to continue the living anionic graft-from polymerization process. It is very interesting to note that the anionic polymerization of various monomers, such as methyl methacrylate, can take place at room temperature without causing any detectable side reactions, which may be associated with the stable benzylic anion initiator. After achieving the desired composition of the graft copolymer, the graft reaction can be terminated by adding a proton source, such as methanol or isopropanol. Thus, by using this easily controllable living graft-from reaction technique, a variety of graft copolymer compositions with well-defined side chain segments, including random and block copolymers, have been produced that are all completely soluble in organic solvents.

Fig. 10 compares the ^{1}H NMR spectrum of a graft copolymer, having an ethylene/1-octene/DVB
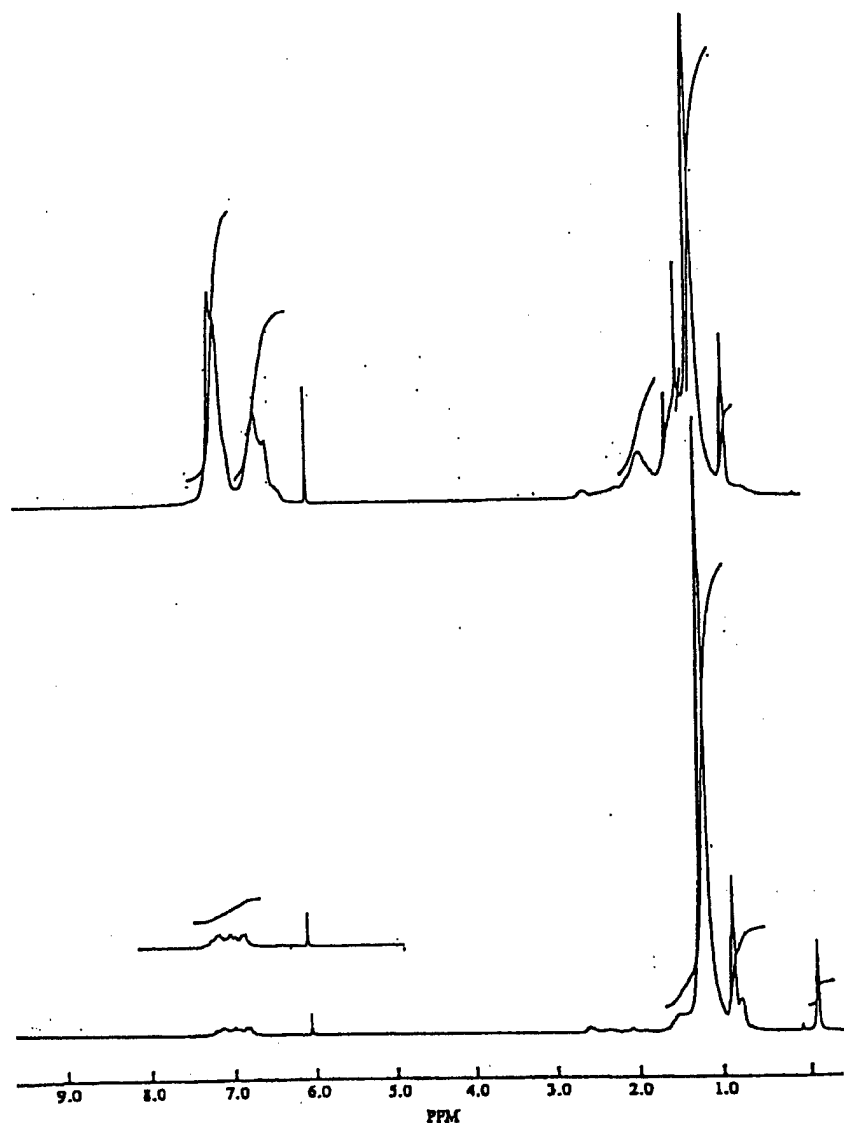
Fig. 10. ¹H NMR spectrum of a silylated ethylene/1-octene/DVB terpolymer (bottom) and a graft copolymer with ethylene/1-octene/DVB backbond and polystyrene side chains (top). Both polymers were derived from the same starting ethylene/1-octene/DVB terpolymer having a DVB content of about 4 mol%.

elastic backbone and several polystyrene side chains, and a corresponding silylated ethylene/1-octene/DVB terpolymer. Fig. 10 (bottom) shows the complete disappearance of all vinyl peaks and a strong peak at 0.05 ppm corresponding to the methyl proton next to Si. Both the metallation and silylation efficiencies were almost 100%. Fig. 10 (top) indicates the graft copolymer containing more than 50 mol% polystyrene side chains. In addition to the chemical shifts for ethylene/1-octene, the new peaks ($\delta =$ 6.4–7.3 ppm) are due to aromatic protons in the PS side chains. Overall, the graft-from reactions were very effective — more than 80% styrene monomer conversion within one hour.

The graft content increased proportionally with increasing monomer concentration and reaction time. Since the graft-from reaction involves a living anionic polymerization, it is reasonable to assume that each benzylic lithium produces one polymer side chain and the each side chain has a similar molecular weight. The graft density, defined, as the number of grafted side chains per 1000 carbons in the polyolefin backbone, is the same as the density of the benzylic anions. The side chain length is basically proportional to the reaction time and monomer concentration.

In metallocene graft-onto reaction cases, the pending styrene units in the α-olefin/DVB copolymer serve as chain transfer agents. As discussed in Section 6.2, the combination of styrene and hydrogen is a very effective chain transfer agent in metallocene-mediated α-olefin polymerization, which can be directly applied to the graft reaction of an olefin/DVB copolymer containing pending styrene units, as illustrated in Eq. (10).

$$(10)$$
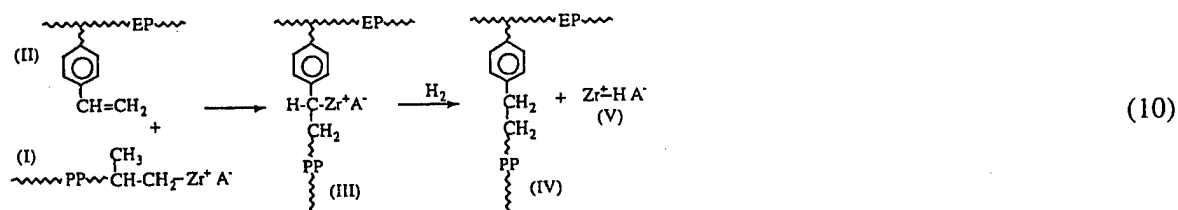
The metallocene polymerization of propylene was carried out in the presence of EP/DVB and hydrogen. During the polymerization of propylene (with a 1,2-insertion manner) the propagation Zr–C site (I) reacts with the pending styrene unit (with a 2,1-insertion manner) in the EP/DVB copolymer to form a graft copolymer (III) having several styrene terminated PP side chains. The catalytic Zr–C site in the graft copolymer (III) becomes inactive to propylene [47] due to the combination of steric hindrance between the active site (Zr–C) and the incoming monomer (propylene with 1,2-insertion), and the formation of a complex between the adjacent phenyl group and the Zr^+ ion. On the other hand, with the presence of hydrogen, the dormant Zr–C site (III) can react with hydrogen to form EP-g-PP (IV) and regenerate a Zr–H species (V) that is capable of reinitiating the polymerization of propylene and continuing the polymerization/graft reaction cycle. This process not only produces a desirable EP-g-PP graft polymer, but also maintains high metallocene catalyst activity. The PP's molecular weight is basically proportional to the [propylene]/[styrene] ratio.

Table 12 summarizes the results of EP-g-PP graft copolymers using a rac-Me$_2$Si[2-Me-4-Ph(Ind)]$_2$ZrCl$_2$/

Table 12
A summary of EP-g-PP graft copolymers

Reaction condition		Yield (g)	Catalyst activity Kg PP/molZr.h	Graft composition		Graft copolymer	
C$_3$/EP-DVB^a (psi/g)	H$_2$ (psi)			EP-DVB (wt%)	PP (wt%)	T_g (°C)	T_m (°C)
20/2.6	0	2.5	0	100	0	−48	–
20/2.6	2	4.9	1864	32.3	67.7	−47	152
20/2.6	6	6.56	3184	30.5	69.5	−47	152
20/2.6	12	7.79	4128	28.5	71.5	−46	152

^{a} EP-DVB: E: 52.1 mol%; P: 43.7 mol% and DVB: 4.2 mol%; M_w = 68,600 and PDI = 2.

MAO catalyst with the presence of propylene and EP-DVB and hydrogen. This systematic study was conducted to evaluate the effect of hydrogen on the catalyst activity and graft copolymer composition. The presence of hydrogen is clearly a key factor in the success of this graft reaction. With an appropriate [propylene]/[hydrogen] ratio, the graft reaction can be as efficient as the homopolymerization of propylene itself. The graft length and density can be controlled by the combination of DVB units in the EP-DVB copolymer and the propylene concentration. Some very desirable EP-*g*-PP graft copolymers containing continuous PP domains and discrete EP domains have been prepared with high impact TPO properties.

7.4. Ring-opening graft-from polymerization [67]

Ring opening polymerization provides a convenient route for preparing polyolefin graft copolymer containing polycondensation polymer side chains. Since the functionalized polyolefins are available, it is possible to use the functional group as an initiator for ring opening reactions. One example is an anionic ring opening reaction of ε-caprolactone (ε-CL) from a hydroxylated PP (PP-OH). In a typical example, a fine powder form of PP-OH ($M_v = 183,000$ g/mol), containing 1.4 mol% hexenol units is metallated with excess *n*-butyllithium to form the lithium alkoxide. A toluene slurry of the powdery solid was then reacted with a 3 molar equivalent of diethylaluminum chloride for 12 h to form the PP-aluminum alkoxide. The monomer, e.g. caprolactone, was then added to a slurry of the PP-OAlEt$_2$ in toluene. The reaction was terminated (after 24 h at room temperature) by the addition of MeOH, and the polymer was isolated via precipitation into acidified MeOH. The polymer mass was extracted with hot acetone in a soxhelt apparatus under N$_2$ for 48 h to remove any ε-CL homopolymer. The resulting PP-*g*-PCL graft copolymers were analyzed by NMR and DSC to determined their compositions and thermal properties (T_m, T_g, and crystallinity). Table 13 summarizes the experimental results of PP-*g*-PCL copolymers that were prepared from two PP-OH containing primary and secondary OH groups.

Runs 1–4 all started with the same PP-OH copolymer containing 1.4% hexenol monomer units. The weight percent PCL in the resulting graft copolymer increased linearly with increasing ε-CL in the feed. The relatively long reaction time can be explained by the heterogeneous reaction conditions. The diffusion of ε-CL into the PP matrix would be the rate limiting step for the reaction. In fact, runs 2 and 4 differ in the reaction time of 24 and 60 h, but resulted in copolymers with 33 and 59 wt% PCL respectively. The amount of homo-PCL produced, i.e. the acetone soluble fraction, also increased with the ε-CL feed. Any residual aluminum alkyl not covalently bound to the polymer could easily initiate the

Table 13
A Summary of PP-*g*-PCL copolymers and reaction conditions (Reproduced with permission from Macromolecules 1994;27:1313. Copyright 1994 Am. Chem. Soc.) [67]

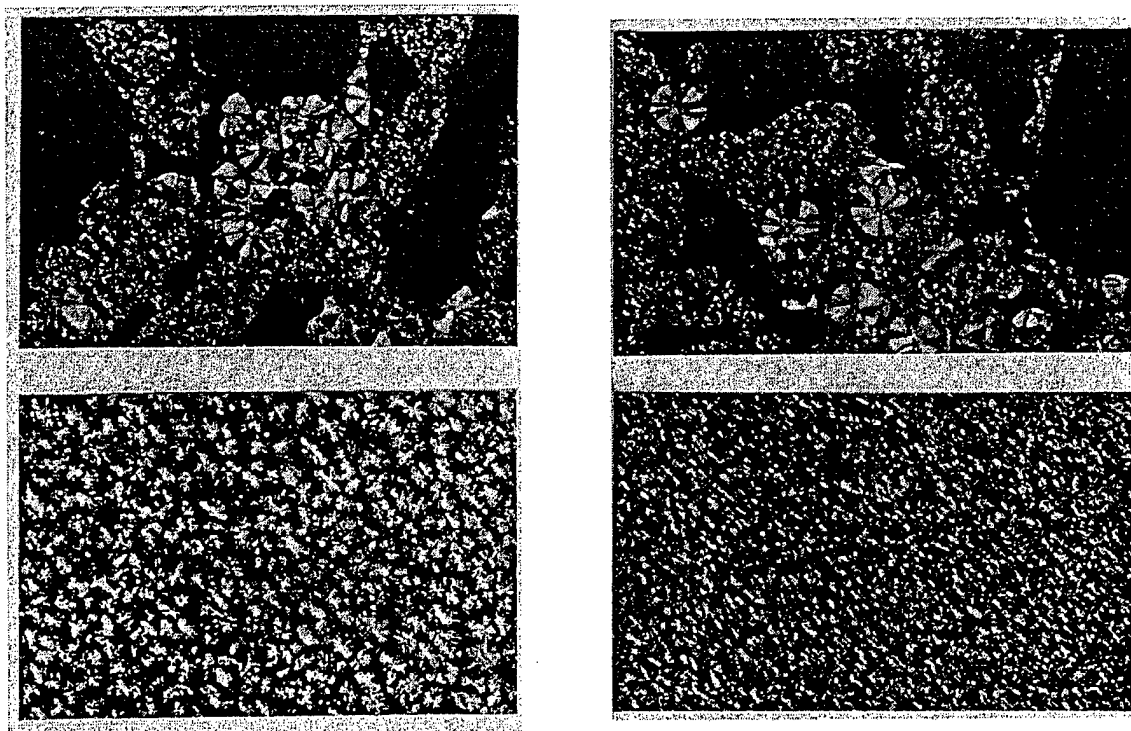| Run	Reaction conditions			Products		
	PP-O-AlEt$_2$ (g)	ε-CL (g)	Time (h)	Acetone soluble (g)	Acetone insoluble (g)	ε-Cl in graft (wt%)
1	2	2.169	24	0.366	2.252	16.8
2	2	4.299	24	0.430	2.763	32.9
3	2	8.243	24	2.581	3.922	56.8
4	2	4.571	60	2.102	4.120	59.5
5	2	6.525	24	1.387	3.603	45.4

Fig. 11. Left: optical micrographs of (top) homopolymer blend with *i*-PP/PMMA = 70/30 and (bottom) two homopolymers with PP-*g*-PMMA containing 30% MMA, *i*-PP/PP-*g*-PMMA/PMMA = 70/10/30. Right: optical micrographs of (top) two homopolymer blend with *i*-PP/PC = 70/30 and (bottom) two homopolymers with PP-*g*-PCL, *i*-PP/PP-*g*-PCL/PC = 70/10/30 (100×). (Reproduced with permission from Macromolecules 1994;27:1313. Copyright 1994 Am. Chem. Soc.).

homo-polymerization of the ε-CL. Excess aluminum alkyl associated with the bound Al-Os may not be completely washed out by the non-polar solvents. Run 5 started with commercial grade propylene and 1,4-hexadiene copolymer containing approximately 1.6% unsaturated monomer units. The polymer was hydroborated with 9-BBN and oxidized to give functionalized PP with the secondary alcohols on either the 4 or 5 position of the hexadiene branch. The secondary alcohol can also be converted to the secondary aluminum alkoxide, which is recognized as an active initiator in the graft-from reaction of ε-CL.

7.5. Polyolefin graft copolymer as the compatibilizer in polyolefin blends

Polyolefin graft copolymers are very effective compatibilizers for improving interactions between their corresponding polyolefins and other materials, including polymers and substrates. Fig. 11 compares polarized optical microscopy of two polymer blend systems, including PP/PMMA [66] and PP/PC [67] with and without graft copolymers as the compatibilizers.

In the first system, a simple polymer blend (70/30 wt% of *i*-PP and PMMA homopolymers) shows two distinct phases — the crystalline PP phase and an amorphous PMMA phase. Within the PP domain, the spherulite size varies greatly with a few extremely large crystallites and predominantly small spherulites. With 10 wt% of PP-*g*-PMMA graft copolymer in PP/PMMA blend, the large phase seperated PMMA domains are dispersed into the inter-spherulite regions, and cannot be detected with the optical microscope.

The mode of nucleation within the PP crystalline phase has changed, as evidenced by the now relatively homogeneous spherulite size.

Bisphenol-A polycarbonate (PC) has excellent high and low temperature physical properties even up to 140°C. Using PP as the matrix material with a compatibilized polycarbonate dispersed phase could greatly improve the mechanical properties, creating a toughened plastic. Such an inexpensive polymer blend may be able to compete with more costly engineering plastics. Since poly(ε-caprolactone) (PCL) and polycarbonate (PC) form a miscible blend, the graft copolymer PP-g-PCL should behave as an emulsifier for PP and PC blends. In Fig. 14 (right), the 70/30 PP/PC blend shows gross phase separation of the spherulitic PP and the amorphous PC phases. The PC phases vary widely in both size and shape due to the lack of interaction with the PP matrix. On the other hand, the blend containing 70/30/10 of PP/ PC/ PP-g-PCL, where the graft contains 57 wt% PCL, shows only small distorted spherulites and a few very small distinct PC phases. The PP-g-PCL is clearly proven to be an effective compatibilizer for PP and PC blends. It should also be noted that the films of the compatibilized blends formed in the melt press were optically clear. This is unlike pure i-PP that forms hazy, translucent films. The lack of large spherulites in both the blend and the graft must minimize scattering.

It is interesting to study the compatibility of PE-g-PS copolymer in HDPE and PS blends. Both a polarized optical microscope and a scanning electron microscope (SEM) were used to examine the surfaces and bulk morphologies, respectively. Of the two blends comprised of an overall 50/50 weight ratio of PE and PS, one is a simple mixture of 50/50 between HDPE and PS and the other is a 45/45/10 weight ratio of HDPE, PS, and PE-g-PS (containing 50 mol% PS). Similar to Fig. 11, the polarized optical micrographs of the two blends are very different. A gross phase separation, with spherulitic PE and amorphous PS phases, is shown in the simple PE/PS blend. The PS phases vary widely in both size and shape due to the lack of interaction with the PE matrix. On the other hand, a continuous crystalline phase results in the compatibilized blend. Basically, the large phase separated PS domains are now dispersed into the inter-spherulite regions and cannot be detected by the optical microscope. The graft copolymer behaves as a polymeric emulsifier, and increases the interfacial interaction between the PE crystalline and the PS amorphous regions to reduce the domain sizes.

Fig. 12 shows the SEM micrographs, operating with secondary electron imaging, revealing the surface topography of the cold fractured film edges. The films were cryro-fractured in liquid N$_2$ to obtain an undistorted view representative of the bulk material. In the homopolymer blend, the polymers are grossly phase separated, as can be seen in Fig. 12(a). The PS component exhibits non-uniform, poorly dispersed domains and voids at the fracture surface. This 'ball and socket' topography is indicative of poor interfacial adhesion between the PE and PS domains, and represents PS domains that are pulled out of the PE matrix. Such pull out indicates that limited stress transfer takes place between the phases during fracture. A similar blend containing graft copolymer shows a totally different morphology in Fig. 12(b). The material exhibits flat mesa-like regions similar to pure PE. No distinct PS phases are observable, indicating that fracture occurred through both phases or that the PS phase domains are too small to be observed. The PE-g-PS is clearly proven to be an effective compatibilizer in PE/PS blends.

8. Synthesis of functional polyolefin diblock copolymers

Diblock copolymer is the most effective interfacial agent [73,74] in polymer blends and composites. Usually, only a small quantity (as low as 1%) of a suitable diblock copolymer is needed to change the
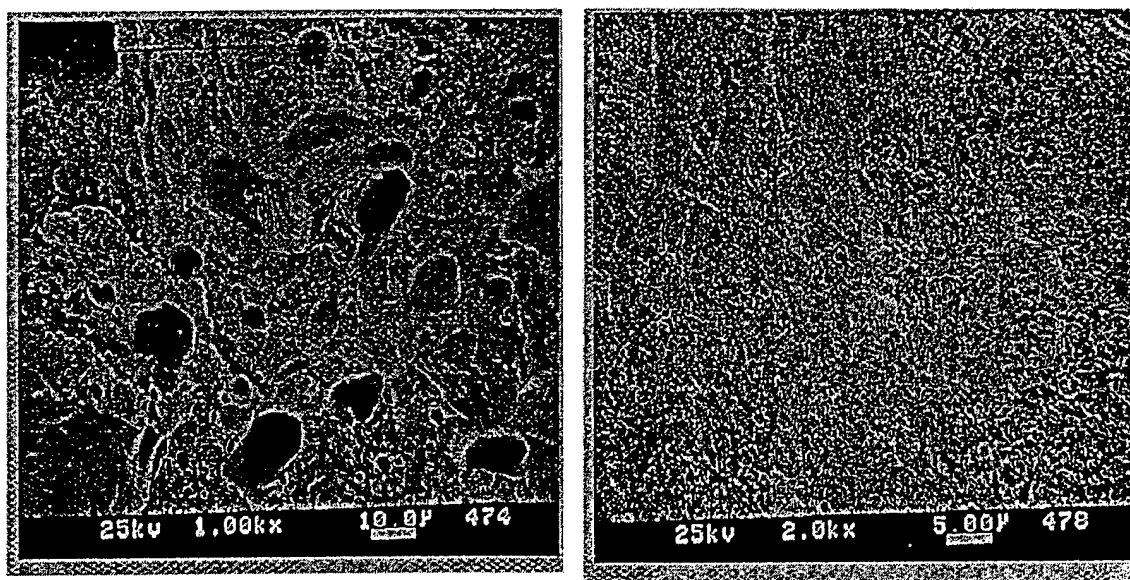
Fig. 12. SEM micrographs of the cross-section of two polymer blends: (a) two homopolymers with PE/PS = 50/50 (1000 ×) and (b) two homopolymers and a PE-*g*-PS copolymer blend with PE/PE-*g*-PS/PS = 45/10/45 (2000 ×) (Reproduced with permission from Macromolecules 1997;30:1272. Copyright 1997 Am. Chem. Soc.) [72].

incompatible binary blends to a uniform micro-phase morphology with strong interfacial adhesion.Traditionally, most diblock copolymers have been prepared by living polymerization processes, namely anionic [75,76], cationic [77,78], and recently metathesis [79,80] with sequential monomer additions. The living coordination polymerization of α-olefin by transition metals is very limited. In addition, the catalyst's sensitivity to functional groups further constrains the chemistry's ability in achieving functional polyolefin diblock copolymer.

In this section, we will discuss a new method by using polyolefin containing a terminal borane or *p*-MS groups, which can be interconverted to living free radical or anionic initiator, respectively, for polymerization of functional monomers. The chemistry employs two different polymerization mechanisms that are the most suitable for preparing individual polymer blocks, i.e. metallocene for polyolefin and free radical or anionic for functional polymer. The combination of two routes produces functional polyolefin diblock copolymers with a broad range of copolymer composition and well-designed molecular structure.

8.1. Polyolefin block copolymers prepared via a terminal borane group [50,51,81–83]

As illustrated in Eq. (11), polyolefin containing a terminal borane group (alkyl-9-BBN) can be prepared by two routes, i.e. in situ chain transfer reaction to B–H group during metallocene polymerization and hydroboration of chain-end unsaturated polymer (see details in Section 6.1). The terminal alkyl-9-BBN group in polymer (I) was then spontaneously oxidized to produce a peroxy-9-BBN (II). The peroxyborane (II) behaves very differently from regular organic peroxides, and consequently decomposes by itself even at ambient temperature to generate an alkoxy radical (C–O ∗) and a borinate radical (B–O ∗). The alkoxyl radical (C–O ∗), located at the end of polyolefin chain, is very reactive and can then be used for the initiation of radical polymerization with the presence of free radical

polymerizable monomers. On the other hand, the borinate radical (B–O *), stabilized by the empty p-orbital of boron through back-donating electron density, is too stable to initiate polymerization. However, the borinate radical may form a weak and reversible bond with the growing chain end during the polymerization reaction. Upon the dissociation of the electron pairs in the resting state, the growing chain end can then react with monomers to extend the polymer chain to form diblock copolymer (IV).
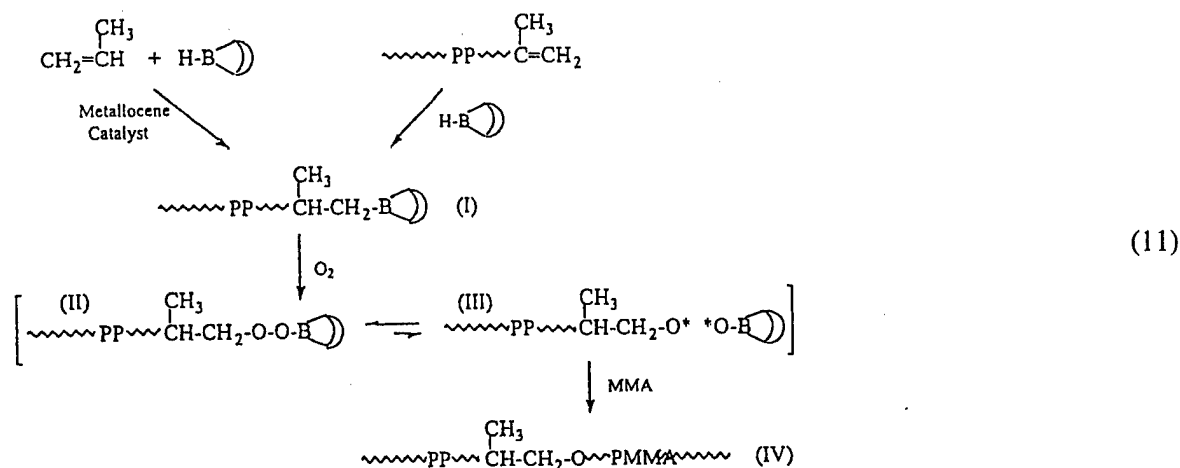
$$(11)$$

Overall, the reaction process resembles a transformation reaction from metallocene coordination polymerization to living free radical polymerization via a borane group at the polymer chain end. It is interesting to note that the reaction involves only one borane group per polymer chain. The whole reaction process provides an ultimate test for examining the efficiency of the borane reagent in the chain extension process.

One example is a borane-terminated PE (PE-t-B) polymer [50] that was subjected to oxidation reaction by oxygen in the presence of free radical polymerizable MMA monomers. The resulting reaction mixture was carefully fractionated by Soxlet extraction using boiling THF to remove any PMMA homopolymer. In most cases, only a very small amount (<10%) of PMMA homopolymer may be initiated by the radical in a bicyclic ring, instead of a polymeric radical, due to the small non-selective oxidation reaction of alkyl-9-BBN. The generally insoluble fraction (but soluble in 1,1,2,2-tetrachloroethane, 1,2,4-trichlorobenzene at elevated temperatures) is PE-b-PMMA diblock copolymer. Table 14 summarizes the experimental results of two sets of chain extension reactions using two starting PE-t-B polymers with $M_n = 19.4 \times 10^3$ and 42.7×10^3 g/mol, respectively.

The experimental result in both comparative sets clearly shows the increase of MMA conversion and the content of PMMA in the diblock copolymer with the increase of the reaction time. The extent of chain extension reaction is basically proportional to the reaction time, which clearly indicates the living free radical polymerization of MMA. High concentration of PMMA in diblock copolymer can be achieved with narrow molecular weight distribution.

Fig. 13 shows the ^{1}H NMR spectrum of three PE-b-PMMA copolymers that were sampled at different reaction times during the same chain extension process. The reaction was started by using a PE-t-B polymer (I) with $M_n = 19,400$ g/mol and $M_w/M_n = 2.1$. The new peak at 3.58 ppm, corresponding to methoxyl groups (CH$_3$O) in PMMA, increased its intensity with the reaction time. Apparently, the PMMA segment in PE-b-PMMA grows with the reaction time, and high molecular weight

Table 14
A summary of PE-b-PMMA diblock copolymers

PE-t-B[a] (g)	Reaction condition		Yield (g)	THF extraction		Diblock copolymer		
	Temperature/time (°C/h)	O_2/MMA (ml/mol)		Insoluble (%)	Soluble (%)	M_n (×10^{-3})	M_w/M_n	PE/PMMA mole ratio
(I)/3	25/6	1.9/1.87	3.98	96	4	49.2	2.1	100:43
(I)/3	25/12	1.9/1.87	6.65	93	7	62.5	2.4	100:62
(I)/3	25/24	1.9/1.87	8.05	90	10	90.3	2	100:102
(II)/5	25/2	1.4/1.87	6.12	97	3	47.5	2.3	100:03
(II)/5	25/6	1.4/1.87	6.78	95	5	61.8	2.4	100:13
(II)/5	25/12	1.4/1.87	8.74	93	7	76.3	1.9	100:22
(II)/5	25/24	1.4/1.87	10.24	89	11	97.6	2.9	100:36

[a] PE-t-B (I): $M_n = 19.4 \times 10^3$ g/mol, $M_w/M_n = 2.1$; PE-t-B (II): $M_n = 42.7 \times 10^3$ g/mol; $M_w/M_n = 2.2$.
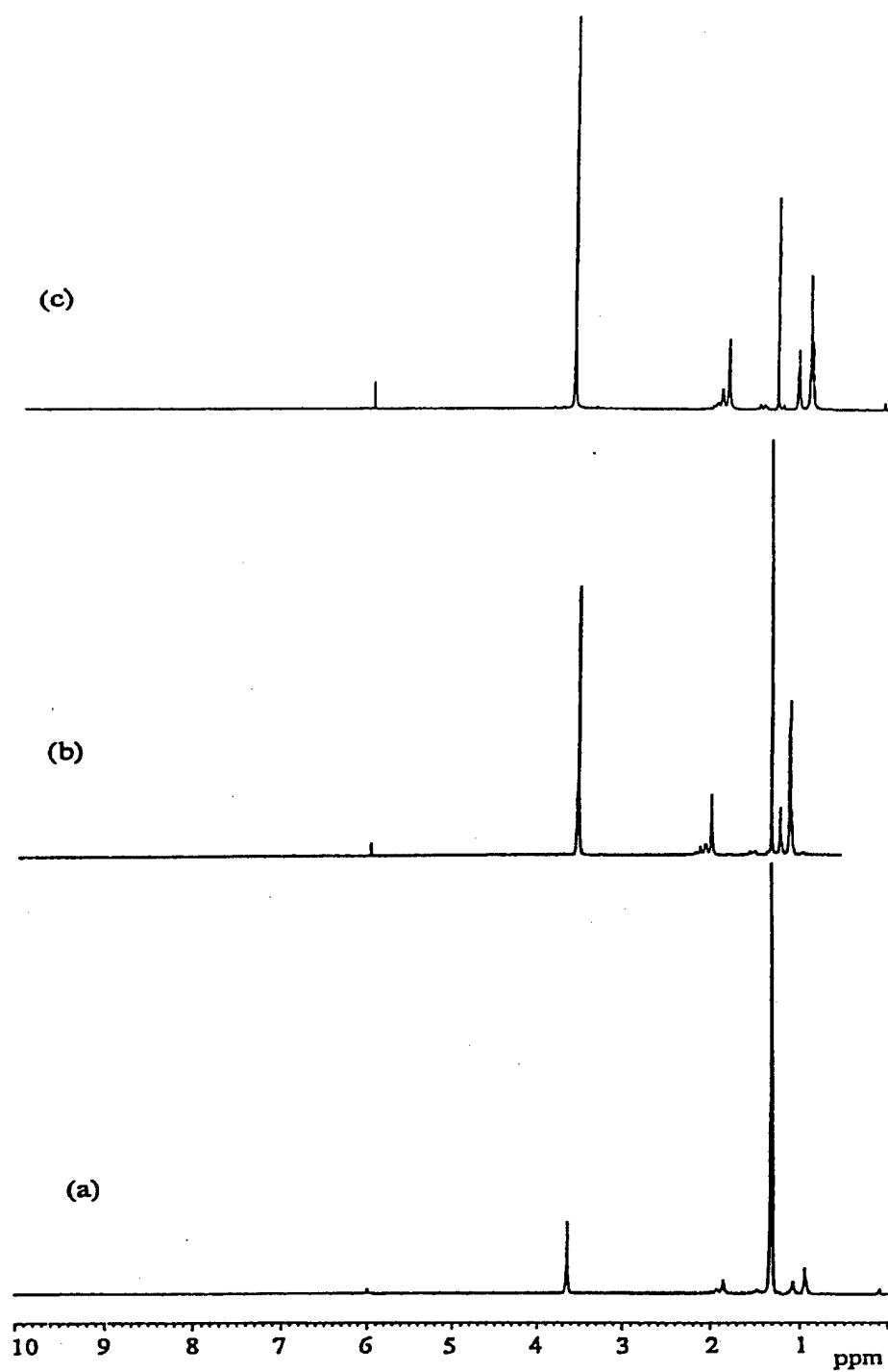
Fig. 13. ^{1}H NMR spectra of PE-*b*-PMMA containing (a) 16, (b) 48 and (c) 85 mol% PMMA contents. (solvent: $C_2D_2Cl_4$; temperature: 110°C).

diblock copolymer with up to 85 mol% of PMMA copolymer (Fig. 13(c)) has been prepared. Considering only one terminal borane group in each PE chain, these experimental results imply the living free radical polymerization in the chain extension process.

Fig. 14 compares the GPC curves of two PE-b-PMMA diblock copolymers and the starting PE-t-B polymer. It is clear that the polymer continuously increased its molecular weight during the entire polymerization process. The polymer's molecular weight distribution was maintained very constant and narrow (M_w/M_n = 2.0–2.2). The inset shows the linear plot of polymer molecular weight vs. the monomer conversion and compares the results with a theoretical line based on the [g of monomer consumed]/[mole of initiator]. A good match with the straight line through the origin strongly supports the presence of living polymerization in the reaction.

The same experimental results were observed in PP case [81], shown in Fig. 15. The molecular weight more than doubles from M_n = 13,000 of PP-t-B to M_n = 29,000 g/mol of PP-b-PMMA, and the molecular weight distribution (MWD) slightly increases from 1.5 to 1.7. The GPC results are consistent with the ^{1}H NMR measurements that show about a 1/1 mole ratio between PP and PMMA in the copolymer. It is very interesting to note the remarkable efficiency of borane terminal group, with only one unit per polymer chain.

The same radical chain extension was also applied to new syndiotactic–polystyrene (s-PS) [51]. Table 15 summarizes the reaction conditions and experimental results of s-PS diblock copolymers containing polymethylmethacrylate (PMMA) and polybutylmethacrylate (PBMA).

In general, both PMMA and PBMA blocks increase along with the reaction time, and chain extension reactions continue even after 12 h. Diblock copolymers with a nearly 1/1 mole ratio of [styrene]/[MMA] or [styrene]/[BMA] have been prepared, despite the heterogeneous reaction conditions. These effective
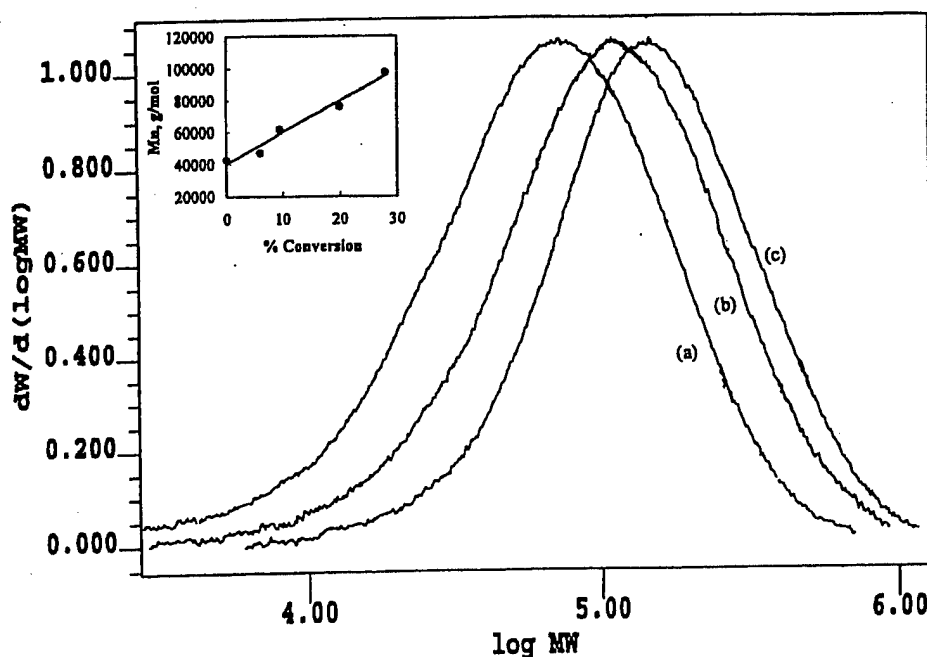

Fig. 14. GPC curves of (a) the starting PE-t-B polymer (M_n = 19,400), and two corresponding PE-b-PMMA copolymers (b) M_n = 58,600, and (c) M_n = 90,300 g/mol.
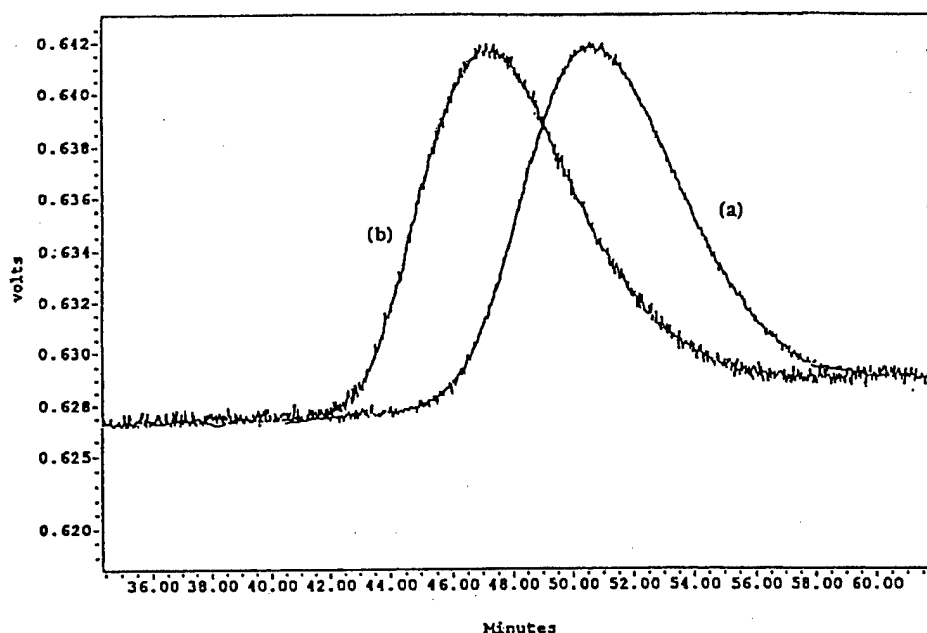
Fig. 15. GPC curves of (a) PP (M_n = 13,000 and PDI = 1.5) (b) the corresponding PP-b-PMMA copolymer (M_n = 29,000 and PDI = 1.7). (solvent: trichlorobenzene; temperature: 135°C). (Reproduced with permission from J. Am. Chem. Soc. 1999;121:6763. Copyright 1999 Am. Chem. Soc.).

and long-lived chain extension reactions again provide strong evidence of the borane group's existence at the polymer chain end and the living free radical chain extension process. DSC curves of s-PS-t-B and the corresponding s-PS-b-PMMA show two identical thermal transition temperatures, including a T_m near 270°C and a T_g near 100°C for the s-PS polymer, in both samples. A clear new T_g at about 130°C (corresponding to the high molecular weight PMMA polymer) was shown in s-PS-b-PMMA sample. Both polymer segments in the s-PS-b-PMMA copolymer must have long consecutive (undisturbed) sequences to form separate domains.

· It's very interesting to note that the borane-mediated radical polymerization is particularly effective with the polar monomers. The rate of propagation may enhance due to the interaction between the boron moiety in the propagating end group and the heteroatom (O, N, Cl) in the polar monomer as illustrated below.

"Coordination"
Radical Addition
Process
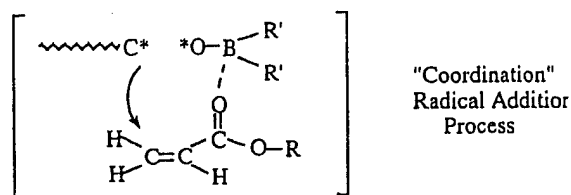
8.2. Polyolefin block copolymers prepared via a p-methylstyrene terminal group [52]

As discussed in Section 6.2, p-methylstyrene (p-MS) terminated polyolefins have been prepared by the combination of metallocene catalysis and chain transfer reaction to p-MS/H_2. The terminal p-MS

80

T.C. Chung / Prog. Polym. Sci. 27 (2002) 39–85

Table 15

A summary of s-PS-b-PMMA and s-PS-b-PBMA diblock copolymers

s-PS-t-B[a] (g)	Reaction condition		Polar monomer (mol)	Yield (g)	Diblock copolymer		Blocks mole ratio
	Temperature/time (°C/h)	O_2 (ml)			s-PS block M_n ($\times 10^{-3}$)	Polar Block M_n ($\times 10^{-3}$)	
(I)/5	25/6	1.9	MMA/1.87	6.25	15	2	100:14
(I)/5	25/12	1.9	MMA/1.87	7.56	15	5	100:35
(I)/5	25/24	1.9	MMA/1.87	9.98	15	14	100:97
(I)/5	25/10	1.9	BMA/1.87	6.72	15	7.1	100:35
(I)/5	25/20	1.9	BMA/1.87	7.56	15	15	100:72
(I)/5	25/24	1.9	BMA/1.87	8.94	15	18.3	100:89
(II)/7	25/6	2.4	MMA/1.87	7.56	70	3	40:04.5
(II)/7	25-Dec	2.4	MMA/1.87	8.13	70	8	100:12
(II)/7	25/24	2.4	MMA/1.87	8.98	70	17	100:25

[a] s-PS-t-B (I): $M_n = 15 \times 10^3$ g/mol, $M_w/M_n = 2.2$; s-PS-t-B (II): $M_n = 70 \times 10^3$ g/mol; $M_w/M_n = 2.1$.

Table 16
A summary of PP-b-PS diblock copolymers

Reaction conditions			Yield (g)	PP-b-PS products		M_n (g/mol)	M_w/M_n
PP[a] (g)	Styrene (g)	Time (h)		THF soluble (g)	PP-b-PS products, PP/PS (mol)		
0.73	0.9	1.0	0.94	n.g	86.9/13.1	–	–
0.73	2.7	1.0	1.54	n.g	60.6/34.4	54.0	2.34
0.69	4.5	3.0	2.77	n.g	52.2/47.8	–	–
0.76	9.0	3.0	3.60	n.g	48.8/51.2	117.5	2.25

[a] PP-t-p-MS sample ($M_n = 25.9 \times 10^3$ g/mol; $M_w/M_n = 2.3$).

group provides the active site to transform metallocene polymerization to living anionic polymerization, as illustrated in Eq. (12). The metallation reaction of p-MS terminated polypropylene (PP-p-MS) was carried out under heterogeneous reaction conditions by suspending the powder form of PP in cyclohexane. A excess of s-BuLi/TMEDA was used to ensure a complete reaction. Usually, the reaction mixture was stirred at room temperature for a few hours before removing the polymer powder from the solution by filtration and washing. The lithiated PP-t-p-MS (II) was used to prepare diblock copolymers. By mixing polymer powder with styrene monomer in cyclohexane solvent, the living anionic polymerization took place to produce PP-b-PS diblock copolymer. After the reaction, the product was vigorously extracted by refluxing THF to remove any PS homopolymer.
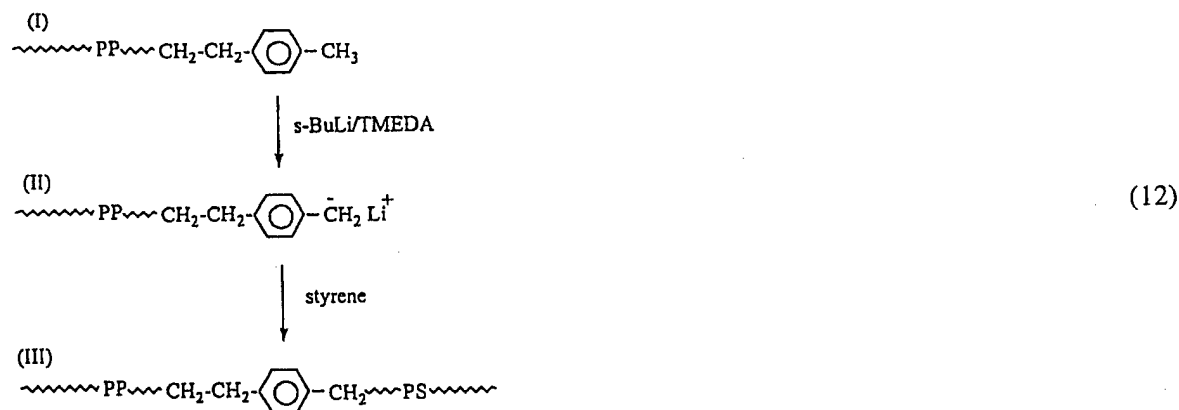

(12)

Table 16 summarizes the experimental results of PP-b-PMMA diblock copolymers by starting from a PP-t-p-MS polymer ($M_n = 25.9 \times 10^3$ g/mol). In all cases (including high molecular weight PP-t-p-MS polymer cases), the soluble PS homopolymer fraction was negligible. Basically, the PP-b-PS product increases its PS content and molecular weight as more styrene is introduced during the reaction. Not all of the styrene was converted in the relatively short reaction time under non-polar solvent conditions.

Fig. 16 (top) shows the ^{1}H NMR spectra of PP-b-PS ($M_n = 44.0 \times 10^3$ g/mol; PDI = 2.34) and Fig. 16 (bottom) compares the GPC curve of PP-b-PS with the starting PP-t-p-MS ($M_n = 25.9 \times 10^3$ g/mol; PDI = 2.3). Despite the doubling of polymer molecular weight, the molecular weight distribution (PDI) remains very constant. The quantitative analysis of the diblock copolymer composition was calculated
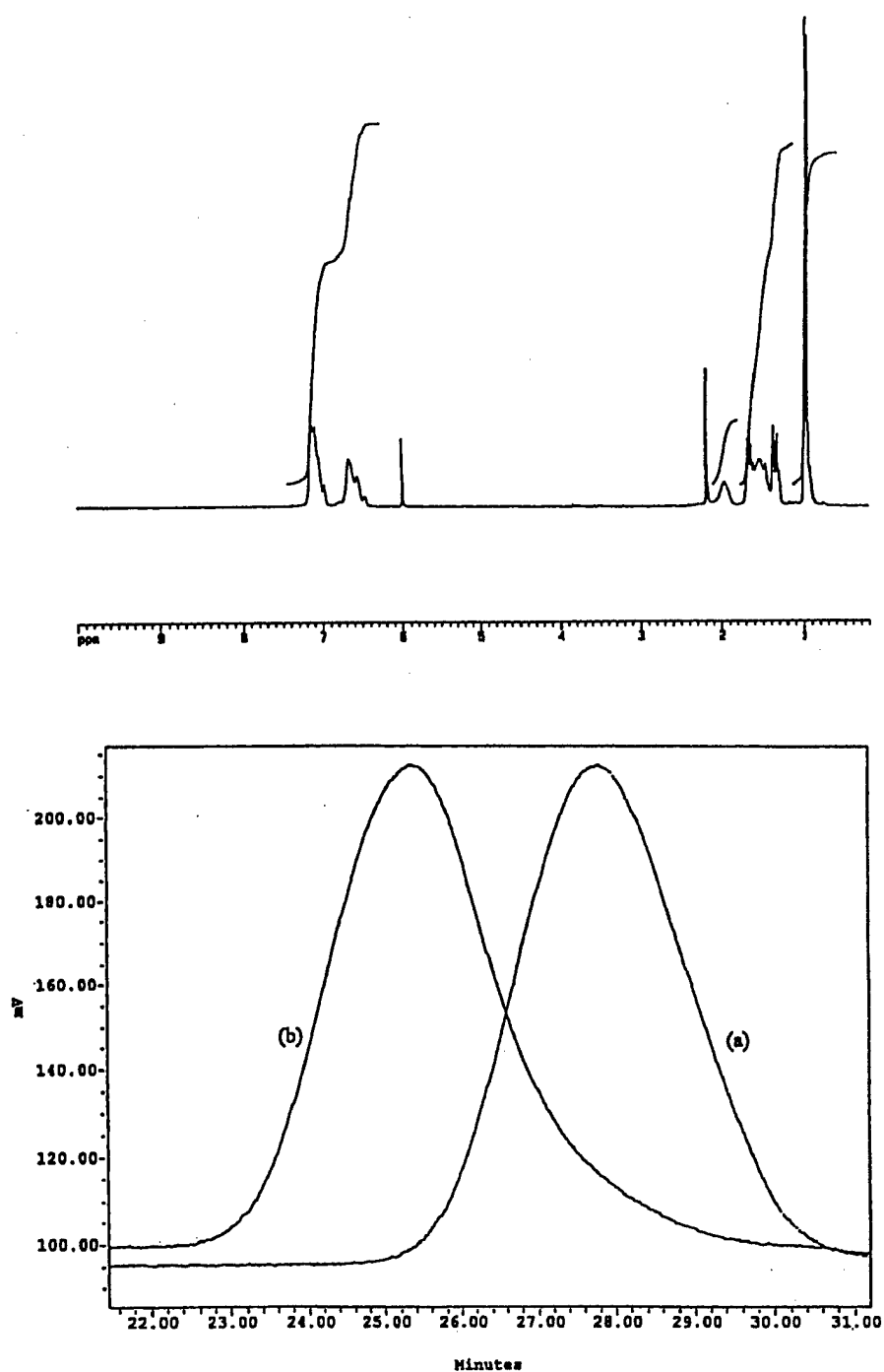
Fig. 16. Top: ^{1}H NMR spectra of PP-*b*-PS diblock copolymer and (bottom) GPC curves of (a) the starting PP-*t-p*-MS and (b) the resulting PP-*b*-PS polymers. (Reproduced with permission from J. Am. Chem. Soc. 2001;123:4871. Copyright 2001 Am. Chem. Soc.).

using the ratio of two integrated intensities between the aromatic protons ($\delta = 6.4$–7.3 ppm) in the PS segment and the methylene protons ($\delta = 1.35$–1.55 ppm) in the PP segment, along with the number of protons both chemical shifts represent.

Overall, the transformation from metallocene to living anionic polymerization was very effective ($>80\%$), and the molecular structure of the copolymer could be easily controlled by the starting p-MS terminated polyolefin and the quantity of monomer introduced during the living anionic chain extension reaction. This diblock reaction benefits from the known and well-defined living anionic polymerization process, and offers a complementary method to the previous one, i.e. transformation from metallocene to living free radical polymerization. The combination provides a powerful tool to prepare a broad range of polyolefin diblock copolymers containing a metallocene-prepared polyolefin block and an anionic or free radical-prepared polymer block.

9. Conclusion

It is both a scientific challenge and an industrial importance to develop a general method of preparing functional polyolefin with block and graft structures, containing both polyolefin and functional (polar) polymer blocks. The reactive polyolefin intermediate offers a very attractive route, with simple reaction process to prepare the desirable block and graft copolymers with relatively well-defined molecular structures. The chemistry is based on three reactive sites, including borane, p-methylstyrene, and divinylbenzene, which permit the facile transformation from metallocene-mediated olefin polymerization to living free radical or living anionic polymerization. This sequential polymerization process, with both changes of catalytic sites and monomers, allows the employment of the best suitable polymerization mechanisms for preparing individual polymer blocks, i.e. metallocene polymerization for polyolefin and free radical or anionic polymerization for functional (polar) polymer.

Acknowledgements

References

[1] Storck WJ. Chem Engng News 2000;78(26):9.
[2] Vasile C, Seymour RB. Handbook of polyolefins. New York: Marcel Dekker, 1993.
[3] VerStrate G. Enyclop Polym Sci Engng 1986;6:522.
[4] Perlson BD, Schababerle CC. In: Ehrig RJ, editor. Plastics recycling; products and process. Munich: Hanser Publishers, 1992. Chapter 4.
[5] Natta G, Mazzanti G, Longi P, Bernardini F. J Polym Sci 1958;31:181.
[6] Heller J, Tieszen DO, Parkinson J. J Polym Sci 1963;A1:125.
[7] Clark KJ, Powell T. Polymer 1965;6:531.
[8] Chung TC. Macromolecules 1988;21:865.
[9] Andresen A, Cordes HG, Herwig J, Kaminsky W, Merk A, Mottweiler R, Pein J, Sinn H, Vollmer HJ. Angew Chem, Int Ed Engl 1976;15:630.
[10] Sinn H, Kaminisky W. Adv Organomet Chem 1980;18:99.

[11] Ewen JA, Jones RL, Razavi A, Ferrara J. J Am Chem Soc 1988;110:6255.

[12] Yang X, Stern L, Marks TJ. J Am Chem Soc 1994;116:10015.

[13] Coates GW, Waymouth RM. Science 1995;267:217.

[14] Francis FC, Brookhart M. J Am Chem Soc 1995;117:1137.

[15] Mecking S, Johnson LK, Wang L, Brookhart M. J Am Chem Soc 1998;120:888.

[16] Clark KJ, City WG. US Patent 3,949,277, 1970.

[17] Langer AW, Haynes RR. US Patent 3,755, 279, 1973.

[18] Purgett MD, Vogl O. J Polym Sci, Part A: Polym Chem 1988;26:677.

[19] Kesti MR, Coates GW, Waymouth RM. J Am Chem Soc 1992;114:9679.

[20] Schneider MJ, Schafer R, Mulhaupt R. Polymer 1997;38:2455.

[21] Correia SG, Marques MM, Ascenso JR, Ribeiro AFG, Gomes PT, Dias AR, Blais M, Rausch MD, Chien JCW. J Polym Sci, Part A: Polym Chem 1999;37:2471.

[22] Gaylord NG, Mehta M, Mehta R. J Appl Polym Sci 1987;33:2549.

[23] Singh R. Prog Polym Sci 1992;17:251.

[24] Jagur-Grodzinski J. Prog Polym Sci 1992;17:361.

[25] Hu GH, Flat JJ, Lambla M. Free radical grafting of monomers onto polymers by reactive extrusion: principles and applications. In: Al-Malaika S, editor. Reactive modifiers for polymers. London: Blackie Academic and Professional, 1997. p. 1–77.

[26] Hogt AH, Meijer J, Jelenic J. Modification of polypropylene by organic peroxides. In: Al-Malaika S, editor. Reactive modifiers for polymers. London: Blackie Academic and Professional, 1997. p. 84–123.

[27] Chung TC. ChemTech 1991;27:496.

[28] Chung TC. J Mol Catal 1992;76:15.

[29] Chung TC. Macromol Symp 1995;89:151.

[30] Chung TC. Trends Polym Sci 1995;3:191.

[31] Chung TC. Polym Mater Encycl 1996;8:6412.

[32] Chung TC. Metallocene-based reactive polyolefin copolymers containing *p*-methylstyrene. In: Scheirs J, Kamisky W, editors. Metelocene-based polyolefins. New York: Wiley, 1999. p. 293–318.

[33] Aggarwal SL. Block copolymers. New York: Plenum Press, 1970.

[34] Riess G, Periard J, Bandereet A. Colloidal and morphological behavior of block and graft copolymers. New York: Plenum Press, 1971.

[35] Lohse D, Datta S, Kresge E. Macromolecules 1991;24:561.

[36] Chung TC. US Patent 4,734,472, 1989.

[37] Chung TC. US Patent 4,812,529, 1989.

[38] Ramakrishnan S, Berluche E, Chung TC. Macromolecules 1990;23:378.

[39] Chung TC, Lu HL, Li CL. Polym Int 1995;37:197.

[40] Chung TC, Rhubright D. Macromolecules 1991;24:970.

[41] Chung TC, Rhubright D. Macromolecules 1993;26:3019.

[42] Chung TC, Lu HL. US Patent 5,543,484, 1996.

[43] Chung TC, Lu HL. US Patent 5,866,659, 1999.

[44] Chung TC, Lu HL. US Patent 6,015,862, 2000.

[45] Chung TC, Lu HL. J Polym Sci Part A: Polym Chem 1997;35:575.

[46] Chung TC, Lu HL. J Polym Sci, Part A: Polym Chem 1998;36:1017.

[47] Lu HL, Hong S, Chung TC. J Polym Sci, Part A: Polym Chem 1999;37:2795.

[48] Lu HL, Hong S, Chung TC. Macromolecules 1998;31:2028.

[49] Chung TC, Dong JY. US Patent 6,096,849, 2000.

[50] Xu G, Chung TC. J Am Chem Soc 1999;121:6763.

[51] Xu G, Chung TC. Macromolecules 1999;32:8689.

[52] Chung TC, Dong JY. J Am Chem Soc 2001;123(21):4871.

[53] Chung TC, Lu HL, Li CL. Macromolecules 1994;27:7533.

[54] Chung TC, Rhubright D. J Polym Sci, Part A: Polym Chem 1993;31:2759.

[55] Machida S, Shikuma H, Tazaki T, Tatsumi T, Kurokawa S. US Patent 5,608,009, 1997.

[56] Doi Y, Ueki S, Soga K. Macromolecules 1979;12:814.

[57] Doi Y, Keii T. Adv Polym Sci 1986;73/74:201.

[58] Yasuda X, Furo M, Yamamoto H. Macromolecules 1992;25:5115.

[59] Killian CM, Tempel DJ, Johnson LK, Brookhard M. J Am Chem Soc 1996;118:11664.

[60] Baumann R, Davis WM, Schrock RR. J Am Chem Soc 1997;119:3830.

[61] Natta G, Beati E, Severine F. J Polym Sci 1959;34:548.

[62] Ranby B, Guo F. Polym Prepr 1990;31:446.

[63] Chung TC, Jiang GJ, Rhubright D. US Patent 5,286,800, 1994.

[64] Chung TC, Jiang GJ, Rhubright D. US Patent 5,401,805, 1995.

[65] Chung TC, Jiang GJ. Macromolecules 1992;25:4816.

[66] Chung TC, Rhubright D, Jiang GJ. Macromolecules 1993;26:3467.

[67] Chung TC, Rhubright D. Macromolecules 1994;27:1313.

[68] Chung TC, Janvikul W, Lu HL. J Am Chem Soc 1996;118:705.

[69] Chung TC, Janvikul W. J Organomet Chem 1999;581:176.

[70] Chung TC, Janvikul W, Bernard R, Jiang GJ. Macromolecules 1993;27:26.

[71] Chung TC, Janvikul W, Bernard R, Hu R, Li CL, Liu SL, Jiang GJ. Polymer 1995;36:3565.

[72] Chung TC, Lu HL, Ding RD. Macromolecules 1997;30:1272.

[73] Riess G, Periard J, Bonderet A. Colloidal and morphological behavior of block and graft copolymers. New York: Plenum Press, 1971.

[74] Lohse D, Datta D, Kresge E. Macromolecules 1991;24:561.

[75] Szwarc M. Adv Polym Sci 1982;47:1.

[76] Young RN, Quirk RP, Fetters L. J Adv Polym Sci 1984;56:1.

[77] Miyamoto M, Sawamoto M, Higashimura T. Macromolecules 1985;18:123.

[78] Kennedy JP. US Patent 4,946,899, 1990.

[79] Risse W, Grubbs RH. Macromolecules 1989;22:1558.

[80] Schrock RR, Yap KB, Yang DC, Sitzmann H, Sita LR, Bazan GC. Macromolecules 1989;22:3191.

[81] Chung TC, Lu HL, Janvikul W. Polymer 1997;38:1495.

[82] Chung TC, Lu HL. J Mol Cat A: Chem 1997;115:115.

[83] Lu B, Chung TC. Macromolecules 1999;32:2525.

For Journal of the American Chemical Society as a Communication to the Editor

A New Living Free Radical Initiator; Alkylperoxy-9-borafluorene

T. C. Chung* and Guangxue Xu

Department of Materials Science and Engineering

The Pennsylvania State University

University Park, PA 16802

* Author to whom all correspondence should be addressed

Abstract

This paper discusses a new living free radical initiator, alkylperoxy-9-borafluorene, which shows spontaneous homolysis at ambient temperature to form active alkoxyl radical and "dormant" borinate radical due to the back-donating of electron density to the empty p-orbital of boron. The alkoxyl radical is active in initiating the polymerization of vinyl monomers, such as acrylic and methacrylic and monomers. On the other hand, the borinate radical is too stable to initiate polymerization, but may form a reversible bond with the propagating radical at the chain end to prevent undesirable termination reactions. The alkylperoxy-9-borafluorene initiator can be formed in situ or prepared by selective oxidation of 9-alkyl-borafluorene with oxygen. The "living" radical polymerization was characterized by predictable polymer molecular weight, narrow molecular weight distribution, and the formation of block copolymers by sequential monomer addition. In addition, the polymers formed are white solids, even without purification.
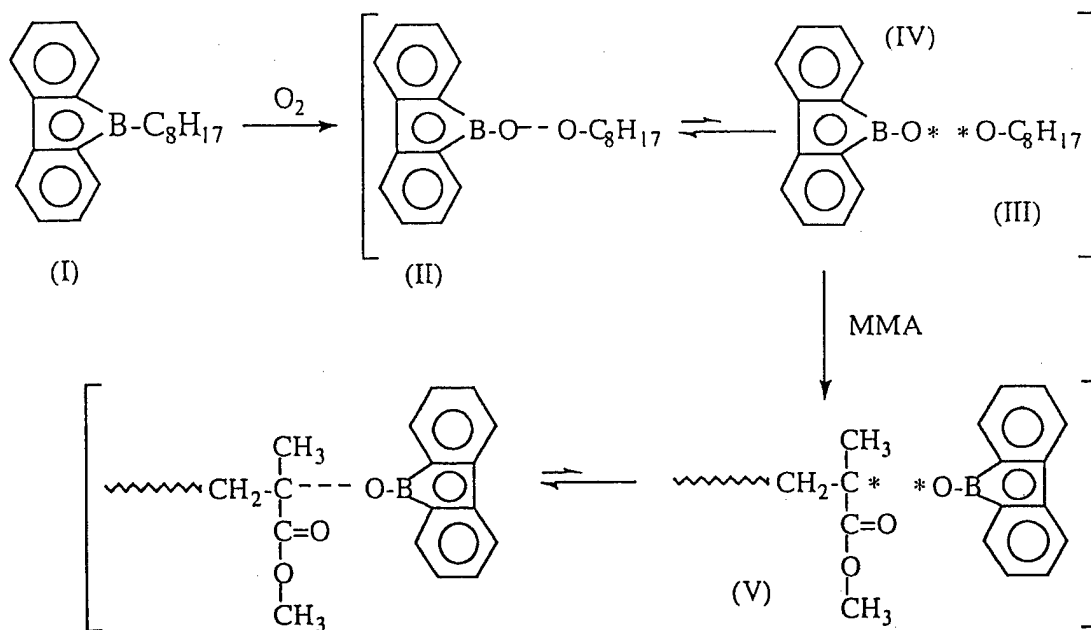
The control of polymer structure has been an important issue in polymer synthesis, both for scientific interests and industrial applications. Living polymerization provides an optimal means of control that can result in polymers with well-defined molecular structures; i.e. desirable molecular weight and polymer chain end, narrow molecular weight distribution, and the formation of block and star polymers. In the past, the most viable techniques for living polymerization reactions were mediated by anionic[1], cationic[2], and recently metathesis[3] initiators.

Free radical polymerization is particularly interesting due to its compatibility with a wide range of functional groups. Early attempts to realize a living free radical polymerization involved the concept of reversible termination of the growing polymer chains by iniferters[4], such as N,N-diethyldithiocarbamate derivatives. However, this approach suffered from poor control of the polymerization reaction and the formation of polymer with high polydispersity.

The first living radical polymerization was observed in reactions involving a stable nitroxyl radical[5] such as 2,2,6,6-tetramethylpiperidinyl-1-oxy (TEMPO), which does not react with monomers but forms a reversible end-capped propagating chain end. Usually, the reactions have to be carried out at an elevated temperature (>100°C) to obtain a sufficient concentration of propagating radicals for monomer insertion. Subsequently, several research groups have replaced the stable nitroxyl radical with transition metal species or reversible chain transfer agents as the capping agents to mediate living free radical systems. These polymerization reactions follow the mechanisms of atom transfer radical polymerization (ATRP)[6] or reversible addition-fragmentation chain transfer (RAFT)[7], respectively. Overall, these systems have a central theme-reversible termination via equilibrium between the active and dormant chain ends at an elevated temperature.

In the past decade, we have been studying a new free radical initiation system based on the oxidation adducts of organoborane and oxygen. The initial objective was centered around the functionalization of polyolefins[8,9] by first incorporating borane groups into the polymer chain that were then spontaneously oxidized by oxygen to form peroxide (B-O-O-C) moieties. Next, these moieties initiated free radical graft-from polymerization at ambient temperature to form polyolefin graft and block copolymers. A few years ago, we discovered a relatively stable radical initiator in the oxidation adducts[9] of alkyl-9-borabicyclononane (alkyl-9-BBN). This initiator exhibits the radical polymerization of methacrylate monomers with a linear relationship between the polymer molecular weight and a low monomer conversion rate (< 15%). The polymers formed during the polymerization show a stable but relatively broad molecular weight distribution (Mw/Mn= ~2.5) compared to those prepared by living polymerization processes. This initiator is very difficult to use for the preparation of block copolymer.

In this paper, we will discuss a new living free radical initiator, alkylperoxy-9-borafluorene, which can initiate living radical polymerization[10] at ambient temperatures. The resulting vinyl polymers are white solids with predictable molecular weight and narrow molecular weight distribution. As illustrated in Equation 1, the peroxide can be easily prepared by spontaneous selective oxidation of alkyldiarylborane (I) with oxygen at ambient temperature.

$$\underset{(I)}{\boxed{\text{B-C}_8\text{H}_{17}}} \xrightarrow{\text{O}_2} \left[\underset{(II)}{\text{B-O--O-C}_8\text{H}_{17}} \rightleftharpoons \underset{(III)}{\text{B-O}\ast\ \ast\text{O-C}_8\text{H}_{17}\ (IV)}\right]$$

$$\downarrow \text{MMA}$$

$$\left[\begin{array}{c}\text{CH}_3\\ \text{wwwCH}_2\text{-C---O-B}\\ \text{C=O}\\ \text{O}\\ \text{CH}_3\end{array} \rightleftharpoons \begin{array}{c}\text{CH}_3\\ \text{wwwCH}_2\text{-C}\ast\ \ \ast\text{O-B}\\ \text{C=O}\\ \text{O}\\ \text{CH}_3\end{array}\ (V)\right]$$

Equation 1

The preparation of precursor 1-octyl-9-borafluorene (I) will be discussed in the supplemental information. In a typical oxidation reaction, a stoichiometric amount of oxygen was syringed into a stirred suspension of 1-octyl-9-borafluorene in benzene. The mixture was stirred for 3 hours at ambient temperature. Evaporation of the volatiles under high vacuum afforded 1-octyl-9-borafluorene oxidation adduct as a colorless viscous product. Figure 1 compares the ^{11}B NMR spectra of the sample before and after the oxidation reaction.

(Figure 1)

The single chemical shift of 1-octyl-9-borafluorene (I) at 60 ppm (vs. etherated BF$_3$) indicates the strong π-electron delocalization around the B atom at the center five-member ring, which provides high bond order and good stability of the aryl-B bonds. Upon oxidation, the chemical shift completely moves to a higher field at 42 ppm, indicating a quantitative oxidation reaction to produce 1-octylperoxyl-9-borafluorene[11] initiator (II). Due to the two strong aryl-B bonds, the

oxidation reaction selectively takes place at the octyl-B bond. Both the ^{1}H and ^{13}C NMR spectra of 1-octylperoxyl-9-borafluorene are provided in the supplemental information.

The 1-octylperoxyl-9-borafluorene initiator (II) behaves very differently from other living radical initiator systems. This peroxylborane is a reactive radical initiator even at ambient temperature. The spontaneous homolytical cleavage of peroxide may take place by generating a reactive alkoxy radical (C-O*) (III) and a stable borinate radical (B-O*) (IV) due to the back-donating of electron density to the empty p-orbital of boron. The alkoxyl radical (III) then initiates the radical polymerization of methyl methacrylate (MMA) at ambient temperature. On the other hand, the borinate radical (IV) is too stable to react with monomer, but serves as the end-capping agent to form a weak and reversible bond[12] with the growing chain end (V) during the polymerization. Upon the dissociation of the electron pair, the growing chain end can react with MMA to extend the polymer chain. The resulting new chain end radical immediately forms a weak bond with the borinate radical (IV). This process minimizes the undesirable chain transfer reaction and termination (coupling and disproportionation) reaction between two growing chain ends.

In a typical polymerization reaction, a 100 ml glass reactor equipped with a magnetic stirrer was introduced with 40 ml THF and 10 ml MMA (1.87 M) by syringe under a nitrogen atmosphere. The reactor was then placed in a water bath (20°C) for 10 minutes before adding 1-octylperoxyl-9-borafluorene (1.7 x 10^{-3} M) to the solution. The mixture was stirred at 20°C with periodic removal of samples from the reactor. The polymer solution was quenched with acidic methanol and the precipitated polymer was collected, washed, and dried in a vacuum oven at 60° C. About 51 mol% monomer conversion was observed after 24 hours of reaction. Figure 2 shows the GPC curves of the poly(methyl methacrylate) polymers sampled during the reaction.

(Figure 2)

It is clear that the polymer continuously increased its molecular weight during the entire polymerization process. The polymer's molecular weight distribution was maintained very constant and narrow (Mw/Mn= ~1.2). Figure 3 plots the polymer molecular weight vs. the monomer conversion and compares the results with a theoretical line based on the [g of monomer consumed]/[mole of initiator]. A good match with the straight line through the origin strongly supports the presence of living polymerization in the reaction.

(Figure 3)

This living radical polymerization was also evidenced in the preparation of block copolymers such as poly(methyl methacrylate-b-butyl methacrylate) by sequential monomer addition. Figure 4 compares the GPC curves of poly(methyl methacrylate-b-butyl methacrylate) diblock copolymer and the corresponding poly(methyl methacrylate) homopolymer. The molecular weight almost doubles from the homopolymer to the diblock copolymer without changing the narrow molecular weight distribution (Mw/Mn= ~1.2). Basically, the copolymer composition is controlled by the monomer feed ratio and reaction time.

(Figure 4)

Overall, it is remarkable to consider the simplicity of this living radical initiator and its polymerization process occurring at ambient temperature with the injection of oxygen to 1-octyl-9-borafluorene in the presence of monomers. The diminished chain-transfer and termination reactions in the homogeneous reaction conditions imply the in situ formation of a stable radical, possibly borinate radical (IV), which serves as the reversible capping agent with the propagating radical during the living radical polymerization. Both the homo- and di-block copolymers formed are white solids with well-defined molecular structures.

Acknowledgment

References:

1. (a) Szwarc, M., *Adv. Polym. Sci.* **1982**, 47, 1. (b) Tung, L. H., Lo, G. Y. and Beyer, D. E., U. S. Patent 4,172,100, 1979. (c) Young, R.N., Quirk, R.P. and Fetters, L. *J. Adv. Polym. Sci.* **1984**, 56, 1.

2. (a) Miyamoto, M., Sawamoto, M. and Higashimura, T. *Macromolecules* **1985**, 18, 123. (b) Kennedy, J. P., U. S. Patent, 4,946,899, 1990.

3. (a) Risse, W. and Grubbs, R. H. *Macromolecules* **1989**, 22, 1558. (b) Schrock, R. R., Yap, K. B., Yang, D. C., Sitzmann, H., Sita, L. R. and Bazan, G. C. *Macromolecules* **1989**, 22, 3191.

4. (a) Otsu, T.; Yoshida, M. Makromol. Chem., Rapid Commun. **1982**, 3, 127. (b) Otsu, T.; Kuriyama, A. *J. Macromol. Sci., Chem.* **1984**, A21, 921. (c) Turner, S. R.; Blevins, R. W. *Macromolecules* **1990**, 23, 1856.

5. (a) Moad, G.; Rizzardo, E.; Solomon, D. H. *Macromolecules* **1982**, 15, 909. (b) Georges, M. K.; Veregin, P. R. N.; Kazmaier, P. M.; Hamer, G. K. *Macromolecules* **1993**, 26, 2987. (c) Hawker, G. J. *J. Am. Chem. Soc.* **1994**, 116, 11185. (d) Hawker, C. J. *Angew. Chem. Int. Ed. Engl.* **1995**, 34, 1456. (e) Hawker, C. J.; Frechet, J. M. J.; Grubbs, R. B.; Dao, J. *J. Am. Chem. Soc.* **1995**, 117, 10763. (f) Wang, D.; Wu, Z. *Macromolecules* **1998**, 31, 6727.

6. (a) Wang, J. S.; Matyjaszewski, K. *J. Am. Chem. Soc.* **1995**, 117, 5614. (b) Wang, J. S.; Matyjaszewski, K. *Macromolecules* **1995**, 28, 7901. (c) Kato, M.; Kamigaito, M.; Sawamoto, M.; Higashimura, T. *Macromolecules* **1995**, 28, 1721. (d) Percec, V.; Barboiu, B. *Macromolecules* **1995**, 28, 7970. (e) Granel, C.; Dubois, P.; Jerome, R.; Teyssie, P. *Macromolecules* **1996**, 29, 8576. (f) Wayland, B. B.; Posznik, G.; Mukerjee, S. L.; Fryd, M. *J. Am. Chem. Soc.* **1994**, 116, 7943.

7. Chiefari, J; Chong, Y. K.; Ercole, F.; Krstina, J.; Jeffery, J.; Le, T.; Mayadunne, R.; Meijs, G. F.; Moad, C. L.; Moad, G.; Rizzardo, E.; Thang, S. H. *Macromolecules* **1998**, 31, 5559.

8. (a) Chung, T. C.; Jiang, G. J.; Rhubright, D. *Macromolecules* **1993**, 26, 3467. (b) Chung, T. C.; Lu, H. L.; Janvikul, W. *Polymer* **1997**, 38, 1495. (c) Lu, B.; Chung, T. C. *Macromolecules* **1998**, 31, 5943. (d) Xu, G.; Chung, T. C. *J. Am. Chem. Soc.* **1999**, 121, 6763. (e) Xu, G.; Chung, T. C. *Macromolecules* **1999**, 32, 8689.

9. Chung, T. C.; Janvikul, W.; Lu, H. L. *J. Am. Chem. Soc.* **1996**, 118, 705.

10. Arimoto, F. S. *J. Polym. Sci.: Part-I* **1966**, 4, 275.

11. For comparison, 1-octyloxyl-9-borafluorene was also synthesized by reacting 9-borafluorene with 1-octanol. This compound, having a [11]B chemical shift at about 43 ppm, showed no catalytic activity in the presence of MMA monomers.

12. No oxygen NMR signal was observed in a [17]O-labelled 1-octylperoxyl-9-borafluorene sample, indicating a paramagnetic character of the compound and oxygen nuclei carrying the unpaired electron.

Figure Captions

Figure 1, ^{11}B NMR spectrum of (a) 1-octyl-9-borafluorene and (b) 1-octylperoxyl-9-borafluorene.

Figure 2, GPC curves of poly(methyl methacrylate) polymers sampled during the polymerization reaction (a) 2, (b) 5, (c) 18 and (d) 24 hours, respectively.

Figure 3, Plot of poly(methyl methacrylate) molecular weight vs. monomer conversion.

Figure 4, GPC curves of (a) poly(methyl methacrylate) (Mn= 52,000 g/mol, Mw/Mn = 1.2) and (b) poly(methyl methacrylate-b-butyl methacrylate)) (Mn= 122,000 g/mol, Mw/Mn = 1.2).
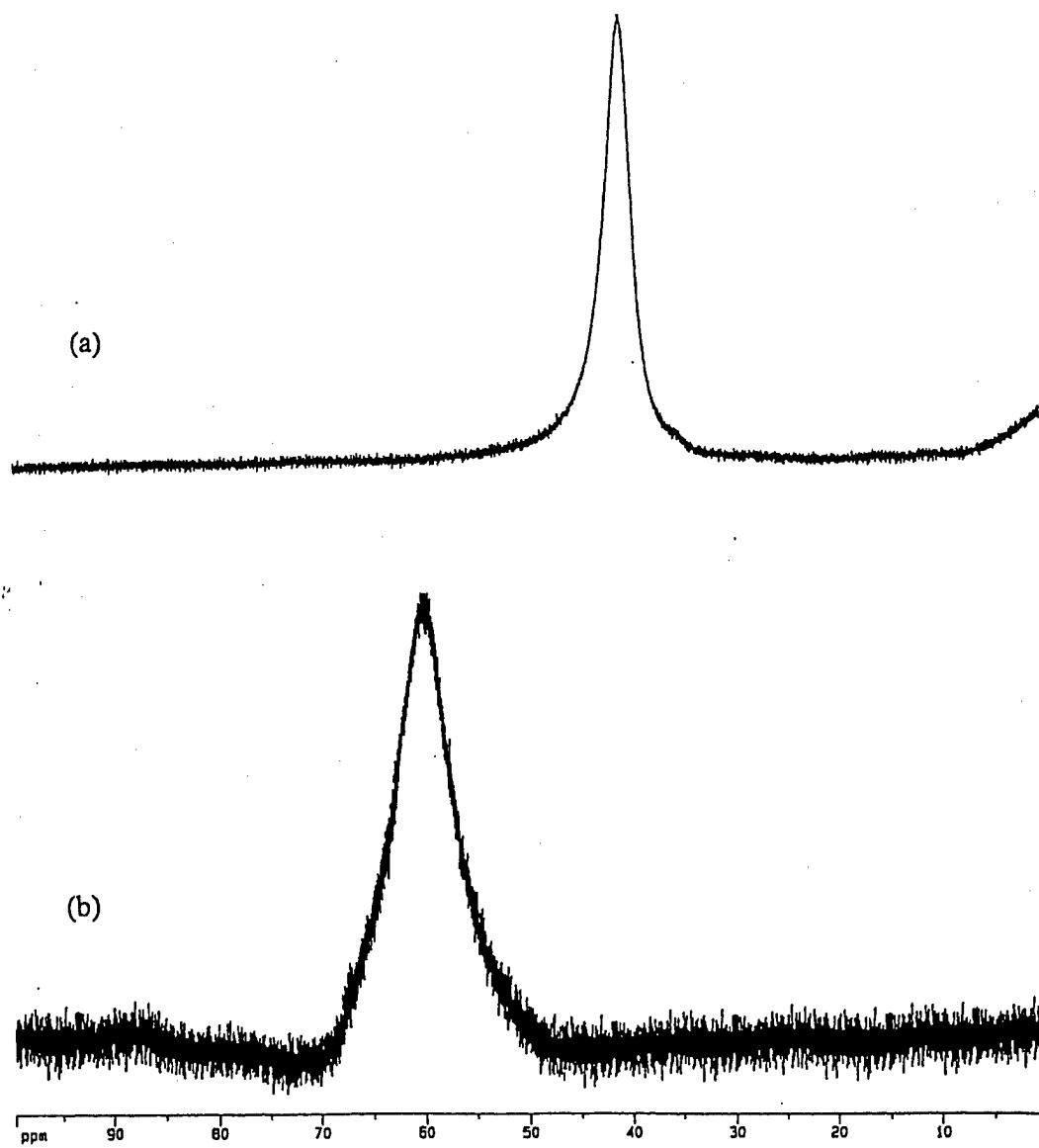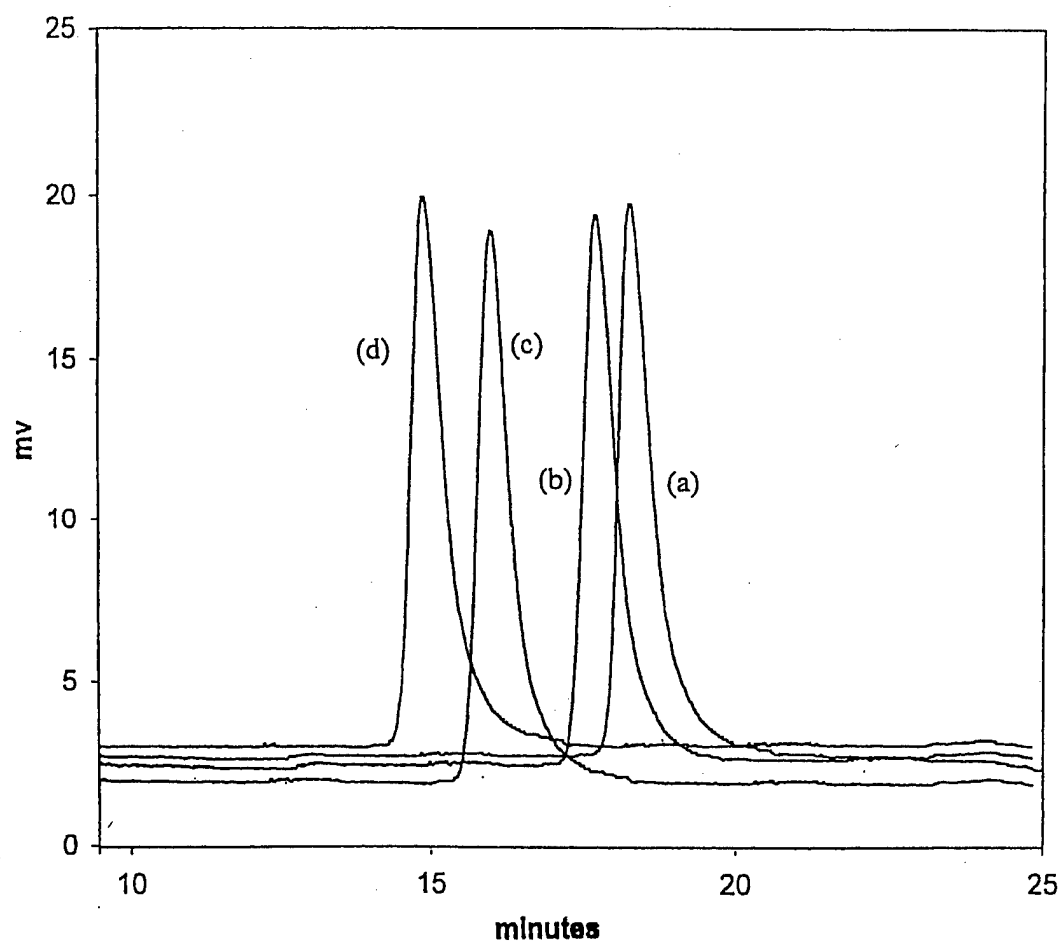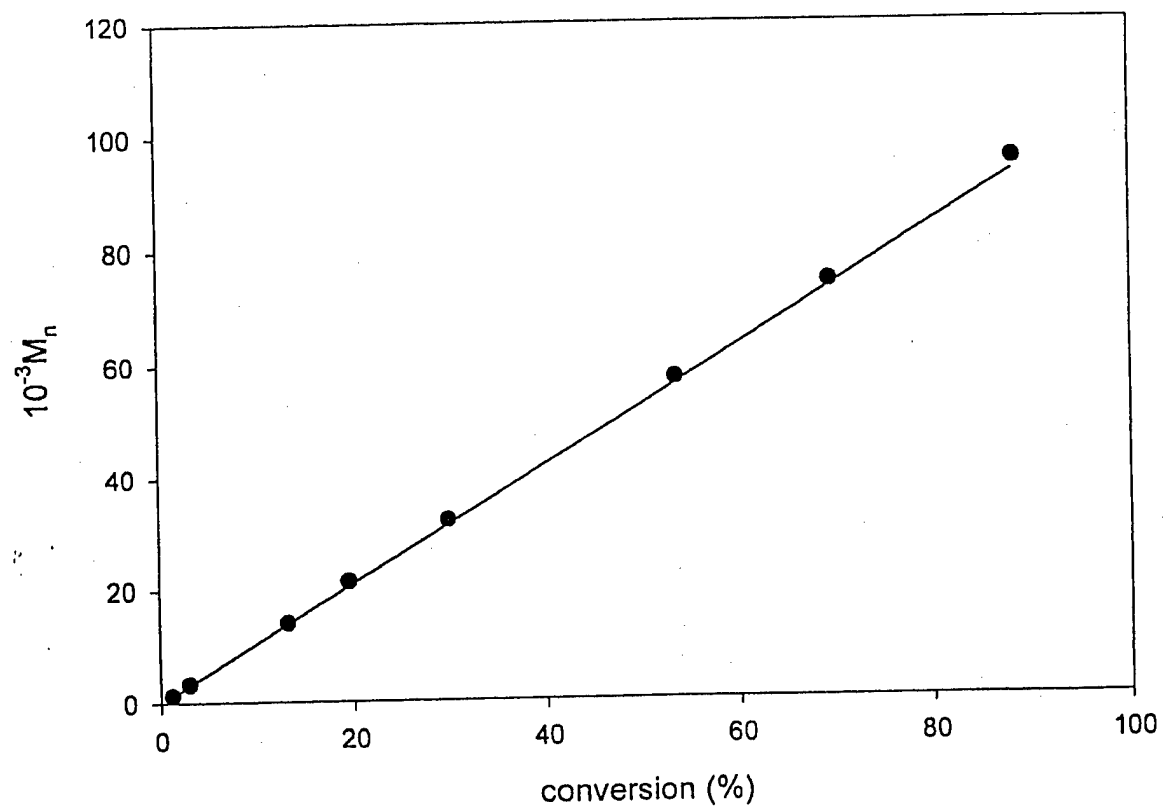
Figure 1

Figure 2

Figure 3

Figure 4